THE EFFECTS OF MATERIALS AND MICRO - CLIMATE VARIATIONS ON PREDICTIONS OF CARBONATION RATE IN REINFORCED CONCRETE IN THE INLAND ENVIRONMENT

Yunusa Aminu Alhassan

A thesis submitted to the Faculty of Engineering and the Built Environment, University of the Witwatersrand, Johannesburg, in fulfillment of the requirements for the degree of Doctor of Philosophy.

Johannesburg, 2014

DECLARATION

I declare that this thesis is my own unaided work. It is being submitted to the Degree of Doctor of Philosophy to the University of the Witwatersrand, Johannesburg. It has not been submitted before for any degree or examination to any other university.

……..

…… day of …… ……..

ABSTRACT

Carbonation of reinforced concrete elements results in the depassivation of reinforcing steel, which very often causes corrosion of the reinforcement and leads to the loss of reinforcing steel cross sections, and bonding with concrete that culminate in the reduction of the load carrying capacity, durability performance and ultimately service life of reinforced concrete structures.

In this thesis, the rate of carbonation of the most commonly used concretes on construction projects in South Africa are determined for different inland exposure conditions and are then related to the concrete mixture design and/or early-age characterisation parameters. The results obtained are expressed in the form of prediction models with concrete mixture design and/or concrete characterisation at early-age as input parameters. In addition, the binder types used in concrete, concrete curing durations and exposure conditions effects on carbonation rate in concrete are also included as predictor variables. On the basis of concrete types, processing and exposure conditions assessed in this work, carbonation have significant effect on blended concretes while concrete given prolonged curing duration and in an outdoor exposed condition present the least rate of carbonation.

The significance of the results obtained in terms of rate of carbonation for different concrete types and exposure conditions will aid in the design, repair and or maintenance of concrete structures in inland environments. The modelled rates of carbonation reflect the carbonation rates of the different binder types and inland exposure conditions in South Africa. The data obtained in the tests and the techniques used provide an effective basis for predicting the rate of carbonation in proposed and existing reinforced concrete structures made with the binder types and located in the inland environment of South Africa.

ACKNOWLEDGEMENTS

I gratefully acknowledge:

My supervisor, Professor Yunus Ballim, for his friendship, encouragement, guidance and patience over the duration of this project and who served as a constant source of inspiration and for investing his time to greatly improve my writing skills for the purpose of this work

The Federal Polytechnic Idah, Nigeria and Tertiary Education Trust Fund, Nigeria, for providing financial support

Cement and Concrete Institute, South Africa, for your unrelenting financial assistance through Professor Yunus Ballim

Postgraduate Merit Award of the University of the Witwatersrand, for providing financial support

Members of staff in the School of Civil & Environmental Engineering, University of the Witwatersrand, South Africa for their material and spiritual support

Dr Petra Gaylard (Data Management and Statistical Analysis) for helpful discussion and the reviewing of the statistical modelling aspect of this thesis

The staff at the Cement and Concrete Institute's Information Centre for their assistance in obtaining literature references

Finally, I extend my deepest gratitude to my family, friends and colleagues and especially my beloved wife, Princess Acho, for all their support, prayers and tolerance throughout the duration of this study. May God bless you all.

TABLE OF CONTENTS **PAGE**

DECLARATION ii

ABSTRACT……iii

ACKNOWLEDGEMENTS……iv

TABLE OF CONTENTS……v

LIST OF FIGURES……xi

LIST OF TABLES……xx

CHAPTER 1 1-1

INTRODUCTION 1-1

1.1 Background 1-1

1.2 Hydration and the Development of Pore Structure and Chemistry……1-3

1.3 Durability Index Testing and Approach……1-5

1.4 Carbonation Rate in Concrete 1-7

Chapter References 1-15

CHAPTER 2 2-1

LITERATURE REVIEW..... 2-1

2.1 Introduction 2-1

2.2 Hydration Reactions..... 2-1

2.2.1 Hydration reactions of plain cement 2-1

2.2.2 Hydration reactions of blended cement..... 2-3

2.3 Nature of Concrete 2-4

2.3.1 Physical and chemical nature of concrete 2-5

2.3.2 The nature of concrete on its durability performance 2-12

2.3.3 Fluid transport properties of concrete and its measurement 2-14

2.3.4 Chemical composition of concrete and its quantification 2-24

2.4 Mechanism of Carbonation in Concrete 2-28

2.4.1 Measurement of carbonation in concrete……...2-29

2.4.2 Derivation of the basic carbonation progression rate equation 2-30

2.4.3 Factors that influence carbonation progression in concrete 2-34

2.5 Existing Models for the Prediction of Carbonation Depth/Rate in Concrete ..... ….2-40

2.5.1 Approach for the development of carbonation rate prediction model in concrete ……..2-52

Chapter References 2-55

CHAPTER 3 3-1

MATERIALS AND METHODS 3-1

3.1 Introduction 3-1

3.2 Variables of the Test Program 3-2

3.2.1 Exposure condition 3-2

3.2.2 Binder type 3-3

3.2.3 Water/binder ratio 3-3

3.2.4 Moist curing period 3-4

3.2.5 Mixing and compaction 3-4

3.2.6 Age at testing 3-5

3.3 Properties of the Materials Used 3-5

3.3.1 Cement 3-5

3.3.2 FA 3-6

3.3.3 GGBS 3-6

3.3.4 CSF 3-6
3.3.5 Composite cement 3-7
3.3.6 Aggregates 3-8
3.3.7 Admixtures 3-12
3.4 Laboratory and Field Testing Procedure 3-12
3.4.1 Concrete mixtures 3-12
3.4.2 Concrete cube samples requirement and storage 3-15
3.4.3 Concrete cube samples preparation and processing 3-16
3.5 Test Methods 3-24
3.5.1 Compressive strength tests 3-24
3.5.2 Durability index tests 3-25
3.5.3 Chemical composition tests 3-32
3.5.4 Micro-climate monitoring at the exposure sites 3-39
3.5.5 Carbonation depth test 3-40
Chapter References 3-42

CHAPTER 4 4-1
RESULTS AND DISCUSSION 4-1
4.1 Introduction 4-1
4.2 Compressive Strength Results 4-1
4.3 Oxygen Permeability Results 4-8
4.3.1 Oxygen permeability at 28 days after casting 4-8
4.3.2 Oxygen permeability at 6, 12 and 18 months after casting 4-17
4.4 Water Sorptivity Results 4-20
4.4.1 Water sorptivity at 28 days after casting 4-20

4.4.2 Water sorptivity at 6, 12 and 18 months after casting..... 4-27
4.5 Results of Chemical Composition Tests 4-31
4.5.1 Calcium hydroxide content 4-31
4.5.2 Wet chemical analysis for calcium oxide content..... 4-37
4.6 Micro-climate Variation at Exposure Sites 4-43
4.6.1 Carbon dioxide variation..... 4-44
4.6.2 Relative humidity variation..... 4-45
4.6.3 Temperature variation 4-47
4.7 Concrete Carbonation Depth Results 4-48
4.7.1 Concrete carbonation rate 4-49
Chapter References 4-73

CHAPTER 5 5-1
MODELLING THE CARBONATION RATE OF CONCRETE 5-1
5.1 Introduction 5-1
5.2 Formulation of a Prediction Model for the Carbonation Rate of Concrete…
..... 5-2
5.3 Multiple Linear Regression: A Review 5-5
5.4 Description of the Response and Predictor Variables..... 5-8
5.5 Preparation of the Response and Predictor Variables..... 5-11
5.5.1 Univariate analysis of the response and predictor variables 5-11
5.5.2 Relationship between the response and predictor variables..... 5-20
5.6 Regression Analysis Between the Response and Predictor Variables 5-32
5.6.1 Developed carbonation prediction models..... 5-43
Chapter References 5-47

CHAPTER 6 ……..6-1

COMPARISON OF CARBONATION PREDICTION FROM DEVELOPED MODELS WITH HISTORICALLY MEASURED CARBONATION..... 6-1

6.1 Introduction 6-1

6.2 Comparison of Carbonation Predictions from Developed Models and Measured Carbonation 6-2

6.2.1 Ballim's data 6-3

6.2.2 Ananmalay's data 6-8

6.2.3 Ballim and Lampacher's data..... 6-15

6.2.4 Lampacher's data 6-21

6.2.5 Yam's data 6-24

6.3 Analyses of Difference Between Predicted Carbonation from Developed Models and Measured Carbonation 6-28

6.3.1 Laboratory cast concrete samples carbonation 6-29

6.3.2 Existing concrete structures carbonation 6-29

Chapter References 6-32

CHAPTER 7 7-1

GENERAL CONCLUSIONS 7-1

7.1 Introduction 7-1

7.2 Observations and Conclusions 7-1

7.3 Recommendation for Future Research..... 7-7

APPENDICES…….A-1

Appendix A: Concrete compressive strength test results….....A-1

Appendix B: Concrete medium-term durability index test results……..A-6

Appendix C: Micro-climate results of the exposure sites…..A-10

Appendix D: Concrete carbonation test results…..A-14

Appendix E: Correlation analysis and scatter plots output……...….A-22

Appendix F: Regression analysis output……...…….A-46

Appendix G: Natural carbonation rate plots.....A-77

LIST OF FIGURES **PAGE**

Chapter 1

Figure 1.1: Schematic representation of the service life of a reinforced concrete structure affected by reinforcement corrosion (Bertolini, 2008) 1-2

Figure 1.2: pH reduction due to carbonation moving as a "front" from the concrete surface (Ballim et al., 2009)..... 1-3

Figure 1.3: Schematic diagram showing the influence of water/cement ratio and degree of hydration on the reduction of capillary pore volume (Gräf & Grube, 1986) 1-4

Figure 1.4: Framework for carrying out durability studies (Alexander & Ballim, 1993; Ballim et al., 2009)..... 1-7

Figure 1.5: Pourbaix diagram for iron-water system at 25°C (Revie & Uhlig, 2008) 1-9

Chapter 2

Figure 2.1: Schematic of the hydration and structures development in cement paste (Mehta & Monteiro, 1993)..... 2-2

Figure 2.2: Representation of the transition zone and bulk cement paste in concrete (Mehta & Monteiro, 1993) 2-5

Figure 2.3: Schematic outline of microstructural development in Portland cement paste (C-A-S-H are included as part of C-S-H for convenience, although they will crystallize as separate phases). The approximate times indicated are: (a) Initial mix; (b) 7 days; (c) 28 days; (d) 90 days (Mehta and Monteiro, 1993)..... 2-7

Figure 2.4: Dimensional ranges of solids and pores in a hydrated cement paste (Mehta & Monteiro, 1993; Gowripalan et al. 1990)..... 2-9

Figure 2.5: Schematic description of the structure of cement gel (Fernandez Bertos et al., 2004) 2-10

Figure 2.6: Types of water associated with the calcium silicate hydrate (Feldman and Sereda, 1968)..... 2-11

Figure 2.7: Permeability cell arrangement (Alexander et al., 1999)..... 2-20

Figure 2.8: (a) Test Set (b) Specimens arranged for saturation (c) Vacuum saturation facility (Alexander et al., 1999)..... 2-23

Figure 2.9: Perkin Elmer Thermogravimetric Analyzer (TGA 4000) 2-25

Figure 2.10 28 day oxygen permeability vs carbonation depth (Ballim, 1994) ..... ….2-44

Figure 2.11: 28 day water sorptivity vs. carbonation depth (Ballim, 1994) 2-46

Figure 2.12: 28 day oxygen permeability vs carbonation depth (Mackechnie, 1996) 2-47

Figure 2.13: 28 day oxygen permeability vs carbonation depth (Mackechnie and Alexander, 2002)..... 2-48

Chapter 3

Figure 3.1: Grading curve of coarse aggregate (Granite) 3-10

Figure 3.2: Grading curve of fine aggregate (Granite crusher sand) 3-12

Figure 3.3: Concrete cube samples in the laboratory room after moist curing, during preconditioning..... 3-19

Figure 3.4: Concrete cube samples inside a micro-climate controlled accelerated carbonation chamber located in a temperature controlled room..... 3-21

Figure 3.5: View of a basement parking garage indicating the location where the concrete cube samples and data logger were placed..... 3-21

Figure 3.6: Concrete cube samples and data logger in a basement parking garage (indoor condition)..... 3-22

Figure 3.7: View of a foot bridge along a busy highway indicating where the concrete cube samples and data logger were placed..... 3-22

Figure 3.8: Concrete cube samples and data logger under a bridge along a busy highway (outdoor sheltered condition) 3-23

Figure 3.9: Outdoor exposed condition showing exposed concrete cube samples and data logger sheltered from rain and sun…..3-23

Figure 3.10: Concrete cube samples on the rooftop of a building in an urban setting (outdoor exposed condition)……...3-24

Figure 3.11: Preparation of discs from a concrete cube sample 3-26

Figure 3.12: (a) Oxygen permeability sample unite (b) Oxygen permeability experimental set-up 3-27

Figure 3.13: Typical plots of logarithm of the ratio heads versus time…….....3-29

Figure 3.14: (a) Water sorptivity experimental set-ups (b) Concrete discs in a vacuum for saturated weight determination……3-30

Figure 3.15: Typical plots of individual concrete discs mass gain versus square-root of time……..3-31

Figure 3.16: TG/DTG curve for PC-40 concrete - 3 days moist curing…….3-34

Figure 3.17: Micro-climate data been downloaded at the end of the month from the data loggers placed at the different exposure sites. 3-40

Figure 3.18: Method of breaking concrete cubes for carbonation depth determination……..3-41

Figure 3.19: A typical concrete cube samples sprayed with phenolphthalein, showing the depth of carbonation……...3-42

Chapter 4

Figure 4.1: Compressive strength vs. Water/binder ratio for the 100% CEM I concretes..... 4-3

Figure 4.2: Compressive strength vs. Water/binder ratio for the 70/30 CEM I-FA concretes..... 4-3

Figure 4.3: Compressive strength vs. Water/binder ratio for the 50/50 CEM I-GGBS concretes 4-4

Figure 4.4: Compressive strength vs. Water/binder ratio for the 90/10 CEM I-CSF concretes 4-4

Figure 4.5: Compressive strength vs. Water/binder ratio for the 100% CEM V concretes 4-5

Figure 4.6: Compressive strength vs. Concrete age for all the concrete types studied 4-5

Figure 4.7: Oxygen permeability index vs. Water/binder ratio for the 100% CEM I concretes 4-11

Figure 4.8: Oxygen permeability index vs. Water/binder ratio for the 70/30 CEM I-FA concretes 4-11

Figure 4.9: Oxygen permeability index vs. Water/binder ratio for the 50/50 CEM I-GGBS concretes 4-12

Figure 4.10: Oxygen permeability index vs. Water/binder ratio for the 90/10 CEM I-CSF concretes 4-12

Figure 4.11: Oxygen permeability index vs. Water/binder ratio for the 100% CEM V concretes 4-13

Figure 4.12: Oxygen permeability index vs. Extent of initial moist curing for all the concrete types studied 4-13

Figure 4.13: Concrete permeability measurement results after 6-months exposure to the inland environment 4-18

Figure 4.14: Concrete permeability measurement results after 12-months exposure to the inland environment 4-18

Figure 4.15: Concrete permeability measurement results after 18-months exposure to the inland environment 4-19

Figure 4.16: Water sorptivity vs. Water/binder ratio for the 100% CEM I concretes 4-23

Figure 4.17: Water sorptivity vs. Water/binder ratio for the 70/30 CEM I-FA concretes..... 4-23

Figure 4.18: Water sorptivity vs. Water/binder ratio for the 50/50 CEM I-GGBS concretes..... 4-24

Figure 4.19: Water sorptivity vs. Water/binder ratio for the 90/10 CEM I-CSF concretes..... 4-24

Figure 4.20: Water sorptivity vs. Water/binder ratio for the 100% CEM V concretes..... 4-25

Figure 4.21: Water sorptivity vs. Extent of initial moist curing for all the concrete type studied 4-25

Figure 4.22: Concrete sorptivity measurement results after 6 months exposure to the inland environment..... 4-28

Figure 4.23: Concrete sorptivity measurement results after 12 months exposure to the inland environment..... 4-29

Figure 4.24: Concrete sorptivity measurement results after 18 months exposure to the inland environment..... 4-29

Figure 4.25: $Ca(OH)_2$ content vs. Water/binder ratio for the 100% CEM I concretes..... 4-33

Figure 4.26: $Ca(OH)_2$ content vs. Water/binder ratio for the 70/30 CEM I-FA concretes..... 4-33

Figure 4.27: $Ca(OH)_2$ content vs. Water/binder ratio for the 50/50 CEM I-GGBS concretes..... 4-34

Figure 4.28: $Ca(OH)_2$ content vs. Water/binder ratio for the 90/10 CEM I-CSF concretes..... 4-34

Figure 4.29: $Ca(OH)_2$ content vs. Water/binder ratio for the 100% CEM V concretes..... 4-35

Figure 4.30: $Ca(OH)_2$ content vs. Concrete age for all the concrete type studied……4-35

Figure 4.31: CaO content vs. Water/binder ratio for the 100% CEM I concretes……4-39

Figure 4.32: CaO content vs. Water/binder ratio for the 70/30 CEM I-FA concretes..... 4-40

Figure 4.33: CaO content vs. Water/binder ratio for the 50/50 CEM I-GGBS concretes..... 4-40

Figure 4.34: CaO content vs. Water/binder ratio for the 90/10 CEM I-CSF concretes..... 4-41

Figure 4.35: CaO content vs. Water/binder ratio for the 100% CEM V concretes ..... ……..4-41

Figure 4.36: CaO content vs. Concrete age for all the concrete type studied 4-42

Figure 4.37: Average monthly carbon dioxide variations for the exposure sites…. 4-45

Figure 4.38: Average monthly relative humidity variations for the exposure sites.. 4-46

Figure 4.39: Average monthly temperature variations for the exposure sites ... 4-47

Figure 4.40: Carbonation depth vs. Exposure period..... 4-48

Figure 4.41: Carbonation depth vs. Square root of exposure period 4-50

Figure 4.42: Carbonation rate vs. Water/binder ratio for the 100% CEM I concretes exposed indoors..... 4-56

Figure 4.43: Carbonation rate vs. Water/binder ratio for the 70/30 CEM I-FA concretes exposed indoors..... 4-57

Figure 4.44: Carbonation rate vs. Water/binder ratio for the 50/50 CEM I-GGBS concretes exposed indoors..... 4-57

Figure 4.45: Carbonation rate vs. Water/binder ratio for the 90/10 CEM I-CSF concretes exposed indoors..... 4-58

Figure 4.46: Carbonation rate vs. Water/binder ratio for the 100% CEM V concretes exposed indoors..... 4-58

Figure 4.47: Carbonation rate vs. Concrete age for all the concrete types exposed indoors..... 4-59

Figure 4.48: Carbonation rate vs. Water/binder ratio for the 100% CEM I concretes exposed outdoor sheltered..... 4-60

Figure 4.49: Carbonation rate vs. Water/binder ratio for the 70/30 CEM I-FA concretes exposed outdoor sheltered..... 4-60

Figure 4.50: Carbonation rate vs. Water/binder ratio for the 50/50 CEM I-GGBS concretes exposed outdoor sheltered..... 4-61

Figure 4.51: Carbonation rate vs. Water/binder ratio for the 90/10 CEM I-CSF concretes exposed outdoor sheltered..... 4-61

Figure 4.52: Carbonation rate vs. Water/binder ratio for the 100% CEM V concretes exposed outdoor sheltered..... 4-62

Figure 4.53: Carbonation rate vs. Concrete age for all the concrete types exposed outdoor sheltered..... 4-62

Figure 4.54: Carbonation rate vs. water/binder ratio for the 100% CEM I concretes exposed outdoors..... 4-63

Figure 4.55: Carbonation rate vs. water/binder ratio for the 70/30 CEM I-FA concretes exposed outdoors..... 4-63

Figure 4.56: Carbonation rate vs. water/binder ratio for the 50/50 CEM I-GGBS concretes exposed outdoors..... 4-64

Figure 4.57: Carbonation rate vs. water/binder ratio for the 90/10 CEM I-CSF concretes exposed outdoors..... 4-64

Figure 4.58: Carbonation rate vs. water/binder ratio for the 100% CEM V concretes exposed outdoors..... 4-65

Figure 4.59: Carbonation rate vs. Concrete age for all the concrete types exposed outdoors..... 4-65

Figure 4.60 Carbonation rate vs. Water/binder ratio for the 100% CEM I concretes exposed to an accelerated condition..... 4-66

Figure 4.61: Carbonation rate vs. Water/binder ratio for the 70/30 CEM I-FA concretes exposed to an accelerated condition..... 4-66

Figure 4.62: Carbonation rate vs. Water/binder ratio for the 50/50 CEM I-GGBS concretes exposed to an accelerated condition..... 4-67

Figure 4.63: Carbonation rate vs. Water/binder ratio for the 90/10 CEM I-CSF concretes exposed to an accelerated condition..... 4-67

Figure 4.64: Carbonation rate vs. Water/binder ratio for the 100% CEM V concretes exposed to an accelerated condition..... 4-68

Figure 4.65: Carbonation rate vs. Concrete age for all the concrete types exposed to an accelerated condition..... 4-68

Figure 4.66: Carbonation rates vs. Exposure conditions for all the 0.5 w/b ratio concretes exposed to natural conditions..... 4-69

Chapter 5

Figure 5.1: A flow chart illustrating the iterative regression process (Chatterjee & Hadi, 2009)..... 5-5

Figure 5.2: Histogram showing the distribution of the response variable 5-12

Figure 5.3: P - P plot for the response variable..... 5-13

Figure 5.4: Histograms showing the distribution of the predictor variable 5-15

Figure 5.5: P - P plots for the predictor variables 5-17

Chapter 6

Figure 6.1: Comparison of predicted carbonation of Model 3 (outdoor sheltered and exposed) and measured carbonation..... 6-19

Figure 6.2: Comparison of predicted carbonation of Model 4 (outdoor sheltered and exposed) and measured carbonation..... 6-19

Figure 6.3: Comparison of predicted carbonation of Model 3 and 4 (outdoor exposed) and measured carbonation 6-24

Figure 6.4: Comparison of predicted carbonation of Model 3 (Grade 30 and 35) and measured carbonation..... 6-27

Figure 6.5: Comparison of predicted carbonation of Model 4 (grade 30 and 35) and measured carbonation..... 6-27

Appendices

Figure E1: Scatter plots of the variables……A-24

Figures G1-G8: Carbonation depth vs. square-root of exposure period……A-78

LIST OF TABLES **PAGE**

Chapter 2

Table 2.1: Coefficients for carbonation prediction model (Watkins and Jones, 1993) 2-42

Table 2.2: 90th percentile carbonation prediction model parameters for exposed conditions in the three localities in South Africa (Alexander, et al., 2007; Yam, 2004) 2-51

Table 2.3: Weather conditions in the three localities in South Africa (Alexander, et al., 2007; Yam, 2004)..... 2-51

Chapter 3

Table 3.1: Oxide analysis of binders (%) used 3-8

Table 3.2: Coarse aggregate (Granite stone) sieve analysis..... 3-9

Table 3.3: Fine aggregate (Granite crusher sand) sieve analysis 3-11

Table 3.4: Mixture proportions (kg/m3) of the various concretes used..... 3-14

Table 3.5: Summary of concrete cube samples treatment for the different tests ..... ….3-16

Table 3.6: Typical oxygen permeability test analysis 3-28

Table 3.7: Typical water sorptivity test analysis and plots 3-31

Table 3.8: Weight loss in the specimens according to the thermal decomposition from the TG/DTG curves 3-35

Table 3.9: Calcium hydroxide contents in the concrete mixtures..... 3-37

Table 3.10: Calcium oxide (CaO) contents in the concrete mixtures 3-39

Chapter 4

Table 4.1: Average compressive strength test results of the concretes..... 4-2

Table 4.2: Average oxygen permeability test results of the concretes 4-9

Table 4.3 Average water sorptivity test results of the concretes 4-21

Table 4.4 Calcium hydroxide content of the concretes 4-32

Table 4.5: Calcium oxide results of the concretes 4-38

Table 4.6: Regression parameters for the different concrete types exposed indoor 4-52

Table 4.7: Regression parameters for the different concrete types exposed outdoor but sheltered 4-53

Table 4.8: Regression parameters for the different concrete types exposed outdoor but unsheltered 4-54

Table 4.9: Regression parameters for the different concrete types exposed to an accelerated exposure 4-55

Chapter 5

Table 5.1: Description of the response and predictor variables 5-9

Table 5.2: Univariate statistics for the response variable 5-12

Table 5.3: Univariate statistics for the predictor (continuous) variables 5-14

Table 5.4: Bivariate correlation coefficients between the variables 5-22

Table 5.5: Table of association between the variables 5-28

Table 5.6: Predictor variable subsets for the prediction of K_{nat} 5-30

Table 5.7: Dummy variable coding for binder types 5-31

Table 5.8: Dummy variable coding for curing periods 5-31

Table 5.9: Dummy variable coding for exposure conditions 5-31

Table 5.10: Predictor variables subsets for the prediction of K_{nat} 5-33

Table 5.11: Results of the multiple linear regression analysis 5-35

Table 5.12: Estimated model coefficients 5-40

Table 5.13: Model coefficients for binder types……5-45

Table 5.14: Model coefficients for curing durations…..5-45

Table 5.15: Model coefficients for exposure conditions….5-46

Chapter 6

Table 6.1: Mixture design and early-age characterisation parameters of concretes (taken from Ballim, 1994)..... 6-4

Table 6.2: Companion concrete carbonation depth and rates (taken from Ballim, 1994) 6-5

Table 6.3: Comparison of measured depths/rates and predicted rates/depths by the developed models..... 6-7

Table 6.4: Mixture design and early-age characterisation parameters of concretes (taken from Ananmalay, 1996) 6-9

Table 6.5: Corresponding carbonation depth results for concrete made with properties shown in Table 6.4 (taken from Ananmalay, 1996)..... 6-10

Table 6.6: Comparison of calculated rate of carbonation ($K_{nat.}$) for the controlled indoor exposure and predicted rate of carbonation ($K_{pred.}$) by the developed models 6-12

Table 6.7: Predicted rate of carbonation by the developed models for the outdoor exposed conditions..... 6-13

Table 6.8: Comparison of measured depth of carbonation for outdoor exposed concretes and predicted depths of carbonation for outdoor exposed condition by the developed models..... 6-13

Table 6.9: Carbonation depths/rates results for the concrete cores obtained from the bridge structures (taken from Ballim and Lampacher, 1996) 6-16

Table 6.10: Comparison of measured depths of carbonation and predicted depth of carbonation by the developed models..... 6-20

Table 6.11: Concrete characterisation results (taken from Lampacher, 2000) .. 6-22

Table 6.12: Carbonation prediction models for the inland environment taken from Yam (2004); Alexander et al. (2007) 6-25

Chapter 7

Table 7.1: Recommended models for use 7-3

Table 7.2: Model coefficients for curing durations……..7-4

Table 7.3: Model coefficients for exposure conditions……....7-4

Appendices

Table A.1: Individual concrete mass and compressive strength results……..A-1

Table B.1: Oxygen permeability results for site exposed concrete….....A-6

Table B.2: Water sorptivity results for site exposed concrete…….A-8

Table C.1: Annual micro-climate variations within the exposure sites…....…A-10

Table D.1: Natural indoor carbonation depth results for all concrete…...…….A-14

Table D.2: Natural outdoor sheltered carbonation depth results for all concrete……..A-16

Table D.3: Natural outdoor exposed carbonation depth results for all concrete……..A-18

Table D.4: Accelerated carbonation depth results for all concrete……...…….A-20

Table E.1: Table of bivariate correlation….....A-23

Table E.2: Association between the categorical variables……...……A-32

Table E.3 Association between the continuous and categorical variables…... A-33

CHAPTER 1

INTRODUCTION

1.1 Background

The combined use of concrete and steel reinforcement became common practice from the beginning of the twentieth century and led to a widespread use of reinforced concrete in the construction of structures throughout the world. As concrete in itself, from the time of the Romans, had shown a good performance even under aggressive environmental conditions, it was initially assumed that reinforced concrete could also be considered as an intrinsically durable construction material (Bertolini, 2008). However, especially from the second half of the twentieth century, deterioration of reinforced concrete structures became a major problem and structural engineers, asset managers as well as material scientists had to focus on the durability performance and service life of reinforced concrete structures. It appeared that very often durability performance of reinforced concrete structures was limited by the corrosion of the steel reinforcement (Arup, 1983; Bertolini, 2008; Bertolini et al., 2013; Mehta, 1991; Page & Treadaway, 1982; Schiessl, 1988; Thorvaldson, 1952; Tutti, 1982; Valenta, 1968).

The service life of reinforced concrete structures affected by steel reinforcement corrosion is marked by two stages viz initiation and propagation stages which are schematically presented in Figure 1.1. The initiation period corresponds to either chloride penetration and accumulation of chloride ions in the vicinity of the reinforcement or the ingress of carbon dioxide up to the level of the reinforcement. The duration of the initiation period depends on the quality of the concrete, particularly the cover concrete and the environmental exposure condition of the concrete.

The propagation period on the other hand is that period of active reinforcement corrosion and is marked by crack formation, spalling and loss of steel cross-section and bonding with concrete, leading possibly to structural collapse (Bertolini, 2008; Tutti, 1982). The service life of a reinforced concrete structure can be defined with respect to the relevant limit state, which for this study is the initiation limit state and marked by corrosion initiation period. The initiation limit state is defined as the time it takes the aggressive agents (carbon dioxide) to get to the level of the steel reinforcement in sufficient quantity or form to initiate active corrosion. During this time, the structure is also expected to be able to meet its specified durability requirements with an acceptable level of safety (Richardson, 2004).

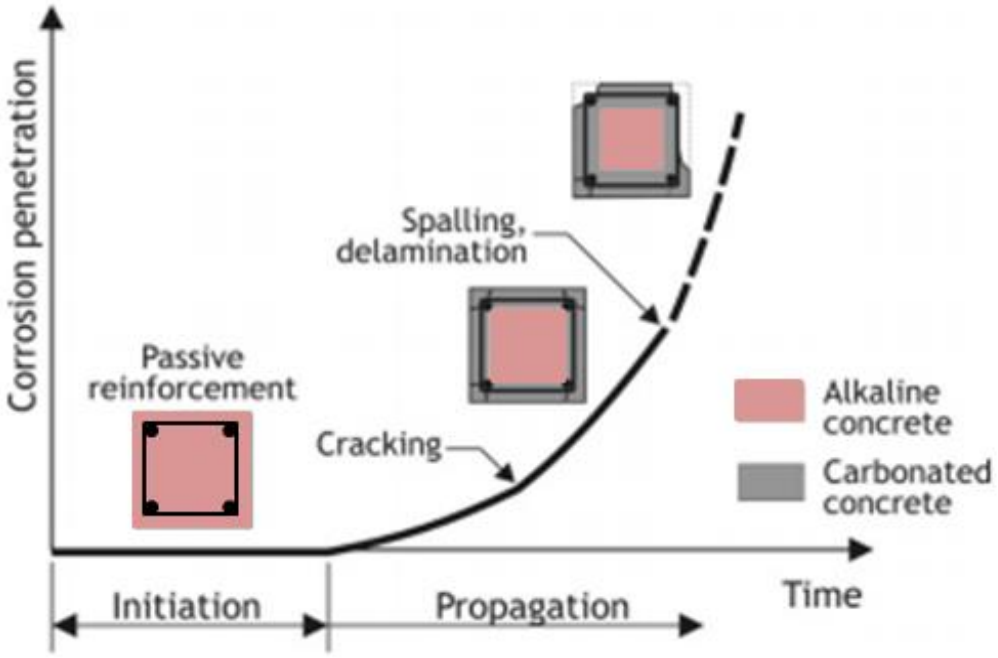


Figure 1.1: Schematic representation of the service life of a reinforced concrete structure affected by reinforcement corrosion (Bertolini, 2008)

Durability performance and service life of reinforced concrete structures situated in the inland environment is often principally affected by the ingress of carbon dioxide. When atmospheric air penetrates reinforced or unreinforced concrete,

carbon dioxide in the air dissolves in the pore water of the concrete to form carbonic acid which then chemically reacts with alkalis (hydroxide) in the cement paste that are produced from the hydration reaction of cement to form carbonate with the release of water. This reaction is commonly referred to as "carbonation" and it moves as a "front" into the concrete as schematically shown in Figure 1.2 (Ballim et al., 2009; Beckett, 1986; Neville, 1981; Roberts, 1981). (A detailed description of the carbonation process can be found in Section 2.4).

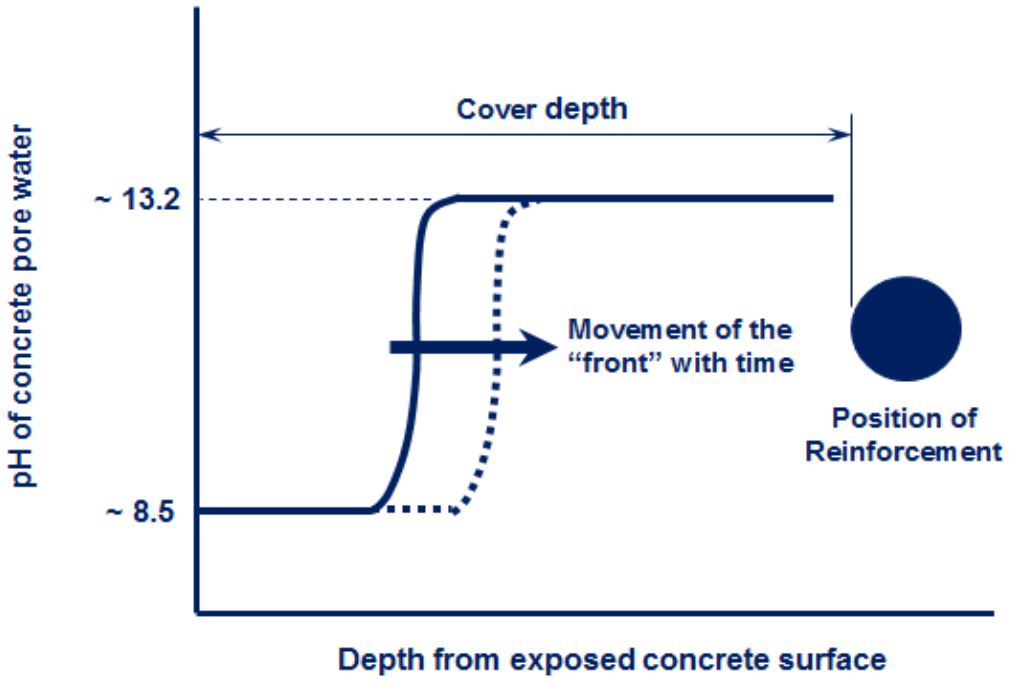


Figure 1.2: pH reduction due to carbonation moving as a "front" from the concrete surface (Ballim et al., 2009)

1.2 Hydration and the Development of Pore Structure and Chemistry

The rate of advance of the carbonation front in concrete depends on the permeability of the concrete and the quantity of the hydroxides, which are, in turn, controlled by the characteristics of the concrete making material and its processing, for example curing and compaction. In addition, carbonation rates also depend on the concrete exposure condition environments (Kobayashi & Uno,

1990; Neville, 1981; Roberts, 1981; Wierig, 1984). While the permeability of concrete depends on many factors among which are the water/binder ratio and processing of the concrete which influences its hydration, the amount of hydroxides (*CH*) available in the concrete depends on the type and content of the binder used. Figure 1.3 shows the effects of water/binder ratio and degree of hydration on the fluid transmissibility of hydrated cement paste as well as its chemistry.

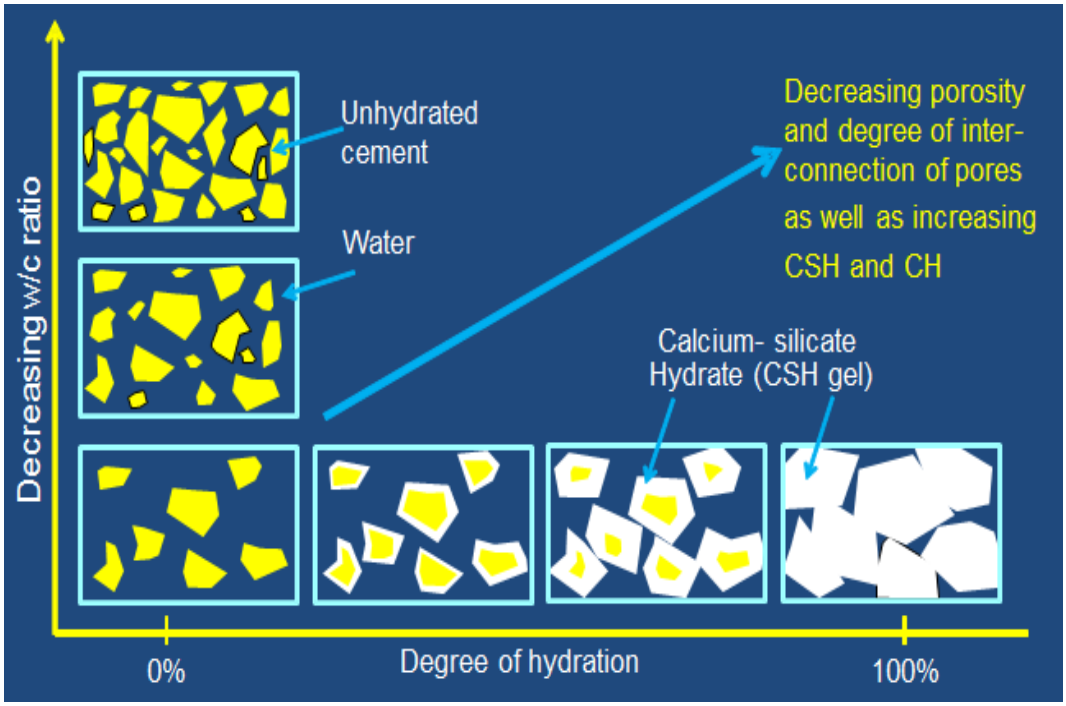


Figure 1.3: Schematic diagram showing the influence of water/cement ratio and degree of hydration on the reduction of capillary pore volume (Gräf & Grube, 1986)

In a hydrated cement paste, mortar or concrete, the size and continuity of the pores at any point during the hydration process would control the permeability of the concrete (Mehta and Monteiro, 1993). The water/binder ratio is indirectly responsible for permeability of the hydrated cement paste because, as indicated in Figure 1.3, this determines first the total space and subsequently the unfilled space after the water is consumed by either cement hydration or evaporation to the

environment (Mehta and Monteiro, 1993). The cement-aggregate interface is similar in composition to the hydrated cement paste; however, this phase presents a zone of high porosity making it the main contributor to the fluid transport properties of concrete.

The hydroxide content in concrete also depends on the water/binder ratio and the degree of hydration; it increases with hydration as noted in Figure 1.3. However, the content of hydroxide in concrete depends more on the binder types used. While the hydroxide content increases with hydration in plain cement, it decreases in the case of blended cement. In either plain or blended cement concrete, hydration reduces the interconnectivity of the pore structure, with the rate of reduction being relatively slow for blended concrete. Generally, the amount of hydroxides and the concrete pore connectivity are functions of the cement hydration reaction which, in its turn, is time and curing dependent. Thus, the rate of carbonation in concrete may reduce as the water/binder ratio reduces and the degree of hydration increases. This issue is more complex and will be more thoroughly discussed in Chapter 2.

1.3 Durability Index Testing and Approach

In South Africa, an approach to improving the durability performance of reinforced concrete construction has been developed. The philosophy involves the understanding that durability will be improved only when measurements of appropriate cover concrete properties can be made. Such measurements must reflect the in-situ properties of concrete, influenced by the dual aspect of material potential and construction quality (Ballim et al., 2009). Designers and constructors can use this approach to optimize the balance between required concrete qualities and cover thickness for a given environment and binder system.

This approach involves a series of tests that measure the fluid transport properties of concrete at a relatively early age, usually 28 days. Additionally, the approach

quantifies the concrete deterioration mechanism, and by relating the mechanism of deterioration to its early-age characteristics parameters, control of concrete quality or predictions of its performance can be achieved. The analysed values obtained from the tests are referred to as Durability Index values.

The durability index approach can be used by designers to predict likely structural responses, from knowledge of environment and material factors. The broad framework of this approach is presented schematically in Figure 1.4 and involves three inter-related aspects (Alexander and Ballim, 1993; Ballim et al., 2009):

- Material indexing, such as permeability, sorptivity, strength etc. in characterizing the concrete. Such quantifiable physical or engineering parameters must be sensitive to the important material and environmental factors such as cement type, water/binder ratio, types and degree of curing etc. The essence of the indexing is to provide a reproducible engineering measure of concrete microstructure and properties of importance to concrete durability;
- Direct durability testing, such as accelerated and long-term evaluations of a range of durability problems. Accelerated testing is necessary since concrete deterioration involves long time periods. On the other hand, long-term testing is important to eliminate the possibility that the chemical and mechanistic effects of accelerated testing do not distort the results so that extrapolation to deterioration rates in normal environment become unrealistic;
- Correlations between the material indexes and direct durability testing results and between these two and actual structural performance are necessary, such that the index tests can be used to either control the quality of concrete during construction or predict the performance of the concrete in the design environment.

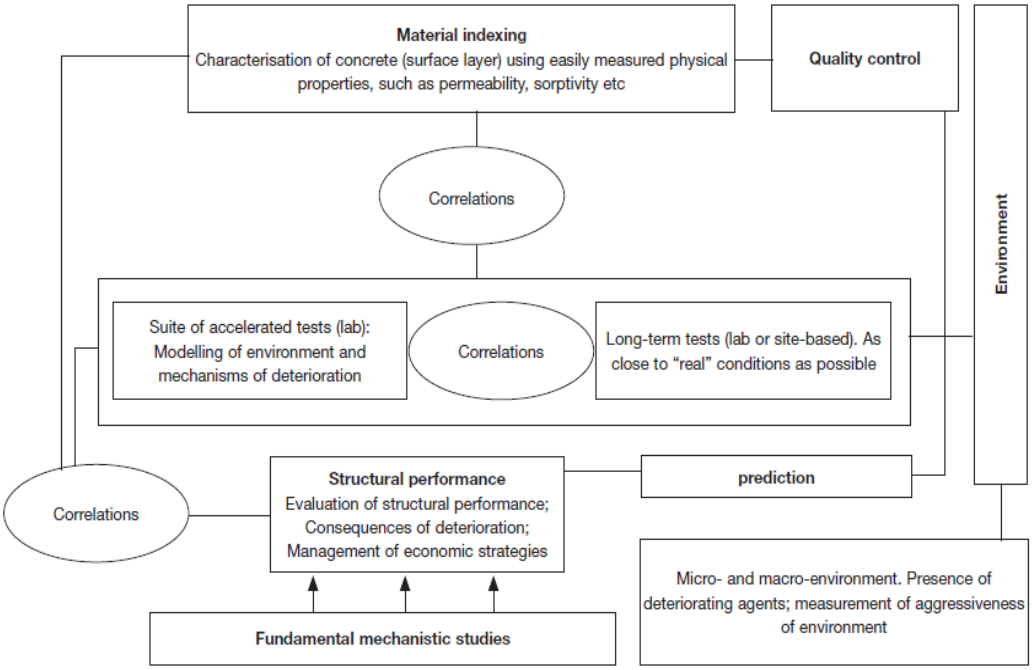


Figure 1.4: Framework for carrying out durability studies (Alexander & Ballim, 1993; Ballim et al., 2009).

1.4 Carbonation Rate in Concrete

The carbonation front advances beyond a particular point when all the carbonatable materials at that point have been converted to carbonates. Thus, the rate of movement of the carbonation front depends on the concrete characteristics as well as the environmental exposure condition and this follows a square-root of time law (Bertolini et al., 2013) (see Section 2.4.1 for derivation). The water released during the carbonation reaction makes the carbonation process self-sustaining but it is limited by the increasing difficulty of the carbon dioxide to penetrate the depth of the concrete (Richardson, 1988). This is because the carbonates produced are deposited in the concrete pores, reducing the permeability by decreasing the pore size and the degree of interconnection between the pores. In addition, carbon dioxide can only move beyond a particular point after all the carbonatable materials at that point have been consumed in the carbonation reaction.

In unreinforced concrete, carbonation has beneficial implications for both strength and durability by the reduction of concrete pore volume and permeability (Neville, 1981). However, in reinforced concrete, carbonation has an important effect in initiating the corrosion of reinforcing steel, therefore reducing the durability performance and service life of reinforced concrete members/elements and structures. As indicated in Figure 1.2, the carbonation reaction process reduces the pH of the concrete pore water from above 13.2 to below 8.5 upon complete carbonation. When this process reaches the reinforcing steel level, the reduced pH causes the passive gamma-ferric oxide layer on the steel to become unstable and the steel is depassivated. Gamma ferric oxide is a thin film of γFe_2O_3 that forms on the surface of steel under an alkaline environment (Hausmann, 1964). If sufficient oxygen and moisture is available, the steel will start corroding with subsequent loss in cross sectional area and bonding with the concrete. Hence, serviceability and load bearing capacity of the reinforced concrete member/element or structure will decrease.

The corrosion of steel is dependent on the electrical potential and pH of the environment in which the steel is placed (Capozucca, 1995). By controlling the potential and or adjusting the pH in the specific domain, it may be possible to prevent corrosion from taking place. Pourbaix devised a compact summary of thermodynamic data in the form of the potential-pH diagram (see Figure 1.5), which relates to the electrochemical and corrosion behavior of any metal in water (Revie & Uhlig, 2008). The Pourbaix diagram has the advantage of showing specific conditions of potential and pH under which steel either does not react or can react to form specific oxides or complex ions. Although the Pourbaix diagram is an essential tool developed for interpreting potential corrosion, predictions must be tested experimentally and validated before being used. Further, since the Pourbaix diagram is based on thermodynamic data, it conveys no information on rates of reaction and provides no measure of how effective any barrier films may be in the presence of specific anions. Similarly, the diagram does not indicate the detailed conditions under which non-stoichiometric metal compound films are possible.

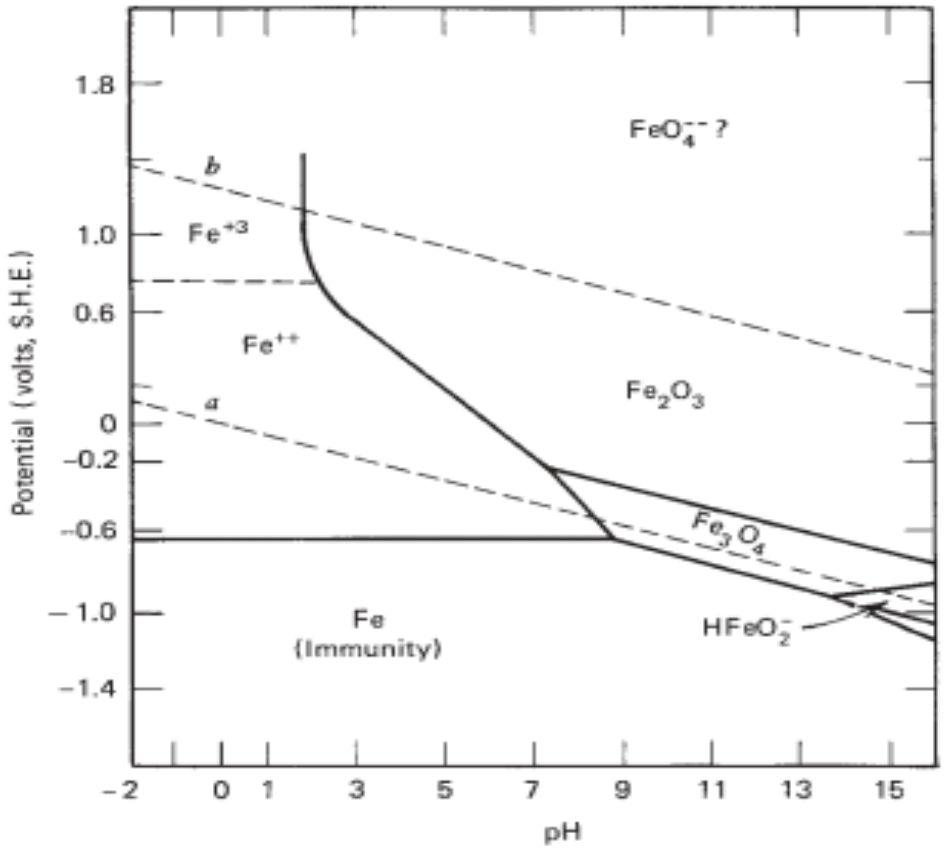


Figure 1.5: Pourbaix diagram for iron-water system at 25°C (Revie & Uhlig, 2008)

Because it can lead to reinforcement corrosion and serious compromise of long-term durability, carbonation of concrete must be considered at the design stage of a proposed reinforced concrete structure as well as during the service life of an existing reinforced concrete structure. To ensure the required service life and durability performance of concrete structures, designers and property owners are expected to have a reliable estimate of the carbonation rate for different binder types used in concrete and for the different inland environmental exposure conditions. This allows the specification of mixture proportions and cover depths for specific binder types and exposure condition for the attainment of the desired service life. Similarly, it is necessary for effective scheduling of maintenance and repair plans for the extension of the residual service life of existing concrete structures.

The problem of concrete carbonation and determining the depth or rate of carbonation has been studied since the late 70's (Arup, 1983; Neville, 1997; Page & Treadaway, 1982; Roberts, 1981; Tutti, 1982). In South Africa, attention was drawn to the problem of concrete carbonation in the early 90's following the increasing incidences of carbonation-induced corrosion damage of concrete structures and hence the need to quantify durability performance and service life of structures in the inland environments (Alexander et al., 2007; Ananmalay, 1996; Ballim, 1994; Ballim & Lampacher, 1996; Bruno, 2010; Lampacher, 2000; Mackechnie & Alexander, 2002; Mackechnie, 1996).

Some of the reasons for attention on concrete carbonation problems are:

- The high cost of maintenance and repair of existing infrastructure;
- The need for improvement in current design specifications for concrete structures since design approaches of the past do not account for the increasing sophistication of modern materials;
- The increasing aggressiveness of the environment due to industrialization and;
- The need to prolong the service life of concrete structures.

Similarly, most of the research on the effect of carbonation on durability performance and service life of concrete structures has been conducted in other regions of the world. The problem with importing these research conclusions to another region is that the materials, concrete and application of concrete technology may be very different for the two regions. Additionally, in developing a relationship between carbonation and durability performance, emphasis needs to be placed on the environmental exposure conditions encountered locally.

Furthermore, changes in the material constituents of concrete and construction methods result in reduced durability (Alexander et al., 2007; Fulton, 1977; Yam, 2004). For instance, the changes in cement characteristics in favour of fast track

construction for economic gains necessitate the increase in fineness of ordinary Portland cement and tricalcium silicate content. This increases the rate of early strength development if such cement is used in making concrete. Similarly, higher w/c ratio concrete will give similar compressive strength as lower w/c ratio concrete at later age, however, the higher w/c ratio concrete will be more porous and permeable even though strength is okay (Fulton, 1977; Rath and Horton, 2001). With the above problems, an improvement in the understanding of the specific deterioration rates and mechanisms common to a particular environment is considered to be crucial component in enhancing the design of future construction. Thus, there is a need for research on the influence of carbonation on concrete made with local materials, under local exposure conditions.

The carbonation process in concrete has been correlated to compressive strength (Atiş, 2003; Sulapha et al., 2003), its chemical composition (Neville, 1981; Parrott, 1994) and possibly concrete mixture design parameters (Uchida & Hamada, 1928; Kishitani, 1960). While most of the published data on concrete carbonation in South Africa links the depth or rate of carbonation to the pore structure of the concrete, little attention is being paid to the chemical composition of the concrete or the mechanism of concrete carbonation. In addition, environmental variations especially at the level of the micro-climate are not addressed directly. Southern Africa has large part of the region characterised by hot, dry conditions with high frequency of bright sunshine periods. For most part, rain periods are almost entirely a summer phenomenon (Ballim, 1994). Consequently, there is a clear need for research in characterising durability for the specific materials and environmental conditions encountered in South Africa.

A need has therefore been recognized for research to be focused towards quantifying the rates of carbonation for different binder types used in concrete, the various inland exposure conditions as well as developing an understanding of the relationship between carbonation and the surface quality of concrete. Past research on the subject has recognized this need and a considerable amount of work has

already been done (see Section 2.4.3). The main findings from this research is that empirical relationships can be established between early-age characterisation parameters of concrete, such as compressive strength, chemical composition or fluid transmissibility, and its rate of carbonation. Such relationships allow a prediction of durability performance and service life of reinforced concrete in an inland environment. However, such relationships cannot be used in regions other than the ones in which it is been developed. Thus, the need for the present study in using the concrete making materials, and processes as well as the micro-climate conditions of the exposure encountered locally in South Africa.

In line with the durability studies presented in Figure 1.4, the present study aims to characterize different concrete types at early-age while companion concrete durability performance (in terms of the depth of carbonation) in the medium-term will be quantified. This quantification will allow the effects of the concrete making materials and processing as well as the inland exposure micro-climates to be evaluated for their effects on concrete durability performance. Based on correlations between the early-age characterisation of concrete and its durability performance in the medium-term, long-term prediction of durability performance and service life of concrete structures exposed to an inland environment can be made.

The principal objective of this research is to develop knowledge of the rate of carbonation of concretes in the inland environment of South Africa, at the micro-climate level, accounting for concrete mixture design and early-age characterization parameters that will enable the reliable prediction of the time to initiation of potential corrosion and therefore, the service life of reinforced concrete structures.

The proposed prediction models are thus intended to provide guidance for:

- Structural engineers and designers, in terms of material proportioning and cover depth determination for proposed reinforced concrete structures in the inland environment as well as service life prediction;
- Property owners and asset managers, for residual service life determination for maintenance and repair scheduling of existing reinforced concrete structures in the inland environment.

In order to determine the characteristics of South African concretes and their durability performance, concretes were made using different binders (100% *CEM* I, 70/30 *CEM I-FA*, 50/50 *CEM I-GGBS*, 90/10 *CEM I-CSF* and 100% *CEM V*) commonly used on construction projects. Processing of the concretes in terms of curing duration and compaction was in line with construction practice in South Africa. This is to ensure that, as far as possible, the concretes tested reflect concrete commonly used on construction projects in South Africa. The concrete thus produced and tested range between low strength grades to high strength grade.

The permeation properties of the concretes were characterised at 28 days after casting using the oxygen permeability and water sorptivity (Durability Index) tests, while its chemical composition was quantified by thermal and wet chemical analysis techniques. Companion concretes exposed to accelerated carbonation at 28 days and different inland environment in South Africa in the medium-term were characterized for their durability performance in terms of carbonation depth using the phenolphthalein test method. The intention was to determine the rate of carbonation for the individual concrete type.

The combined concrete permeation properties, chemical composition and carbonation depth results effectively characterise South African concretes and their durability performance. The results were used to develop empirical models

that account for mixture design and early-age characterisation parameters to predict rates of carbonation.

To test the significance and reliability of the carbonation predictions from the developed models, concrete carbonation rate were obtained from carbonation studies on laboratory cast concrete samples and existing concrete structures exposed to the inland environment of South Africa whose mixture design and/or early-age characterization results were known. These data were analysed and compared to the predicted carbonation results from the developed models in this study. The model results provide a range of carbonation rates that can be expected for South African concretes of the types modeled and under the specific ambient conditions assessed.

In undertaking this research, the following materials, processing and environmental variables were considered:

- Binder types used in preparing the test concretes: *CEM I; CEM I/FA; CEM I/GGBS; CEM I/CSF; CEM V*;
- The same aggregates was used in making all the concretes – granite crusher sand and stone;
- Concrete samples were given varying initial moist curing durations: 3, 7 and 28 days;
- Concrete compressive strength ranges from low strength grades to high strength grades;
- Concrete samples were exposed to an accelerated carbonation condition and three inland exposure conditions: indoor; outdoor sheltered; outdoor exposed.

The thesis has been divided into chapters that are arranged as follows:

- Chapter 2 of this thesis presents a discussion on the hydration reactions of plain and blended cement as well as on the nature of concrete with

emphasis on its physical and chemical nature. A review of the literature on concrete permeation, chemistry, carbonation mechanism and existing carbonation models is also presented in Chapter 2. The Chapter concludes by formulating an approach to modelling the carbonation rate in concrete;

- Details of the laboratory investigation are presented in Chapter 3. The chapter also presents the details of the field studies;
- In Chapter 4, the results and discussion of the laboratory investigation are presented. Also presented in Chapter 4 are the analyses and discussion of the results of the field studies;
- Using the results obtained from the laboratory and field studies presented in Chapter 4, Chapter 5 gives the results of the modelling analysis. The chapter also describes and interprets the variables and outcomes of the developed prediction models;
- The comparison of the depth and rate of carbonation from the developed models to the historically obtained carbonation data from the literature was performed in Chapter 6. The carbonation data used for the comparison were for inland exposure condition concrete;
- A general discussion on important observations and conclusions noted in the preceding chapters are covered in Chapter 7. The chapter also presents the possible areas for future research in the field of concrete durability and deterioration.

Chapter References

Alexander, M. G., Mackechnie, J., & Yam, W. (2007). *Carbonation of concrete bridge structures in three South African localities*. Cement and Concrete Composites, 29(10), 750-759.

Alexander, M. G., & Ballim, Y. (1993). *Experiences with durability testing of concrete: A suggested framework incorporating parameters and results from accelerated durability tests*. 3rd Canadian Symposium on: Cement and Concrete. Ottawa, Canada. pp. 248-263.

Ananmalay, N. (1996). *Characterising the strength and durability performane of South African silica fume concretes*. MSc Dissertation, University of the Witwatersrand, Johannesbourg.

Arup, H. (1983). *The mechanisms of the protection of steel by concrete*. Society of Chemical Industry, pp. 151-157.

Atiş, C. D. (2003). *Accelerated carbonation and testing of concrete made with fly ash*. Construction and Building Materials, 17(3), 147-152.

Ballim, Y. (1994). *Curing and the durability of concrete.* PhD Thesis, University of the Witwatersrand, Johannesbourg.

Ballim, Y., Alexander, M., & Beushausen, H. (2009). *In:Owens G (ed) Fulton's concrete technology*. 9th edn Cement and Concrete Institute, Midrand. pp. 155-188.

Ballim, Y., & Lampacher, B. (1996). *Long-term carbonation of concrete structures in the Johannesburg environment*. Journal-South African Institution of Civil Engineers, 38, 5-9.

Beckett, D. (1986). *Carbonation and its influence on the durability of reinforced concrete buildings*. Construction Repairs and Maintenance, pp14–*16*.

Bertolini, L. (2008). *Steel corrosion and service life of reinforced concrete structures*. Structure and Infrastructure Engineering, 4(2), 123-137.

Bertolini, L., Elsener, B., Pedeferri, P., Redaelli, E., & Polder, R. B. (2013). *Corrosion of steel in concrete: prevention, diagnosis, repair*: Wiley. com.

Bruno, S. (2010). *Modelling the carbonation of concrete usinf early age oxygen permeability index tests.* MSc University of Cape Town, Cape Town.

Capozucca, R. (1995). *Damage to reinforced concrete due to reinforcement corrosion*. Construction and Building Materials, 9(5), 295-303.

Fulton, F.S. (1977). *Concrete technology: a South African handbook.* 5th (Revised Metric) ed. Johannesburg: The Portland Cement Institute.

Gräf, H., & Grube, H. (1986). *Experimental testing method of water and gas permeability of mortar and concrete*: Part 1. Beton, *36*(5), 184-187.

Hausmann, D. (1964). *Electrochemical behavior of steel in concrete*. Journal of the American Concrete Institute, No. 61-10, Vol. 61(Issue No. 2, 1964), Pp. 171-188.

Kishitani, K. (1960). *Consideration on durability of reinforced concrete*. Transactions of the Architectural Institute of Japan. 65: 9-16.

Kobayashi, K., & Uno, Y. (1990). *Influence of alkali on carbonation of concrete, part 2-Influence of alkali in cement on rate of carbonation of concrete*. Cement and Concrete Research, 20(4), 619-622.

Lampacher, B. J. (2000). *Durability of concrete structures.* PhD Thesis, University of the Witwatersrand, Johannessburg.

Mackechnie, J., & Alexander, M. (2002). *Durability predictions using early-age durability index testing.* Paper presented at the Proceedings of the Ninth Durability and Building Materials Conference (Australian Corrosion Association, Brisbane, Australia, 2002).

Mackechnie, J. R. (1996). *Predictions of reinforced concrete durability in the marine environment*. PhD Thesis, University of Cape Town, Cape Town.

Mehta, P. K. (1991). *Durability of concrete--fifty years of progress?* ACI Special Publication, 126.

Neville, A. (1981). *Properties of Concrete (3rd edn.)* Pitman. London, UK.

Neville, A. M. (1997). *Properties of concrete. 4th and final ed*. Harlow, UK: Pearson Education Limited.

Page, C., & Treadaway, K. (1982). *Aspects of the electrochemistry of steel in concrete*.

Parrott, L. J. (1994). *Design for avoiding damage due to carbonation-induced corrosion*, Durability of Concrete- 3rd International Conference, Nice, France 1994, pp.283-298.

Raath B, Horton J. (2001). *Is faster and faster, better and better*. In: Proceedings of Conference on Concrete for the 21st Century: Modern Concrete Progress through Innovation. Concrete Soc. Southern Africa; 2001. p. 13–4

Revie, R. W., & Uhlig, H. H. (2008). *Corrosion and corrosion control: An introduction to corrosion science and engineering. 4th Edition*: Wiley-Interscience, John Wiley & Sons Inc, Hoboken, New Jersey.

Richardson, M. G. (1988). *Carbonation of reinforced concrete: Its causes and management*: Citis.

Richardson, M. G. (2004). *Fundamentals of durable reinforced concrete*: Taylor & Francis.

Roberts, M. H. (1981). *Carbonation of concrete made with dense national aggregates*. Watford, Building Research Establishement., Information Paper IP 6/81.

Schiessl, P. (1988). *Corrosion of Steel in Concrete: Report of the Technical Committee 60 CSC, RILEM* (the International Union of Testing and Research Laboratories for Materials and Structures): Chapman & Hall.

Sulapha, P., Wong, S., Wee, T., & Swaddiwudhipong, S. (2003). *Carbonation of concrete containing mineral admixtures*. Journal of materials in civil engineering, 15(2), 134-143.

Thorvaldson, T. (1952). *Chemical aspects of the durability of cement products.* Paper presented at the Proceedings of the 3rd Intern. Symp. Chem. Cem.

Tutti, K. (1982). *Corrosion of steel in concrete*. Swedish Cement and Concrete Institute: CIB, Research Report.

Uchida, S. & Hamada, M. (1928). *Durability tests of steel and concrete*. Journal of Architecture and Building Science. 516: 1-18.

Valenta, O. (1968). *Durability of concrete.* Paper presented at the Proceedings of the 5th International Congress on the Chemistry of Cement.

Wierig, H. (1984). *Longtime studies on the carbonation of concrete under normal outdoor exposure.* Proceedings of the RILEM, Hannover University, 239-249.

Yam, W.K. (2004). *Carbonation of concrete bridge structures in three South African localities.* MSc (Eng.) Thesis. University of Cape Town, Cape Town.

CHAPTER 2

LITERATURE REVIEW

2.1 Introduction

The literature reviewed has been organized into four sections and is presented in this order:

- Brief discussion on the hydration reactions of plain and blended Portland cement.
- Detailed discussion on the nature of concrete with emphasis on the physical and chemical properties of its binder phase and its effect on concrete durability. The fluid transport properties and the chemical composition of concrete as well as the various techniques for their quantification are also included here.
- The mechanism of carbonation in concrete, its measurement and the derivation of the carbonation progression equation. Included in the section are factors that influence the carbonation process in concrete.
- The reviews of existing models for the prediction of the carbonation progression in concrete as well as the approach used in the formulation of the proposed prediction models for carbonation rate in concrete.

2.2 Hydration Reactions

2.2.1 Hydration reactions of plain cement

In the presence of water the silicates and aluminates in plain cement form products of hydration calcium silicate hydrate (*C-S-H*), calcium hydroxide (*CH*) and calcium sulphoaluminate (*C-A-S-H*). Figure 2.1, taken from Mehta and Monteiro (1993), shows a schematic of the hydration process and structure development in cement paste. As hydration continues, the system of water-filled interconnected pores becomes partially filled with hydration products, reducing

the inter-connectivity of the pore structure. Incomplete hydration resulting from inadequate curing however leaves the surface zone more permeable and vulnerable to attack from external influence, thus leading to reduced durability performance and service life of concrete incorporating such cement paste.

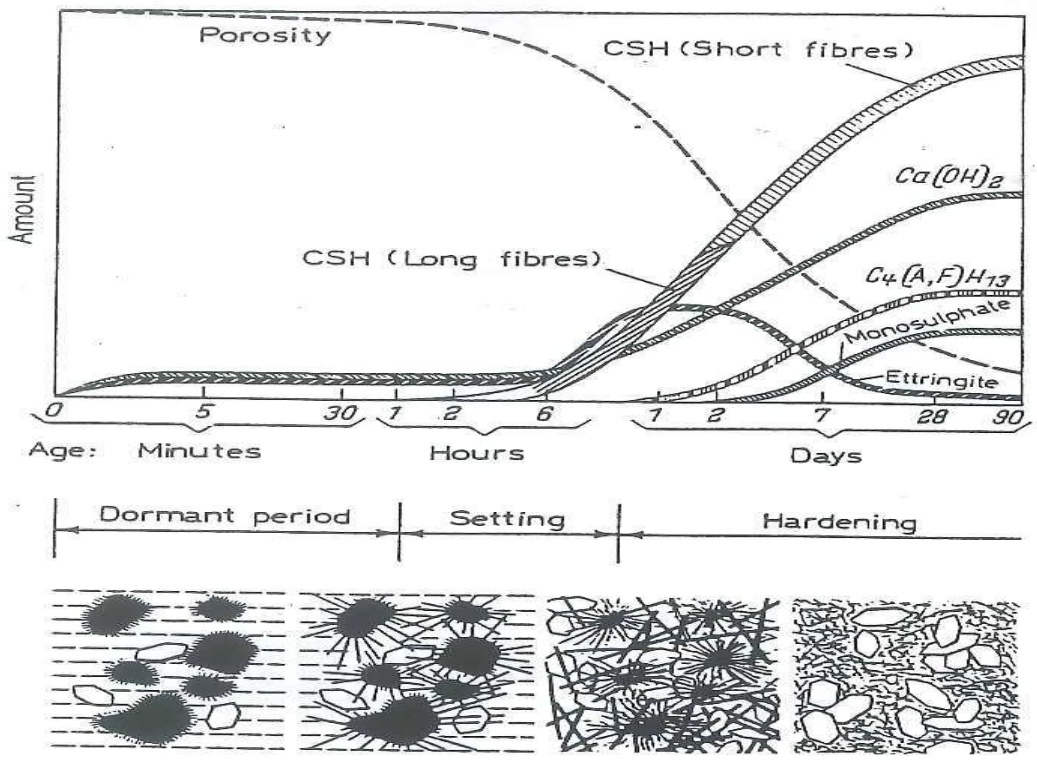


Figure 2.1: Schematic of the hydration and structures development in cement paste (Mehta & Monteiro, 1993)

In idealised form, the cement hydration reactions can be written as (Bertolini et al., 2013; Mehta & Monteiro, 1993):

Silicates

$$C_3S + 6H \rightarrow C_3S_2H_3 + 3CH \quad 2.1$$

$$C_2S + 4H \rightarrow C_3S_2H_3 + CH \quad 2.2$$

Aluminates

$C_3A + 3CSH_2 + 25H \rightarrow C_3A.3CS.31H$ (Ettringite) 2.3

$C_3A + CSH_2 + 10H \rightarrow C_3A.CS.12H$ (Monosulphate) 2.4

2.2.2 Hydration reactions of blended cement

Blended cements are obtained by inter-grinding or blending plain cement with supplementary cementitious materials (*SCM*). Among these, blended cement with the addition of fly ash (*FA*) and condensed silica fume (*CSF*) which are pozzolanic in nature and ground granulated blast furnace slag (*GGBS*) which is a latent hydraulic material are of particular interest with regards to durability performance in the present study. *SCM* like *FA* and *CSF*, that are pozzolanic in nature are mainly glassy siliceous materials that may contain aluminous compounds but have low calcium content. In themselves they do not have binding properties, but acquire them in the presence of *CH*, giving rise to hydration products similar to those of plain cement. While *SCM* like *GGBS*, which is a latent hydraulic material differs from the rest of the *SCM* in that it forms product of hydration on its own similar to plain cement when mixed with water. However, the reactions are very slow because the amount of *CH* released by *GGBS* in the reaction is too low to allow a rapid dissolution of the glass phase. Thus, *GGBS* often uses the *CH* from cement to go into reaction. The reaction between *SCM*, *CH* and water is known as pozzolanic reaction (Bertolini et al., 2013). In simplified form, the pozzolanic reaction can be written as:

$SCM + CH + water \rightarrow C - S - H$ 2.5

The hydration characteristics of blended cement differ from those of plain cement. The hydration of blended cement consumes *CH* and thus reduces its amount in relation to a cement paste obtained with plain cement. The microstructure of blended cement and blended cement concrete also differs. In blended cement very fine products of hydration will be observed leading to a refinement of the pore

structure (Bertolini et al., 2013). Consequently, an increase in the resistance to penetration of aggressive agents can be obtained for blended concretes. However, the hydration reactions of blended cement are slower than those of plain cement. Therefore, this beneficial effect will be achieved only if the early-age wet curing of the concrete is long enough. In addition, since pozzolanic reaction consumes *CH*, the alkaline content of the paste in concrete is reduced. This is of fundamental importance to the carbonation of concrete, since the permeability of concrete and its chemical interaction determines the ease with which aggressive elements may enter the concrete and reduce its durability performance (Addis, 1986). As will be discussed later, the properties of concrete are largely the properties of its paste content. The long-term durability of the material depends on the structure and composition of the paste.

2.3 Nature of Concrete

Concrete is a composite material made of aggregate and the reaction products of the cement and mixing water (i.e. the porous cement paste). This makes concrete a multi-phase material comprising a binder, filler and interfacial transition zone as represented in Figure 2.2, taken from Mehta and Monteiro (1993). Discussion on the different phases in concrete is given below:

1. A binder phase known as hardened cement paste (*hcp*) is made up of a solid phase (calcium silicate hydrates - *CSH*, calcium hydroxide - *CH*, calcium sulphoaluminate - *CA$\underline{S}$H* and unhydrated clinker grains); voids (interlayer space in *C-S-H*, capillary voids and air voids); and a water phase (capillary water, adsorbed water, interlayer water and chemically combined water);

2. A filler phase, commonly consist of aggregates – coarse and fine, comprising mainly gravel and fine sand fractions of naturally weathered or crushed rock materials;

3. The last phase in concrete is called the Interfacial Transition Zone (*ITZ*). The *ITZ* is the space between the bulk cement paste and aggregates (see Figure 2.2). The *ITZ* is composed of the same elements as the hcp but its microstructure and

properties are different and it is weaker than the binder and filler phases. Hence the *ITZ* exercises a far greater influence on the mechanical and durability behaviour of concrete.

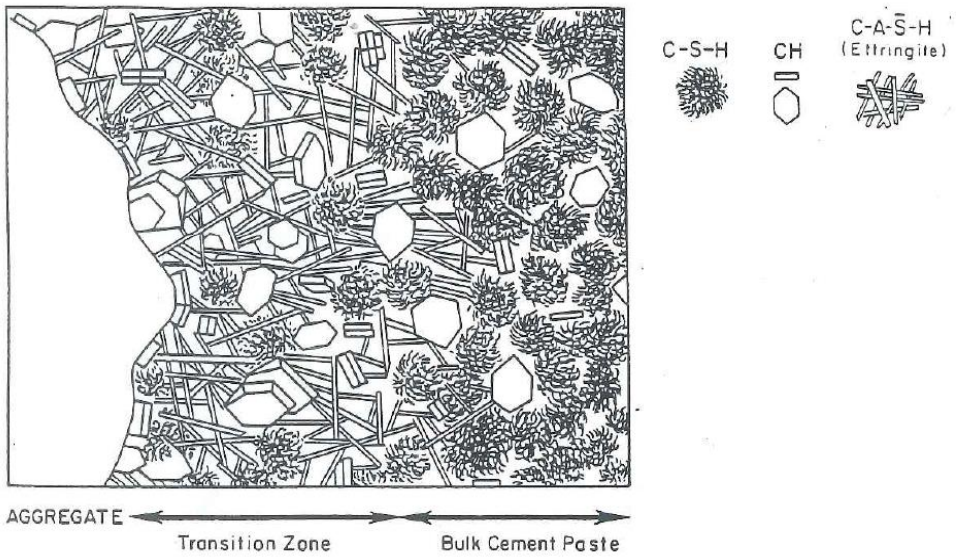


Figure 2.2: Representation of the transition zone and bulk cement paste in concrete (Mehta & Monteiro, 1993)

The deterioration of concrete and its long-term durability performance is dependent on the structure and composition of the hcp and *ITZ*. Similarly, the ability of concrete to protect embedded steel and withstand various types of degradation mechanisms depend also on the structures and compositions of the hcp and the *ITZ*. These phases in concrete also determine the concrete fluid transport and chemical properties (Mehta, 1988). Thus, the formation of *hcp* and *ITZ* in concrete, its structure and composition will be considered in more detail.

2.3.1 Physical and chemical nature of concrete

Concrete resists aggressive environments by its physical and chemical resistance which is derived from its dense microstructure and complex pore system as well as from its chemical interaction. The structure of the *hcp* and *ITZ* determines

concrete pore structure while their composition influences its chemistry. The durability performance of concrete therefore depends on the structure and composition of the hcp and *ITZ*. This is in turn influenced by the fluid transport properties of the hardened concrete and the chemical interaction between the constituents of the hcp and the aggressive agents.

For instance, carbonation of reinforced concrete is responsible for the depassivation of reinforcing steel. The rate of advance of carbon dioxide (CO_2) into concrete is determined by both the ease of access for CO_2 (fluid transport properties) as well as the ability of the elements of the *hcp* (and *ITZ*) to bind CO_2 (chemical interaction), thereby making the CO_2 increasingly unavailable for depassivating the steel. The concrete chemical composition is influenced by the solid phase of the hcp and *ITZ*. While the structure of the *hcp* and *ITZ* especially its voids and water phases, dictates the pore structure hence the fluid transport properties of concrete. The aggregate phase in concrete acts as filler and is responsible for the unit weight, elastic modulus and dimensional stability of the concrete. This phase has no direct contribution to the chemical properties of concrete. The discussion below focuses on both these aspects (fluid transport properties and chemical interaction) in considering the influence of the structures and composition of the hcp and *ITZ* on the durability performance and service life of concrete.

The hydrated cement paste (hcp)

Figure 2.3 as presented by Mehta and Monteiro (1993) shows a schematic outline of the microstructural development in Portland cement paste. The end product of the developmental stage at 28 or 90 days is a reduced content of the unhydrated cement clinker and the water-filled capillary pores if properly cured. The largest volume of the hydration product in the hcp are *C-S-H, CH* and *C-A-S̲-H* which have the greater influence on the physical and chemical nature of concrete (Mehta & Monteiro, 1993).

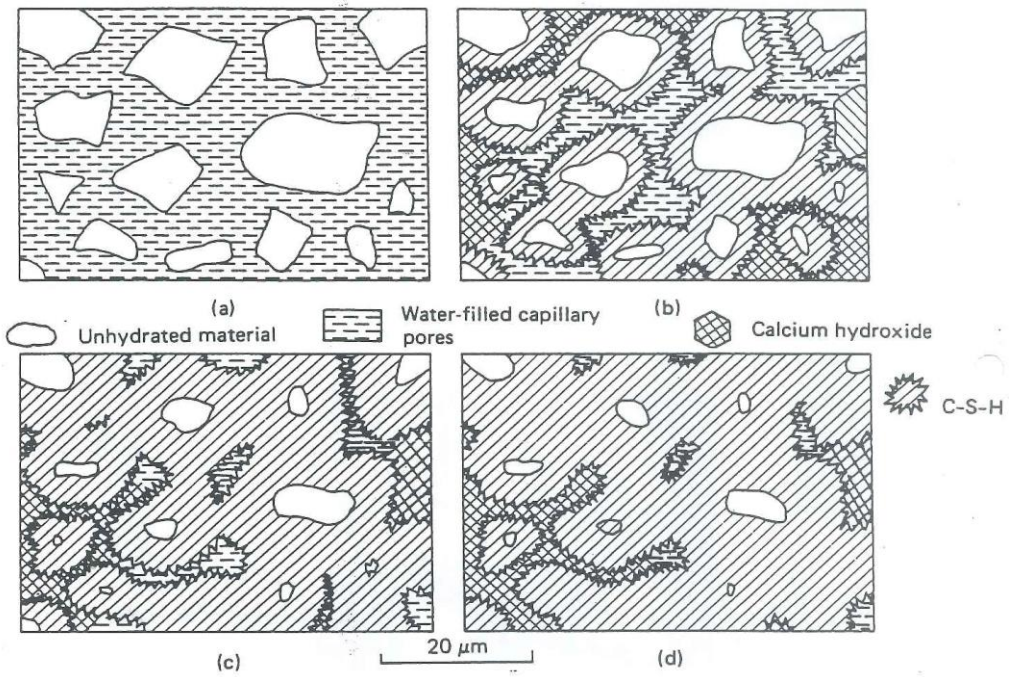


Figure 2.3: Schematic outline of microstructural development in Portland cement paste (*C-A-S-H* are included as part of *C-S-H* for convenience, although they will crystallize as separate phases). The approximate times indicated are: (a) Initial mix; (b) 7 days; (c) 28 days; (d) 90 days (Mehta and Monteiro, 1993)

The larger part of this discussion is drawn from the work of Mehta and Monteiro (1993). The *C-S-H* makes up 50-60% of the solid *hcp* and has no defined stoichiometry but determines the phase property of the paste. While the *CH* phase of the solid constitutes 20-25% has a definite stoichiometry, and its strength contributing potential is limited. The *CH* crystals possess less adhesion capacity because of the lower surface area and correspondingly weak Van der Waal forces of attraction. The other solid product is the *C-A-S-H* which occupies 15-20% of the solid and plays minor role in the behaviour of concrete microstructure. The last phase is the inner cores of unhydrated clinker grains that exist in the microstructure of the *hcp* long after hydration. The percentage of unhydrated clinker depends on the cement particle size distribution and its degree of hydration. This phase of the *hcp* dictates on the chemical composition of the concrete and hence its chemical interaction with aggressive agents.

Concrete with a well hydrated cement paste is composed of insoluble hydrates of calcium (*C-S-H, CH* and *C-A-S-H*) that exist in a state of stable equilibrium with high-pH pore fluid. Depending on the concentration of Na^+, K^+ and OH^- ions the pH value ranges from 12.5 to 13.5. The chemical composition of *C-S-H* is not well defined since the ratios between the oxides vary with the degree of hydration, w/c ratio and temperature (Mehta & Monteiro, 1993). However, *C-S-H* contributes to strength and it is volumetrically and chemically stable in non-aggressive environment. The hexagonal crystal of *CH* derived from the hydration of calcium silicate is a constituent part of the hcp and has dimensions of the order of a few μm.

CH as well as *NaOH* and *KOH* that are present in small amounts, are very important with regards to protecting the reinforcement because they cause an alkaline pH up to 13.5 in the pore liquid. In addition they also stabilize the *C-S-H*, the main binding agent of cement (Czernin, 1980; Moskvin, 1983). *C-A-S-H* presents a minor influence to the chemical properties of the concrete. The maintenance of the pH level in the pore fluid of concrete is important to the long-term durability of concrete. In blended concretes, the quantity of *CH* is low due to its consumption in the pozzolanic reaction (see Equation 2.5) and the dilution of clincker cement in the concrete. The chemical composition of concrete in terms of its *CH* content is important to steel reinforcement embedded in concrete. Since the alkaline content in concrete protects the steel by passivation as well as buffering the ingress of CO_2 by going into reaction in the presence of water.

The *hcp* also consists of a void phase that represents the pore structure of the concrete. This phase plays major role in the physical properties of the *hcp* and hence the physical properties of the concrete in terms of its fluid transport. The different types of voids in the *hcp* are the interlayer pores in *C-S-H* (gel pores), capillary voids, entrained air voids and the entrapped air bubbles. Mehta and Monteiro (1993) prepared the schematic diagram shown in Figure 2.4, giving range of pore sizes for the different pore types.

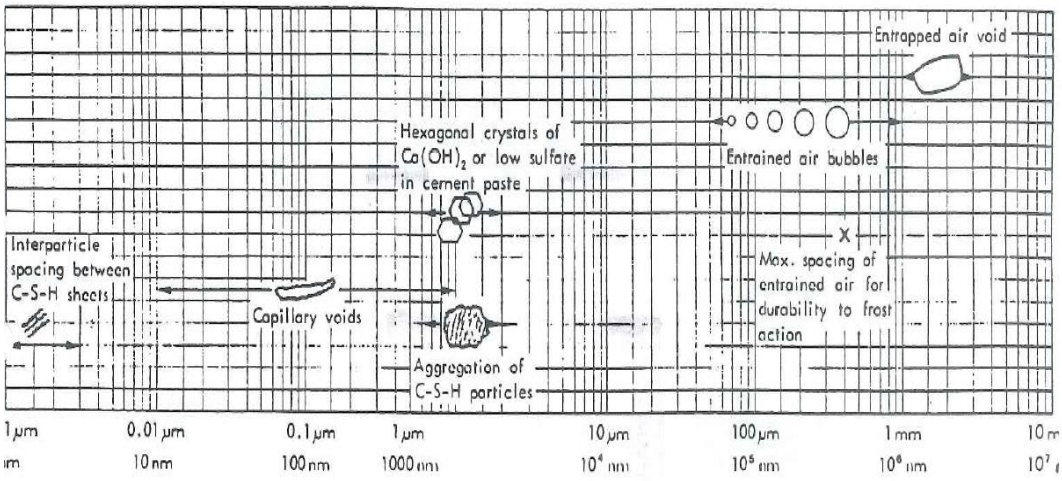


Figure 2.4: Dimensional ranges of solids and pores in a hydrated cement paste (Mehta & Monteiro, 1993)

The interlayer pores in *C-S-H* have widths of approximately 18Å in-between gel particles and account for about 28% of the porosity in the *C-S-H* phase as observed by Powers (Powers, 1958). Power's observation is however in contrast to Feldman and Sereda (1968) observation. Feldman and Sereda suggested that the pores in the interlayer of the *C-S-H* vary from 5Å - 25Å. Voids in the interlayer pores in *C-S-H* have no effect on the strength and permeation of the *hcp* but do contribute to the *hcp* drying shrinkage and creep. Ions and gas molecules which are aggressive to concrete are smaller than the size of typical gel pores. Thus, this void size range has no direct effect on the durability performance of the concrete.

The capillary voids are the spaces not filled by the solid compound of the hardened paste, which is space not taken up by the cement or the hydration product. The capillary voids are irregular in shape and influences strength and permeability of the *hcp* when larger than 50 nm and are often referred to as macro pores (see Figure 2.5). The entrapped air voids and incomplete compaction voids have sizes greater than 1 mm and are created unintentionally. These voids are also irregular in shape and arise as a result of air trapped in the cement paste during

concrete mixing. The entrapped air voids and compaction voids have substantial effects on concrete fluid transport property hence its degradation.

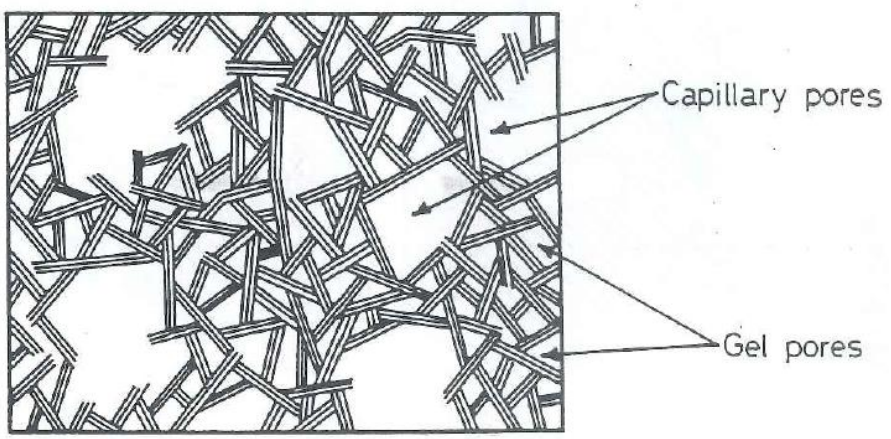


Figure 2.5: Schematic description of the structure of cement gel (Fernandez et al., 2004)

The third component of the *hcp* is water contained in the voids that exists as capillary, adsorbed, interlayer and chemically combined waters (see Figure 2.6 after Feldman and Sereda (1968)). The capillary water is present in voids that are larger than 50Å while the adsorbed water is water adsorbed onto the solid surface in the *hcp* by the influence of attractive forces. The removal or loss of the adsorbed water may cause shrinkage of the *hcp*. The interlayer water is the water that is associated with *C-S-H* structure and is held by hydrogen bonding. This form of water can be lost only on strong drying and when this happens the *C-S-H* structure shrinks considerably. Chemically combined water is water that is an integral part of the microstructure of various cement hydration products. This water is not lost on normal drying, and is only released when the hydrates decompose on heating. This phase of the *hcp* also influence its permeation properties and hence that of the concrete.

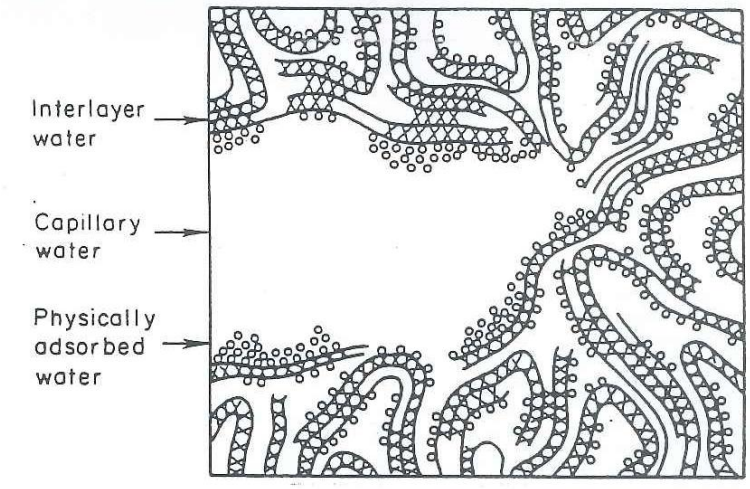


Figure 2.6: Types of water associated with the calcium silicate hydrate (Feldman and Sereda, 1968)

The Interfacial Transition Zone (ITZ)

The *ITZ* phase of the concrete represent a small region next to the particles of coarse aggregate and it is composed of the same elements as the *hcp* (see Figure 2.2). However, its microstructure and properties are different from those of the *hcp*. The *ITZ*, although similar to the *hcp* in terms of its components, is different in terms of morphology, composition and density (Mindess & Young, 1981). Thus, this phase present a zone of particularly high porosity (hence fluid transport) in concretes than does the *hcp*. This phase exist as a thin shell typically 10-15 um thick around large aggregate and is generally weaker than the aggregate and bulk *hcp* (Mehta & Monteiro, 1993).

One of the reasons for the weaker microstructure of the *ITZ* is that, the water film that forms around large aggregate particles in the fresh concrete increases the *ITZ* w/c ratio and thus bleeding (Mindess & Young, 1981). Similarly, the dissolution of calcium sulphate and calcium aluminate compounds produced calcium, sulphate, hydroxyl and aluminate ions which combined to form *C-A-S-H* and *CH*. The higher w/c ratio in the vicinity of the coarse aggregate allows space for the crystalline products of *C-A-S-H* and *CH* to grow in the *ITZ* producing a relatively

larger crystal. This forms a more porous framework in the *ITZ* than in the bulk *hcp*.

The density and hence strength of the *ITZ* is however improved by the progress of hydration since the poorly crystalline *C-S-H* and a second generation of smaller crystals of *C-A-S-H* and *CH* start filling the empty space that exist between the framework created by the larger *C-A-S-H* and *CH* crystals (Mehta & Monteiro, 1993). During stress-induced cracking, the *C-A-S-H* and *CH* crystals serve as preferred cleavage sites owing to their tendency to form an oriented structure. The *ITZ* is therefore the main contributor to the fluid transport properties of concrete and hence the rate of concrete deterioration.

2.3.2 The influence of nature of concrete on its durability performance

The rate of carbonation in concrete and thus its durability performance is controlled by the proportion of the binder phase (*hcp* and *ITZ*), as well as its properties. The properties of the binder phase in concrete depend on its microstructure (i.e. the type, amount and distribution of solids and voids in the *hcp* and *ITZ*). The size and continuity of the pores in the *hcp* and *ITZ* in concrete would determine its fluid transport properties and this is closely related to the capillary porosity and the solid-space ratio. The capillary pores and its degree of interconnectivity as well as the entrapped air influences the pore structure of the concrete. While the composition of the solid phase in the *hcp* and *ITZ* determine the concrete chemical interaction. In determining the resistance to degradation of concrete, not only should the total capillary porosity, size and interconnectivity of the capillary pores be considered, but also the composition of the *CSH* and *CH* that exist in the *hcp* and *ITZ*.

The microstructure of concrete can be seen on three different scales. In increasing level of scale we have the microstructures of the *hcp*, mortar and then concrete. This scale is attributed to the decreasing *hcp* content and increasing *ITZ* volume,

thereby making the fluid transport properties increasing with the scale. Most deterioration mechanisms involve the movement of gases or liquids into or out of the pore structure of concrete. Thus, the fluid transport properties of a concrete are an important determinant of its ability to resist deterioration (Mehta, 1993).

The durability performance of a concrete exposed to a given aggressive environment is also influenced by the chemical interaction between the constituents of the *hcp/ITZ* and the aggressive agent. The chemical composition of concrete which is derived from the thermodynamic stability of its hydrates, determines the resistance to aggressive agents from the environment. Similarly, the nature of the interaction of the paste component of the concrete with the aggressive agents also contributes to resistance of the concrete. Because of its strong alkaline character, *hcp* (and therefore, concrete) is easily deteriorated in an acidic environment, or a pH- reducing environment – which then de-stabilises the hydrates. In determining the resistance to degradation of concrete and its role in protecting the embedded steel reinforcement, the quantity of the hydrates is also very important. The composition of the *hcp* influences the concrete chemistry and is responsible for the chemical protection of the embedded steel reinforcement.

It has been established that the perviousness of concrete as well as its chemical composition plays an important role in the control of concrete durability (Hilsdorf, 1989). Accordingly, testing of transport parameters for concrete, such as permeability, absorption or diffusivity behaviour in most cases has been done on the basis of durability consideration. Similarly, the control of concrete durability especially chloride diffusion and carbonation is also affected by binder chemistry of concrete (Dhir, et al., 1999; Parrott, 1994). In the following sections these transport mechanisms and chemical composition that are normally associated with the ingress of deleterious materials into concrete are discussed. Also presented are the different means for their measurement and quantification.

2.3.3 Fluid transport properties of concrete and its measurement

The transport properties of concrete are important to predicting their durability, since deterioration mechanisms are all related to the ease with which a fluid or ion can move through the concrete microstructure (Mehta, 1988). The fluid transport property of concrete is predominantly influenced by the structure of the *hcp*, especially at the interface (*ITZ*) with aggregate particles. The passage of potentially aggressive species is primarily influenced by the penetrability of the concrete. Concrete penetrability is broadly defined as the extent to which the concrete permits gases, liquids or ionic species to move through its pore structure. It normally embraces the concepts of permeation, sorption, diffusion and migration and is quantified in terms of the transport parameters (Alexander & Mindess, 2005).

The processes involved in fluid and ion movement include flow under pressure, distinct mechanisms of capillary action and flow under a concentration gradient. These mechanisms are characterised by the material properties of permeability, sorptivity, and diffusivity respectively (Richardson, 2002). There are a number of mechanism by which fluids move through the pore structure of concrete and the laws governing these movements are equally varied. Definitions of some of the terms related to fluid transport in concrete are presented below.

Permeation

This describes the movement of fluids through concrete pore structure under an externally applied pressure head whilst the pores are saturated with that fluid. Permeability is a measure of the capacity of concrete to transfer fluids by permeation. Permeability refers to saturated flows caused by an applied pressure differential with the flow velocity (V) given by Darcy's law:

$$V = -K\frac{dh}{dL} \qquad 2.6$$

Where,

K = coefficient of permeability

dh/dL = hydraulic gradient

If the flow velocity is expressed in terms of the pressure differential, Equation 2.7 is applicable.

$$V = -\frac{k}{\mu}\frac{dp}{dL} \qquad 2.7$$

Where,

k = intrinsic permeability coefficient of the material

μ = fluid viscosity

dp/dL = pressure differential

The intrinsic permeability coefficient is dependent on material characteristics, making it a useful method of expressing the permeation characteristics of concrete. Equation 2.8 can then be used to relate the intrinsic permeability coefficient to the Darcy coefficient of permeability.

$$k = \frac{K\mu}{\rho g} \qquad 2.8$$

Where,

g = acceleration due to gravity (m/s^2)

ρ = density

The permeation of concrete is dependent on the pore structure of concrete, the characteristic of the permeating fluid and the applied pressure differential.

Absorption

This is the process whereby fluid is drawn into the concrete to fill the unsaturated pores under the action of capillary forces. It is generally quantified by monitoring

the increase in mass as the liquid penetrates the pore structure. The capillary potential is dependent on the geometry of the pores and the saturation level of the concrete. Water absorption caused by wetting and drying action at the concrete surface is the dominant fluid transport mechanism in the outer skin of the concrete for most inland structures in an exposed condition. Absorption leads to high surface concentrations and steep gradients, thus driving moisture inward, thereby increasing the carbonation process.

The rate of movement of a wetting front through a porous material (e.g. concrete) under the action of capillary suction is called sorptivity. Using the one dimensional case of water absorption with defined boundary conditions, it is possible to define sorptivity in terms of the extended Darcy equation as shown in Equation 2.9.

$$q = -K(\theta)\frac{dY}{dX} \qquad 2.9$$

Where,

q = flow velocity

K = hydraulic conductivity

θ = water content

dy/dx = capillary potential

The cumulative water absorption per unit area i, is dependent on the square root of time and may be expressed as shown in Equation 2.10 (Alexander et al., 1999).

$$i = St^{1/2} \qquad 2.10$$

Where,

i = depth of infiltration

S = sorptivity of the material

t = elapsed time

Sorptivity is related to the hydraulic gradient and capillary potential gradient, and may be used to define the absorption ability of concrete. While the hydraulic diffusivity may be considered the fundamental water absorption property of porous materials, its determination is complicated. Sorptivity on the other hand is relatively simple to determine and is directly related to the hydraulic diffusivity. Extensive experimental work has confirmed the theoretical basis for sorptivity and sorptivity tests have gained popularity due to their simplicity and accuracy (Ballim, 1994; Gummerson et al., 1980; Hooton et al., 1993; Kelham, 1988).

Sorptivity is affected by internal influences such as initial water content and microstructural configuration and external factors such as temperature, transmission fluid and sample geometry. Water absorption is also affected by the orientation of the material as the flow is influenced by capillary and gravity driven forces (Gummerson et al., 1980). However, most researchers argue that gravity effects are very small in relation to capillary suction.

Diffusion

This is the process by which liquids, gases or ions are transported through the pore structure of concrete under the action of a concentration gradient. Diffusion occurs in partially or fully saturated concrete and is an important internal transport mechanism for most concrete structures exposed to salts. Rates of diffusion are dependent on temperature, moisture content of concrete, type of diffusant and the inherent diffusibility of the material. The process of diffusion is described by Fick's first law for steady state diffusion. This law, stated in Equation 2.11 may be used to describe the rate of diffusion of a gas/ion into a uniformly permeable material (Ballim et al., 2009; Richardson, 2002).

$$J = -D_{eff}\frac{d_c}{d_x} \qquad 2.11$$

Where,

J = mass transport rate (g/m^{2}s)

D_{eff} = effective diffusion coefficient (m^2/s)

dC/dx = concentration gradient (g/m^3m)

C = concentration of fluid (g/m^3)

x = distance (m)

The negative prefix denotes that the flux occurs along a declining concentration gradient. Diffusion does not constitute a major transport mechanism in inland concrete where the main deterioration mechanism is carbonation, but diffusion tests provide useful information with regard to durability of concrete structure fully submerged in sea water or salt-contaminated soil. Diffusion occurs in partially and fully saturated concrete and is the dominant transport mechanism for most marine structure. In the marine environment, diffusion of chloride ions is of particular importance due to the depassivating effect of chlorides on embedded steel, which ultimately may lead to corrosion. The modelling of ionic diffusion in concrete is done using modifications of Fick's second law of diffusion (for non-steady state diffusion).

The major driving mechanism in the carbonation of concrete is diffusion of CO_2, which is dependent on the diffusivity of the concrete. Fick's law of diffusion has been used to describe the depth of carbonation and hence the basis of the majority of carbonation prediction models. However, measuring diffusion is usually a difficult process at the same time there are techniques available that can measure permeability of concrete on site and in the laboratory. Permeability tests provide useful information with regard to durability and are particularly sensitive to changes in the pore fraction (Därr & Ludwig, 1973).

It is of importance to this research as the South African Durability Index test will be used to quantify the pore structure of concrete at early ages and will be used as a proxy for characterising the diffusion process in concrete as well as the pore volume and connectivity. The South African Durability Index (*DI*) approach is

based on a suite of three tests that characterise the penetrability of concrete by quantifying the rate of transport of different fluids through it. The *DI* tests characterise the potential durability of concrete according to the transport mechanism of oxygen permeability for permeation, water sorptivity for absorption and chloride conductivity for diffusion (Alexander et al., 1999; Ballim, 1994).

The *DI* tests have also been shown to be sensitive to those material, constructional, and environmental factors that influence durability and they provide reproducible engineering measures of the microstructure of concrete (Alexander et al., 2001; Ballim, 1994; Gouws et al., 2001; Mackechnie & Alexander, 2002; Mackechnie, 1996). The tests characterise the quality of concrete as affected by choice of material and mix proportions, placing, compaction and curing techniques and environment. Test equipment and procedures are described in detail in the literature (Alexander et al., 1999). However, only the basic principles for the oxygen permeability and water sorptivity tests will be discussed, as they are relevant to concrete deterioration due to carbonation, which is the main focus of this study.

The results obtained from the South Africa oxygen permeability test are comparable to other test methods in the measurement of the microstructure of concrete. In a comparative international study of various test methods for durability indicators, the oxygen permeability test was found to be able to detect differences in w/b ratio, binder type, and curing condition on a highly significant statistical level (Beushausen & Alexander, 2008; Romer, 2005; Torrent & Fernández, 2007). The same study revealed that results obtained with the South Africa oxygen permeability test equipment correlate well with other existing test methods for oxygen permeability, such as the Cembureau method and the Torrent Permeability Tester.

Oxygen permeability test

The oxygen permeability test involves the determination of the oxygen permeability index (*OPI*) of a concrete specimen (typically a concrete core of 30 ±2 mm thick and 70±2 mm diameter) from the rate of pressure decay through the specimen when placed in a falling head permeameter. The rate of pressure decay of a falling head permeameter is governed by the Darcy equation, allowing the coefficient of permeability (*k*) to be determined (Ballim, 1994).

The falling head permeameter shown in Figure 2.7 taken from Alexander et al. (1999) was originally developed at the University of the Witwatersrand by Ballim (1994). It applies an initial pressure to one side of a concrete specimen with the other side at normal atmospheric pressure. As permeation occurs through the specimen, the decrease in pressure with time is measured. From the slope of the log of pressure head versus time, the oxygen permeability coefficient may be determined using Equation 2.12 (Alexander et al., 1999; Ballim, 1994).

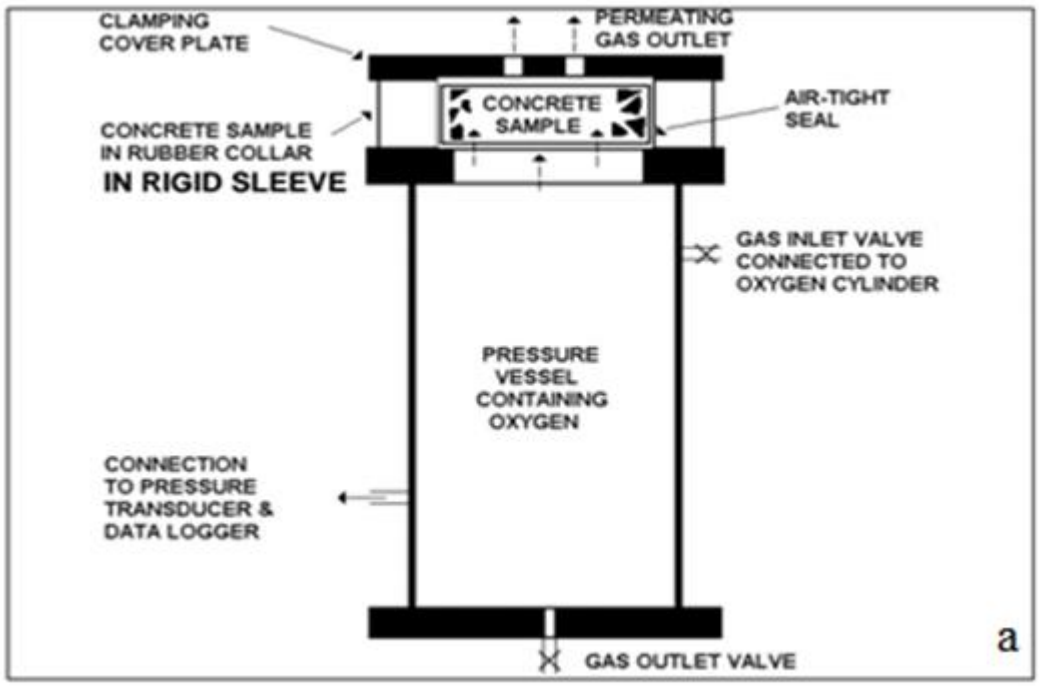


Figure 2.7: (a) Permeability cell arrangement (Alexander et al., 1999)

$$k = \frac{\omega V g dz}{RA\theta} \qquad 2.12$$

Where,

k = coefficient of permeability (m/s)

ω = molecular mass of oxygen, 0.032 (kg/mol)

V = volume of oxygen under pressure in permeameter (m^3)

g = acceleration due to gravity, 9.81 (m/s^2)

R = universal gas constant, 8.313 (Nm/K mol)

A = cross - sectional area of sample (mm^2)

d = average sample thickness (m)

θ = absolute temperature (K)

z = slope of the line determined in regression analysis of $\log\left(\frac{P_0}{P_t}\right)$ vs t.

P_0 = pressure at start of test (kPa)

P_t = pressure at time t (kPa)

t = time (s)

The oxygen permeability index (*OPI*) is then given as the negative log of the average of the coefficient of permeability of the samples, which for four samples is as given in Equation 2.13.

$$OPI = -log_{10}\left[{}^{1}/_{4}\ (k_1 + k_2 + k_3 + k_4)\right] \qquad 2.13$$

The *OPI* for concrete ranges from 8 to 11, that is, over three orders of magnitude. The higher the index, the less permeable is the concrete. The oxygen permeability test therefore gives an indication of the gas permeation properties of the concrete and can provide a rapid estimation of the resistance of a particular concrete to the transport of gas, especially with respect to carbon dioxide diffusion into the concrete (Alexander et al., 1999). The *OPI* is strongly influenced by the amount

and continuity of larger pores where most of the flow will occur and which are likely to have been caused by poor compaction and/or bleeding (Mackechnie, 1996). The *OPI* values obtained for concrete can provide a basis of comparison and a means of estimating the degree of influence on the microstructure of the binders. The movement of oxygen through concrete is also one of the fundamental parameters governing the rate of corrosion and is therefore indispensable in any attempt to meaningfully study the corrosion and or carbonation of steel in concrete.

Water sorptivity test

An important parameter of the pore structure of concrete, including its dimensional effects, is the rate and degree to which it absorbs water. Sorptivity is the rate of movement of a water front through a porous material (e.g. concrete) under capillary action. The dominant mechanism controlling rate of water ingress into unsaturated or partially saturated concrete is absorption, where fluid is drawn by capillary suction. Capillary suction depends significantly on the orientation and connectivity of the pores. It is significant near the surface of the concrete but tends to decrease with depth. The test is therefore a useful measure of the near surface characteristics of the concrete (Alexander et al., 1999).

Water sorptivity test method developed by Ballim (1994) is a variation of that developed by Kelham (1998) and provides a measure of the sorptivity of a specimen based on the principles relating to the flow of water in partially saturated porous media. The water sorptivity test involves the determination of the porosity and sorptivity values of a concrete specimen (typically a concrete core of 30±2 mm thick and 70±2 mm diameter) by periodically placing the specimen onto a free water surface. The rate of absorption is then monitored by weighing the specimen on an electronic balance. The free water surface consists of layers of absorbent material placed in a plastic tray containing a solution of distilled water saturated with $Ca(OH)_2$. Figure 2.8 taken from Alexander et al. (1999) shows the arrangement and experimental set-up for the water sorptivity test. An estimate of

the total pore volume is obtained by vacuum saturating the sample after the absorption test.

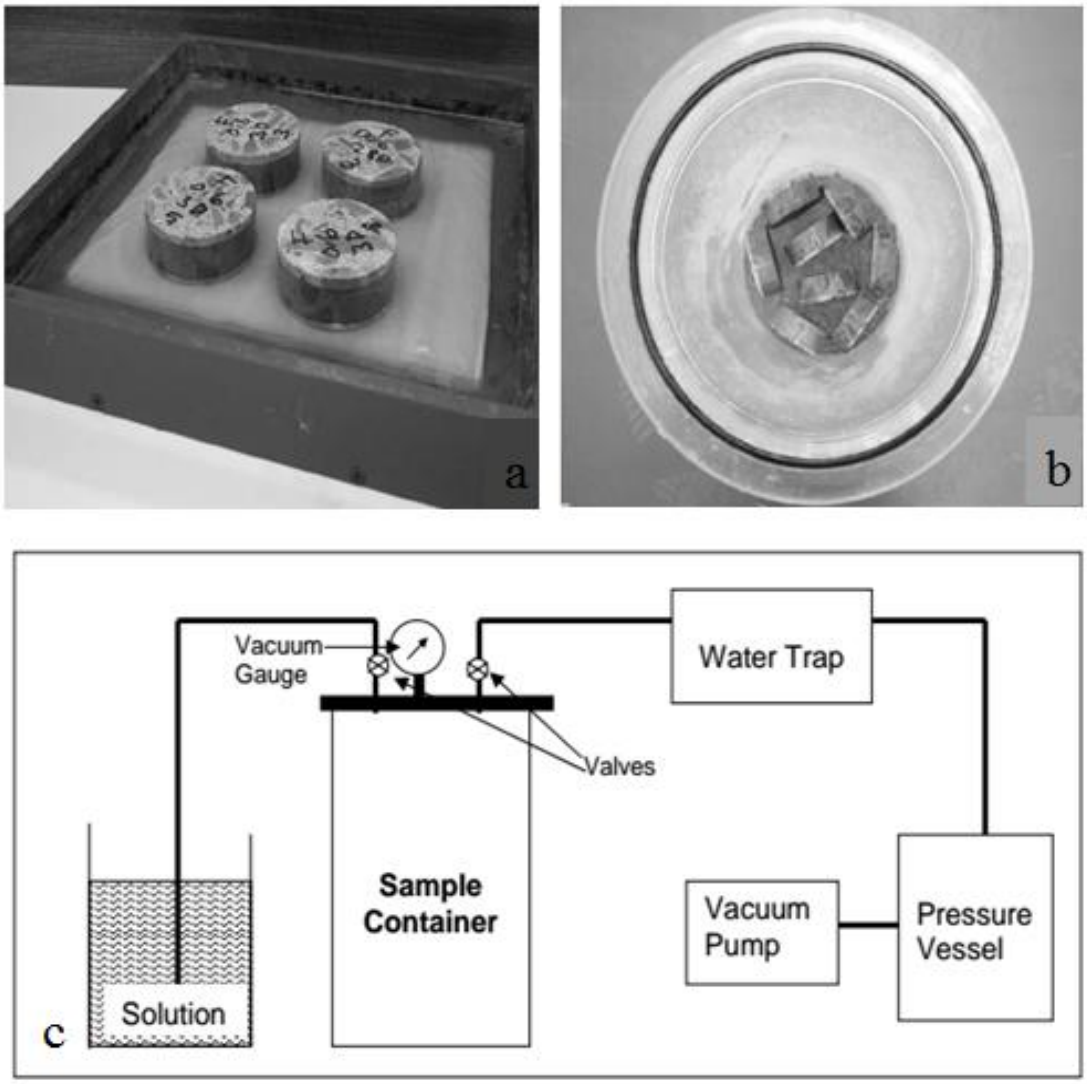


Figure 2.8: (a) Test Set (b) Specimens arranged for saturation (c) Vacuum saturation facility (Alexander et al., 1999)

The porosity (n) of each specimen, as a percentage may be determined from Equation 2.14.

$$n = \frac{M_{sv} - M_{so}}{Ad\rho_w} X\ 100 \qquad 2.14$$

Where,

M_{sv} = vacuum saturated mass of the specimen to the nearest 0.01 g

M_{so} = initial mass of the specimen at time t = 0 to the nearest 0.01 g

A = cross- sectional area of the specimen to the nearest 0.02 mm^2

d = average specimen thickness to the nearest 0.02 mm

ρ_w = density of water in g/mm^3

The water sorptivity (S) of the specimen can be obtained from the test using Equation 2.15.

$$S = \frac{Fd}{M_{sv} - M_{so}} \qquad 2.15$$

Where,

F = the slope of the best fit line obtained by plotting mass of water absorbed (M_{wt}) against time (t) expressed in $g/\sqrt{hr}$

d = the average specimen thickness to the nearest 0.02 mm, in mm

2.3.4 Chemical composition of concrete and its quantification

The chemical composition of concrete depends on the mix constituents, especially the cement and/or binder content and its composition. In addition, the chemical composition of the binder also depends on the degree of hydration and degree of pozzolanic activity for blended cement. The chemical parameter limiting concrete carbonation is the amount of carbonatable material (hydroxides) that is available in the concrete matrix. Thus, the amount of hydroxide in the pore structure of the concrete has an influence on the rate of carbonation. Different methods exist for the quantification of the hydroxides content in concrete and the main techniques discussed here are the thermal and wet chemical analytical methods.

Thermal analysis test

Thermal analysis is a general term which covers a variety of techniques that record the physical and chemical changes occurring in a substance as a function of temperature (Da Silva et al., 2009; Ramachandran, 1979). Thermogravimetry (*TG*) continuously measures the change in mass of a material as a function of time and temperature over a fairly wide temperature range, using a predetermined heating rate. Thermogravimetric analysis (*TGA*) can be used to quantify the hydroxides contents in a powder sample extracted from concrete (Parrott & Killoh, 1989; Platret & Deloye, 1994).

The thermal decomposition behaviour of concrete can be studied using a *TGA* instrument that monitors the mass and temperature change of a sample. An example is the Perkin Elmer TG400 thermogravimetric analyzer coupled to a Setaram differential analyzer presented in Figure 2.9. The instrument enables the *TG* curve and the derived differential thermogravimetric curve (*DTG*) to be obtained simultaneously on a powdered sample.



Figure 2.9: Perkin Elmer Thermogravimetric Analyzer (TGA 4000)

The gypsum ($CaSO_4$), hydroxide (*CH*) and calcite ($CaCO_3$) content in a powdered sample can then be estimated from the weight loss measured from the *TG* curves

between the initial and final temperatures of the corresponding peaks on the *DTG* curve. The following dehydration, dehydroxylation and decomposition reactions correspond to the loss of $CaSO_4$, *CH* and $CaCO_3$ at the following temperature ranges 100-127°C, 400-500 ^{o}C and 650-750 ^{o}C respectively as given in Equations 2.16 to 2.18 (Da Silva et al., 2009). (A detailed procedure for the estimation of the hydroxide content from the *TG/DTG* curves can be found in Chapter 3, Section 3.5.3).

1. Calcium sulphate dehydration

$$CaSO_4.2H_2O \rightarrow CaSO_4 + 2H_2O \qquad 2.16$$

2. Calcium hydroxide dehydroxylation

$$Ca(OH)_2 \rightarrow CaO + H_2O \qquad 2.17$$

3. Calcium carbonate decomposition

$$CaCO_3 \rightarrow CaO + CO_2 \qquad 2.18$$

Thermogravimetric analysis (*TGA*) is thus a convenient method to determine the *CH* contents in a sample of paste extracted from concrete and reduced into powder. The thermal analysis technique (*TGA*) has been used by numerous researchers (Bhatty et al., 1986; Borges et al., 2010; Dweck et al., 2000; Midgley, 1979; Parrott & Killoh, 1989; Saeki & Monteiro, 2005; Villain et al., 2007) for the quantification of the *CH* content in concrete, mortar and paste. Among these Geraldine et al. (2007) uses the *TGA* technique to determine carbonation profile in concrete by quantifying the $CaCO_3$ and *CH* of specimen obtained from concrete. They however supplemented the *TGA* method with the chemical analysis test of the same concrete specimen. The aim of their study was to monitor the carbonation progression in concrete for the prediction of service life.

In a similar study, Parrot and Killoh (1989) used the *TGA* technique to determine the presence of *CH* in a 36 year old concrete structure. Specimens obtained by drilling at different depths were analysed by the *TGA* method for $CaCO_3$ and *CH* content with the intention of predicting the service life of the structure. Javed et al.

(1986) also used the *TGA* technique to estimate the quantity of *CH* present in plain and blended cement paste. Their aim was to compare the hydration rate of different mixtures. Duchesne and Berube (1994) used the *TGA* method to measure the *CH* content of paste made with Portland cement blended with *PFA*, *CSF* and *GGBS* with the intention of quantifying the rate of reaction for the different paste type.

Wet chemical analysis test

Chemical analysis can be used in the identification and determination of the elemental composition of cementitious materials (St John et al., 1998). Although wet chemical analysis is being superseded by X-ray fluorescence analysis (Norrish & Chappell, 1977) it is still in use (Atiş, 2003; Lampacher, 2000; Midgley, 1979; Villain et al., 2007). Thus, the wet chemical analysis approach was used in this study for the quantification of the calcium oxide (*CaO*) content in the powdered samples obtained from the concrete. The acid dissolution method of the wet chemical technique was employed, and standard test methods are available in most national standard (ASTM C85-66; BSI 1881, 1988). The method involves acid dissolution of samples obtained from concrete to determine the *CaO* content in the hardened paste. The amount of *CaO* content obtained from the sample can also be used for the determination of the cement content in the concrete, if the composition of the cement is known. Although acid dissolution attack aggregates, while some components of silica fume are not soluble in either hydrochloric or nitric acid, the method is still being used in the quantification of *CaO* content in concrete, mortar or paste (Atiş, 2003; Lampacher, 2000).

The wet chemical analysis method, using the acid dissolution as explained in the British standard (BSI 1881, 1988) for determination of cement content was preferred in the quantification of the *CaO* content in powdered samples because of its simplicity. The principle behind the determination of the *CaO* content in concrete is straightforward. A chemical compound that constitutes a large proportion of the cement and is essentially absent from the other components of

the concrete (aggregate) is identified. The concrete is then analysed for that component. If the entire component originated from cement and the proportion of the component in cement is known, the *CaO* content can be calculated. For example, Portland cement typically contains 64.5% *CaO*, if a concrete contain 13% Portland cement and 84% aggregate containing no *CaO* (the other 3% is combined water of hydration), then the percentage of *CaO* in the concrete can be calculated thus:

$$CaO\ content\ (\%) = 13\ X\ {}^{64.5}/_{100} \qquad 2.19$$

Hence, the acid dissolution method can conveniently be used to determine the *CaO* content in paste sample obtained from either plain or blended concrete. Since the conditions of extraction can be expected to dissolve all the calcium oxide regardless of the extent of pozzolanic reaction. For instance, the *CaO* content of both plain and blended concrete (with *FA, GGBS, CSF*) was calculated by Atis (2003) using the acid dissolution method. In another study, Lampacher (2000) used the acid dissolution method to quantify the *CaO* content of plain and blended concrete samples obtained from existing concrete structures with the intention of determining cement content. The acid dissolution method was also used by Geraldine et al. (2007) in the estimation of *CaO* content in powder samples obtained from concrete, with the aim of calculating the cement content. In a more thorough study, Midgley (1997) used the chemical extraction to measure the calcium ions that are taken into solution in a study to determine the hydroxide content in set Portland cement.

2.4 Mechanism of Carbonation in Concrete

Carbonation is a reaction between carbonic acid and hydroxides in cement paste that form carbonates. Carbonic acid can be introduced in the pore structure of *hcp* by dissolution of gaseous atmospheric carbon dioxide (CO_2) in pore water or by direct penetration of rain water with dissolved CO_2. Cementitious pastes are basic (*pH* as high as 13.5) and the carbonation reaction reduces the *pH* of the paste to

less than 8.5 when fully carbonated (Glass et al., 1991). Carbonates formed in the carbonation reaction are larger molecules and of lower solubility than the hydroxides, thereby increasing the density of the cement pastes of the concrete and locally, the strength (Neville, 1997). Reduction of the *pH* of the cement paste is a concern for reinforcing steel embedded in concrete because steel is more susceptible to corrosion at lower *pH* level. As a result, carbonation studies most often concern themselves with this potential corrosion and the rate at which carbonation progresses from the exposed concrete face towards the reinforcing steel.

2.4.1 Measurement of carbonation in concrete

No standard method to measure concrete carbonation exists, although several publications do discuss methods of analysis, e.g. Rilem Recommendation CPC 18, ASTM C 856, etc. (Neville, 1997). Carbonation of concrete can be measured using either of the following methods: phenolphthalein solution, rainbow indicator, measuring the pH of pore solutions, thin-section examination with petrographic microscope, x-ray diffraction, infra-red absorption. While some of the methods require a significant amount of time and often expensive equipment, the phenolphthalein solution and rainbow indicator methods are quick and economical. Although the phenolphthalein solution and rainbow indicator methods do not identify areas of partial carbonation, the rainbow indicator requires subjective analysis in determining the location of the colour change which is not as vivid as the phenolphthalein solution. Thus, the phenolphthalein solution was considered as sufficient for carbonation measurement in this project.

The phenolphthalein method involves spraying freshly broken concrete surfaces with 1 or 2% phenolphthalein solution (Wierig, 1984). The surface where the pH is greater than 9 turns magenta and a gradually lightening shades of pink for pH of 8 – 9 (see Figure 3.19). The location where the surface is colourless represents the depth to which full or nearly full carbonation has been achieved and the *pH* of the

cement is at or below 8 (See Figure 3.19). Phenolphthalein testing can be sufficient to determine the extent of carbonation, but it is critical to understand what is actually being measured. The test does not indicate the level of carbonation in the cement paste, but only the location where the *pH* is above or below 9. A *pH* of 9 or lower is generally accepted as 'fully carbonated'. A *pH* greater than 9, however, is not an indicator that no carbonation has occurred. However, the "frontal" nature of the progress of the reaction means that the point of colour change is sufficiently close to the zone of uncarbonated concrete (or something similar).

2.4.2 Derivation of the basic carbonation progression rate equation

Carbonation progression into concrete follows a square-root of time law which is based on a few assumptions (Tutti, 1982). Derivation of the square-root of time equation is necessary if it is to be used appropriately and modelled in line with the governing assumptions. The carbonation rate in concrete is controlled by the ingress of CO_2 into the concrete pore system by diffusion, with a concentration gradient of CO_2 acting as the driving force. Therefore, the CO_2 always has to pass through concrete sections that have already undergone carbonation in order to participate in a reaction at some depth into the concrete.

Applying Fick's first law of diffusion, the amount,- (m) of CO_2 diffusing through a concrete layer is given by:

$$m = -DA\frac{C_1 - C_2}{x}t \qquad 2.20$$

Where,

m = mass of CO_2 (g)

D = diffusion coefficient of CO_2 through carbonated concrete (m^2/s)

A = area through which the transport is taking place (m^2)

C_1 = CO_2 concentration at the concrete surface (g/m^3)

C_2 = CO_2 concentration at the carbonation front (g/m^3)

x = thickness of the penetrated concrete layer (m)

t = time (s)

It is assumed that the carbonation front cannot move on except when all carbonatable matter, (a, in g/m^3 -) has reacted within a reference volume, Ad_x. The total mass of CO_2, m that has to be transported to the carbonation front to transform this matter, a thereby progressing the carbonation front by, dx is given by:

$$m = a.A.d_x \qquad 2.21$$

Since this is similar to the flux that goes through this reference volume in a reference time, dt to move a distance dx forward, substituting Equation 2.21 in the simplified form of Fick's first law gives:

$$-DA\frac{(C_1-C_2)}{x}t = aAdx \qquad 2.22$$

The boundary condition for the CO_2 concentration C_2 at the carbonation front is that it is zero. Using this boundary condition and solving Equation 2.22 by integration results in:

$$x^2 = \frac{2D}{a}(C_1)t \qquad 2.23$$

If all constant parameters of Equation 2.23 (diffusion coefficient, CO_2 concentration difference and the amount of carbonatable material) are combined into one single constant K, Equation 2.23 will result in the well-known equation:

$$x = K\sqrt{t} \qquad 2.24$$

Where,

x = depth of carbonation

t = time

K = carbonation rate, dependent on the surrounding concentration of CO_2, the possible absorption of CO_2 in the concrete and the permeability of the material.

The assumptions inherent in the derivation of Equation 2.24 are that:

1. The pore structure of the cement paste in concrete (pore size distribution and degree of interconnection of the pores) remains uniform with depth into concrete;

2. The value and quality of the pore structure remains constant with depth from the surface of the concrete inwards;

3. The degree of hydration and the amount of carbonatable material remains constant with depth.

Note that these assumptions are rarely true in practice, especially under conditions of limited curing of the surface zone.

The assumptions in the derivation of the square-root of time equation, demonstrate that the application of Fick's law of diffusion using constant parameters is subject to many limitations. However, numerous prediction models for the development of the depth of carbonation with time exist based on this theory. For higher concrete ages, the depth of carbonation observed is often less than expected according to a $\sqrt{t}$ relation. In controlled climates such as laboratory, satisfactory results may be obtained. However correlation with actual carbonation rates is often poor, especially for outdoor exposure with changing temperature and humidity conditions.

Although Equation 2.24 is the commonly accepted form of the carbonation rate equation, numerous researchers (Bentur and Jaegerman, 1991; Wierig, 1984; Meyer, 1968; Smolczyk, 1980; Nischer, 1984) have proposed the following

alternative equation, claiming that this form gives better correlation with the measured results:

$$x = Kt^n \qquad 2.25$$

Where, n < 0.5 and the terms are as described for Equation 2.24.

Based on long term observations of the carbonation rate of concrete subjected to natural weather conditions, Wierig (1984) concluded that a √t approach is sufficiently accurate to describe the progress of carbonation as long as the concretes are sheltered from rain. Similarly, a study on existing concrete structures in South Africa by Yam (2004) and Alexander et al. (2007) observed a √t relationship for carbonation progression in inland concrete structures while deviations from the √t relationship was noted for concrete structures in the marine environment. Furthermore, Lampacher (2000) in a study of the durability performance of inland concrete structures in South Africa ranging in age between 19 and 70 years, used the √t relationship for the ingress of CO_2. Since the shortest conceivable initiation time is used when assessing the service life of the concrete structure (Tutti, 1982), the square-root of time equation can be utilized in most cases. The square-root of time relationship is therefore an upper limit value for the penetration of the carbonation front.

For reliable modelling of the mechanism or process of carbonation in concrete, the environmental exposure condition is vital in the determination of a time function for the rate of carbonation. However, the derivation of the rate of carbonation from the square-root of time law is influenced by numerous factors which can be grouped into concrete characterisation (concrete making materials and processing) and the environmental exposure condition of the concrete. The above mentioned factors affect the rate of carbonation or the rate of ingress of CO_2 into concrete. Detailed explanations of these factors in relation to the rate of carbonation are presented in the next section.

2.4.3 Factors that influence carbonation progression in concrete

Carbonation rate in concrete is greatly affected by both external and internal factors to the concrete. Thus, the factors that encourages the process of carbonation in concrete can be classified into two distinct categories: environmental factors (extrinsic) and concrete properties (intrinsic).

Environmental Factors

The relative humidity (*RH*) at the concrete exposure site determines the drying rate of the concrete and thus the concrete internal humidity or the saturation degree of pores in the concrete. Concrete under low humidity does not react with CO_2 because there is insufficient water for the CO_2 to dissolve and form carbonic acid. On the other hand, penetration of CO_2 into saturated concrete under a condition of high humidity is difficult. The most favourable exposure condition for carbonation to progress is between 50 to 70 % of relative humidity (Verbeck, 1958; Richardson, 2002; Neville, 1997; Fernandez et al., 2004).

The rate of carbonation in concrete can be significantly reduced under cyclic wetting and drying conditions, when compared with constant *RH* conditions (Bakker, 1994). For instance, when a concrete surface becomes saturated with water as a result of rain period, diffusion of CO_2 into the concrete becomes negligible and the advance of the carbonation front is halted. The concrete has to dry out to the depth to which the carbonation front had reached just before the wetting period, in order for the carbonation front to advance. Schubert (1976) has shown that periodic rewetting significantly reduces carbonation due to the slower rate of CO_2 diffusion through the partially saturated pores of the cement paste matrix.

The penetration of CO_2 in concrete is given by the diffusion mechanism, according to Fick's first law, where the gas penetration is proportional to the difference of CO_2 concentration between the two environments. Thus, the higher

the concentration between the external and internal environment of concrete, the higher the CO_2 penetration will be and, consequently, the higher the carbonation depths observed in a period of time (Da Silva et al., 2009; Nischer, 1984; Hamada, 1969; Fukushi, 1985). Since diffusion is a concentration gradient-driven transport of gas, the partial pressure of CO_2 affects the rate of diffusion and the rate of the carbonation reaction.

Temperature is another environmental factor that affects the reaction rate of the carbonation process. Depending on the temperature to which the concrete is exposed, there is a tendency to accelerate hydration reactions of cement, thus improving the microstructural conditions or increasing the carbonation reaction. However, if temperature is high, it can cause micro-cracking of the material. Micro-cracking is the preferential way for aggressive agent – to penetrate into concrete. Similarly, depending on the temperature, the dissolution and saturation degrees of different species with water change. At lower temperatures, less calcium hydroxide and more carbon dioxide will dissolve in the pore water, but the reaction rate will generally be reduced (Balen & Gemert, 1994). The diffusivity of CO_2 is increased due to increase in activation energy with an increase in temperature.

Concrete Properties

The carbonation process in concrete depends also on the microstructure and chemical composition of the cover concrete. Factors that affect the concrete pore structure and chemical composition influence the rate of carbonation in concrete as well. The concrete microstructure largely depends upon the w/b ratio, the paste content, cement content, binder type, aggregate type, aggregate content, water content, quality of mix constituents as well as all the concrete processing practice such as mixing, transportation, placing, compacting, curing etc. While the chemical composition of the concrete is a function of the cement and/or the binder type and content as well as the degree of hydration. The discussion below focuses

on both these aspects in considering the influence of the material and processing properties on carbonation rate in concrete.

The effects of concrete microstructure and chemical composition on carbonation rate as influenced by the following factors are explained.

1. Cement type affects CO_2 buffering capacity and the physical parameters of the concrete. Finely ground Portland cement decreases the permeability of cement paste hence the rate of carbonation. Similarly, Portland cement has high hydroxide content thus high buffering capacity against CO_2 ingress. However, the effect of blended cement concretes on the rate of carbonation depends on the interplay of the effects of the *SCM* on the concrete permeability as well as its hydroxide content. Manmohan and Mehta (1981) have shown that a significant effect of the addition of FA to Portland cement was that it effected a refinement of the pore structure upon hydration, by transforming large pores into fine pores. As a result of this effect, Mehta (1983) noted a decrease in cement paste permeability after the addition of *FA*.

   Although, the addition of *FA* decreases the fluid transport properties of concrete, the influence of such concrete regarding the rate of carbonation is uncertain since the carbonation process is a function of the *CH* content of the concrete too. The pozzolanic reaction consumes *CH* leaving less active materials to resist CO_2 ingress. This led Alexander (1989) to conclude that: "Fly ash concrete may or may not carbonate faster than comparable plain cement concrete under similar conditions depending on such interlinked factors as permeability and *CH* content".

   In a survey of the literature on the effects of *FA* on concrete carbonation, Thomas et al. (1990) conclude that for equal strength grade, depths of carbonation were similar for *FA* and *OPC* concretes while Alonso et al. (1990) note that blended cements are not as effective as plain cement in

passivating reinforcing steel and therefore, increases the probability of corrosion.

For *GGBS* blended concretes, research appears to indicate that *OPC/GGBS* paste cured for 28 days have similar total porosity values as plain *OPC* paste at the same w/c ratio (Pigeon & Regourd, 1983). However, the *GGBS* pastes have more gel pores and fewer capillary pores than corresponding *OPC* paste. This does not appear to have a significant effect on the permeation properties of the material in concrete. As Reeves (1985) shows that the water permeability of a 70/30 *GGBS/OPC* concrete is slightly higher than that of a plain concrete. Similarly, research conducted by Osborne (1999) shows that the replacement of *OPC* with *GGBS* increases the rate of carbonation as well as the permeability of the concrete. He also noted increased carbonation and permeability with increasing *GGBS* replacement. However, the extent of increase in the carbonation rate decreases as the total binder content of the concrete increases.

CSF on the other hand causes pore blocking in the hydrating cement, densifying the hydrating gel structure (Mehta & Gorve, 1982). This is as a result of its high reactivity (Roy, 1997) and its ability to form nucleation sites for cement hydration (Mitchell et al., 1998). These effects give *CSF* blended concrete reduced rate of carbonation, despite the fact that its *CH* content is low in comparison to plain cement concrete.

2. w/c ratio affects the physical parameters of concrete and may influence the amount of hydrated cement present and hence buffering capacity of the concrete. Permeability of concrete generally decreases with w/c ratio and hence, the rate of carbonation is reduced, other factors being held constant. The positive influence of w/c ratio on the rate of carbonation of concrete is as a result of the increasing volume and degree of interconnectivity of the capillary pores. Similarly, since permeability increases with w/c ratio, the rate of ingress of CO_2 also increases. A study by Henry and Kurtz (1963) shows

increasing fluid transport ability with increasing w/c ratio. This largely explains the noted increases in concrete carbonation rate by numerous researchers as w/c ratio increases (Atiş 2003; Ho & Lewis, 1987; Loo et al., 1994; Mackechnie & Alexander, 2002; Sisomphon & Franke, 2007; Sulapha et al., 2003).

3. Cement content in concrete affects its buffering capacity. While cement content is not a basic parameter in determining the permeability of concrete (Addis, 1986), it does have an influence on the carbonation progression in concrete. For instance, the rate of carbonation in concrete is influenced by the amount of hydration products available for reaction. Hence, for the same permeability a concrete with more cement will show a slower rate of carbonation progression.

4. Although aggregate type has no direct effect on concrete carbonation, it may lead to "through-aggregate" carbonation (BRE, 2001). However, the size of the aggregate and its content has effect on concrete permeability because of the role of the *ITZ*. Thus, the rate of carbonation increases with an increase in aggregate size and content as a result of increased volume of the *ITZ*.

5. Curing is a process aimed at encouraging the hydration of cement during the early period of casting hence ensuring that the engineering properties of concrete develop to their required potential. Curing has very significant effect on the permeability of concrete. Continued hydration of concrete decreases both the size and continuity of the pores in *hcp* as well as its composition. Thus, curing may either increase or decrease the rate of carbonation in concrete depending on the type of binder used. While curing has positive effect on rate of carbonation in plain cement concrete, the effect depends on the inter-play between permeability and hydroxide content in blended cement concrete (Alexander, 1989).

The chemical composition of the cover concrete depends on the mix constituents, especially the binder type and content, and the chemical composition of the binder. Additionally, the chemical composition of concrete also depends on the degree of hydration and degree of pozzolanic activity in the case of blended binders. Curing influences the degree of hydration and pozzolanic activity thus the chemical composition of the concrete. With the use of *SCM*, hydroxide components in the cement paste are reduced due to its consumption. With this reduction, carbonation rates would tend to increase, as there is less material to react with the CO_2.

However, *SCM* have the effect of decreasing permeability of the cement paste which tends to decrease the diffusivity of the ingress of CO_2. If the reduction in permeability has a higher impact than the reduction in hydroxide components, then the overall carbonation is reduced. The chemical parameter of importance to carbonation is the amount of carbonatable material (hydroxides) that is available in the concrete matrix. It has been observed that, given a sufficiently high CO_2 concentration, unhydrated products (C_2S, C_3S) as well as the *CSH* gel and other hydration products such as ettringite will carbonate. While at ambient CO_2 concentration, only the *CH* will mainly carbonate. Thus, the rate of carbonation is slow at low CO_2 concentration.

Considering the mentioned limitations in the derivation of the square-root of time law stated in section 2.4.2 for the progression of the carbonation front in concrete and the various factors that influences this progression as enumerated in section 2.4.3, numerous attempts to correlate the rate of carbonation with the concrete physical and/or chemical properties has been atttempted in a bid to model the mechanism of carbonation in concrete (Ballim, 1994; Mackechnie, 1996; Parrott & Killoh, 1989; Bruno, 2010). In the following section, an attempt is made to review some existing empirical models on carbonation progression in concrete.

2.5 Existing Models for the Prediction of Carbonation Depth/Rate in Concrete

Reinforced concrete structures are expected to carbonate in their natural environmental exposure condition. Surprisingly, the majority of articles on concrete carbonation modelling have been focused on laboratory concrete specimens that were carbonated under controlled or accelerated exposure. Following an intense literature review, only four unique publications on experimental modelling of concrete carbonation in the inland environment by Dhir et al. (1989), Watkins and Jones (1993), Parrott (1994) and BRE (2001) were found. These works will be discussed in detail later in the section. Since environmental exposure conditions affect the rate of carbonation in concrete, it is questionable if the numerous experiments (and hence the models) that were and continue to be conducted in the absence of a natural environmental exposure conditions are truly representative of the behaviour of in-service structures.

It has already been discussed in Chapter One that one of the criteria that is often used to define the end-of-service life of carbonation-affected reinforced concrete structures service life, is the time it takes the carbonation front to reach the level of the reinforcing steel (Initiation Limit State – *ILS*). Considerable experimental works have been done on the time it takes the CO_2 to move from the concrete surface to the reinforcing steel level. The main intent of the majority of the research work is to correlate the properties of concrete to the depth or rate of carbonation in the companion concrete. The following section reviews the experimental work and the corresponding results from various researchers in their attempt to model the advance of carbonation.

Similar to findings from Kikuchi et al. (1988), Osborne (1999) and Hilsdorf (1989), Dhir et al. (1989) proposed an empirical equation (Equation 2.26) to predict the depth of carbonation in concrete. The equation represents a model and is based on the relationship between the intrinsic permeability of plain and blended concrete and the carbonation depth of companion concrete. Equation 2.26

was derived by regression analysis between the depth of carbonation in concrete and its permeability values.

$$D = (t/20)^{\gamma}(22.8logK - 6.9) \quad 2.26$$

Where,

D = depth of carbonation (mm) after t years normal exposure

t = design life of the concrete structures (years)

K = intrinsic permeability of the concrete (10^{-17} m^2)

γ = time exponent (γ = 0.5, if w/c ≤ 0.6 and γ = 0.4 if w/c > 0.6)

Dhir et al. (1989) study represents a notable contribution to understanding the relationship between concrete microstructure, its environmental exposure conditions and the carbonation process in concrete. The variable time exponent accounts for the carbonation process for the different concrete types. In addition, the concept of employing the intrinsic permeability in a prediction model is appealing as test specimens for a variety of concretes can be made and the permeability measurements obtained after 28 days. Furthermore, the principle of using the inherent characteristics of the concrete, in the absence of site environmental conditions, to obtain estimates for carbonation performance of concretes appears to be reasonable, provided the intrinsic values are compared to actual site specific data to validate the model.

Whilst the Dhir et al. modelling attempt was based on a study of the natural environmentally exposed concretes and the consideration of the time exponent as well as the concrete fluid transport properties in the model, the chemical composition of the concrete was however, not given specific consideration in the model. Additionally, the environmental exposure conditions considered where those of the UK and which will definitely be different from inland South Africa both in its weather and its concrete materials and technology. Clearly, the Dhir et al. model, even though comprehensive, cannot be used by South African building

owners and design engineers in the design of concrete structures as it can be expected to give inaccurate predictions.

Watkins and Jones (1993), in an assessment of over 800 buildings in Hong Kong in the late 1980's in terms of depth of carbonation, strength, cement content, density, permeability, porosity and age, developed a prediction model that is similar to the general carbonation prediction model presented in Equation 2.24. However, the time exponent *n*, varied between 0.5 and 1, while the rate of carbonation *K*, varies in accordance to the strength of the concrete. Table 2.1 gives the *K* and *n* exponent, based on Honk Kong's concrete making materials and environmental conditions respectively. The authors gave the climatic condition in Hong Kong in terms of the CO_2, *RH* and temperature variation as ranging between 0.03 - 0.1%, 70 - 84% and 15 – 28^0C respectively.

Table 2.1: Coefficients for carbonation prediction model (Watkins and Jones, 1993)

Strength of concrete (MPa)	*K*	*n*
15 - 24.99	6.43	0.570
25 - 34.99	4.28	0.592
35 - 44.99	3.07	0.614

The correspondence of the data with theoretical models appears to be reasonable and it enables the depths of carbonation to be predicted under a number of varying conditions with some precision. This leads directly to an ability to predict the initiation period for concrete of varying grades. The Watkins and Jones model (1993), although applicable to a variety of concrete grades and exposures, has similar short-comings as the Dhir et al. model. Additionally, since this model was developed based on study on existing structures, it is not applicable to proposed concrete structures as early-age concrete characterisation results were not used.

In a more thorough research, Parrott (1994) proposed a carbonation prediction model that is potentially quite broad in application, taking into account variations in cement types (through calcium oxide content), w/c, strength and curing through permeability. Parrot's model although based on UK exposure condition is applicable for a variety of RH conditions. The Parrott model is similar in concept to the generally accepted empirical carbonation prediction model and it explicitly considers the permeability of the concrete, thereby allowing for a broader application. Parrott's model is given in Equation 2.27.

$$d = \frac{aK^{0.4}}{C^{0.5}} t^n \qquad 2.27$$

Where,

d = carbonation depth (mm)

t = exposure time (years)

k = air permeability of cover concrete (10^{-16} m^2)

n = the time exponent

a = calibration coefficient for a particular environmental effect

C = calcium oxide content in the hydrated cement matrix which can react with CO_2, expressed in kg/m^3 of cement matrix. C depends on the cement type, *RH* and proportion of cement which has reacted.

Despite the fact that Parrott model is comprehensive in terms of its coverage of the factors that influences concrete carbonation rate, it is unlikely to accurately predict the carbonation process of South Africa concrete structures. This is because it was developed under an environmental exposure conditions different from that in South Africa, in terms of temperature and relative humidity condition. Additionally, different concrete making materials and technology were used in the production of the concrete used.

Another attempt to develop prediction model for the carbonation depth in concrete was conducted in the UK by the Building Research Establishment (*BRE*). The *BRE* (2001) model was similar to Parrott's model and was developed using carbonation depth over time for concrete made using different cement types, cement contents, w/c ratios and different curing regimes. Equation 2.28 present the BRE model developed based on regression analysis between the response (carbonation depth) and predictor (concrete permeability and cement content) variables.

$$d = (3.165t^{0.49}\ X\ k^{0.5}\ + 1.47t^{0.59})/C \qquad 2.28$$

Where,

d = depth of carbonation (mm)

K = oxygen permeability values of the concrete at 28 days

C = is the normalized cement content

t = time of exposure (years)

The *BRE* model has similar shortcomings as the Parrott model suffered in terms of its applicability in South Africa.

It is evident from the above discussion that despite the sophistication of the various prediction models for the estimation of rate of carbonation in concrete, the accuracy of the prediction will be questionable when used under South African environmental exposure conditions. This is mainly attributed to as stated above - the differences in the concrete making materials and concrete technology as well as the environmental exposure condition. For instance in Equation 2.27, "a" is determined to be 64 for the "European" climate. Clearly the climate in South Africa will differ greatly from that of Europe.

With the above mentioned short-comings of models developed under different climatic and concrete technology conditions, South African researchers have

made numerous attempts to model the rate of carbonation in concrete for the prediction of the durability performance and service life of concrete structures. This section describes the attempts by South African researchers in the prediction of carbonation depths thus rates in concrete. Attempts by South African researchers in the prediction of concrete carbonation rates and the development of carbonation rate prediction models includes, amongst others attempt by Ballim (1994), Mackechnie (1996), Ballim and Lampacher, (1996), Lampacher (2000), Mackechnie and Alexander (2002), Yam (2004), Alexander et al. (2007) and Bruno (2010).

Ballim (1994) made the foremost attempt in the development of prediction model for carbonation of concrete in South Africa using the fluid transport properties of concrete. Concretes were cast using plain and blended binders and were treated to varying degree of initial moist curing. The oxygen permeability and water sorptivity of the concrete were measured at 28 days after casting while the depth of carbonation of companion concretes exposed to a controlled laboratory environment were measured at 10 and 20 months. Plots of the early-age permeation properties of the concretes against equivalent carbonation depth shown in Figures 2.10 and 2.11, taken from Ballim (1994) shows good correlation.

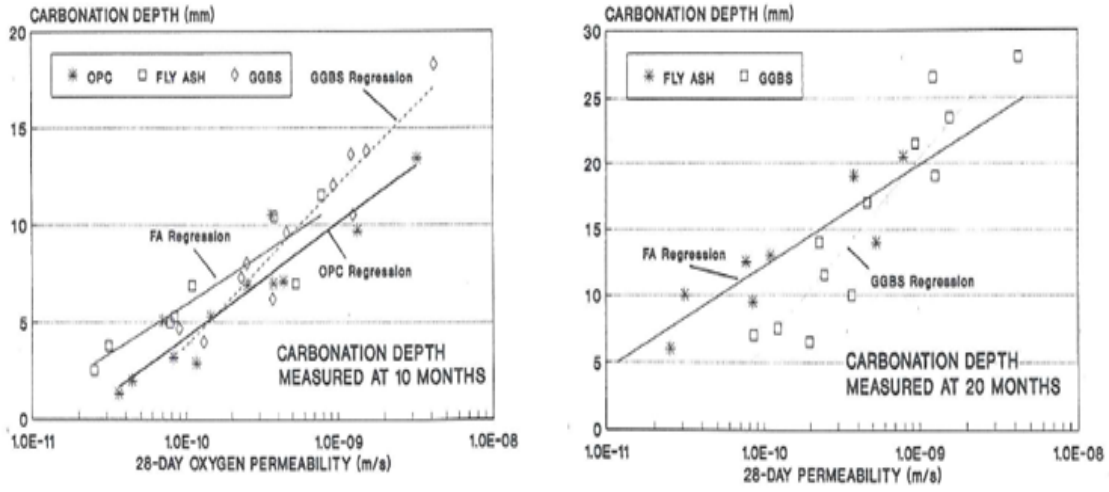


Figure 2.10: 28 day oxygen permeability vs carbonation depth (Ballim, 1994)

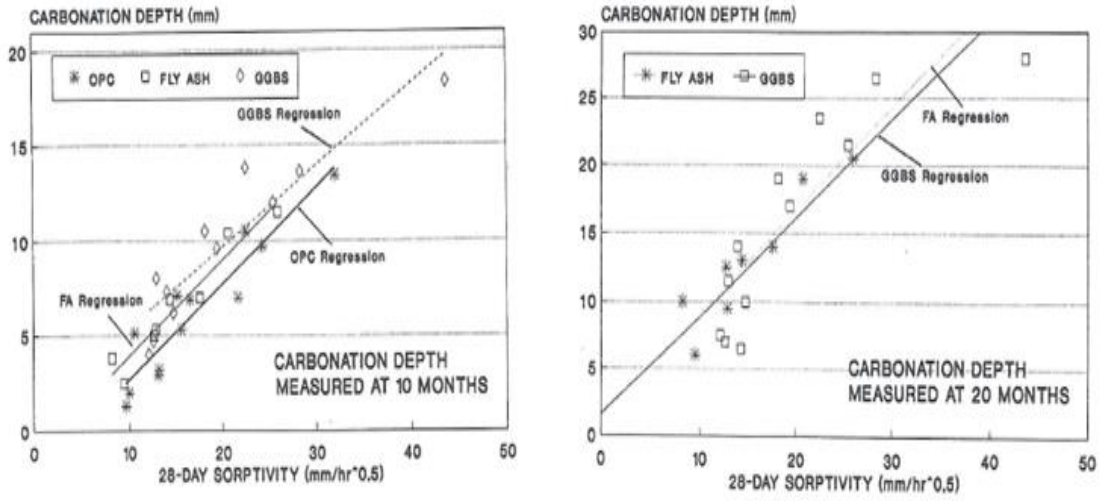


Figure 2.11: 28 day water sorptivity vs. carbonation depth (Ballim, 1994)

The relationships shown in Figures 2.10 and 2.11 were presented in Equations 2.29 and 2.30, between the concrete carbonation depth and the oxygen permeability index and water sorptivity respectively.

$$X = \lambda_9 . In(K) + \lambda_{10} \qquad 2.29$$

$$X = \lambda_{11} . S + \lambda_{12} \qquad 2.30$$

Where,

X = carbonation depth (mm)

K = oxygen permeability

S = water sorptivity

$\lambda_{9\ to\ 12}$= are coefficients dependent on the binder type

In a similar study, Mackechnie (1996) related the 28-day oxygen permeability values for both plain and blended concretes to the 12-months carbonation depth after exposure to the marine environment. Good correlations were also obtained over a wide range of concretes as shown in Figure 2.12. Mackechnie however did not present this relationship in the form of an equation.

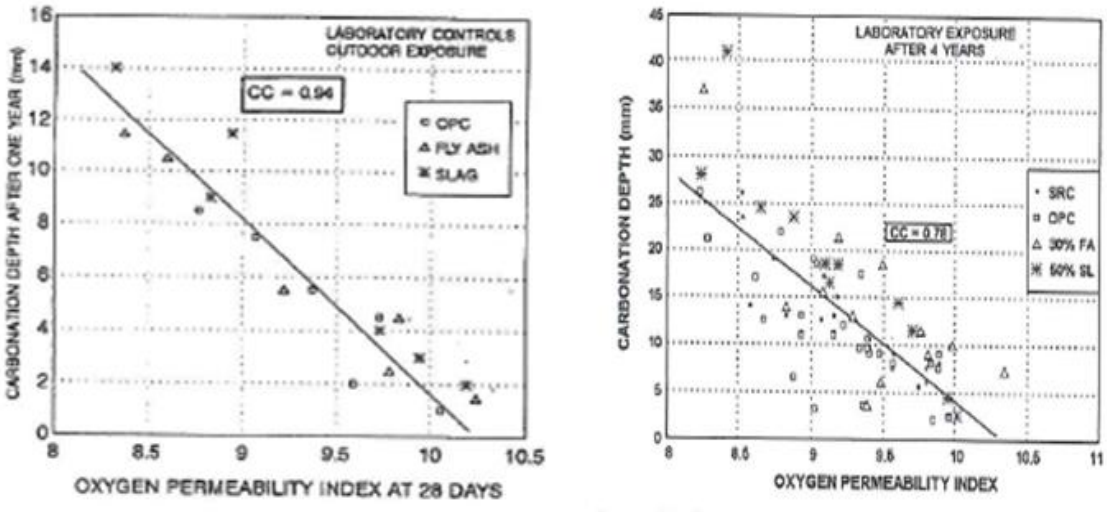


Figure 2.12: 28 day oxygen permeability vs carbonation depth (Mackechnie, 1996)

Mackechnie and Alexander (2002) proposed an empirical relationship that was similar to the general carbonation model, for the prediction of the depth of carbonation in concrete. In their study, Plain and blended concretes of different grade were exposed to the marine environment of South Africa for up to 6 years, and the carbonation depth measured at intervals of 1, 4 and 6 years, using the

phenolphthalein method. The pore structures of the companion concretes were characterized using the oxygen permeability test at 28 days after casting. Figure 2.13 shows the correlation between the oxygen permeability values recorded at 28 days and the carbonation depths, which shows good correlation. This relationship was presented in the form of an Equation.

$$X = K_c t^{0.4} \qquad 2.31$$

Where,

X = carbonation depth (mm)

K_c = material coefficient

t = time (years)

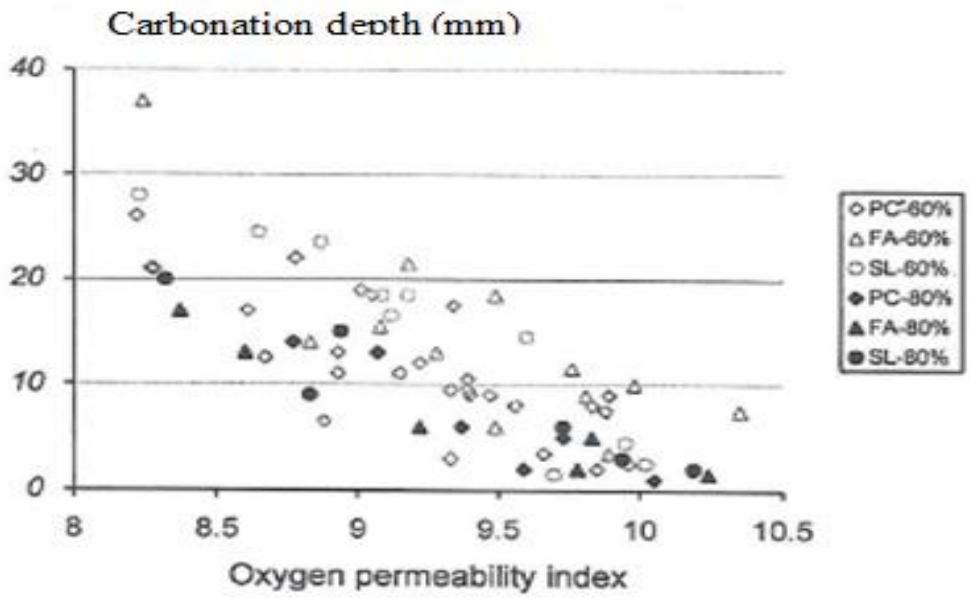


Figure 2.13: 28 day oxygen permeability vs carbonation depth (Mackechnie and Alexander, 2002)

The studies by Ballim (1994), Mackechnie (1996) and Mackechnie and Alexander (2002) represent a notable contribution to understanding the relationship between concrete early-age permeation properties and the carbonation rate in concrete. The models or relationship developed by these authors will however not allow for the

prediction of the performance of concrete not represented in the data set as small samples sizes were used. In addition, these authors attempts at predicting the carbonation depths in concrete, did not consider the chemistry of carbonation in terms of the concrete chemical composition. Furthermore, the Mackechnie (1996) and Mackechnie and Alexander (2002) models are not applicable to the inland environment since samples were exposed to the marine environmental exposure conditions.

In a more thorough research, Bruno (2010) assessed the oxygen permeability of plain and blended concretes, as well as the accelerated carbonation depths of the companion concretes. His intention was to develop a model for predicting the depth of carbonation in concrete. Using the *OPI* values of the concrete, exposure condition effects and the quantification of the chemical composition of the concrete, Bruno proposed a regression model shown in Equation 2.32, for the prediction of carbonation depth in concrete.

$$X = \sqrt{\frac{2D_{dry}C\beta}{a}} * \sqrt{t_e} \qquad 2.32$$

Where,

X = depth of carbonation

D_{dry} = effective diffusion coefficient and is calculated from the oxygen permeability, k

C = ambient carbon dioxide concentration (mol/m^3)

β = relative humidity factor

a = the amount of carbonatable material in the concrete matrix (mol/m^3)

t_e = effective time of carbonation over the service life of the concrete.

Bruno's model, although comprehensive in the coverage of the factors that influence the process of carbonation and also has the advantage of differentiating exposure conditions and concrete types, is based on an accelerated carbonation

process. In addition, the amount of carbonatable materials in the concrete and the environmental conditions parameters were obtained theoretically. This limits the applicability and usefulness of the model in natural exposure conditions.

Ballim and Lampacher (1996) in a study of the durability performance of existing concrete structures aged between 19 and 30 years located in the inland environment of South Africa propose an average rate of carbonation to 3.67 mm/√years. A lack of relationship between the depth of carbonation and either the oxygen permeability index or water sorptivity at later age was noted by the authors. The poorly known variations in mix constituents, the degree of initial curing received and the subsequent environmental exposure history of these structures are the possible reasons given by the authors for the lack of correlation.

Lampacher (2000) in a more detailed study of the durability performance of existing concrete structures in the inland environment of South Africa presented the average rate of carbonation to be 3.16 mm/√year. In his study, carbonation depths of existing concrete structures, ranging in age between 19 and 70 years, were measured. Also measured were the concretes permeation properties (in terms of oxygen permeability index and water sorptivity), compressive strength, *CaO* and cement contents and the modulus of elasticity. Lampacher did not however relate the concrete carbonation depth to any of these concrete properties measured.

The study by Ballim and Lampacher (1996) and Lampacher (2000) represent a contribution to understanding the relationship between concrete permeation properties at later ages, exposure condition and carbonation depth of existing concrete structures. The coefficients obtained by these authors for these concrete structures are functions of the variability in material properties and exposure conditions on the carbonation process. Although the outcomes of their study cannot be directly applicable to proposed concrete structures, it can be used for maintenance and repair scheduling for inland structures. Similarly, their study also

buttress the point that the rate of carbonation in concrete decreases at an increasing time of exposure. Hence, the reduced average rate of carbonation from 3.67 to 3.16 mm/√year when the exposure duration increases from 19-30 years to 19-70 years.

Alexander et al. (2007) drawing data from Yam (2004) presented similar studies to that of Watkins and Jones (1987), Ballim and Lampacher (1996) and Lampacher (2000), in which the depths of carbonation were obtain for 90 in-service reinforced concrete bridges that are between the ages of 11 and 76 years. The structures investigated were drawn from three South African localities – Cape Peninsula, Durban and Johannesburg. The depths of carbonation for the different structures were obtained and the general square-root of time equations applied in order to derive the various rate of carbonation. In the study, prediction models that were similar to the general carbonation model were developed, except for the variables K and n in Equation 2.25 which were different. The differences in the values of the variables were attributed to the variable concrete strength and exposure conditions of the bridges. Table 2.2 gives the values of K and n for the different localities and concrete strength grades, while Table 2.3 presented the weather conditions in the three localities. The CO_2 concentrations for these localities are similar - about 0.035%.

Table 2.2: 90th percentile carbonation prediction model parameters in Equation 2.25 for exposed conditions in the three localities in South Africa (Alexander et al, 2007; Yam, 2004)

Localities	Strength grade	*K*	*n*
Cape Peninsula	Grade 20	5.94	0.4
	Grade 30	3.48	0.4
	Grade 40	2.95	0.4
Durban	Grade 25	7.01	0.4
	Grade 35	5.53	0.4
	Grade 45	4.38	0.4
Johannesburg	Grade 25	5.00	0.5
	Grade 30	4.65	0.5

Table 2.3: Weather conditions in the three localities in South Africa (Alexander et al, 2007; Yam, 2004)

Rainfall seasons	Cape Peninsula		Durban		Johannesburg	
	Av. RH (%)	Temp (^oC)	Av. RH (%)	Temp (^oC)	Av. RH (%)	Temp (^oC)
Wet March - September	78	14	79	23	68	19
Dry Oct - April	71	19	73	18	51	13

The study by Yam (2004) and Alexander et al. (2007) represents a notable contribution to understanding the relationship between strength, exposure condition and carbonation depth of existing structures. The different coefficients obtained by these authors for the variable *K* and n for different localities and strength grades of concrete are as a result of the variability in material and exposure conditions on the carbonation process. The models developed will not allow prediction of the performance of proposed concrete structures since the effects of construction variability in terms of curing were not captured. Furthermore, this model cannot be used during the design stage of proposed concrete structure since they lack early-age parameters.

Relationships have been developed for predicting the carbonation depth/rate from material and environmental factors. However, some of these relationships or models require too many parameters to be practical. For instance, Bruno's model require measurement of diffusion masses of CO_2 concentration inside and outside the samples, and diffusion constant that varies as relative humidity changes. While most of the models do not consider all factors that affect carbonation depth/rate, for example, the equations developed by Ballim (1994), Mackechnie and Alexander (2002), are not dependent upon environmental conditions. The fluid transport properties of the concrete may help capture some of the material properties and curing effects, the effect of the concrete chemistry and varying curing periods are often not considered.

2.5.1 Approach for the development of carbonation rate prediction model for concrete

Justification is drawn from the process of carbonation and the factors that influences carbonation in concrete as presented in section 2.4.2 and 2.4.3, for the choice of input variables in the proposed models. In principle, the rate of penetration of the carbonation reaction front depends upon the atmospheric concentration of CO_2, the CO_2 binding capacity of cover concrete and the gas diffusion coefficient of the carbonated surface layer (Parrott, 1987; Dhir et al., 1989; Hilsdorf, 1989; Tutti, 1982; Papadaki et al., 1989).

Thus, for a prediction model of CO_2 ingress into concrete to be reliable and useful, provision must be made for different cementitious materials used in making concrete, construction effects and conditions of exposure. Existing prediction models reviewed generally fail to address all of these issues adequately. It is therefore necessary that this research be conducted in order to develop local models for concrete durability performance and service life predictions. From the findings of the review on local models, there appear to be sufficient reason to believe that a more reliable and quantitative model may be devised which could

have sufficiently broad application to be practical for specifications and predictions.

The use of the square-root of time equation for the prediction of carbonation rate is limited by:

- The variations with depth from the exposed surface of the moisture content.
- The degree of cement and carbonation reactions.
- The pore structure of the concrete.
- The CO_2 binding capacity.
- The CO_2 diffusion coefficient.

The above-mentioned variables are as a result of curing effect, cement composition and moisture history. In the formulation of the CO_2 ingress into concrete, it is assumed that:

- The coefficient of CO_2 diffusion can be represented by the permeation properties of the cover concrete.
- The binding capacity is related to the *CH* and *CaO* content and degree of reaction of the cement.
- Variation of atmospheric concentration of CO_2 can be ignored.
- Under wetter exposure conditions there is progressive departure from the square-root of time function predicted by simple diffusion theory.

In the literature reviewed above, the oxygen permeability and water sorptivity tests on concrete at early-age is known to correlate with the resistance of the concrete pore structure to CO_2 ingress (Ballim, 1994; Bruno, 2010; Lampacher, 2000; Mackechnie, 1996). These tests are sensitive to both material and construction effects and can be used on laboratory and site concretes. The chemical composition of concrete that is of importance to the ingress of CO_2 is the hydroxide content which can be quantified by either the *TGA* or wet chemical

analysis technique (Midgley, 1997). It was noted from the review on factors that influence CO_2 ingress that the exposure conditions surrounding concretes, the curing duration of the concrete and the binder types used in making concretes affects its buffering of the CO_2 ingress (BRE, 2001; Dhir et al., 1989; Parrott, 1994).

Similarly, relationships exist between concrete early-age characterisation parameters and the depth of carbonation (Ballim, 1994; Mackechnie, 1996; Basheer et al., 2001; Dhir et al., 1994). Further, the rate of carbonation can be obtained from the depth of carbonation using the square-root of time law (Tutti, 1982; Alexander et al., 2007; Lampacher, 2000, Ballim and Lampacher, 1996). Thus, with the above information, prediction models can be developed by relating the rates of carbonation to the numerous factors know to influence or affect it, using a computational regression approach on measured data.

This chapter has placed the current study into context by reviewing the process of carbonation in concretes, its measurement, factors that influence the rate of CO_2 ingress as well as existing models for the prediction of carbonation in concrete. Attempts by South African researchers to develop models to improve the predictive ability for the carbonation process under South African environmental condition were also reviewed. Based on the shortcomings of existing models, an approach was formulated for the development of models for the carbonation rate in concrete. The next chapter will discuss the materials and experimental program involved in the quantification of the early-age characterisation parameters, exposure conditions and the medium-term durability performance of concretes.

Chapter References

Addis, B.J. (1986). (Ed), *Fulton's Concrete Technology*, Sixth (Rev.) Edition, 288-290. Portland Cement Institute, Midrand, South Africa.

ASTM C85. 1971. *Standard method of test for cement content of hardended portland cement concrete designation C85-66, 1971*. Annual Book of ASTM Standards, Part 10, 1971, Philadelphia, Pa. pp. 42-45.

Alexander, M., Skalny, J., & Mindess, S. (1989). *Role of aggregates in hardened concrete.* Material Science of Concrete III, Skalny, J. and Mindess, S. eds., The American Ceramic Society, Inc. Westerville, Ohio, 119-146.

Alexander, M., Mackechnie, J., & Ballim, Y. (1999). *Guide to the use of durability indexes for achieving durability in concrete structures*. Research monograph(2), 36.

Alexander, M., Mackechnie, J., & Ballim, Y. (2001). *Use of durability indexes to achieve durable cover concrete in reinforced concrete structures.* American Ceramic Society, Inc., Materials Science of Concrete VI(USA), 2001, 483-511.

Alexander, M., Mackechnie, J., & Yam, W. (2007). *Carbonation of concrete bridge structures in three South African localities.* Cement and Concrete Composites, 29(10), 750-759.

Alexander, M., & Mindess, S. (2005). *Aggregates in concrete*: Taylor & Francis.

Alexander, M. G., Ballim, Y., & Mackechnie, J. R. (1999). *Concrete durability index testing manual.* Research monograph, No. 4.

Alexander, M. G., Streicher, P. E., & Mackechnie, J. R. (1999). *Rapid chloride conductivity testing of concrete, Research Monograph No. 3, 35 pp.* Department of Civil Engineering, University of Cape Town, Cape Town.

Alonso, M.C., Andrade, C. Moragues, A. and Goni, S. (1990). *Influence of the use of blended cements on the corrosion behaviour of reinforcements*. Proc. Of 2nd Int. Conf. on Engineering Materials. Bologna, Italy. Vol. 1, Parts 3. Pp. 837-844.

Atiş, C. D. (2003). *Accelerated carbonation and testing of concrete made with fly ash.* Construction and Building Materials, 17(3), 147-152.

Bakker, R. (1994). *Prediction of service life reinforcement in concrete under different climatic conditions at given cover*. Paper presented at the Corrosion and Protection of Steel in Concrete, International Conference, Sheffield (UK),(Swamy, RN (Ed.)).

Van Balen, K., & Van Gemert, D. (1994). *Modelling lime mortar carbonation*. Materials and Structures, 27(7), 393-398.

Ballim, Y. (1994). *Curing and the durability of concrete.* PhD Thesis, University of the Witwatersrand, Johannesburg.

Ballim, Y. (1993). *Curing and the durability of OPC, fly ash and blast-furnace slag concretes.* Materials and structures, 26(4), 238-244.

Ballim, Y., Alexander, M. and Beushausen, H., (2009). *Durability of concrete. In Owens, G. & Perrie, B. Fulton's concrete technology*. Cement and Concrete Institute. pp.155-188.

Ballim, Y., Alexander, M., & Beushausen, H. (2009). *In:Owens G (ed) Fulton's concrete technology* (pp. 155-188). 9th edn Cement and Concrete Institute, Midrand.

Ballim, Y., & Lampacher, B. (1996). *Long-term carbonation of concrete structures in the Johannesburg environment*. Journal-South African Institution of Civil Engineers, 38, 5-9.

Basheer, L., Kropp, J., & Cleland, D. J. (2001). *Assessment of the durability of concrete from its permeation properties: a review*. Construction and building materials, 15(2), 93-103.

Bertolini, L., Elsener, B., Pedeferri, P., Redaelli, E., & Polder, R. B. (2013). *Corrosion of steel in concrete: prevention, diagnosis, repair*: Wiley. com.

Bentur, A., & Jaegermann, C. (1991). *Effect of curing and composition on the properties of the outer skin of concrete*. Journal of materials in civil engineering, 3(4), 252-262.

Beushausen, H., & Alexander, M. G. (2008). *The South African Durability Index tests in an international comparison.* Journal of the South African Institute of Civil Engineers, vol.50, no.1, March 2008, pp.25-31.

Bhatty, J. I., Dollimore, D., Gamlen, G., Mangabhai, R., & Olmez, H. (1986). *Estimation of calcium hydroxide in OPC, OPC/PFA and OPC/PFA/polymer modified systems.* Thermochimica acta, 106, 115-123.

BRE. (2001). *Modelling degradation processes affecting concrete*, Ed. Keith Quillin. Building Research Establishement.

Bruno, S. (2010). *Modelling the carbonation of concrete usinf early age oxygen permeability index tests.* MSc University of Cape Town.

Borges, P. H., Costa, J. O., Milestone, N. B., Lynsdale, C. J., & Streatfield, R. E. (2010). *Carbonation of CH and C–S–H in composite cement pastes containing high amounts of BFS*. Cement and Concrete Research, 40(2), 284-292.

BSI 1881. (1988). *Methods for analysis of hardened concrete, London*. British Standard Institution, Part 124, pp. 21.

Czernin, W. (1980). *Cement chemistry and physics for civil engineers*: Bauverlag.

Da Silva, F., Helene, P., Castro-Borges, P., & Liborio, J. (2009). *Sources of variations when comparing concrete carbonation results.* Journal of materials in civil engineering, 21(7), 333-342.

Därr, G., & Ludwig, U. (1973). *Determination of permeable porosity*. Matériaux et Construction, 6(3), 185-190.

Duchesne, J., & Bérubé, M. (1994). *The effectiveness of supplementary cementing materials in suppressing expansion due to ASR: Another look at the reaction mechanisms part 1: Concrete expansion and portlandite depletion*. Cement and Concrete Research, 24(1), 73-82.

Dhir, R., Hewlett, P., & Chan, Y. (1989). *Near-surface characteristics of concrete: prediction of carbonation resistance.* Magazine of Concrete Research, 41(148), 137-143.

Dhir, R. K., Hewlett, P. C., Byars, E. A., & Bai, J. P. (1994). *Estimating the durability of concrete in structures*. Concretes Society, London, Vol. 28, No. 6, pp. 25-30.

Dweck, J., Buchler, P. M., Coelho, A. C. V., & Cartledge, F. K. (2000). *Hydration of a Portland cement blended with calcium carbonate*. Thermochimica Acta, 346(1), 105-113.

Feldman, R. F., & Sereda, P. J. (1968). *A model for hydrated Portland cement paste as deduced from sorption-length change and mechanical properties*. Matériaux et Construction, 1(6), 509-520.

Fernandez Bertos, M., Simons, S., Hills, C., & Carey, P. (2004). *A review of accelerated carbonation technology in the treatment of cement-based materials and sequestration of CO_2.* Journal of Hazardous Materials, 112(3), 193-205.

Fukushi, I. (1985). *Carbonation and durability of reinforced concrete buildings*. Cement Concr.(Jpn), 461, 8-16.

Glass, G., Page, C., & Short, N. (1991*). Factors affecting the corrosion rate of steel in carbonated mortars.* Corrosion Science, *32*(12), 1283-1294.

Geraldine, V., Mickael, T. & Gereard, P. (2007). Measurement methods of carbonation profiles in concrete: hermogravimetry, chemical analysis and gammandensimetry. Cement and Concrete Research (37), 1182-1192.

Gouws, S., Alexander, M., & Maritz, G. (2001). *Use of durability index tests for the assessment and control of concrete quality on site*. Concrete Beton, 98, 5-16.

Gowripalan, N., Cabarera, J., Cusens, A., & Wainwright, P. (1990). *Effect of curing on durability*. Concrete International, 12(12).

Gummerson, R., Hall, C., & Hoff, W. (1980). *Water movement in porous building materials—II. Hydraulic suction and sorptivity of brick and other masonry materials.* Building and Environment, 15(2), 101-108.

Hamada, M. (1968). *Neutralisation (carbonation) of concrete and corrosion of reinforcing steel.* Proc. 5th Int. Symp. on Chem. of Cement, Tokyo, 1968, pp. 343-384.

Henry, R., & Kurtz, G. (1963). *Water vapor transmission of concrete and of aggregates*: DTIC Document.

Hilsdorf, H., & Kropp, J. (2004). *Performance criteria for concrete durability* (Vol. 12): CRC Press.

Hilsdorf, H. K. (1989). *Durability of concrete-a measurable quantity?* Paper presented at the DURABILITY OF STRUCTURES. IABSE SYMPOSIUM, SEPTEMBER 6-8 1989, LISBON (IABSE REPORT VOLUME 57/1).

Ho, D., & Lewis, R. (1987). *Carbonation of concrete and its prediction*. Cement and Concrete Research, 17(3), 489-504.

Hooton, R., Mesic, T., & Beal, D. (1993). *Sorptivity testing of concrete as an indicator of concrete durability and curing efficiency*. Paper presented at the Proceedings of the third Canadian symposium on cement and concrete, Ottawa, Ontario.

Javed, B. I., Dollimore, D., Gamlen, G., Mangabhai, R., & Olmez, H. (1986). *Estimation of calcium hydroxide in OPC, OPC/PFA and OPC/PFA/polymer modified systems*. Thermochimica acta, 106, 115-123.

Kelham, S. (1988). *A water absorption test for concrete*. Magazine of Concrete Research, 40(143), 106-110.

Kikuchi, M. and Mukai, T. (1988). Carbonation of concrete containing fly ash coarse aggregate. CAJ Review.

Kikuchi, M., Dosho, Y., Narikawa, M., & Miura, T. (1998). *Application of re-cycled aggregate concrete for structural concrete. Part 1-experimental study on*

the quality of recycled aggregate and recycled aggregate concrete. Paper presented at the Proceedings of the International symposium: Use of recycled concrete aggregate.

Lampacher, B. J. (2000). *Durability of concrete structures.* PhD Thesis, University of the Witwatersrand, Johannessburg.

Loo, Y., Chin, M., Tam, C., & Ong, K. (1994). *A carbonation prediction model for accelerated carbonation testing of concrete.* Magazine of Concrete Research, 46(168), 191-200.

Mackechnie, J., & Alexander, M. (2002). *Durability predictions using early-age durability index testing.* Paper presented at the Proc. Ninth Durability and Building Materials Conference, Australian Corrosion Association, Brisbane, Australia.

Mackechnie, J. R. (1996). *Predictions of reinforced concrete durability in the marine environment.* PhD Thesis, University of Cape Town, Cape Town.

Manmohan, D., Metha, P.K. (1981). *Influence of pozzolanic, slag and chemical admixtures on pore size distribution and permeability of hardened cement paste,* Cement, Concrete and Aggregates, 3 (1981) 63-67.

Mehta, P. K. (1983). *Pozzolanic and cementitious byproducts as mineral admixtures for concrete-a critical review*. ACI Special Publication, 79.

Mehta, P. (1988). *Durability of concrete exposed to marine environment--a fresh look.* ACI Special Publication, 109.

Mehta, P.K. and Gjorve, O.E. (1982). *Properties of portland cement concrete containg fly ash and condensed silica fume*. Cem. Concr. Res., 12(5): 587-595.

Mehta, P., & Monteiro, P. (1993). *Concrete: Structure, Properties, and Materials,* Prentice-Hall, Englewood Cliffs, NJ, 1993.

Meyer, A. (1968). *Investigations on the carbonation of concrete.* Paper presented at the Proc. 5th Int. Symp. On the Chemistry of Cement.

Midgley, H. (1979). *The determination of calcium hydroxide in set Portland cements.* Cement and Concrete Research, *9*(1), 77-82.

Mindess, S., & Young, J. F. (1981). *Concrete,* Prentice Hall. Englewood Cliffs, NJ, 481.

Mitchell, D., Hinczak, I., & Day, R. (1998). *Interaction of silica fume with calcium hydroxide solutions and hydrated cement pastes*. Cement and Concrete Research, 28(11), 1571-1584.

Moskvin, V. M. (1983). *Concrete and reinforced concrete deterioration and protection*: Mir Publishers.

Neville, A. M. (1997). *Properties of concrete. 4th and final ed.* Harlow, UK: Pearson Education Limited.

Nischer, P. (1984). Einflub der Betongute auf die karbonate sierung, Zement und Beton, Vol. 29 No. 1 pp. 11-15.

Norrish, K., & Chappell, B. (1977). *X-ray fluorescence spectrometry*. Physical methods in determinative mineralogy, 201-272.

Osborne, G. (1999). *Durability of Portland blast-furnace slag cement concrete*. Cement and Concrete Composites, 21(1), 11-21.

Parrott, L. J. (1994). *Design for avoiding damage due to carbonation-induced corrosion,* Durability of Concrete- 3rd International Conference, Nice, France 1994, pp.283-298.

Parrott, L.J. (1987). *A review of carbonation in reinforced concrete*. British Cement Association Report C11-0987, pp.121.

Parrott, L., & Killoh, D. (1989). *Carbonation in a 36 year old, in-situ concrete*. Cement and Concrete Research, 19(4), 649-656.

Papadakis, V. G., Vayenas, C. G., & Fardis, M. (1989). *A reaction engineering approach to the problem of concrete carbonation.* AIChE Journal, 35(10), 1639-1650.

Pigeon, M., & Regourd, M. (1983). *Freezing and thawing durability of three cements with various granulated blast furnace slag contents*. ACI Special Publication, 79.

Platret, G., & Deloye, F. (1994). *Thermogravimetry and carbonation of cements and concretes.* Actes des Journées des Sciences de l'Ingénieur du Réseau des Laboratoires des Ponts et Chaussées, 237-243.

Powers, T. C. (1958). *Structure and physical properties of hardened Portland cement paste.* Journal of the American Ceramic Society, 41(1), 1-6.

Ramachandran, V. (1979). *Differential thermal method of estimating calcium hydroxide in calcium silicate and cement pastes*. Cement and Concrete Research, *9*(6), 677-684.

Richardson, M. (2002). *Fundamentals of durable concrete, modern concrete technology*: Published by Spon Press, London.

Romer, M. a. F. L., L. . (2005). *RILEM TC 189-NEC: Non-destructive evaluation of the concrete cover: Comparative test. Part I: Comparative test of penetrability methods. Part II: Comparative test of covermeters*, Materials and Structures, vol.38, no.284, Dec. 2005, . pp.895-911.

Roy, D. M. (1999). *Alkali-activated cements opportunities and challenges.* Cement and Concrete Research, 29(2), 249-254.

Saeki, T., & Monteiro, P. J. (2005). *A model to predict the amount of calcium hydroxide in concrete containing mineral admixtures*. Cement and Concrete Research, 35(10), 1914-1921.

Saetta, A.V. and Vitaliani, R.V., (2004), *'Experimental investigation and numerical modeling of carbonation process in reinforced concrete structures Part I: Theoretical formulation',* Cement and Concrete Research, Vol. 34, pp. 571-579.

Smolczyk, H. (1980). *Slag structure and identification of slags.* Paper presented at the Proceedings, 7th International Congress on the Chemistry of Cement. Vol. 1, III. Paris. Pp.1-17.

Sisomphon, K., & Franke, L. (2007). *Carbonation rates of concretes containing high volume of pozzolanic materials*. Cement and Concrete Research, 37(12), 1647-1653.

St John, D. A., Poole, A. B., & Sims, I. (1998). *Concrete petrography: a handbook of investigative techniques*: Arnold; Copublished in North, Central and South America by J. Wiley.

Sulapha, P., Wong, S., Wee, T., & Swaddiwudhipong, S. (2003). *Carbonation of concrete containing mineral admixtures*. Journal of materials in civil engineering, 15(2), 134-143.

Osborne, G. (1989). *Carbonation and permeability of blastfurnace slag cement concretes from field structures.* Proc. Of 3rd Int. ACI Special Publication, 114.

Thomas, M.D.A., Mathews, J.D. and Cripwell, J.B. (1990). *The durability of PFA concrete – A survey of existing structures.* Building Research Establishement Report PD.87/90. BRE, Watford.

Torrent, R., & Fernández Luco, L. (2007). *State of The Art Report (STAR): RILEM TC 189-NEC: Non-Destructive Evaluation of the Covercrete*. Zurich, Switzerland, 223.

Tutti, K. (1982). *Corrosion of steel in concrete.* Swedish Cement and Concrete Institute: CIB, Research Report.

Verbeck, G. (1958). *Carbonation of hydrated Portland cement*. Cement and Concrete, 17-36.

Villain, G., Thiery, M., & Platret, G. (2007). *Measurement methods of carbonation profiles in concrete: Thermogravimetry, chemical analysis and gammadensimetry.* Cement and Concrete Research, 37(8), 1182-1192.

Watkins, R., AP PITT, J., & JONES, A. (1993). *CARBONATION: A DURABILITY MODEL RELATED TO SITE DATA*. Proceedings of the ICE-Structures and Buildings, 99(2), 155-166.

Wierig, H. (1984). *Longtime studies on the carbonation of concrete under normal outdoor exposure.* Proceedings of the RILEM, Hannover University, 239-249.

Yam, W.K. (2004). *Carbonation of concrete bridge structures in three South African localities.* MSc (Eng.) Thesis. University of Cape Town, Cape Town; 2004.

CHAPTER 3

MATERIALS AND METHODS

3.1 Introduction

This chapter describes the laboratory and field tests program undertaken in this study to assess the influence of carbonation on the durability performance and service life of reinforced concrete. The intention of this study was twofold, firstly to explore the rate of carbonation for different binder types used in concrete subjected to different inland exposure conditions. Secondly, to predict the long-term durability performance and service life of reinforced concrete structures in the inland environment using concrete mixture design parameters and concrete early-age characterisation parameters. The objectives of the investigation were:

a) to quantify the properties of concrete at an early-age (28 days) using permeability, sorptivity, strength and chemical characteristics;
b) to quantify the response of concrete exposed to an accelerated carbonation environment at early-age (28 days);
c) to quantify the response of concrete exposed to the natural inland environment to carbonation effects in the medium-term (24 months);
d) to determine the adequacy of using concrete mixture design parameters and concrete early-age characterisation parameters to predict the long-term durability performance and service life of reinforced concrete.

This chapter provides details of the test program and also the procedure used in monitoring the micro-climate of the inland exposure sites. The results, detailed analysis and discussion of the results and the broad implications of micro-climate variations on concrete carbonation as well as the effect it has on concrete durability performance and service life are presented in Chapter 4. Chapter 5 covers a discussion of objective (d) above with a view to developing prediction models.

Concretes made of different binder types and exposed to different environmental conditions will react differently in terms of their hydration and hence carbonation rates and this will have different effects on reinforced concrete durability performance and service life. These effects will arise more as a result of variations in the permeation properties of the concrete than in the chemical properties. Hence, a further objective of the test program was to measure variation in permeation properties of the concrete after exposure to different micro-climates in the medium-term.

3.2 Variables of the Test Program

3.2.1 Exposure condition

Natural exposure conditions were chosen based on the EN Classification *XC3* and *XC4* (EN206, 1997) as:

a) indoor;
b) outdoor sheltered;
c) outdoor exposed.

These exposure conditions are the higher aggressiveness classification for carbonation-induced corrosion of reinforced concrete in the inland environment. In order to replicate these conditions, concrete cube samples were stored in a basement parking garage (indoor exposure), under a bridge alongside a busy highway (outdoor sheltered) and on the roof top of a building in an urban setting (outdoor exposed).

An accelerated carbonation exposure condition was also investigated. Concrete cube samples were placed in a carbonation chamber where the micro-climatic conditions were at the optimum values known to maximise the rate of carbonation (Wierig, 1984). The accelerated effect was investigated to provide guidance on the possible development of a test method for accelerated carbonation as well as for

use in the prediction of the natural carbonation. Furthermore, the accelerated testing was undertaken to confirm trends observed on site with regard to corrosion activation and rates of carbon dioxide (CO_2) ingress.

3.2.2 Binder type

Binder types were selected to ensure that the concretes tested reflected concretes commonly used in construction projects in South Africa. Five binder types were used as follows:

a) ordinary Portland cement (*PC*), commercially available as *CEM I*;

b) a 70 % *CEM I* / 30 % fly ash (*FA*) blend;

c) a 50 % *CEM I* / 50 % ground granulated blastfurnance slag (*GGBS*) blend;

d) a 90 % *CEM I* / 10 % condensed silica fume (*CSF*) blend;

e) Portland composite cement (*PCC*), commercially available as *CEM V*.

3.2.3 Water/binder ratio

In the selection of the water/binder (w/b) ratios, it was decided that concrete ranging from high strength structural concrete to low strength mass concrete should be considered. This is to ensure that concrete grades tested reflected concrete commonly used on construction sites in South Africa. The following w/b ratios were selected to produce these concretes:

a) 0.4 w/b;
b) 0.5 w/b;
c) 0.6 w/b;
d) 0.75 w/b.

The binder content required to achieve the above concrete qualities for the different binder types were determined from trial methods by adjusting the water and or binder content (Addis & Goodman, 2009).

3.2.4 Moist curing period

In order to have models that are of relevance to the South African concrete industry, concretes with different strength and qualities of near surface zone – in terms of fluid flow and chemical properties as well as conditions concretes are likely to face on construction sites, the following curing conditions were selected:

a) 3 days moist, then exposed to air;
b) 7 days moist , then exposed to air;
c) 28 days moist, then exposed to air.

Hence, it was considered that water curing for up to 7 days represented the full range of site conditions concrete are exposed to in most construction sites, while the 28 days water curing condition represented "ideal" curing which is often not achieved on construction site and is used as a reference.

3.2.5 Mixing and compaction

The same procedure was used in the making of the concretes in terms of the mixing and compaction process for all the concrete mixtures tested in this study. Concretes were compacted using the same method and given similar compaction duration. The intention was to produce concretes under similar processing influence. This is because the degree of concrete compaction affects its microstructure and this may in turn create variability in the carbonation processes of the concrete as well as its permeation and chemical properties.

3.2.6 Age at testing

Two test ages (early-age and medium-term) were selected at which the concrete were characterised in terms of their physical and/or chemical properties and one test age (medium-term) for durability performances characterisation of the concretes in terms of their carbonation depth:

a) Early-age (28 days) characterisation of concrete – to provide an early-age measure of the properties of concrete on which the long-term durability performance and service life of the concretes could be based, and Medium-term (6, 12 and 18 months) characterisation of concrete – to provide a medium-term measure of the variations of the permeation properties of the concrete with advance of carbonation and other exposure effects;
b) Medium-term (6, 12, 18 and 24 months) carbonation depth tests – to provide a medium-term measure of the durability performance of the concrete with variation in micro-climate.

3.3 Properties of the Materials Used

3.3.1 Cement

The cement used in making the concretes was an *OPC* available as *CEM I* and of strength grade 52.5 N, obtained from Pretoria Portland Cement (*PPC*) (Ltd) in a single bulk delivery. Upon receipt at the laboratory the cements were stored in airtight containers to prevent deterioration. Approximately 800 g was obtained from one of the pockets and sent to *PPC* Technical Services Division for chemical analysis. The results of the analysis are presented in Table 3.1. The result obtained show that this cement lies in the typical value of South Africa *CEM I* and satisfies the requirement of SABS EN 197-1 (SABS, 2000).

3.3.2 FA

The *FA* used was obtained from Ash Resources (Pty) Ltd in a single bulk delivery. Upon receipt at the laboratory the *FA* was stored in airtight containers to prevent deterioration. Approximately 800 g was obtained from one of the pocket and sent to *PPC* Technical Services Division for chemical analysis. The results of the analyses are presented in Table 3.1. The chemical composition analysis of the *FA* shows that the *FA* is typical of South Africa *FA* and conforms to SABS 1491: Part 2 (SABS, 1989b).

3.3.3 GGBS

The *GGBS* used in the concretes was obtained from the Vanderbijlpark plant of slagment (Pty) Ltd in a single bulk delivery. Upon receipt at the laboratory the slags were stored in airtight containers to prevent deterioration. Approximately 800 g was obtained from one of the pockets and sent to *PPC* Technical Services Division for chemical analysis. The results of the analyses are presented in Table 3.1. The results of the chemical analysis show that the *GGBS* is typical of South Africa *GGBS* and it satisfies the requirement of SABS 1491: Part 1 (SABS, 1989a).

On the basis of the calculated hydraulic index (H.I. = 1.62), the *GGBS* used in this study would be considered of an acceptable quality. Additionally, the H.I results lie within the typical values of South African *GGBS*.

3.3.4 CSF

The *CSF* used in the concretes was obtained from Holcim South Africa (Pty) Ltd in a single bulk delivery. Upon receipt at the laboratory the *CSF* were stored in airtight containers to prevent deterioration. Approximately 800 g was obtained from one of the pocket and sent to *PPC* Technical Services Division for chemical

analysis. The results of the analyses are presented in Table 3.1. The result shows that the *CSF* is typical of South Africa *CSF* and satisfies the requirement of SABS 1491: Part 3 (SABS, 1989c).

3.3.5 Composite cement

The composite cement used in making the concretes was an all-purpose Portland composite cement (*PCC*) available as *CEM V A (S-V)* and of strength class 32.5 N obtained from Holcim South Africa (Pty) Ltd in a single bulk delivery. Upon receipt at the laboratory the composite cements were stored in airtight containers to prevent deterioration. Approximately 800 g was obtained from one of the pocket and sent to *PPC* Technical Services Division for analysis. The results of the analyses are presented in Table 3.1. The result obtained shows that the composite cement chemical composition values lie in the typical range of South Africa *CEM V* and satisfies the requirement of SANS 50197-1/SABS EN 197 – 1:2000 (SABS, 2000). The South African *CEM V* contains a combination of *GGBS* and *FA* as mineral component at a combined 36-60 % by mass.

Table 3.1: Oxide analysis of binders (%) used

Oxides	*CEM I*	*FA*	*GGBS*	*CSF*	*CEM V*
LOI	3.04	0.69	None	4.00	4.02
SiO_2	21.85	52.96	36.59	88.73	30.02
Al_2O_3	5.10	30.19	13.35	0.60	11.59
CaO	62.84	4.50	36.33	1.35	43.77
Fe_20_3	3.41	3.33	0.78	2.61	2.41
MgO	2.28	0.91	7.35	0.86	2.34
TiO_2	0.43	1.56	0.65	0.01	0.65
Mn_2O_3	0.45	0.07	0.72	0.09	0.17
Na_2O	0.07	0.21	0.24	0.20	0.13
K_2O	0.32	0.79	1.11	2.25	0.68
P_2O_5	0.09	0.45	0.02	0.14	0.14

3.3.6 Aggregates

In the development of the experimental component of the study, it was felt that thermogravimetric analysis (*TGA*) and wet chemical analysis techniques could be used to characterise the early-age chemical composition of the concretes. The use of these techniques in the analysis of concrete is often hampered by similarities in the chemical composition of aggregates and the binder component of the concrete. In order to avoid this problem, it was decided to use granite as both coarse and fine aggregate. These materials were obtained from Jukskei quarry in Johannesburg, South Africa. Jukskei quarry is one of the main sources of aggregates used in many parts of South Africa. On receipt, the aggregates were air dried under laboratory condition. Both the coarse and fine aggregates satisfied the requirements of SABS 1083 (SABS, 1979).

Coarse aggregate

The granite stone used was classified as "-19 mm" and found to have grading as shown in Table 3.2. The corresponding grading curve is shown in Figure 3.1. It is notable from the grading curve that the coarse aggregate sample contained sizes less than 19 mm and was not single-sized. Based on the ASTM C125 definition, a 19 mm nominal maximum stone size (i.e. the smallest sieve opening through which the entire amount of aggregate is permitted to pass) must have the entire aggregate pass through the 25 mm sieve which is the case for the stone grading in Figure 3.1.

Table 3.2: Coarse aggregate (Granite stone) sieve analysis

Sieve size (mm)	Mass retained (g)	Cumulative % mass retained	% mass Passing	Cumulative % mass passing
26.5	0	0	1587.5	100.0
19.0	400.3	25.2	1187.2	74.8
13.2	782.2	74.5	405.0	25.5
9.5	328.6	95.2	76.4	4.8
6.7	55.5	98.7	20.9	1.3
Pan	20.9	100.0	0	0
Sample size:	1587.5 g			

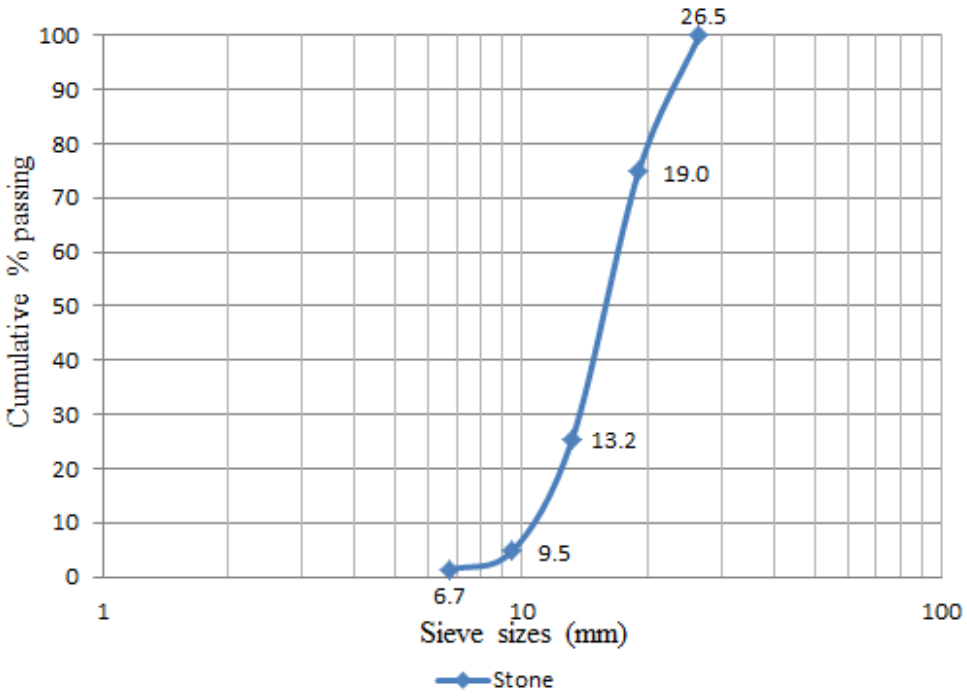


Figure 3.1: Grading curve of coarse aggregate (Granite)

Fine aggregate

A sample of material obtained from the Jukskei quarry, classified as granite crusher sand was found to have grading as shown in Table 3.3. The corresponding grading curve is shown in Figure 3.2. It can be seen from the analysis that the material as received was good for concrete sand as it meets the requirement of ASTM C125.

Granite crusher sand has the advantage of superior particle shape, uniformity of grading and is less likely to contain deleterious substances (such as clay minerals and organic matter) compared to natural sand (pit sand). In addition, it has the advantage of reducing water requirement and saves cement. Although the fineness modulus for the granite crusher sand falls outside of the recommended limits of 1.6 to 3.5 (SABS, 1976), visual inspection of the trial mixes confirmed that the effect on workability and cohesiveness was not large enough to warrant blending with finer sand. Again, as stated before, the intention of the experimental program

was to produce concrete with materials commonly used on construction projects in South Africa.

Table 3.3: Fine aggregate (Granite crusher sand) sieve analysis

Sieve size (mm)	Mass retained (g)	Cumulative % mass retained	% mass Passing	Cumulative % mass passing
6.75	0	0	755.3	100.0
4.75	58.8	7.8	696.5	92.2
2.36	157.6	28.7	538.9	71.4
1.18	141.4	47.4	397.5	52.6
0.60	115.4	62.7	282.1	37.4
0.30	97.9	75.6	184.2	24.4
0.15	69.4	84.8	114.8	15.2
0.075	45.6	90.8	69.2	9.2
Pan	69.2	100.0	0	0
Sample size:	755.3 g			

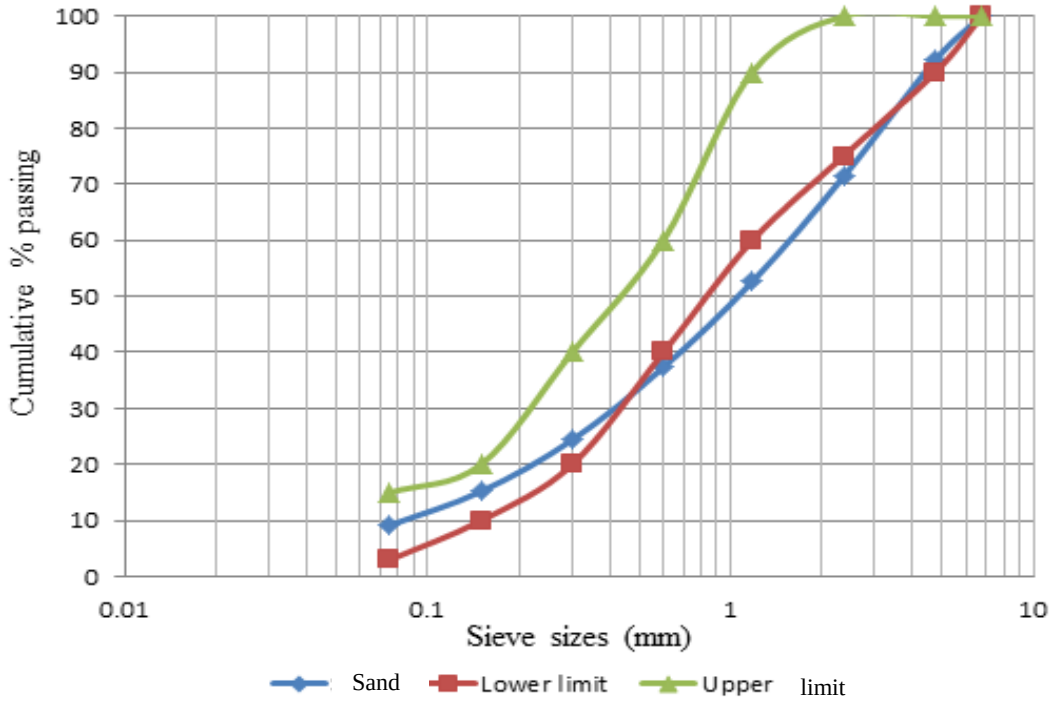


Figure 3.2: Grading curve of fine aggregate (Granite crusher sand)

3.3.7 Admixtures

The plasticizer used in some of the mixes was Chryso Plast 90. It is supplied as a light brown liquid, easily dispersed in water and has a relative density of 1.02±0.02 %. It complies with EN 934 (934-2, 2001).

3.4 Laboratory and Field Testing Procedure

3.4.1 Concrete mixtures

Concrete was prepared using the materials described in section 3.3, with binder types and w/b ratios as discussed in sub sections 3.2.2 and 3.2.3 respectively. The concretes were produced for each mixture by keeping the water content the same for each w/b ratio and the resulting slump measured as shown in Table 3.4. However, plasticizer was added to the 0.4 and 0.5 w/b ratio mixtures to ensure a

minimum slump of 25 mm and 40 mm respectively. For all mixtures, the maximum slumps were not controlled.

Table 3.4 shows the mixture proportions of each of the concrete used in the study. These proportions were determined on the basis of trial mixes (Addis & Goodman, 2009).

Table 3.4: Mixture proportions (kg/m^3) of the various concretes used

Binder combination	Concrete mixture label	Binder					Aggregate		Water content	Water/ binder ratio	Admixture (l)	Slump (mm)	28 day compressive strength (MPa)
		CEM I	*FA*	*GGBS*	*CSF*	*CEM V*	Coarse	Fine					
100% CEM I	PC-40	450	-	-	-	-	990	800	180	0.4	4.00	30	75.93
	PC-50	400	-	-	-	-	990	877	200	0.5	3.25	60	64.5
	PC-60	350	-	-	-	-	1015	869	210	0.6	-	100	49.23
	PC-75	300	-	-	-	-	1050	810	225	0.75	-	140	36.00
70/30 CEM I-FA	FA-40	315	135	-	-	-	990	800	180	0.4	1.75	40	62.80
	FA-50	280	120	-	-	-	990	877	200	0.5	1.70	85	52.13
	FA-60	245	105	-	-	-	1015	869	210	0.6	-	170	37.80
	FA-75	210	90	-	-	-	1050	810	225	0.75	-	185	28.10
50/50 CEM I-GGBS	SL-40	225	-	225	-	-	990	800	180	0.4	1.65	25	61.10
	SL-50	200	-	200	-	-	990	877	200	0.5	1.60	40	48.40
	SL-60	175	-	175	-	-	1015	869	210	0.6	-	60	30.83
	SL-75	150	-	150	-	-	950	900	225	0.75	-	110	22.87
90/10 CEM I-CSF	SF-40	405	-	-	45	-	990	800	180	0.4	4.25	30	91.40
	SF-50	360	-	-	40	-	990	877	200	0.5	3.50	45	76.93
	SF-60	315	-	-	35	-	1015	869	210	0.6	-	85	59.47
	SF-75	270	-	-	30	-	950	900	225	0.75	-	115	41.40
100% CEM V	CC-40	-	-	-	-	450	990	800	180	0.4	1.90	25	58.87
	CC-50	-	-	-	-	400	990	877	200	0.5	1.75	65	47.93
	CC-60	-	-	-	-	350	1015	869	210	0.6	-	120	37.17
	CC-75	-	-	-	-	300	1050	810	225	0.75	-	160	24.43

3.4.2 Concrete cube samples requirement and storage

The 123 concrete cube samples cast for each of the concrete mixtures shown in Table 3.4 were divided for the purpose of curing and testing as shown in Table 3.5. This Table shows that for the compressive strength and chemical composition testing, fifteen concrete cubes were cast and tested for each concrete mixture at three test ages to monitor the quality and chemical composition of the concretes. Fifty four concrete cube samples were cast and tested for the early-age and medium-term oxygen permeability and water sorptivity at four ages after an initial 3, 7 and 28 days of initial moist curing. Table 3.5 also shows that for the accelerated carbonation test and each of the natural exposure carbonation test, four samples were tested each for carbonation depth at four ages for the three initial moist curing periods after casting.

Table 3.5: Summary of concrete cube samples treatment for the different tests

Test	Initial moist curing period	No. of cubes per mixtures	Preconditioning	Testing ages
Compressive strength test	3,7 and 28 days	9	Nil	Test at 3, 7 and 28 days.
Chemical composition test	3, 7 and 28 days	6	Nil	Test at 3, 7 and 28 days
Durability index test (Early-age)	3, 7 and 28 days	6	Laboratory air drying after each of the curing regimes until tested	Test between 28-32 days
Accelerated carbonation depth test (Early-age)	3, 7 and 28 days	12	Laboratory air drying for 14 days after each of the curing regimes and then placed in a carbonation chamber until tested	Test after 7, 14, 21 and 28 days.
Durability index test (Medium-term)	3, 7 and 28 days	54	Laboratory air drying for 14 days after each of the curing regime and then placed on exposure sites until tested.	Test after 6, 12 and 18 months.
Natural carbonation depth test (Medium-term)	3, 7 and 28 days	36	Laboratory air drying for 14 days after each of the curing regimes and then placed on exposure sites until tested	Test after 6, 12, 18 and 24 months.

3.4.3 Concrete cube samples preparation and processing

Mixing procedure

Concrete cube samples measuring 100 x 100 x 100 mm were cast using each of the concrete mixtures listed in Table 3.4. The solid materials were weight batched on a laboratory balance to an accuracy of 50 g. The water and plasticizer was

volume batched using different cylinders. Mixing was carried out in a 50 liter pan mixer and the following procedure was used:

- Introduce dry materials into the mixer in the order of stone, binder and sand;
- Activate the mixer and add the water over the second minute of mixing;
- Mix for a further one minute.

At the end of each mixing cycle, the mix was manually distributed in the pan using a hand-held scoop. This ensured a uniform distribution of the material as some segregation was noticed resulting from the operation of the mixer. For some mixtures, the amount of admixture content was varied to bring it to the required workability. A slump test was then performed to ascertain if the mix fell within the desired slump range. If the slump criterion was not met, plasticizer was incrementally added and mixed for 1 minute before repeating the slump test. This procedure was repeated until the desired slump range was obtained (see Table 3.4 for the individual concrete slump value).

To reduce variability in the concrete cube samples produced and in the test results since the concrete pan mixer cannot produce the required concrete volume per mixture in a single operation, the concretes were produced in batches. Three mix batches were produced per concrete mixtures. The first batch of concrete mix was for the production of 33 concrete cube samples, used for the compressive strength, chemical composition, early-age durability index and accelerated carbonation depth tests. The second batch of concrete mix was for the production of 36 concrete cube samples used for the natural carbonation depth testing. The last batch of concrete mix was used for the production of 54 concrete cube samples used for the medium-term site durability index test for monitoring the variation in the permeation properties of the concrete mixtures. The individual concrete slump values reported on Table 3.4 are averages of three measurements.

Compaction

The 100 mm cube moulds were loosely filled with concrete and compacted by holding each mould onto a high-speed vibrating table, then topped-up during vibration. The vibration period varied from 20 – 30 seconds. The compacted concrete moulds were then marked and placed in a laboratory room where the temperature and relative humidity were at prevailing laboratory condition (23±2 ^{o}C for temperature and 60±5 % for relative humidity) and were covered with plastic sheet.

Curing

The concrete cube samples were de-moulded after 22±2 hours, grouped into three sets and each set subjected to the following curing conditions:

a) The first set of samples were placed in a water curing tank at 22±1 ^{o}C for the next 2 days then tested, or stored in laboratory air at the prevailing temperature of 23±2 ^{o}C and relative humidity of 60±5 % up to the time of testing, or preconditioned for 14 days in the laboratory room before exposure to carbonating environments;
b) The second set of samples were placed in a water curing tank at 22±1 ^{o}C for the next 6 days then tested, or stored in laboratory air at the prevailing temperature of 23±2 ^{o}C and relative humidity of 60±5 % up to the time of testing, or preconditioned for 14 days in the laboratory room before exposure to carbonating environments;
c) The last set of samples were placed in a water curing tank at 22±1 ^{o}C for the next 27 days then tested, or stored in laboratory air at the prevailing natural temperature of 23±2 ^{o}C and relative humidity of 60±5 % up to the time of testing, or preconditioned for 14 days in the laboratory room before exposure to carbonating environments.

At the end of the water curing periods, as stated above, the samples were either tested for compressive strength or chemical composition or stored in the

laboratory room until tested at between 28 and 32 days for early-age permeation properties or were preconditioned for 14 days in a laboratory room without temperature or RH control before exposure to an accelerated or natural carbonating environments. Hence, nominal water curing periods of 3, 7 and 28 days were used. These curing periods were chosen on the basis that they represent on-site conditions, viz: average, good and ideal curing respectively.

Preconditioning and exposure

At the end of the stated moist curing period, the appropriate concrete cube samples were removed from the water tank and transferred to the laboratory room (see Figure 3.3) at the prevailing natural conditions until tested or transferred to different exposure sites. The temperature and relative humidity in the laboratory room during exposure were monitored and ranged between 18 - 23 ^{o}C and 54 - 63 % respectively.

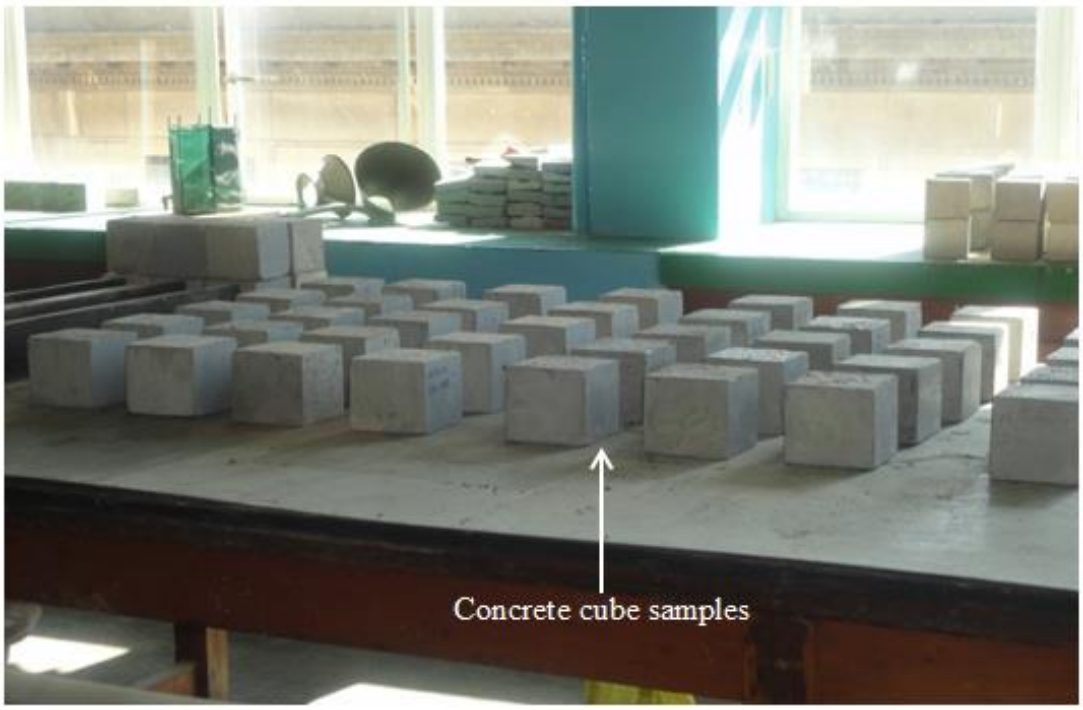


Figure 3.3: Concrete cube samples in the laboratory room after moist curing, during preconditioning

While in the laboratory room, the concrete cube samples for carbonation depth testing were surface-dried and four contiguous surfaces of each cube were coated using water based epoxy (sold as “Stonehard”, manufactured by StonCore Africa (Pty) Ltd. South Africa). The four coated surfaces included the top and bottom surfaces as cast. Two coats of the epoxy were applied, with the second coat being applied approximately 24 hours after the first.

At the end of the preconditioning period the samples were taken to the different exposure sites and arranged such that carbonation of the concrete cubes took place through two opposite formed faces. The concrete cubes were arranged with a spacing of at least 50 mm between neighbouring concrete cubes. The same arrangements were used for the accelerated carbonation exposure condition (see Figures 3.4 to 3.10). It was reasoned that exposing the concrete cubes samples to the same laboratory air preconditioning for 14 days would stabilize the internal moisture conditions of the concrete and the effect of an unusual weather conditions when first exposed outdoors will have a similar effect on all comparable concretes.

It should be noted that the concrete casting process ranged over 12 weeks. And in regard to the laboratory preconditioning environment, the variations in temperature and relative humidity in the laboratory room over this period will have influenced the rate of hydration for the concretes cube samples and it is likely that this may have affected the durability index test results at early-ages. These possible effects must be borne in mind when interpreting the permeability and sorptivity tests results.

Photographs of concrete cube samples and data loggers, in the accelerated carbonation chamber and on the different inland exposure conditions are shown in Figures 3.4 to 3.10.

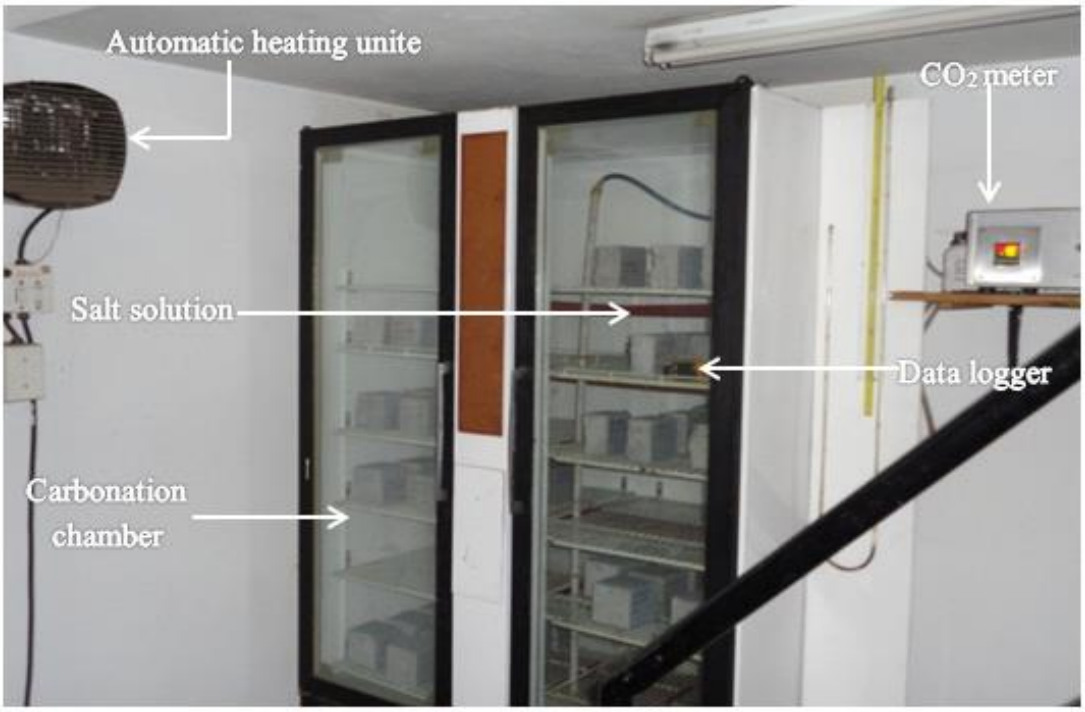


Figure 3.4: Concrete cube samples inside a micro-climate controlled accelerated carbonation chamber located in a temperature controlled room

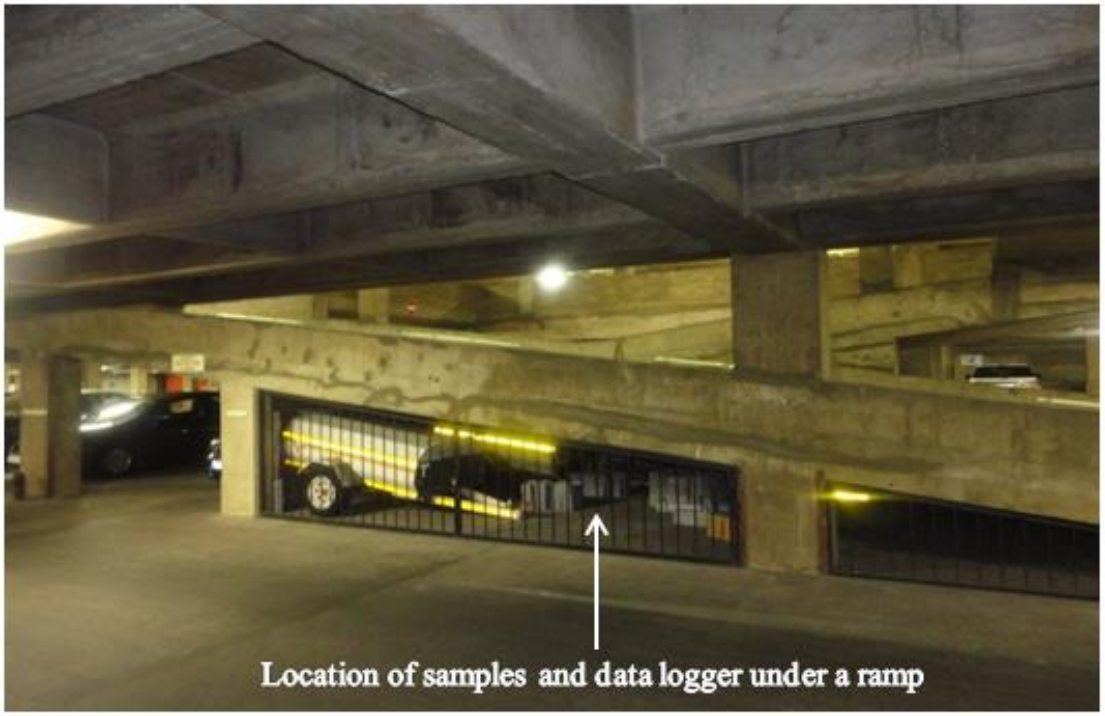


Figure 3.5: View of a basement parking garage indicating the location where the concrete cube samples and data logger were placed

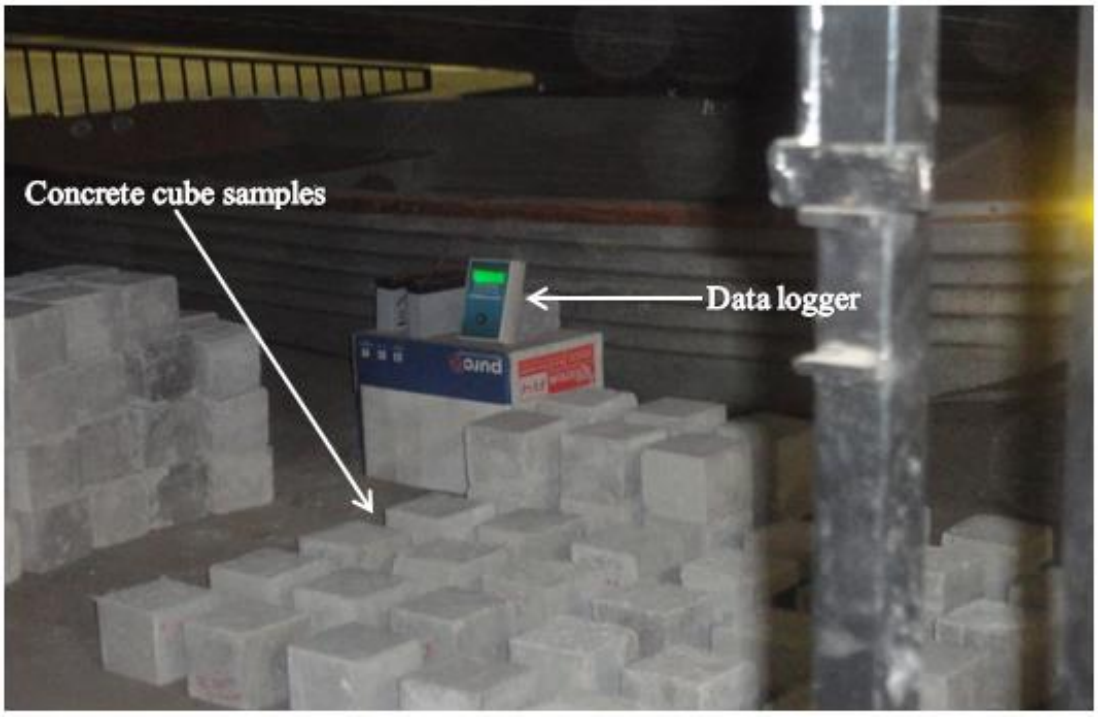


Figure 3.6: Concrete cube samples and data logger in a basement parking garage (indoor condition)



Figure 3.7: View of a foot bridge across a busy highway indicating where the concrete cube samples and data logger were placed

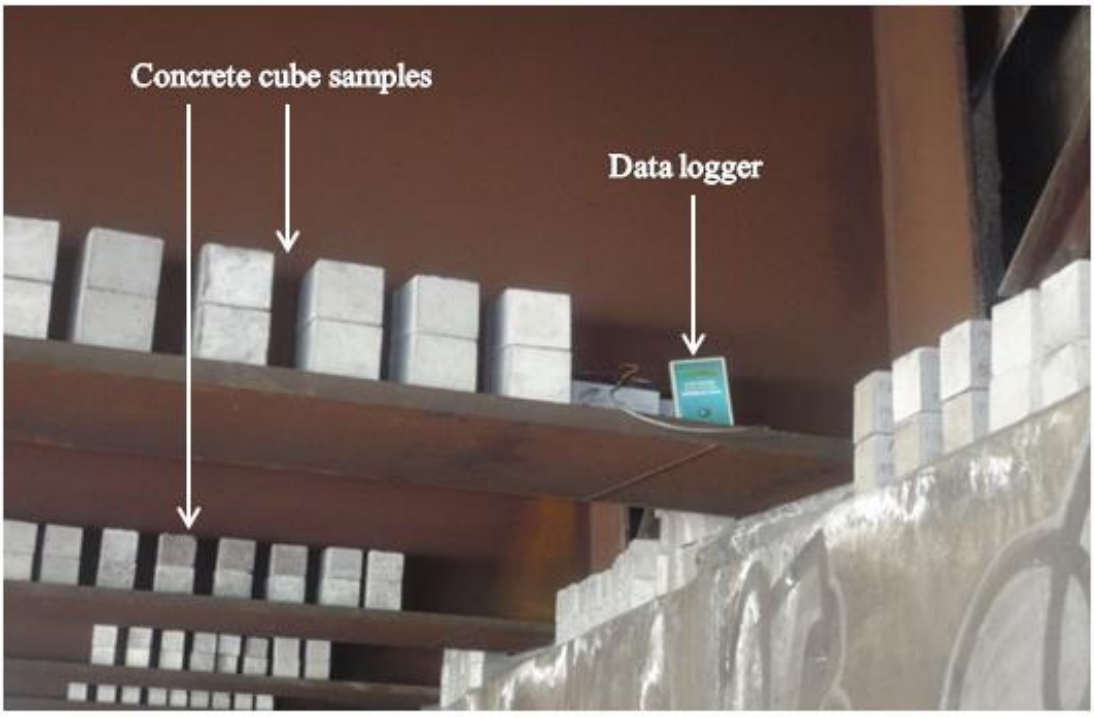


Figure 3.8: Concrete cube samples and data logger under a foot bridge across a busy highway (outdoor sheltered condition)

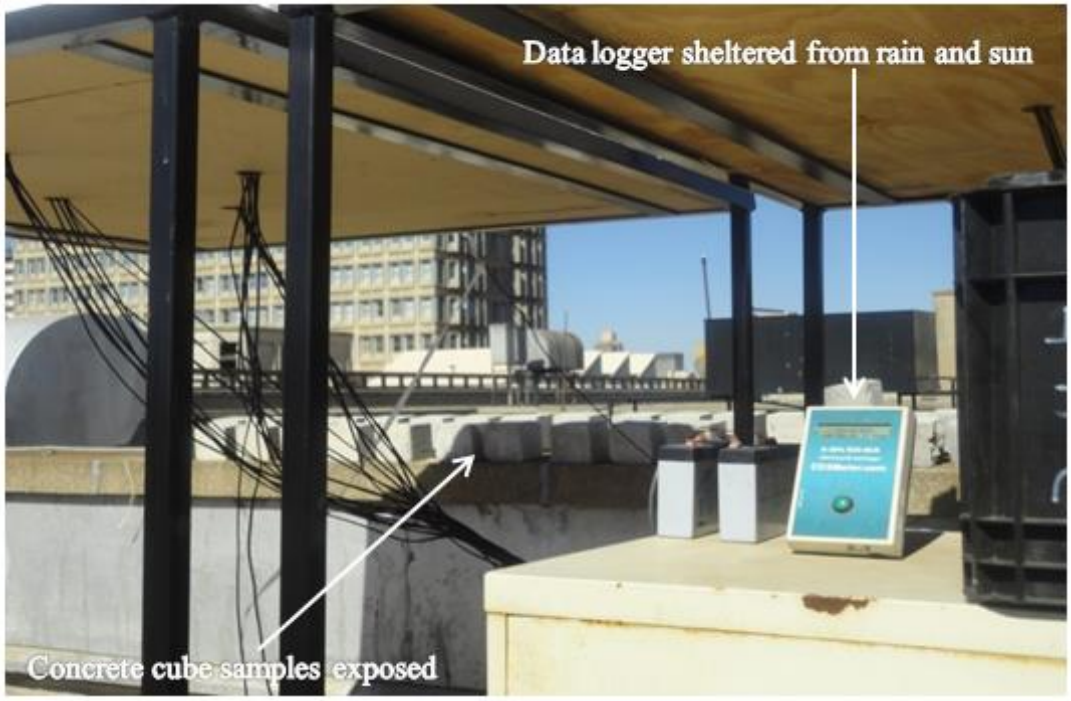


Figure 3.9: Outdoor exposed condition showing exposed concrete cube samples and data logger sheltered from rain



Figure 3.10: Concrete cube samples on the roof top of a building in an urban setting (outdoor exposed condition)

3.5 Test Methods

3.5.1 Compressive strength tests

In order to characterise the concrete mixtures in compressive strength terms, 100 x 100 x 100 mm concrete cube samples were tested in compression at 3, 7 and 28 days after casting under standard curing conditions. Compressive strength tests were conducted to monitor the quality of the produced concrete, the strength development of the different concrete mixtures and the possibility of using the compressive strength values of the concrete to predict its durability performance and service life. The compressive strength test were carried out in accordance with the SANS (1994) method using an Amsler compression testing machine with a capacity of 2000 kN. All samples were weighed in a saturated, surface dry condition to an accuracy of 5 g before being tested.

3.5.2 Durability index tests

Durability index tests for early-age durability characterisation of the concrete mixtures were carried out on specimen obtained from concrete cube samples at 28 days after casting. For some concrete cube samples, the work schedule did not allow obtaining specimen at 28 days and on occasions, were conducted after 28 days and in no case later than 32 days. This is in accordance with the proposed durability index tests method (Alexander et al., 1999). To monitor the permeation properties of the near-surface concrete in the medium-term for the different exposure conditions, durability index tests were performed on specimens (discs) obtained from concrete cube samples after 6, 12 and 18 months of exposure.

The oxygen permeability and water sorptivity tests were the only durability index test conducted on the discs. The tests were performed in a temperature and humidity controlled room following the procedures outlined in the Draft SANS test specification of 2010, which is a revised version of the Durability Index Testing Manual (Alexander et al., 1999). The durability index tests were performed at the Durability Laboratory, School of Civil and Environmental Engineering, University of the Witwatersrand, South Africa.

Preparation of test discs for the durability index tests

At the appropriate time as indicated in Table 3.5, concrete cube samples were removed from the laboratory room or exposure sites for the coring operation. Coring of the concrete cube samples was carried out perpendicular to the casting direction using a high speed, water-cooled diamond tipped core barrel (with a nominal inner diameter of 70 mm) attached to a coring drill. The first 5 mm from either side of the exposed faces of the core is cut off using a water-cooled moveable bed diamond saw and discarded. Using the same cutting tool, the required disc thickness (30±2 mm) was cut from either side of the core as shown in Figure 3.11. The test discs obtained from the opposite faces of the concrete cube sample were marked with the correct reference number on the original

interior face. The discs were then transferred to a 50±2 ºC ventilated oven to be dried for a minimum of 7 days ± 4 hours before being tested for oxygen permeability and water sorptivity tests.

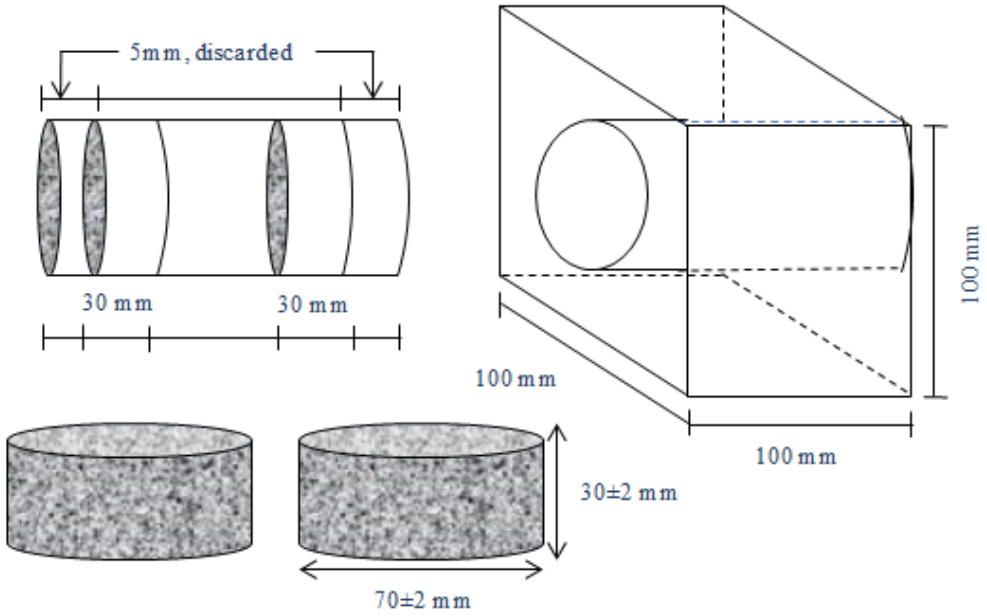


Figure 3.11: Preparation of discs from a concrete cube sample

Oxygen permeability test

At the end of the oven drying period, the discs (70±2 mm Ø and 30±2 mm thick) were taken out of the oven and kept in a laboratory room where the temperature and relative humidity were controlled at 22±1 ºC and 60±5 % respectively and treated as follows:

a) Weigh to an accuracy of 0.01 g to determine the oven dry weight;
b) Measure the thickness and diameter at 4 points equally spaced around the perimeter using a vernier caliper and the averages determined;
c) Left in the laboratory room for approximately 2 - 4 hours to allow it cool to room temperature before testing;
d) Place the discs in the compressible collar within the rigid sleeve with the test face (outer face) at the bottom (see Figure 3.12). Figures 3.12 (a) and

(b) show a typical sealing arrangement and the oxygen permeability experimental set-up respectively.

The discs were then tested for oxygen permeability using the falling head permeameter as described in the Durability Index Testing Manual (Alexander et al., 1999), originally developed by Ballim (1994). The test is based on deriving the D'Arcy coefficient of permeability by monitoring a falling pressure head. Four discs are tested for each concrete mixture by applying an initial pressure of 100 kPa to one side of the concrete disc with the other side at normal atmospheric pressure. As permeation occurs, the decrease in pressure with time is measured at an interval of 15 minutes for 2 hours (a minimum of 8 readings is required per test). The pressure decay curve is measured directly from gauges using data logging from transducers and converted to a linear relationship by plotting the logarithm of the ratio of pressure heads versus time. This plot can be conducted on a standard spreadsheet software system (see Table 3.6 and Figure 3.13).

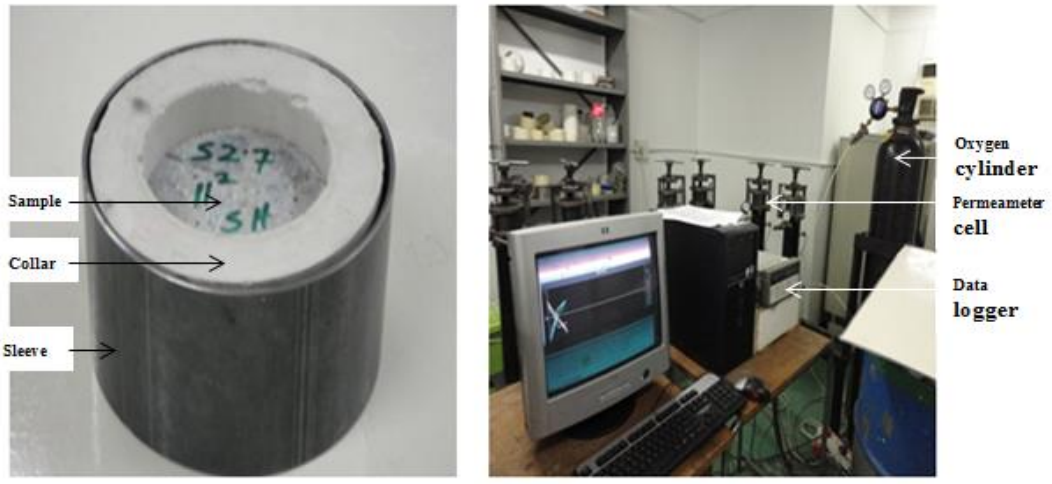


Figure 3.12: (a) Oxygen permeability sample unit (b) Oxygen permeability experimental set-up

Estimation of the discs permeability value

The pressure readings were captured at regular intervals by the data loggers and stored on the computer system for a set of four concrete discs during the oxygen permeability test. These results were then used as input onto the analysis spreadsheet (Alexander et al., 1999). This analysis spreadsheet performs the calculations described in section 2.3.3 and the results of the permeation property of the discs in terms of oxygen permeability are given as average coefficients of permeability, *k* or as average oxygen permeability index, *OPI* value. A typical result from the analysis spreadsheet is shown in Table 3.6 and the individual concrete discs pressures versus time plots presented in Figures 3.13. From Table 3.6, the average results for the discs permeability are highlighted in red.

Table 3.6: Typical oxygen permeability test analysis

University of Cape Town and University of Witswatersrand							
Departments of Civil Engineering							
Oxygen Permeability Test Analysis							
Sample ID:	PC-40-3			Operator:	AY		
Date:	8/12/2012						
Average k (m/s):	1.2E-10	COV:	25.9	%			
OPI:	9.9						
1		2		3		4	
Diameter (mm)	68.63	Diameter (mm)	68.28	Diameter (mm)	68.42	Diameter (mm)	68.15
Thickness (mm)	30.62	Thickness (mm)	29.99	Thickness (mm)	30.76	Thickness (mm)	28.47
k (m/s)	7.17019E-11	k (m/s)	1.36461E-10	k (m/s)	1.21897E-10	k (m/s)	1.32275E-10
r^2	0.9999	r^2	0.9995	r^2	0.9996	r^2	0.9998
Time	Pressure	Time	Pressure	Time	Pressure	Time	Pressure
(hh.min)	(kPa)	(hh.min)	(kPa)	(hh.min)	(kPa)	(hh.min)	(kPa)
16.07	102.8	16.07	104.8	16.07	105.9	16.07	102.8
16.22	101.6	16.22	102.3	16.22	103.6	16.22	100.3
16.37	100.4	16.37	99.9	16.37	101.4	16.37	97.9
16.52	99.1	16.52	97.5	16.52	99.4	16.52	95.5
17.07	97.8	17.07	95.2	17.07	97.3	17.07	93.2
17.22	96.6	17.22	92.9	17.22	95.3	17.22	90.9
17.37	95.4	17.37	90.8	17.37	93.3	17.37	88.8
17.52	94.2	17.52	88.7	17.52	91.4	17.52	86.7
18.07	93.1	18.07	86.6	18.07	89.6	18.07	84.6

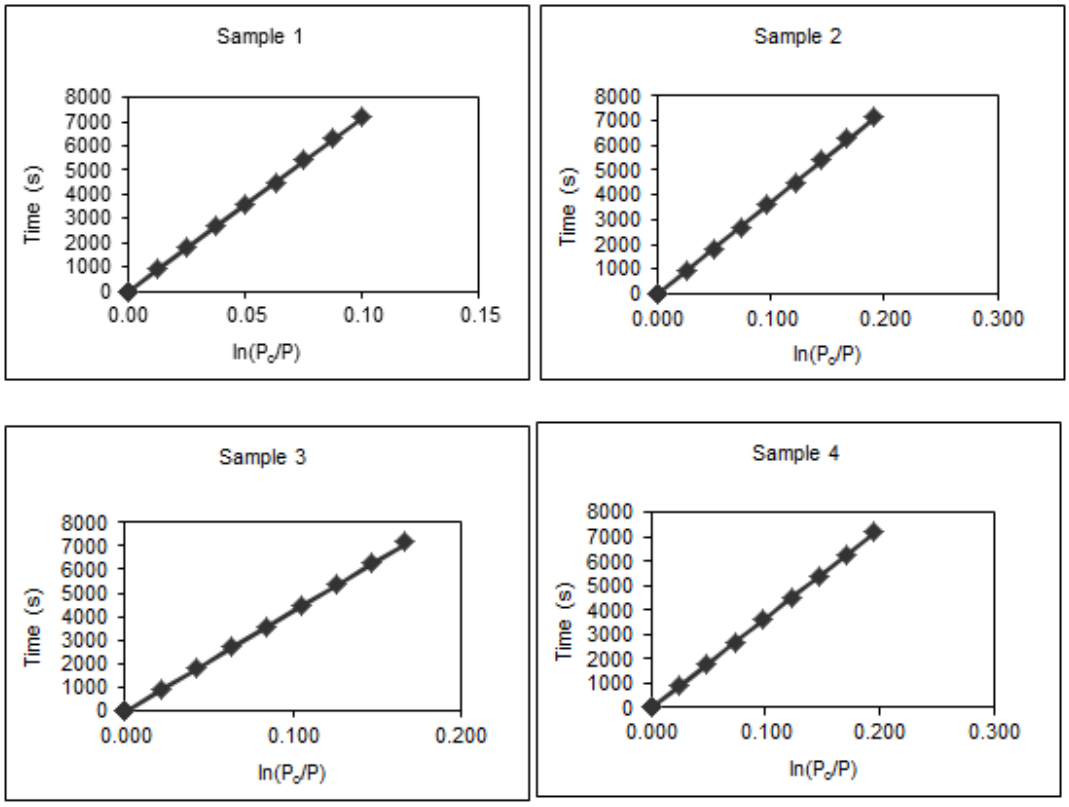


Figure 3.13: Typical plots of logarithm of the ratio heads versus time

Water sorptivity test

For the water sorptivity test, the method originally developed by Ballim (1994) but more carefully described in the Durability Index Testing Manual (Alexander et al., 1999), was followed. A layer of tape was placed on the circumferential surface of the discs. By periodically placing the discs onto a free water surface that consist of layers of absorbent paper placed in a plastic tray containing a solution of distilled water saturated with $Ca(OH)_2$, the rate of absorption is monitored by weighing the discs on an electronic balance. The discs were weighed at 0, 3, 5, 7, 9, 12, 16, 20 and 25 minutes, after patting it once on a damp piece of absorbent paper before being placed on the scale. The discs were then vacuum saturated to determine the saturated mass (see Figures 3.14).

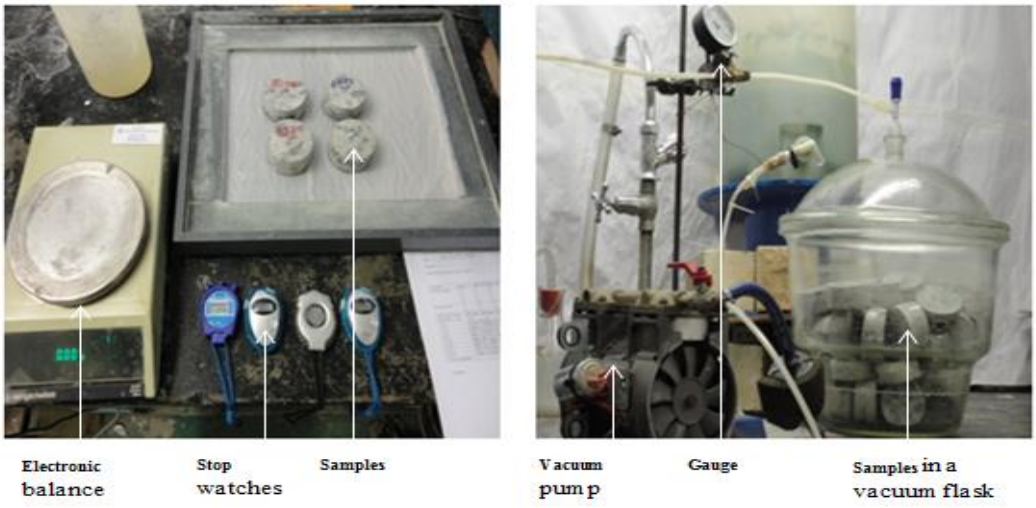


Figure 3.14: (a) Water sorptivity experimental set-ups (b) Concrete discs in a vacuum for saturated weight determination

Estimation of the discs water sorptivity value

The discs mass readings at the stated intervals and its vacuum saturated mass obtained during the water sorptivity test for a set of four concrete discs are used as input onto a standard analysis spreadsheet (Alexander et al., 1999). The analysis spreadsheet performs the calculations described in section 2.3.3 and the results of the permeation property of the discs are obtained as average sorptivity in mm/√hr. and porosity in %. A typical result from the analysis spreadsheet is shown in Table 3.7, and the individual concrete discs mass gained versus square root of time plots are given in Figure 3.15. From Table 3.7, the average results for the discs sorptivity and porosity value are highlighted in red.

Table 3.7: Typical water sorptivity test analysis and plots

University of Cape Town and University of Witswatersrand
Departments of Civil Engineering
Sorptivity Test Analysis

Sample ID: PC-40-3 Operator: AY
Date: 9/3/2012

Av. Sorptivity: 8.2 COV: 9.6
Av. Porosity: 10.9 COV: 16.1

Sample ID	1	2	3	4
Diameter (mm)	68.63	68.28	68.42	68.15
Thickness (mm)	30.62	29.99	30.76	28.47
Time (min)	Mass (g)	Mass (g)	Mass (g)	Mass (g)
0	259.42	249.13	254.13	231.49
3	260.09	249.94	254.8	232.31
5	260.27	250.14	254.97	232.52
7	260.41	250.31	255.13	232.7
9	260.54	250.44	255.25	232.84
12	260.72	250.62	255.4	233.03
16	260.92	250.85	255.59	233.28
20	261.12	251.04	255.74	233.45
25	261.28	251.24	255.91	233.66
Saturated Mass (g)	270.17	260.68	265.75	243.04
R^2 (Must be >0.98)	0.9992	0.9992	0.9998	0.9998
Range	3-25 min	3-25 min	3-25 min	3-25 min
Sorptivity (mm/hr$^{0.5}$)	8.2	8.0	9.2	7.3
Porosity (%)	9.5	10.5	10.2	13.5

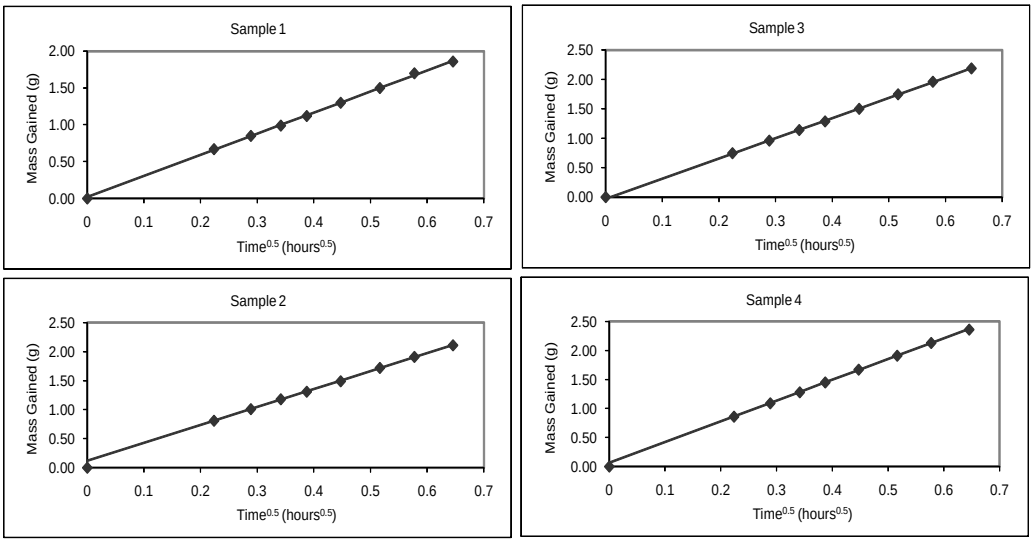


Figure 3.15: Typical plots of individual concrete discs mass gained versus square root of time

3.5.3 Chemical composition tests

The chemical composition of the concrete mixtures was determined from concrete cube samples after 3, 7 and 28 days of standard moist curing periods after casting. Thermogravimetric analysis (*TGA*) and wet chemical analysis tests were performed on powdered specimens obtained from the concrete cube samples. The chemical composition of the specimens were determined in terms of the $Ca(OH)_2$ and *CaO* content using the *TGA* and wet chemical analysis tests respectively.

Thermogravimetric analysis (TGA) test

Powdered samples for the *TGA* test were obtained from a 100 x 100 x 100 mm concrete cube samples at the end of each standard moist curing period. A water-cooled, moveable diamond saw was used to cut a 7±2 mm surface slice from the cube, perpendicular to the direction of casting. The cut slice was discarded and the remainder of the concrete cube was placed in an oven at 50±2 ^{o}C to remove much of the evaporable water. At the end of the oven drying period, which was for a minimum of 14 days, the cut face was drilled to a depth of 20±5 mm using a 7mm diameter drill bit. A number of closely-spaced holes were drilled on the interior cut face, avoiding the edges of the concrete cube sample, and the drill powder was carefully collected. The powdered specimens obtained from drilling a cube was then placed in an agate mortar, further ground using a pestle and then sieved through a 63 µm sieve size. The material passing the sieve was preserved under vacuum in airtight bottles and kept up till the time when the *TGA* tests were carried out. The *TGA* test was performed at the School of Chemistry, University of the Witwatersrand, South Africa.

The thermal decomposition behaviour of the powder samples were studied by tracing mass and heat changes using a Perkin Elmer TG400 thermogravimetric analyser coupled to a Setaram differential analyser. The thermal analyser used in this study, enables the thermogravimetric curve (*TG*) and the derivative thermogravimetric curve (*DTG*) to be obtained simultaneously on the specimen. A

powdered specimen weighing 12±2 mg was heated from ambient temperature to 1000 ^{o}C with a 10 ^{o}C per minute heating rate under a nitrogen atmosphere. A plot of temperature against mass loss (*TG* curve) and derivative mass loss (*DTG* curve) is obtained automatically for the analysis. A typical plot of the result analysis is shown in Figure 3.16. The weight loss obtained from the *TG* and the *DTG* curves were used to estimate the amounts of calcium hydroxide ($Ca(OH)_2$) and calcium carbonate ($CaCO_3$) present in the specimen. To illustrate the process of analysis of these results the measurements obtained from three specimens are presented in Table 3.9 and analysed in the section that follows.

Estimation of calcium hydroxide ($Ca(OH)_2$) content in the specimen

The *TG-DTG* plots from the thermal analysis were similar for all the specimens studied. However, the intensity of the peaks varied with hydration time (curing periods) and binder type. Figure 3.16 is a typical *TG-DTG* plot for powder specimen obtained from concrete cube sample made from concrete mixture label PC-40 and moist cured for 3 days.

From the plot, the content of calcium hydroxide and calcium carbonate were estimated from the weight losses measured from the *TG* curve between the initial and final temperatures of the corresponding *DTG* Peaks, considering the following dehydration and de-composition reactions and theoretical weight losses (Dweck et al., 2000):

- Calcium hydroxide decomposition

  $$Ca(OH)_2 \leftrightarrow CaO + H_2O \qquad 3.1$$

- Calcium carbonates decomposition

  $$CaCO_3 \leftrightarrow CaO + CO_2 \qquad 3.2$$

In the estimation of the $Ca(OH)_2$ content of the specimen Equations 3.1 and 3.2 were used, corresponding to the second and third peaks on the *DTG* curve in Figure 3.16. The third peak is as a result of the de-carbonation of $CaCO_3$, formed

by carbonation of *Ca(OH)₂* during specimen preparation. The percentage weight loss at the de-hydroxylation and de-carbonation region was estimated by determining the equivalent weight loss on the *TG* curve at the peak points on the *DTG* curve where such losses occur as shown in Figure 3.16 (Borges et al., 2010; Villain et al., 2007). The results of the respective temperature and weight losses from Figure 3.16 are presented in Table 3.8.

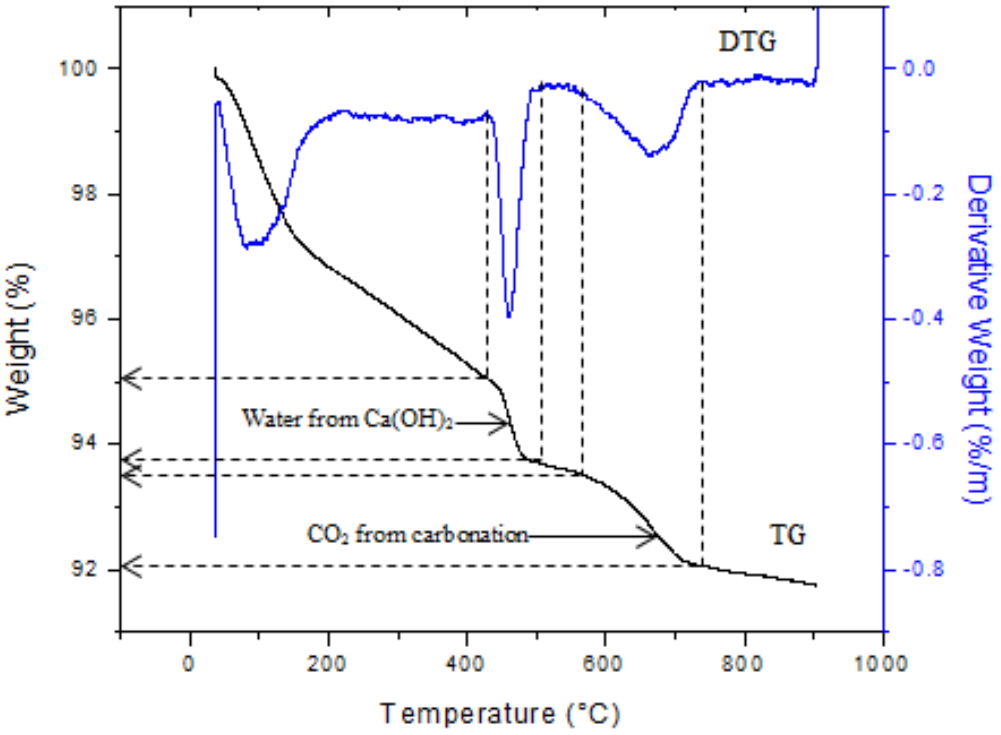


Figure 3.16: TG/DTG curves for PC-40 concrete - 3 days moist curing

Table 3.8: Weight loss in the specimens according to the thermal decomposition from the *TG/DTG* curves

Concrete mixture label/chemical composition	Temperature range (°C) on DTG curve	Retained mass at beginning of peak	Retained mass at end of peak	Estimated weight loss (%)
PC40-3				
$Ca(OH)_2$	428.98 - 491.64	95.05	93.74	1.31
$CaCO_3$	515.16 - 727.97	93.67	92.67	1.00
PC40-7				
$Ca(OH)_2$	426.08 - 510.14	94.72	93.38	1.34
$CaCO_3$	510.14 - 730.09	93.38	92.36	1.02
PC40-28				
$Ca(OH)_2$	426.88 - 507.23	94.06	92.58	1.48
$CaCO_3$	507.23 - 709.73	92.58	91.34	1.25

Considering the stoichiometry of the decomposition of *Ca(OH₂* and *CaCO₃* following the reactions indicated in Equations 3.1 and 3.2, equations were derived for the estimation of the *Ca(OH)₂* contents (see Equations 3.3 to 3.7):

The *H₂O* content from the *TG/DTG* de-hydroxylation loss was calculated using equation 3.1:

$$Ca(OH)_2 \rightarrow CaO + H_2O$$

$$74\ g/mol \quad 56\ g/mol \quad 18\ g/mol \qquad \text{(Molar mass)}$$

$$CH_{dh-loss}(\%) = \frac{dh_{loss}.74}{18} = 4.11\,.\,dh_{loss} \qquad 3.3$$

Where,

$\%CH_{dh-loss}$ = Percentage loss of *Ca(OH)₂* during de-hydroxylation

dh_{loss} = *H₂O* loss from the *TGA* in the de-hydroxylation region

Note that *CaCO₃* was formed as a results of carbonation of *Ca(OH)₂* during the preparation of the specimen following Equation 3.3

$$Ca(OH)_2 + CO_2 \rightarrow CaCO_3 + H_2O \quad 3.4$$

$74\ g/mol \quad 44\ g/mol \quad 100\ g/mol \quad 18\ g/mol$ (Molar mass)

Thus, the amount of *Ca(OH)₂* arising from the decarbonation of *CaCO₃* can be estimated using equation 3.2;

$$CaCO_3 \rightarrow CaO + CO_2$$

$100\ g/mol \quad 56\ g/mol \quad 44\ g/mol$ (Molar mass)

$$CC(\%) = \frac{dc_{loss} \cdot 100}{44} = 2.27\ .\ dc_{loss} \quad 3.5$$

$$CH_{dc-loss}\ (\%) = \frac{CC.74}{100} = \frac{2.27\ .dc_{loss}\ .74}{100} = 1.68\ .\ dc_{loss} \quad 3.6$$

Where,

$CC(\%)$ = Percentage loss of *CO₂* during de-carbonation

$\%CH_{dh-loss}$ = Percentage loss of *Ca(OH)₂* during de-hydroxylation

$\%CH_{dc-loss}$ = Percentage loss of *Ca(OH)₂* during de-carbonation

The total amount of calcium hydroxide (CH_{total}) was estimated by adding the results obtained from Equations 3.3 and 3.6 as shown by Equation 3.7.

$$CH_{total}(\%) = \%CH_{dc-loss} + \%CH_{dh-loss}$$

$$\boldsymbol{CH_{total}(\%) = 1.68\ x\ dc_{loss} + 4.11\ x\ dh_{loss}} \quad \mathbf{3.7}$$

Where,

$CH_{total}\%$ = Total amount of *Ca(OH)₂* in the concrete specimen

dc_{loss} = *CO₂* loss from the *TGA* in the de-carbonation region

Equation 3.7 in conjunction with the weight loss calculation approach shown in Table 3.9 was used in the estimation of the $Ca(OH)_2$ content from the thermal analysis results as given by Figure 3.16. In order to normalise the estimated $Ca(OH)_2$ contents for the purpose of comparison, the $Ca(OH)_2$ contents were calculated on a cement weight basis as in the example presented in Table 3.9 for PC-40 concretes at varying initial moist curing periods. Similar procedure were followed in the estimation of the $Ca(OH)_2$ contents for all the concrete mixtures tested in this study.

Table 3.9: Calcium hydroxide contents in the concrete mixtures

Concrete mixture label	Curing period (day)	$Ca(OH)_2$ content from *TGA* (%) (Equation 3.8)	Cement content in specimen (%) (from chemical test)	$Ca(OH)_2$ per unite of cement content (%)
PC - 40	3	7.06	25.91	17.9
	7	7.21	26.44	21.3
	28	8.17	29.27	23.8

Wet chemical analysis test

The specimens used for the wet chemical analysis test were obtained from 100 x 100 x 100 mm concrete cube samples made from the concrete mixtures in Table 3.4, following the method described in BS 1881: Part 124: 1988 (BSI 1881, 1988). The wet chemical analysis test on the obtained specimen was carried out at the Water Quality Laboratory, School of Civil and Environmental Engineering, University of the Witwatersrand, South Africa.

The procedure used in estimating the *CaO* contents involved placing 5 ± 0.005 g powder specimen in a beaker containing 100 mL of distilled water and 10 mL of hydrochloric acid (32 % AR solution). The solution was first brought to the boil to induce a reaction and then cooled to room temperature. The contents of the beaker were then transferred to a 500 mL volumetric flask and topped up with distilled

water. After agitating for a short while, the mixture was filtered through ash-less filter paper. 25 mL of the resultant precipitate was then added to solution containing 100 mL distilled water, 10 mL of triethanolamine solution, 10 ml sodium hydroxide (*NaOH*) and 0.15 g calcein indicator. After agitating briefly, the solution was titrated against a standard Ethylenediamine-tetra-acetic acid (*EDTA*) solution. The volume of *EDTA* solution required to titrate the test solution is used as the basis for calculating the calcium oxide content. The whole test was repeated for another 5 ± 0.005 g powder specimen and the average volume of *EDTA* for the 2 tests was used to calculate the calcium oxide content of the specimen.

Estimation of calcium oxide (CaO) content in the specimen

From the titration results of the wet chemical analysis, the percentage of *CaO* in the concrete specimens was determined using the following equations as stated in BS 1881 (BSI 1881, 1988).

$$E = \frac{20Xh}{t} \qquad 3.8$$

$$D = \frac{2V_1E}{M_a} \qquad 3.9$$

Where,

E = the calcium oxide equivalent of the *EDTA* solution (in mg CaO/mL);

h = concentration of *CaO* in standard calcium solution in g/L = 1.00 g/L;

t = volume of *EDTA* used in titration in ml = 19.5 ml;

D = the *CaO* content in the concrete specimen in %;

V_1 = the volume of *EDTA* solution used in the titration (in mL);

M_a = the mass of the analytical concrete specimen (in mg).

The *CaO* contents were calculated using equation 3.9 and an example of the results is presented in Table 3.10 for specimen obtained from PC-40 concretes at

varying initial moist curing periods. Similar procedures were followed in the estimation of the *CaO* contents for all the concrete mixtures tested in this study.

Table 3.10: Calcium oxide (*CaO*) contents in the concrete mixtures

Concrete mixture label	Curing period (day)	Concrete specimen mass, Ma (g)	Volume of EDTA, V (mL)	CaO content in specimen D (%) (Equation 3.10)
PC - 40	3	5.013	41.89	16.58
	7	5.081	43.33	16.92
	28	5.038	47.56	18.73

3.5.4 Micro-climate monitoring at the exposure sites

The micro-climate of the natural exposure sites were monitored in terms of the carbon dioxide, relative humidity and temperature variations during the exposure period of the concrete cube samples. Automated CO_2/*RH*/*Temperature* data loggers, able to capture and store micro-climate data at varying time intervals, were positioned at each of the natural exposure sites. Variations in the micro-climate of the sites were monitored continuously with a recording interval of 60 seconds. Micro-climate data was downloaded at the end of each month from the data loggers into a computer system (see Figure 3.17). These micro-climate data were analysed for each exposure sites in terms of the minimum, maximum and mean values for the month.

The micro-climatic condition in the accelerated carbonation chamber was also monitored continuously over the exposure period. The aim is to ensure that the condition in the chamber is within the optimum range for the maximization of the carbonation process at all times during the exposure duration.



Figure 3.17: Micro-climate data been downloaded at the end of the month from the data loggers placed at the different exposure sites.

3.5.5 Carbonation depth test

The durability performance of the concrete was quantified by carrying out carbonation depth test on concrete cube samples cast using the concrete mixtures shown on Table 3.4. The depth of carbonation was measured at the times shown in Table 3.5 for both the accelerated and natural exposure samples.

To determine the carbonation depth, concrete cube samples were split in a plane parallel to the uncoated surface by applying a line load in compression on two opposite faces of the sample (see Figure 3.18). This was achieved using a loading platen with a welded 10 mm mild steel bar, on the top and bottom of the sample. A solution of 1 % phenolphthalein in ethanol was sprayed onto the freshly broken surface of the concrete. A plastic container fitted with a nozzle was used to give a fine spray of the phenolphthalein solution.



Figure 3.18: Method of breaking concrete cubes for carbonation depth determination

The carbonated zone was indicated by the absence of colour change of the cement paste phase (see Figure 3.19). The depth of the uncoloured zone (carbonation depth) was determined by taking the average of six measurements from the surface of the uncoated face (three on each face). The depth of this zone was measured to an accuracy of 0.5 mm using a vernier caliper. Obvious distortions, such as the presence of aggregate particles or air voids near the surface were avoided when the six measurements were taken.

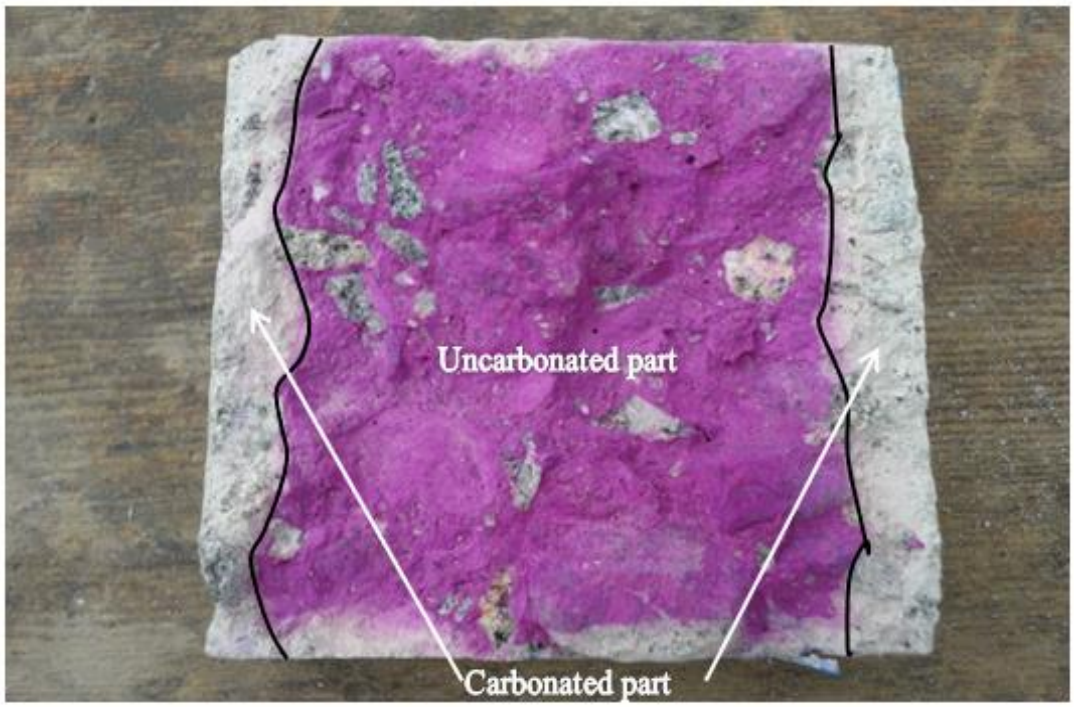


Figure 3.19: A typical concrete cube sample sprayed with phenolphthalein, showing the depth of carbonation

This Chapter has described the laboratory and field studies undertaken to characterise the early-age and medium-term properties of concrete as well as the medium-term durability performance of the concrete in terms of the depth of carbonation. The chapter also presents the approach to the monitoring of the micro-climate of the different exposure sites. The next chapter presents the results obtained from the laboratory and field work. The analysis and discussion of the results as well as the influence the different exposure conditions, curing duration and binder types have on the concrete carbonation depth/rate were also covered in the chapter.

Chapter References

ASTM C125, *Standard terminalogy relating to concrete and concrete aggregates*.

EN 934. (2001). *Concrete admixtures for concrete, mortar and grout. Part 2: Concrete admixtures, definitions, requirements, conformity, marking, labelling, Brussels*. European Committee for Standardization.

Addis, B., & Goodman, J. (2009). *Concrete mix design. In G. Owens (Ed.), Fulton's concrete technology* (Vol. 9th, pp. 219-228). Midrand, South Africa: Cement & Concrete Institute.

Alexander, M. G., Ballim, Y., & Mackechnie, J. R. (1999). *Concrete durability index testing manual*. Research monograph, No. 4.

Ballim, Y. (1994). *Curing and the durability of concrete.* PhD Thesis, University of the Witwatersrand, Johannesbourg.

Borges, P. H., Costa, J. O., Milestone, N. B., Lynsdale, C. J., & Streatfield, R. E. (2010). *Carbonation of CH and C–S–H in composite cement pastes containing high amounts of BFS*. Cement and Concrete Research, *40*(2), 284-292.

BSI 1881. (1988). *Methods for analysis of hardened concrete, London*. British Standard Institution, Part 124, pp. 21.

Dweck, J., Buchler, P. M., Coelho, A. C. V., & Cartledge, F. K. (2000). *Hydration of a Portland cement blended with calcium carbonate*. Thermochimica Acta, 346(1), 105-113.

EN206. (1997). *Concrete - Specification, Performance, Production and Conformity', (BSI, Draft for Public Comment)* British Standard Institution.

SABS. (1989a). *Portland cement extenders, part 1, ground granulated blastfurnace slag SABS 1491-Part 1*: South African Bureau of Standards, Pretoria.

SABS. (1989b). *Portland cement extenders, part 2 fly ash SABS 1491-Part 2*: South African Bureau of Standards, Pretoria.

SABS. (1989c). *Portland cement extenders, part 3, condensed silica fume SABS 1491-Part 3* South African Bureau of Standards, Pretoria.

SABS. (2000). *Cement—Part 1: Composition, specifications and conformity criteria for common cements SABS,ENV 197-1:* South African Bureau of Standards, Pretoria.

SANS. (1994). *South African Standard Code of practice, First revision, Concrete test - compressive strength of hardened concrete* SANS 5863.

Villain, G., Thiery, M., & Platret, G. (2007). *Measurement methods of carbonation profiles in concrete: thermogravimetry, chemical analysis and gammadensimetry*. Cement and Concrete Research, 37(8), 1182-1192.

Wierig, H. (1984). *Longtime studies on the carbonation of concrete under normal outdoor exposure.* Proceedings of the RILEM, Hannover University, 239-24.

CHAPTER 4

RESULTS AND DISCUSSION

4.1 Introduction

This chapter provides all the results obtained in this study in accordance with the manner in which they were reported in Chapter 3. Since these results will be used in the development of prediction models - which mirror the aims of the study, discussion of the results will be presented in order to also assess the quality of the experimental work. In addition, comparing the results obtained to those from similar studies will be useful. Thus, the early-age characterisation results of the concretes in terms of compressive strength, oxygen permeability, water sorptivity, chemical compositions and accelerated carbonation depth are presented and discussed. This is followed by discussion of the micro-climatic variations of the exposure sites in terms of carbon dioxide (CO_2) concentration, relative humidity (*RH*) and *temperature*. Similarly, the medium-term durability performances in terms of carbonation depth of companion concretes are presented, analysed and discussed as well as the discussion of the carbonation rates obtained from the carbonation depths results.

4.2 Compressive Strength Results

Table 4.1 shows the average compressive strengths in MPa obtained for the concrete cubes at 3, 7 and 28 days after casting. Each value shown in this table represents the average of three individual concrete cube compression tests. The individual results of sample mass and failure stress are presented in Table A1 in Appendix A. From Table A1, the variability of the mass and strength results for individual concrete set for all the concrete types tested are suitably low. This signifies that the concrete samples were generally well prepared.

Table 4.1: Average compressive strength test results of the concretes

Binder type	Concrete mix label	Average compressive strength (MPa)		
		3 days	7 days	28 days
100% CEM I	PC-40	46.57	63.47	75.93
	PC-50	31.17	42.03	64.50
	PC-60	25.07	31.53	49.23
	PC-75	21.30	26.30	36.00
70/30 CEM I-FA	FA-40	36.27	43.53	62.80
	FA-50	22.07	31.10	52.13
	FA-60	18.90	22.80	37.80
	FA-75	13.60	16.07	28.10
50/50 CEM I-GGBS	SL-40	24.77	34.03	61.10
	SL-50	18.80	27.43	48.40
	SL-60	13.80	18.23	30.83
	SL-75	8.73	12.63	22.87
90/10 CEM I-CSF	SF-40	51.07	70.87	91.40
	SF-50	37.67	51.93	76.93
	SF-60	26.93	37.10	59.47
	SF-75	22.13	28.53	41.40
100% CEM V	CC-40	24.50	32.77	58.87
	CC-50	19.23	29.37	47.93
	CC-60	16.97	23.47	37.17
	CC-75	9.40	13.80	24.43

The results in Table 4.1 are presented graphically in Figures 4.1 - 4.5, which show the relationship between compressive strength and water/binder (w/b) ratio for each concrete type at the different concrete ages considered. In order to allow comparison of the strength gain for the concretes tested across binder type, Figure 4.6 shows the compressive strength plotted against concrete ages after casting for the different w/b ratios investigated. Although compressive strength for the concretes were evaluated as a baseline and quality control to ensure that mixing, compaction and curing were carried out properly, correlation between compressive strength results and durability performance of the concretes in the medium-term is also useful. The reason for this is the possible development of prediction models using strength as an input parameter.

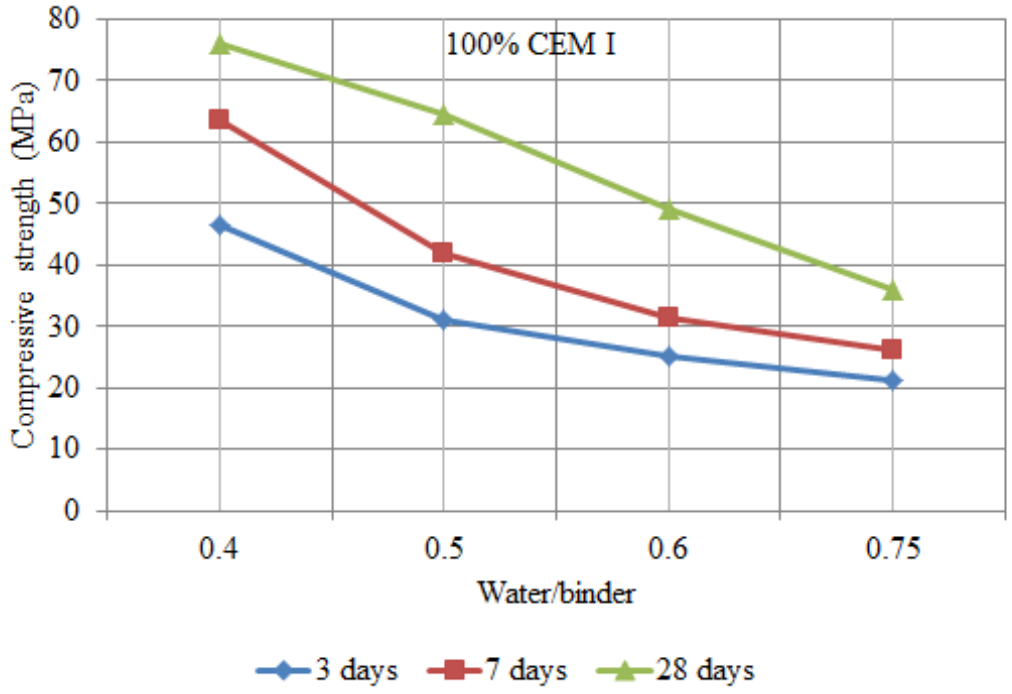


Figure 4.1: Compressive strength vs. Water/binder ratio for the 100% CEM I concretes

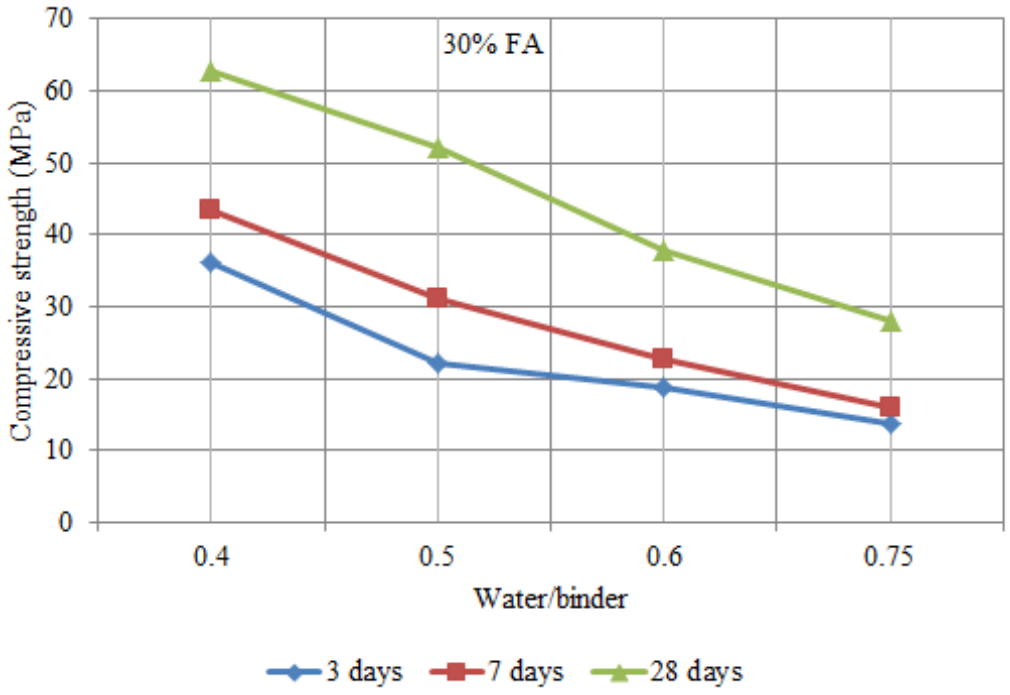


Figure 4.2: Compressive strength vs. Water/binder ratio for the 70/30 CEM I-FA concretes

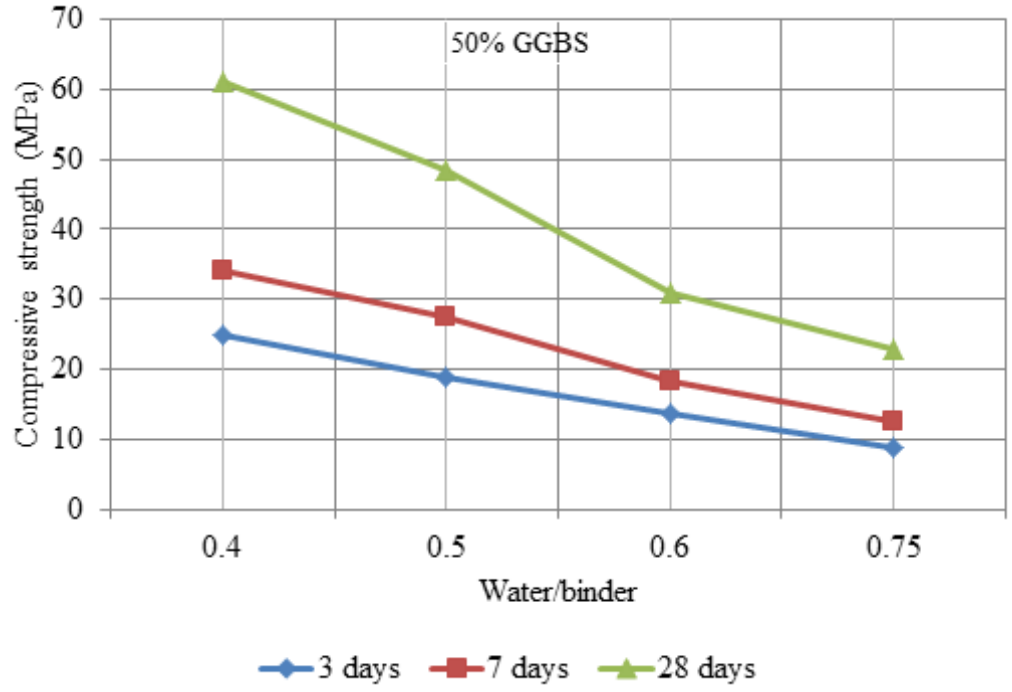


Figure 4.3: Compressive strength vs. Water/binder ratio for the 50/50 CEM I-GGBS concretes

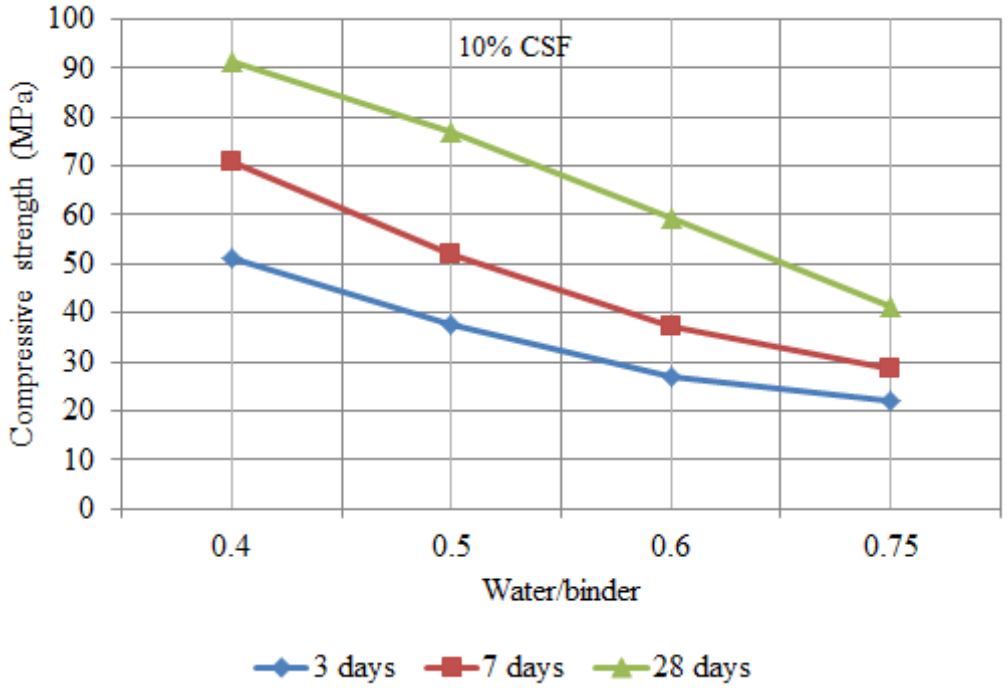


Figure 4.4: Compressive strength vs. Water/binder ratio for the 90/10 CEM I-CSF concretes

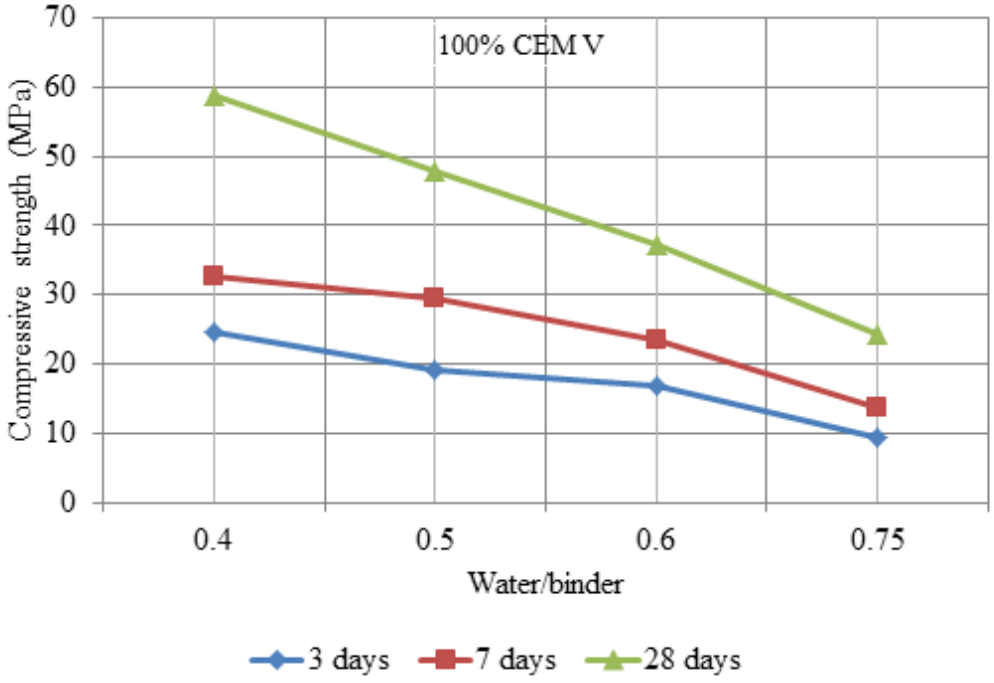


Figure 4.5: Compressive strength vs. Water/binder ratio for the 100% CEM V concretes

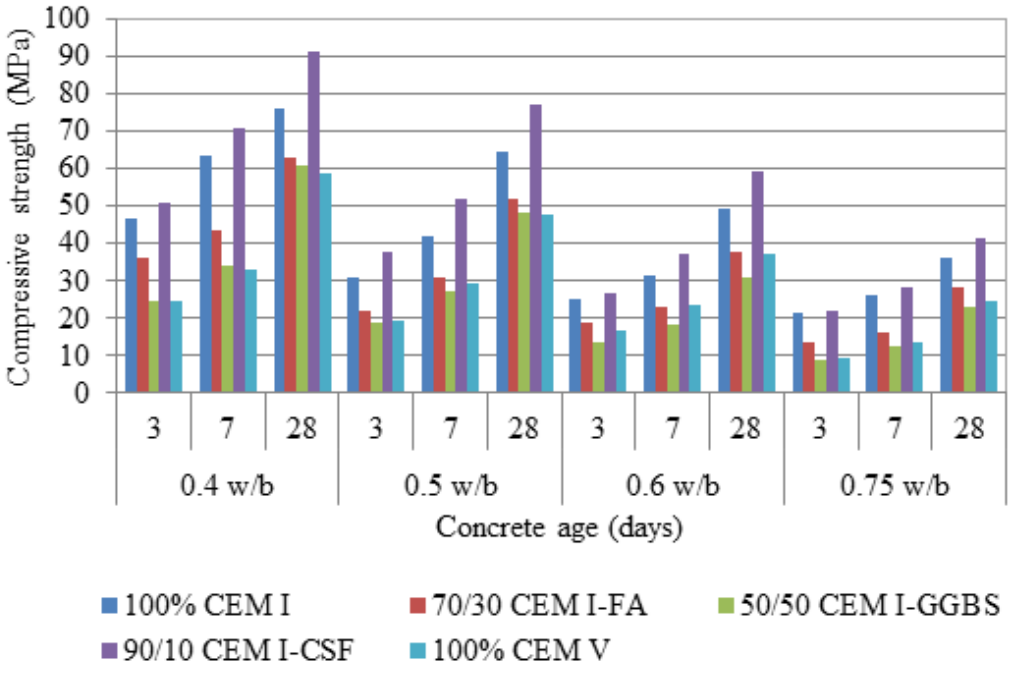


Figure 4.6: Compressive strength vs. Concrete age for all the concrete types studied

The use of different binder types influenced concrete strength development, with decreasing w/b ratio resulting in improved strength. From the compressive strength plots shown above (see Figures 4.1 - 4.5), it can be seen that compressive strength decreases with an increase in w/b ratio for all concrete types and for all moist curing ages investigated. The influence of binder content and w/b ratios on compressive strength at different concrete ages for all concrete types tested is shown in Figure 4.6. From Figure 4.6, it can be noted that blended concretes presented reduced compressive strength in comparison to the *CEM I* concretes at all w/b ratio and curing ages except the *CSF* concretes. Similar influences have been found in results for paste and concretes systems published elsewhere (ACI, 1987; Alexander & Magee, 1999; Alexander & Moyo, 2012; Ballim, 1994; Khan & Lynsdale, 2002; Khan et al., 2000; Mackechnie & Alexander, 2002; Mehta & Gjørv, 1982; Bruno, 2010).

Note that as the moist curing age of the concrete increases, hence the hydration of its binder components, the gain in compressive strength with blended concretes becomes more apparent (see Figures 4.2, 4.3 and 4.5) especially at low w/b ratio. Analyzing the ratios of the 28 days and 7 days compressive strengths for all the concrete types tested, the *FA*, *GGBS* and *CEM V* concretes presented higher values compared to the *CEM I* concretes while the *CSF* concretes gives the lowest ratio. Increased compressive strength gain at later ages for these supplementary cementing materials (*SCM*) can be attributed to their slower hydration rate and chemical pozzolanic effect (especially for *FA* and *CSF*), as well as to the physical effect of the generally tiny *SCM* particles. Detwiler and Mehta (1989) and Goldman and Bentur (1993) suggested in their work that the improvement in compressive strength in blended cement concrete is primarily dependent on the micro filler effect of the *SCM*.

Due to the higher replacement level used and its inherent slower rate of hydration, a slight reduction in compressive strength occurred for the *GGBS* blended concretes at all ages compared to the *FA* concretes especially at higher w/b ratio

(see Figure 4.6). Similar observations were also noted by other researcher (Alexander & Magee, 1999; Ballim, 1994; Mackechnie, 1996; Bruno, 2010). It can also be noted from Figure 4.6 that the difference in compressive strength between the *FA*, *GGBS* and *CEM V* concretes and the *CEM I* and *CSF* concretes are higher at early ages (3 and 7 days) compared to later age (28 days). The reduced compressive strength presented by the *FA*, *GGBS* and *CEM V* concretes can be attributed to either the slower rate of hydration of the *SCM* components in the concretes, their calcium hydroxide depletion tendency or the dilution effect of the *SCM* in the concrete mixture.

The increased compressive strength of the *CSF* blended concrete in comparison to *CEM I* and other blended concretes can be attributed to its high reactivity (Roy, 1999). Similarly, *CSF* has elevated pozzolanic activity and it is an effective filler, thereby reducing concrete porosity and improving strength (Bertolini et al., 2013). The addition of *CSF* to cement paste has been shown to give rise to high early strengths, attributed to either the *CSF* particles causing pore blockage in the hydrating cement, which densifies the hydrating gel structure (Bonen & Khayat, 1995; Lagerblad et al., 1993; Mehta & Gjørv, 1982; Shah & Slate, 1968) or that the *CSF* particles act as nucleation sites for cement hydration, thereby accelerating the hydration process (Larbi & Bijen, 1990; Mitchell et al., 1998). The observation of increased compressive strength of *CSF* blended concretes is noted in the literature (Alexander & Magee, 1999; Alexander & Moyo, 2012; Mehta & Gjørv, 1982; Bruno, 2010).

From the compressive strength results of the concretes obtained in this study, for equal w/b ratio and moist curing ages, the different concrete types can be ranked in terms of compressive strength from the lowest as 50% *GGBS* blended concrete < 100% *CEM V* concrete < 30% *FA* blended concrete < 100% *CEM I* concrete < 10% *CSF* blended concrete. The ranking is generally true at equal w/b ratio and concrete ages under continuous moist curing. The greatest improvement in compressive strength of concrete can be achieved through the use of *CSF* blended

concretes. Improvement in the compressive strength for concretes may be achieved through extended initial moist curing. These results clearly show that the experimental work was of acceptable quality, since the results obtained follow expected trends and are comparable to results from similar studies. Hence, the compressive strength results of the concrete may be used in the development of the carbonation models.

4.3 Oxygen Permeability Results

4.3.1 Oxygen permeability at 28 days after casting

The average results of oxygen permeability obtained for the concretes at 28 days after casting are shown in Table 4.2. In this table, the oxygen permeability test results are presented as both coefficient of oxygen permeability, k (m/s) and oxygen permeability indexes (*OPI*). Each value shown in the table represents the average of permeability measurement on four individual specimens (discs) or, in some cases, the results of only three permeability measurements. Some oxygen permeability test results had to be discarded because the test disc had a crack or flaw through the thickness during preparation of the disc, causing a "short circuit" for oxygen flow during testing.

Cracks or flaws through the disc thickness were easily identified as these discs showed unusually high permeability values or a test result from the same set of discs showed a clear outlier result. Cracks or flaws through discs thickness were common with the blended cement discs obtained from concrete cubes whose mixtures have high w/b ratio as well as concrete cubes given short periods of initial moist curing. The oxygen permeability test analysis results and plots for the different concrete types may be found in the file named "Early-age Oxygen Permeability Test Results" on the accompanying CD.

The measured individual disc permeability results for all the concrete discs tested satisfy the linearity requirement (Ref SANS Draft Specification) as indicated by the test results, that is, the R^2 values are all greater than 0.98. However, the variability requirement and the average permeability measurement results for some sets of discs was not satisfied. Variability noted in the variance of the test results can be explained as due to the sensitivity of the oxygen permeability test to compaction (Alexander et al., 1999), as well as to experimental treatment given to the concrete cube samples.

Table 4.2: Average oxygen permeability test results of the concretes

Concrete mix label	Average oxygen permeability results at 28 days					
	Extent of initial moist curing					
	3 days		7 days		28 days	
	k ($x10^{-10}$ m/s)	*OPI*	*k* ($x10^{-10}$ m/s)	*OPI*	*k* ($x10^{-10}$ m/s)	*OPI*
PC-40	1.2	9.9	1.2	9.9	1.0	10.0
PC-50	1.9	9.7	1.5	9.8	1.3	9.9
PC-60	2.5	9.6	2.4	9.6	2.3	9.6
PC-75	6.5	9.2	5.8	9.2	3.4	9.5
FA-40	1.0	10.0	0.8	10.1	0.5	10.3
FA-50	1.7	9.8	1.2	9.9	1.0	10.0
FA-60	2.4	9.6	2.4	9.6	2.3	9.6
FA-75	6.1	9.2	5.2	9.3	3.5	9.5
SL-40	1.7	9.8	1.2	9.9	1.2	9.9
SL-50	2.7	9.6	2.7	9.6	2.6	9.6
SL-60	5.0	9.3	4.7	9.3	4.3	9.4
SL-75	12.0	8.9	6.5	9.2	6.4	9.2
SF-40	0.9	10.1	0.7	10.1	0.4	10.4
SF-50	1.1	10.0	1.0	10.0	0.8	10.1
SF-60	2.0	9.7	2.0	9.7	1.5	9.8
SF-75	5.3	9.3	4.3	9.4	2.6	9.6
CC-40	1.2	9.9	1.0	10.0	1.0	10.1
CC-50	2.2	9.7	1.7	9.8	1.1	10.0
CC-60	7.0	9.2	4.6	9.3	2.6	9.6
CC-75	59.0	8.2	24.0	8.6	12.0	8.9

Although results of permeability measurements of the concretes are more discriminating when presented as *k*, the *OPI* representation will be used as the results are more commonly reported in this form. Additionally, the OPI representation is mainly used to broadly classify the quality of concrete. This classification ranged from excellent to very poor.. This is because it is considered more useful to present concrete oxygen permeability measurement as an index. In addition, oxygen permeability test results are often presented as an index among practicing engineers in the construction industry in South Africa. Hence, the oxygen permeability results of the concretes are presented as an index in this section and in subsequent discussion. A poor quality concrete with high connectivity of the pores will therefore have a high *k* value (low *OPI* value) and would allow easier passage of oxygen through the concrete. While concretes with very low *k* value (high *OPI* value) would impede the passage of oxygen through the concrete and, by implication, limit the access of corrosion agents to the steel thus slowing the corrosion process, given sufficient concrete cover.

The oxygen permeability test results of the concretes presented in Table 4.2 are shown graphically in Figures 4.7 - 4.11, which show the relationship between *OPI* at 28 days and w/b ratio for each concrete type at the varying extent of initial moist curing considered. In order to allow comparison of the permeability measurement results for the concretes tested across binder types, Figure 4.12 shows the *OPI* of the concrete at 28 days plotted against the initial moist curing period after casting, for the different w/b ratios investigated.

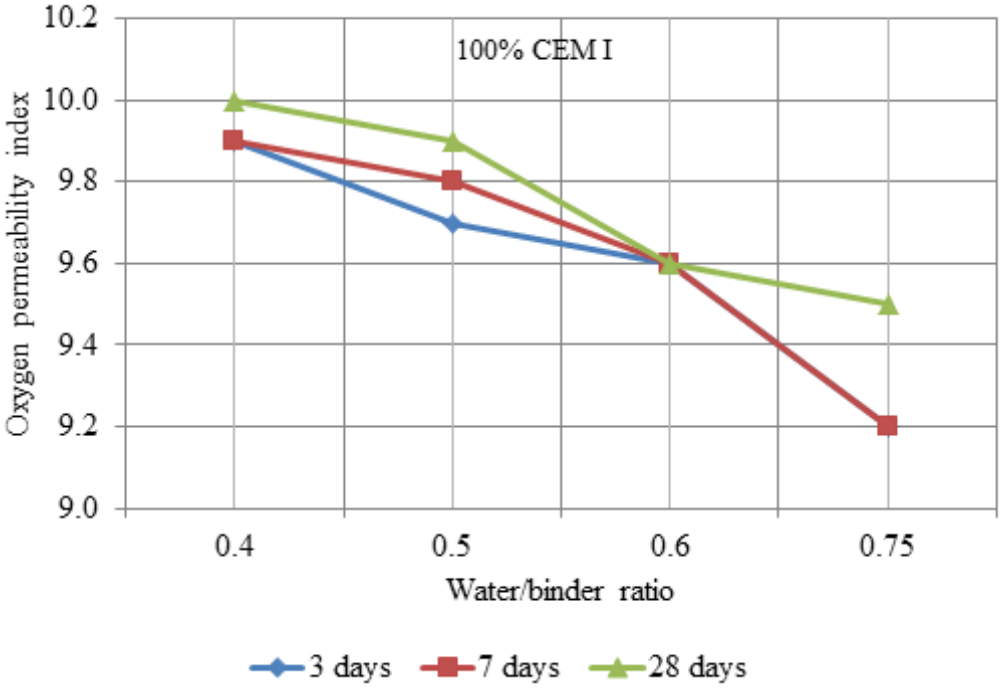


Figure 4.7: Oxygen permeability index vs. Water/binder ratio for the 100% CEM I concretes

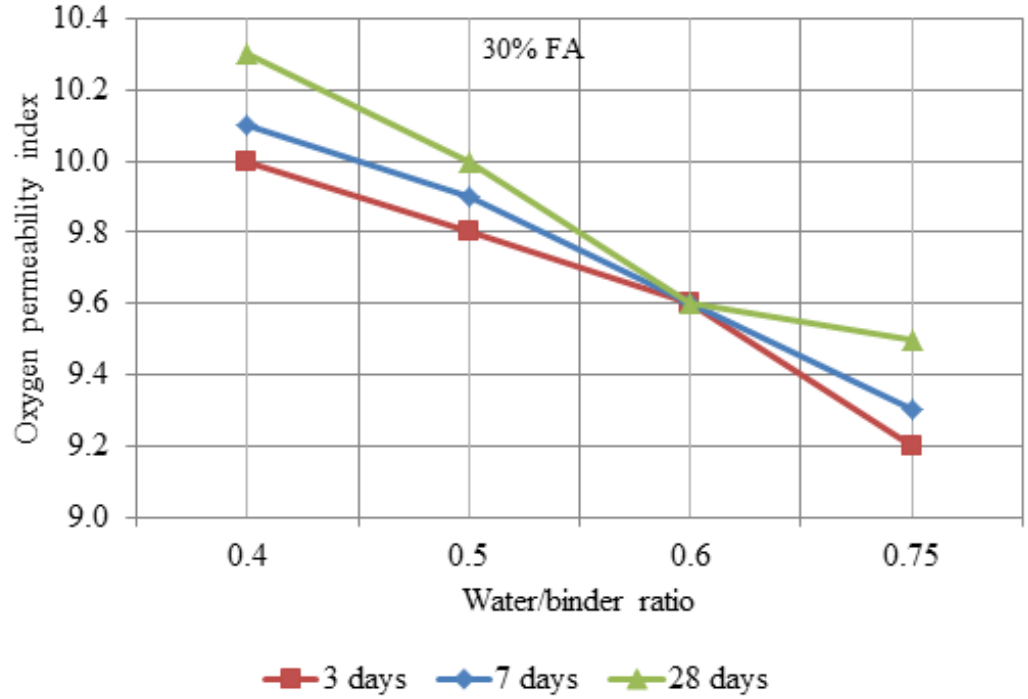


Figure 4.8: Oxygen permeability index vs. Water/binder ratio for the 70/30 CEM I-FA concretes

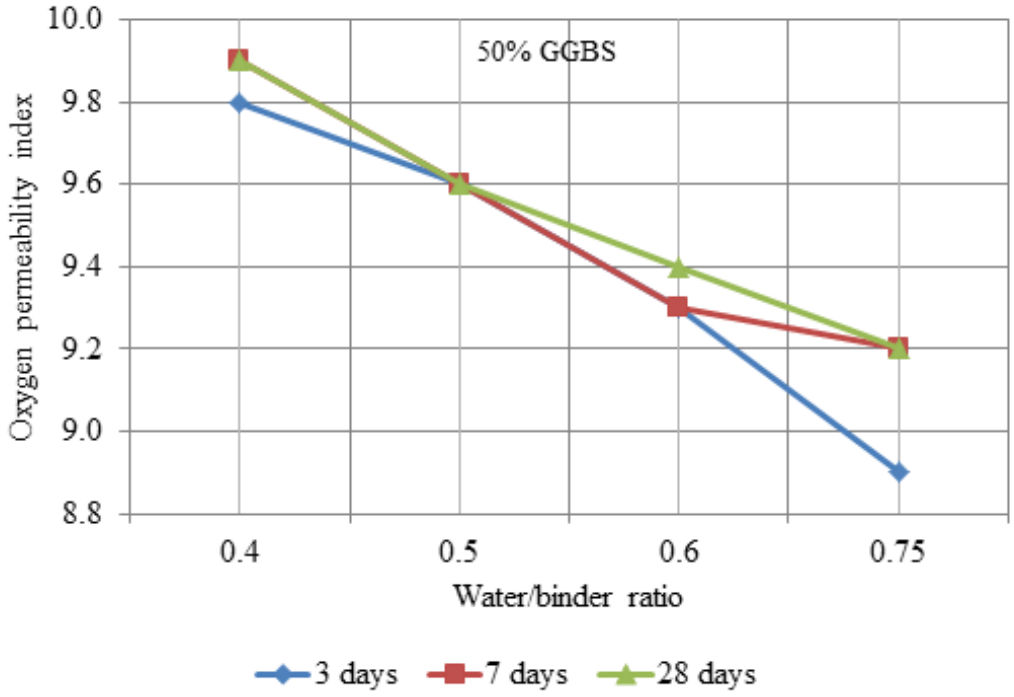


Figure 4.9: Oxygen permeability index vs. Water/binder ratio for the 50/50 CEM I-GGBS concretes

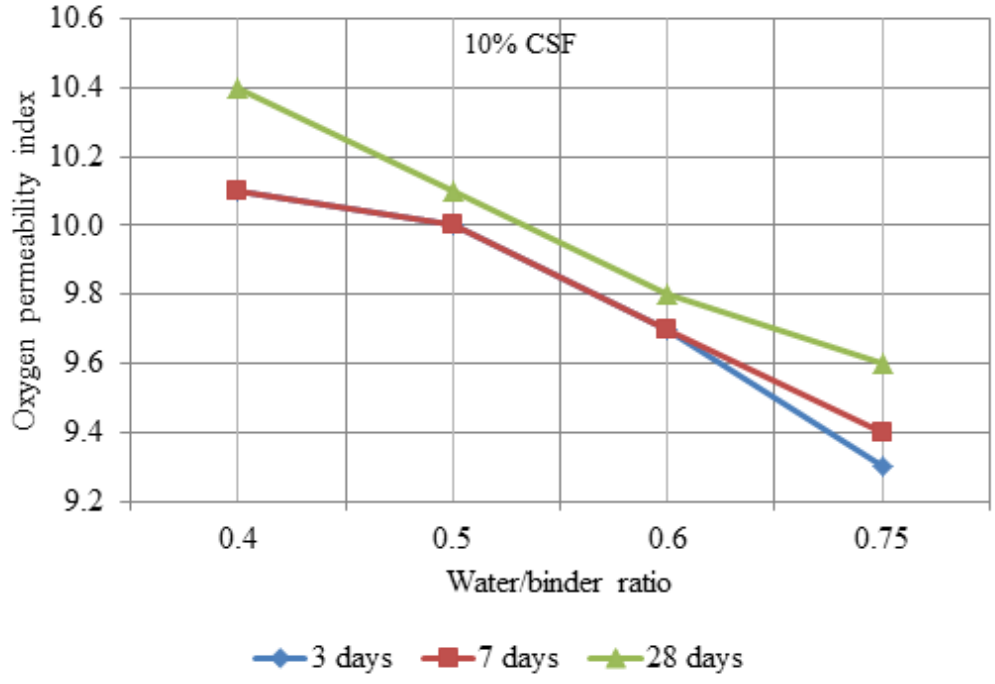


Figure 4.10: Oxygen permeability index vs. Water/binder ratio for the 90/10 CEM I-CSF concretes

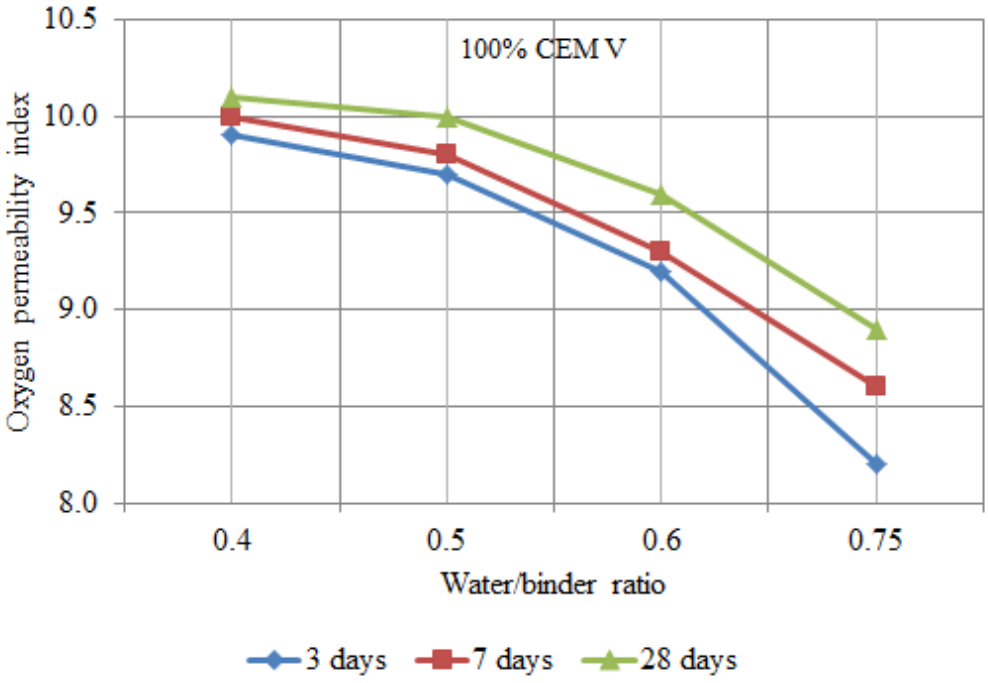


Figure 4.11: Oxygen permeability index vs. Water/binder ratio for the 100% CEM V concretes

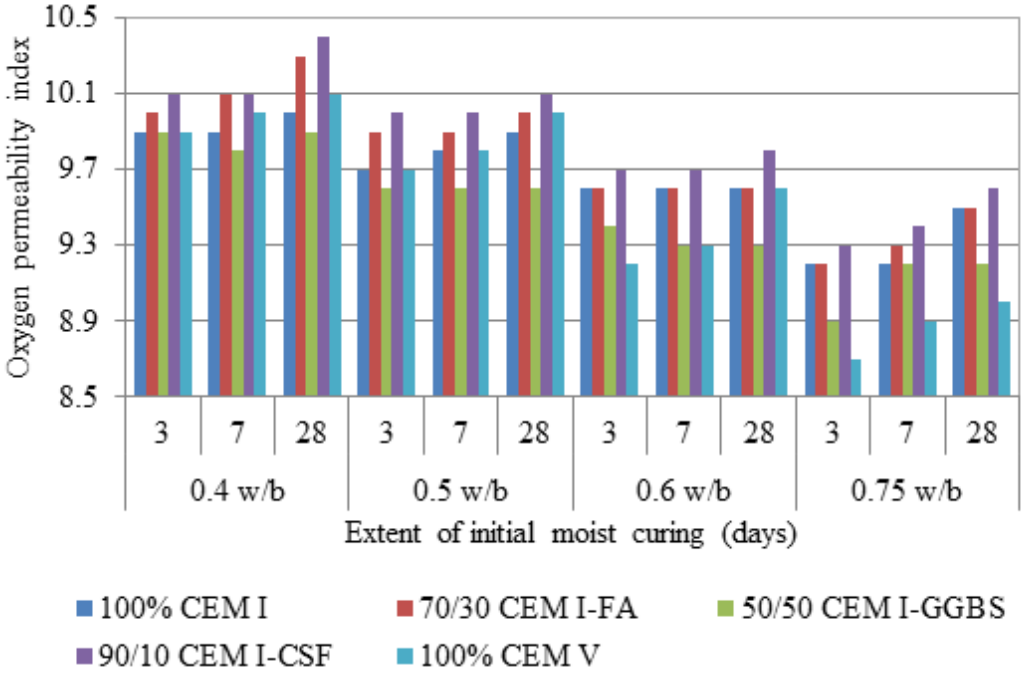


Figure 4.12: Oxygen permeability index vs. Extent of initial moist curing for all the concrete types studied

The use of different binder types influenced the permeation property of the concretes, with increasing w/b ratio resulting in decreased OPI values. From the *OPI* plots of the concretes presented in Figures 4.7 - 4.11 it can be seen that the *OPI* values decrease with an increase in w/b ratio and as the extent of initial moist curing period decreases for all the concrete types tested. The influence of binder content and w/b ratio on the permeation properties of the concretes can be seen clearly in Figure 4.12. From Figure 4.12, it can be noted that *CSF* and *FA* blended concretes showed higher OPI values than the other concrete types at all w/b ratios and curing ages.

Although the *OPI* values are clustered for some concrete mixtures of the same binder type, there are distinct trends of improvement in concrete permeability as the w/b ratio decreases for all the concrete types investigated. The improved permeability for all the concretes as w/b ratio decreases is attributed to the reduction in the volume and size of the pores within the concrete microstructure (Khan & Lynsdale, 2002; Mehta & Manmohan, 1980).

The similarities in the permeability noted in some of the results can be attributed to experimental design. Concretes were exposed to an uncontrolled laboratory environment after the initial 3, 7 and 28 days moist curing period, before being tested for oxygen permeability at between 28 and 32 days. The continued hydration of the concrete during the air drying period is likely to be the reason for the similarity in permeability, since hydration does not cease instantaneously. Similar results were also observed by Alexander and Moyo (2012) in their work.

Henry and Kurtz (1963) noted that permeability of concrete increases considerably with increasing w/b ratio because of the increasing volume and degree of interconnection of capillary pores within the cement paste. In addition, as w/b ratio decreases or as curing time increases (therefore the degree of hydration increases), the reduction of concrete paste porosity is mainly due to the reduction in pores of larger dimensions that have been filled or are connected by

C-S-H gel pores. Similarly, Graf and Grube (1986) state that as hydration proceeds, the initially water filled and fully interconnected pores within the cement paste are filled with hydration products and become discontinuous.

As the initial moist curing age of concrete increases and hence hydration, the improvement in permeability with the blended concretes becomes more apparent (see Figures 4.8 - 4.11) especially at higher w/b ratios. The increased gain in impermeability at later ages for the *SCM* blended concretes can be attributed to a combination of the pozzolanic and micro filler effects of *SCM*, especially for *FA* and *CSF* thus leading to refinement of the pore (Khan & Lynsdale, 2002; Khan et al., 2000). The influence of varying degrees of initial moist curing and w/b ratio on the permeability of the concretes made from the different binder types is shown in Figure 4.12. From Figure 4.12, it can be seen that only CSF and FA blended concretes presence improved permeability in comparison to the *CEM I* cement concretes. The *GGBS* and the *CEM V* concretes also showed improved performance at higher w/b ratios.

It is known that the addition of *SCM* in concrete leads to the formation of more refined hydration products and hence improved permeability in comparisons to the *CEM I* concrete (Mehta & Gjørv, 1982; Mehta, 1983; Neville, 1997). The *GGBS* concretes however did not exhibit this characteristic and lower *OPI* values were observed in comparison to the *CEM I* concrete and the *FA* blended concretes. This can be attributed to its higher replacement level, but more to its slower hydration rate and increased sensitivity to moist curing (Osborne, 1999). The possible effect of better pore refinement by the *GGBS* concretes will probably be achieved only if the extent of initial moist curing is long enough. The *FA* blended concretes however performed better than the *CEM I* concretes at all w/b ratios under continuous initial moist curing.

Manmohan and Mehta (1981) have shown that *FA* refines the concrete pore structure upon hydration by transforming large pores into fine pores. Mehta

(1983) reports a decrease in cement paste permeability from between 11 – 13 $x10^{-11}$ m/s to 1 $x10^{-11}$ m/s after the addition of *FA*. Similarly, Berry and Malhotra (1987) show that well cured concrete pipes with *FA* replacement of 30 and 50 % were less permeable than equivalent *CEM I* concrete pipes. Generally, the results obtained from the present study are as expected and similar results were also obtained by other researcher elsewhere (ACI, 1987; Alexander & Magee, 1999; Alexander & Moyo, 2012; Ballim, 1994; Khan & Lynsdale, 2002; Khan et al., 2000; Mackechnie & Alexander, 2002; Mehta & Gjørv, 1982; Bruno, 2010).

The improved permeability for the *CSF* blended concretes compared to the *CEM I* and other blended concretes can be attributed to its dilution effects and its high reactivity (Roy, 1999). In addition, the *CSF* particles causes pore blockage in hydrating cement, which densifies the hydrating gel structure (Bonen & Khayat, 1995; Lagerblad et al., 1993; Mehta & Gjørv, 1982; Shah & Slate, 1968). Furthermore, *CSF* also accelerates the hydration process by acting as nucleation sites for cement hydration (Larbi & Bijen, 1990; Mitchell et al., 1998).

From the permeability measurement results of the concretes obtained in this study, for equal w/b ratio and extent of initial moist curing periods the different concrete types can be ranked in terms of permeability as measured from the oxygen permeability test from the lowest as 100% *CEM V* concrete < 50% *GGBS* blended concrete < 100% *CEM I* concrete < 30% *FA* blended concrete < 10% *CSF* blended concrete. The ranking is generally true for all w/b ratios under continuous initial moist curing. The greatest improvement in concrete permeability can be achieved through the use of *CSF* and *FA SCM*. Improvements in the permeation properties for the other concretes may be achieved through extended initial moist curing. The permeability result for all the concretes tested clearly show that the experimental work is of an acceptable quality, since results obtained follow existing trends and are comparable to results from other similar studies. Hence the oxygen permeability test results of the concretes may be used in the development of the carbonation prediction models.

4.3.2 Oxygen permeability at 6, 12 and 18 months after casting

Results of oxygen permeability test at 6, 12 and 18 months after casting and exposure for the 0.5 w/b ratio concretes are presented in Table B1 in Appendix B. In the table, the oxygen permeability test results for the different exposure conditions investigated are presented as both *k* and *OPI*. Each value shown in Table B1 represents the averages of permeability measurement on four individual concrete discs.

The results of the concrete individual disc linearity and variability requirement did not meet the SANS Draft Specification. This can be as a result of either the carbonation effect on the concrete, the penetration of pollutants or aggressive agents and/or the sensitivity of the oxygen permeability test. These lead to a decision not to include some of the permeability measurements in the plots and in further analysis.

The results presented in Table B1 are shown graphically in Figures 4.13 to 4.15, which show the relationship between the medium-term *OPI* values of the concretes and the extent of initial moist curing for the different exposure conditions investigated. These figures also allow comparison of the permeability measurements of the concretes in the medium-term across binder types as well as the influence of varying degree of initial concrete moist curing in the medium-term. Similarly, the effect of carbonation on the permeation properties of the concretes exposed to different conditions in the medium-term can be quantified.

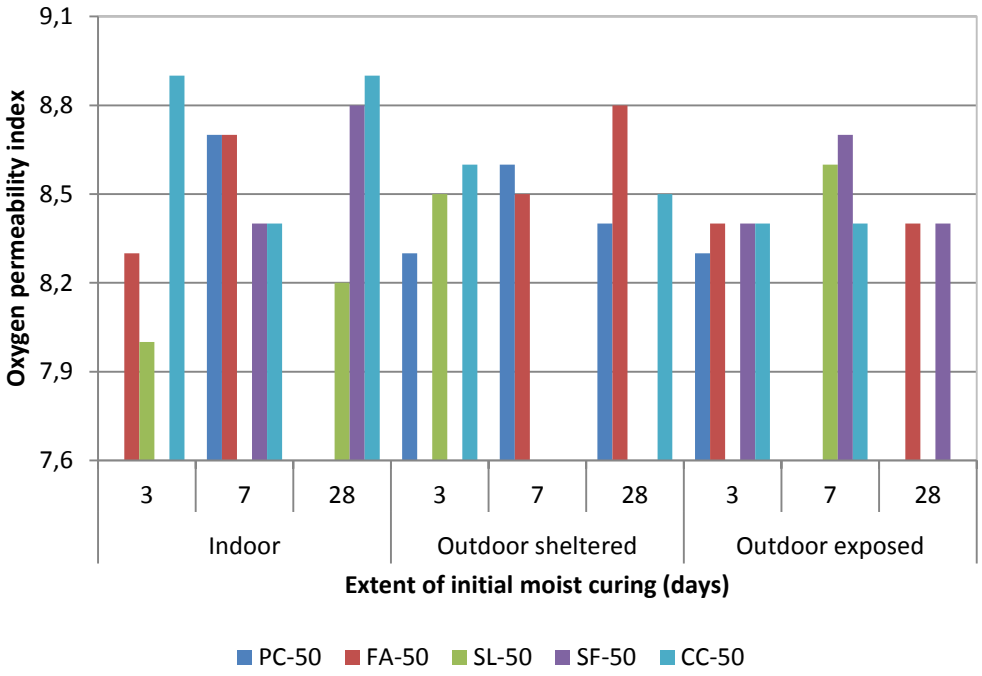


Figure 4.13: Concrete permeability measurement results after 6-months exposure to the inland environment

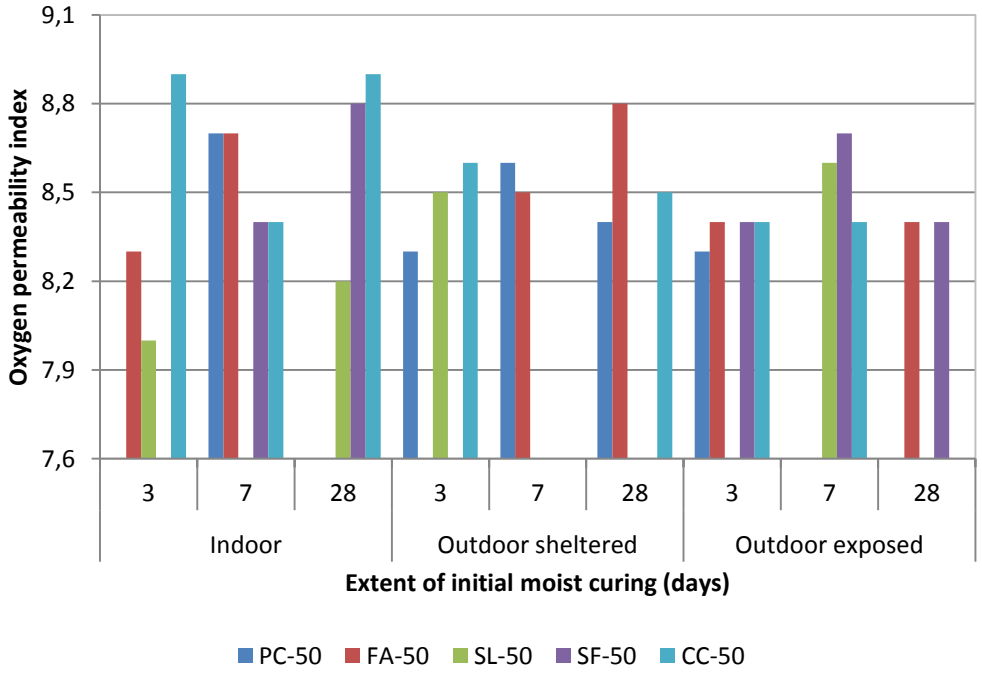


Figure 4.14: Concrete permeability measurement results after 12-months exposure to the inland environment

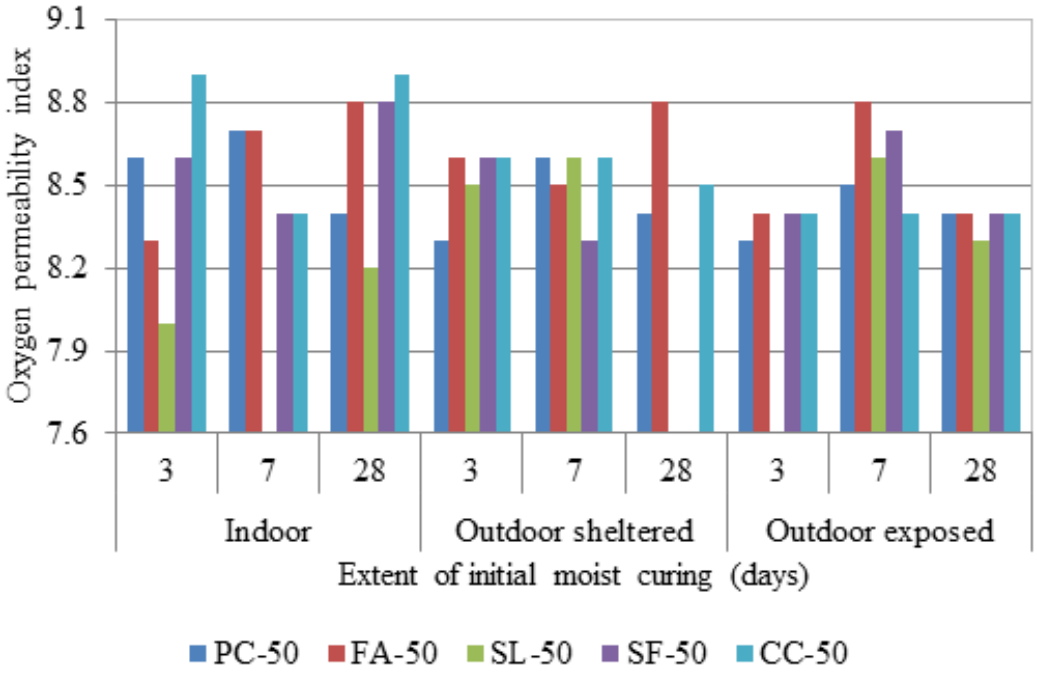


Figure 4.15: Concrete permeability measurement results after 18-months exposure to the inland environment

Figures 4.13 - 4.15 show the relationship between the medium-term permeability values of the concretes and the extent of the initial moist curing periods for the different inland environment investigated. Based on these results, it is difficult to make clear and convincing conclusions about the trends observed.

It is known that carbonation reaction products are approximately 12% greater in volume than the original calcium hydroxide from which they are derived. Some researchers (Blight, 1991; Neville, 1981; Verbeck, 1958) have found carbonation to reduce the permeation properties of concrete. Neville (1981) in his study attributed the reduction in permeation of matured and carbonated concretes to increased rate of hydration from the water released by the carbonation process and the pore blocking effect of the calcium carbonate produced. However, Neville (1981) stated that state that carbonation may not reduce the permeability of blended concretes. Ballim (1994) tested a number of blended and unblended concretes for oxygen permeability after exposure for 10 months to an inland

environment. He noted an increase in permeability for all the concrete types tested. Ballim's results do not show a reduced permeability for plain concrete as noted by Neville. Similarly, Lampacher (2000) noted increased permeability on concrete specimens he obtained from existing concrete structures located in an inland environment, which he notes are mostly unblended concretes.

Apart from the lack of trend noted in the permeability results of the different concrete types investigated in this study, there were general increases in the medium-term permeability results for all the concretes tested when compared to the permeability results of equivalent concretes at early-age (28 days). These conflicting permeability results indicate that the effects of carbonation on permeation properties of concretes or the effects of extended exposure time on concretes are not yet fully understood and requires further investigation.

4.4 Water Sorptivity Results

4.4.1 Water sorptivity at 28 days after casting

The average results of water sorptivity obtained for the concretes at 28 days after casting are presented in Table 4.3. In this table, the water sorptivity test results of the concretes are presented as sorptivity (mm/√hr.) and porosity (%). Each value shown in Table 4.3 represents the average of sorptivity and porosity measurements on four individual discs or, in some cases, the results of only three sorptivity and porosity measurements.

Note that the same discs used for the oxygen permeability test were re-used for the water sorptivity test, this is in line with the Draft SANS specification (2010), a revised version of the Durability Index Testing Manual (Alexander et al., 1999). The water sorptivity test analysis result for the different concrete types may be found in the file named "Early-age Water Sorptivity Test Results" on the accompanying CD. The individual disc sorptivity measurement results for all the

concrete discs tested satisfy the linearity requirement as noted from the test results. This was also the case for the variability around the average sorptivity measurement results for all the set of discs investigated.

Table 4.3: Average water sorptivity test results of the concretes

Concrete mix label	Average water sorptivity and porosity at 28 days					
	Extent of initial moist curing					
	3 days		7 days		28 days	
	Sorptivity ($mm/hr^{0.5}$)	Porosity (%)	Sorptivity ($mm/hr^{0.5}$)	Porosity (%)	Sorptivity ($mm/hr^{0.5}$)	Porosity (%)
PC-40	8.2	10.9	7.8	9.8	6.8	9.2
PC-50	8.5	10.3	8.1	10.3	8.0	9.7
PC-60	10.6	11.1	9.9	11.0	9.7	10.3
PC-75	15.5	13.6	13.8	12.3	13.6	12.2
FA-40	8.3	10.7	7.7	10.0	7.5	9.8
FA-50	9.3	11.3	9.0	11.3	9.0	10.2
FA-60	14.4	12.3	12.3	11.7	11.7	11.0
FA-75	18.5	12.9	13.5	13.3	13.3	13.1
SL-40	6.4	11.3	5.9	10.3	5.3	9.8
SL-50	9.2	11.8	8.3	11.4	8.0	11.4
SL-60	11.9	12.6	9.2	12.8	8.0	11.4
SL-75	19.5	13.7	13.3	15.1	8.9	13.2
SF-40	5.3	10.4	4.5	9.3	3.4	9.5
SF-50	6.7	11.1	6.6	11.3	5.3	10.8
SF-60	8.5	12.6	7.5	12.3	5.5	10.8
SF-75	12.7	15.4	12.1	14.7	8.4	14.6
CC-40	8.5	11.2	7.2	10.8	6.7	10.8
CC-50	10.0	11.9	8.8	10.8	8.6	10.7
CC-60	19.9	12.0	12.3	10.7	10.7	10.8
CC-75	20.0	11.2	17.4	11.4	16.2	11.0

Although discernible trends are noted in the porosity results of the concrete, only the sorptivity values from the water sorptivity test results will be used in describing the permeation properties of the concretes. This is because the transport process of concrete cannot be explained simply by the pore volume (which is what the porosity results represent) but also by its pore connectivity.

The degree of continuity of the pore system has to be taken into account since aggressive agents penetrate into concrete is through this medium. The aim of the water sorptivity test is for possible inclusion of the sorptivity results in the development of carbonation prediction models for concrete.

The sorptivity values of the concretes represent the rate of movement of a water front through the disc under capillary suction, normalised by porosity. The lower the sorptivity value, the more resistant is the concrete to penetration of moisture. Concretes made of higher w/b ratio allow easier access of moisture through the pore structure, while concretes with low w/b ratio (thus low sorptivity values) would impede the access of moisture and will therefore limit the access of aggressive agents to the steel and slow the corrosion process, given sufficient concrete cover.

The water sorptivity test results of the concretes presented in Table 4.3 are shown graphically in Figures 4.16 - 4.20, which show the relationship between the sorptivity values at 28 days and w/b ratio for the different concrete types at varying extents of initial moist curing periods. In order to allow comparison of the sorptivity measurement results for the concretes tested across binder types, Figure 4.21 shows the concrete sorptivity values at 28 days plotted against the initial moist curing period after casting for the different w/b ratios investigated.

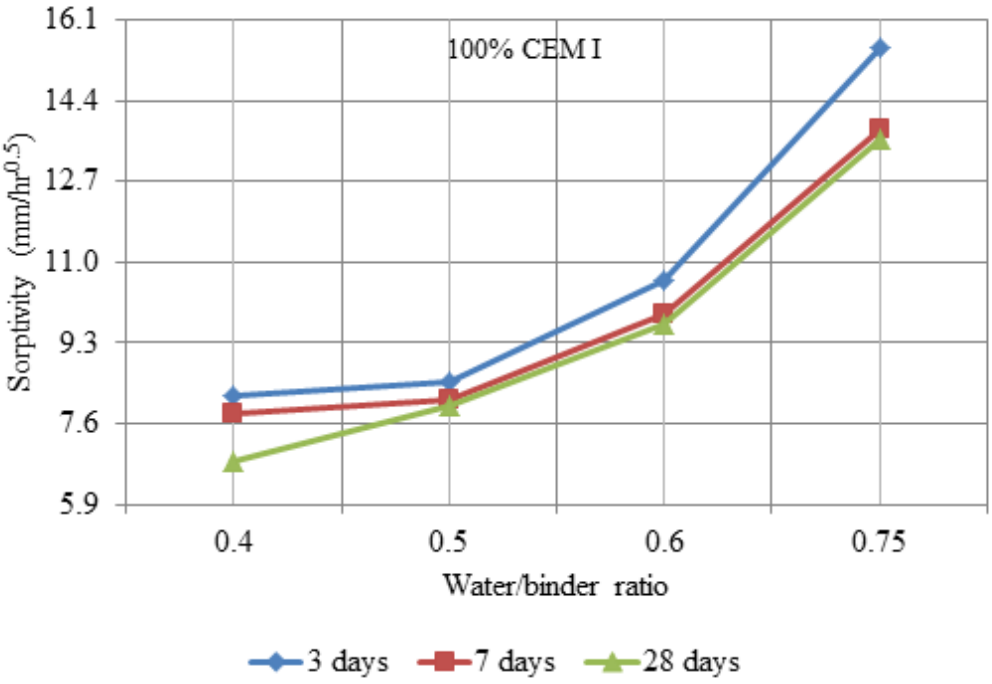


Figure 4.16: Water sorptivity vs. Water/binder ratio for the 100% CEM I concretes

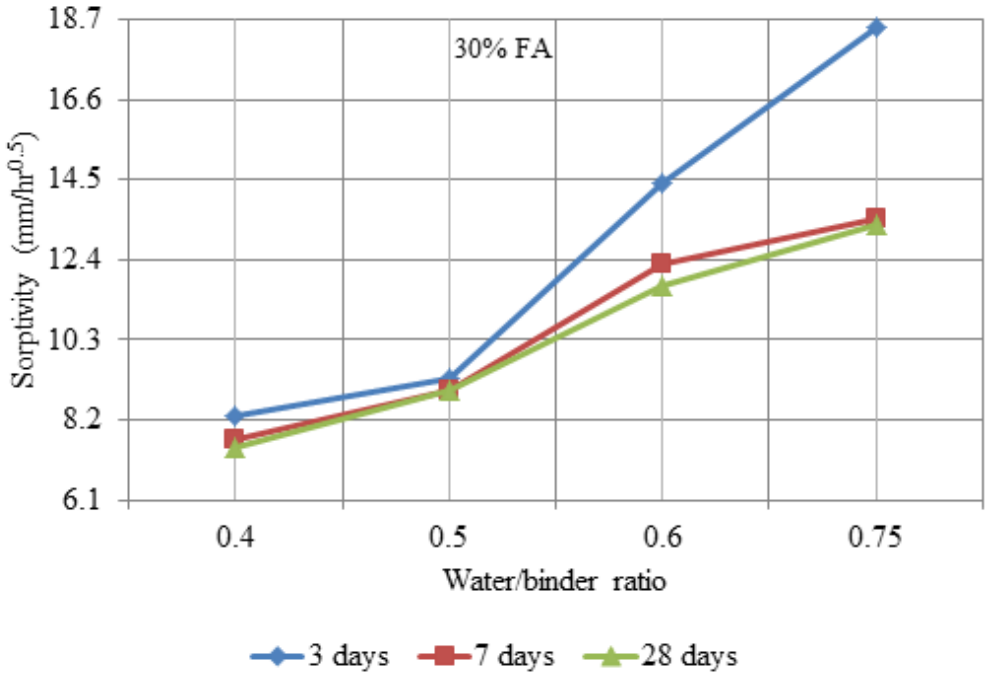


Figure 4.17: Water sorptivity vs. Water/binder ratio for the 70/30 CEM I-FA concretes

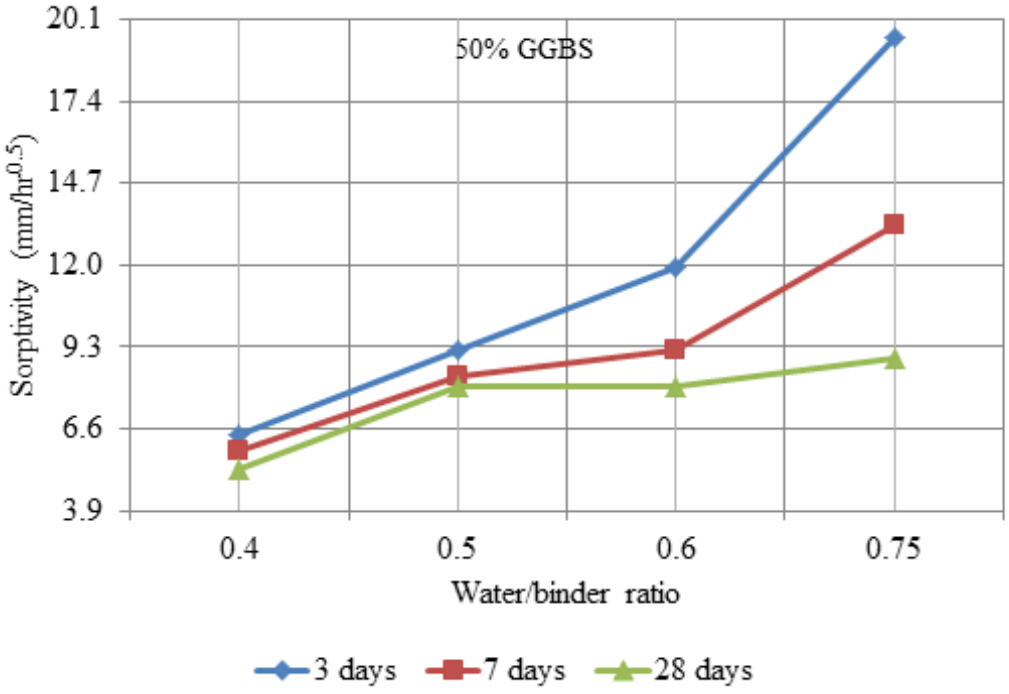


Figure 4.18: Water sorptivity vs. Water/binder ratio for the 50/50 CEM I-GGBS concretes

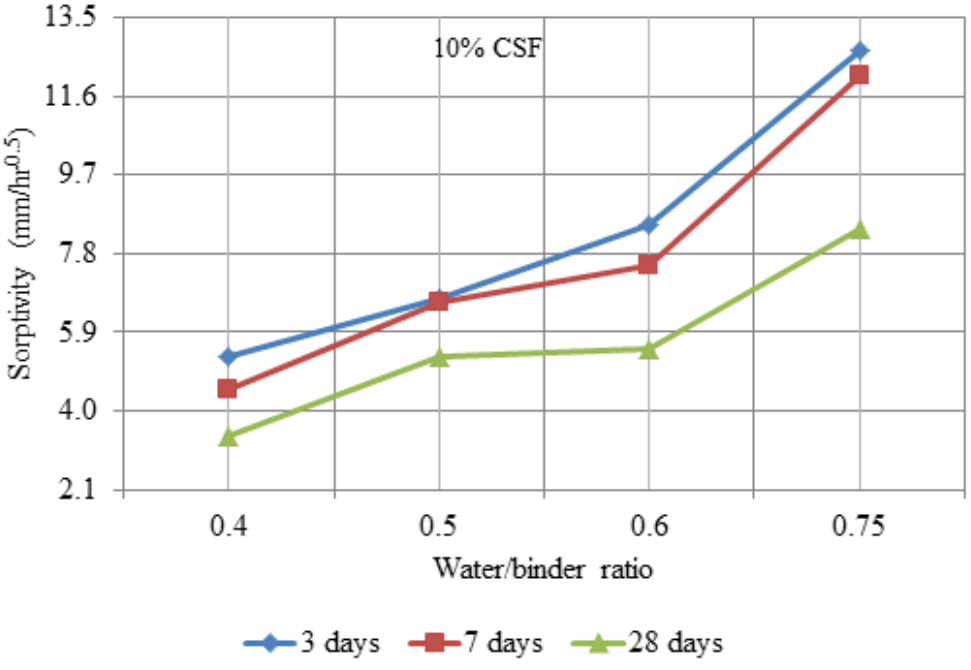


Figure 4.19: Water sorptivity vs. Water/binder ratio for the 90/10 CEM I-CSF concretes

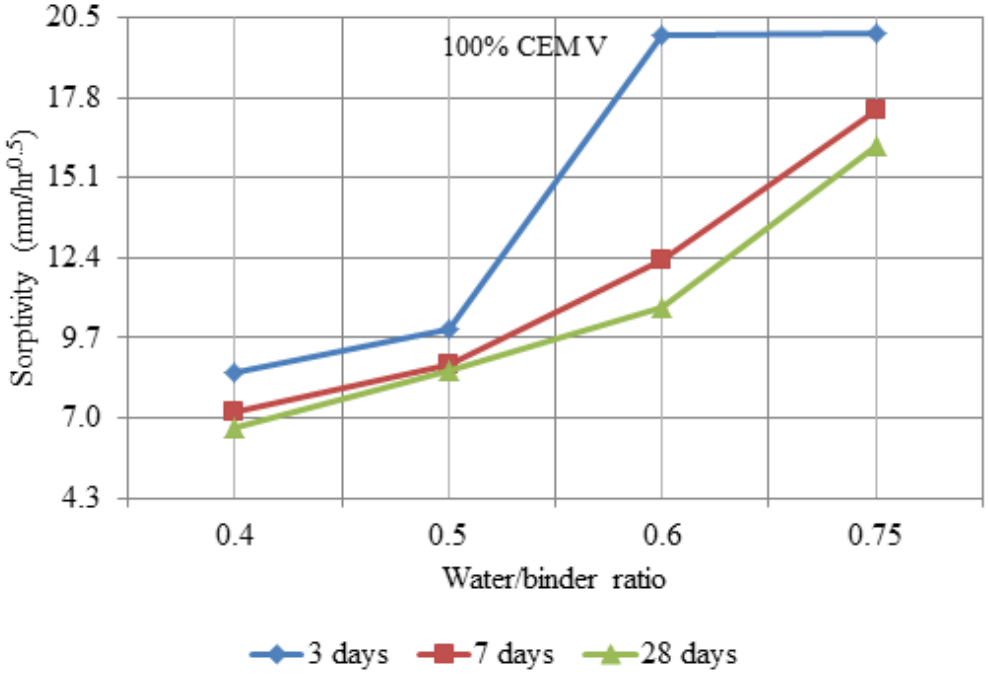


Figure 4.20: Water sorptivity vs. Water/binder ratio for the 100% CEM V concretes

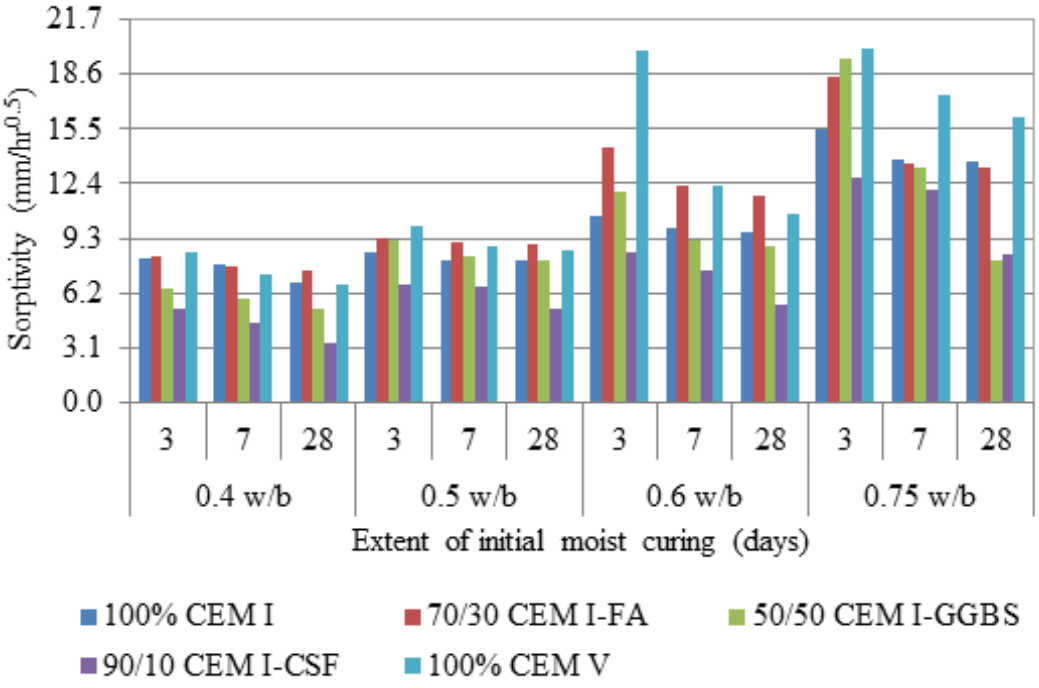


Figure 4.21: Water sorptivity vs. Extent of initial moist curing for all the concrete type studied

Although the oxygen permeability and water sorptivity tests both give an indication of the microstructure of the concrete, the mechanisms of fluid flow are different. However, much of the discussion for the oxygen permeability test results holds similarly for the water sorptivity test results of the concretes. Thus, varying the binder type influences the concrete absorption rate, while a decreased w/b ratio results in improved concrete resistance to the penetration of moisture. From the sorptivity plots presented above (see Figures 4.16 - 4.20), it can be seen that the sorptivity values decrease as the w/b ratio reduces and the extent of initial moist curing period increases for all the concrete types investigated. However, the decrease in sorptivity values as a result of the decrease in w/b ratio are more marked than the increase in the extent of initial moist curing especially for the *CEM I* concretes. Similar lower sensitivity of the concretes to the extent of extended initial moist curing was noted with the permeability results. As stated above, similar reasoning also applies for the sometimes clustered water sorptivity results of the concretes.

Figure 4.21 shows the influence of the extent of initial moist curing periods and w/b ratios on concrete absorption for all the concrete types investigated. From this figure the beneficial use of *SCM* in improving concrete pore structure can be seen for the *GGBS* and *CSF* blended concretes in comparison to the *CEM I* concretes. In addition, blended concretes presented better sorptivity values at lower w/b ratio and extended initial moist curing periods. Improvement in sorptivity for these blended concretes can be attributed to the pozzolanic effect of the *SCM* at later ages and also to their pore filling effect.

The improved sorptivity for all the concretes at low w/b ratio and prolonged duration of initial moist curing are attributed to the reduction in the volume and size of the pores within the concrete microstructures as well as the interconnections. Continued hydration leading to a reduction in capillary porosity is also another reason for the better sorptivity noted for these concretes (Khan & Lynsdale, 2002; Khan et al., 2001; Mehta & Manmohan, 1980). It can also be

noted from Figure 4.21 that the *GGBS* blended concretes presented better sorptivity values than the FA concretes, which is in contrast to the results obtained from their oxygen permeability testing.

From the water sorptivity results of the concretes obtained in this study, for equal w/b ratio and extent of initial moist curing period, the different concrete types can be ranked in terms of sorptivity from the lowest as 30% *FA* blended concrete < 100% *CEM V* concrete < 100% *CEM I* concrete < 50% *GGBS* blended concrete < 10% *CSF* blended concrete. The ranking is generally true at all w/b ratios and extent of initial moist curing periods. The greatest improvement in concrete sorptivity can be achieved through the use of *CSF* and *GGBS SCM*. Improvements in the permeation properties for concretes may be achieved through extended initial moist curing periods. The sorptivity results for all the concrete types tested clearly show that the experimental work was of acceptable quality, since the results obtained follow expected trends and are comparable to results from other similar studies. Hence, the water sorptivity test results of the concretes may be used in the development of carbonation prediction models.

4.4.2 Water sorptivity at 6, 12 and 18 months after casting

Results of water sorptivity test at 6, 12 and 18 months after casting and exposure for the 0.5 w/b ratio concretes are presented in Table B2 in Appendix B. In the table, the water sorptivity test results for the different exposure conditions studied are presented in terms of sorptivity ($mm/hr^{0.5}$) and porosity (%) values of the concretes. Each value shown in Table B2 represents the averages of sorptivity measurements on four individual concrete discs.

The results presented in Table B2 are shown graphically in Figures 4.22 - 4.24, which show the relationship between the medium-term sorptivity results of the concretes and the extent of initial moist curing for the different exposure conditions investigated. These figures also allow comparison of the water

sorptivity across binder types as well as the influence of varying degree of initial moist curing periods in the medium-term. In addition, the effect of carbonation on the permeation properties of the concretes exposed to different inland environmental conditions in the medium-term can also be quantified. The results of the individual concrete disc sorptivity measurements and the variability around the average sorptivity and porosity values satisfied the requirements of SANS Draft Specification as indicated by the test results, that is R^2 values are all greater than 0.98.

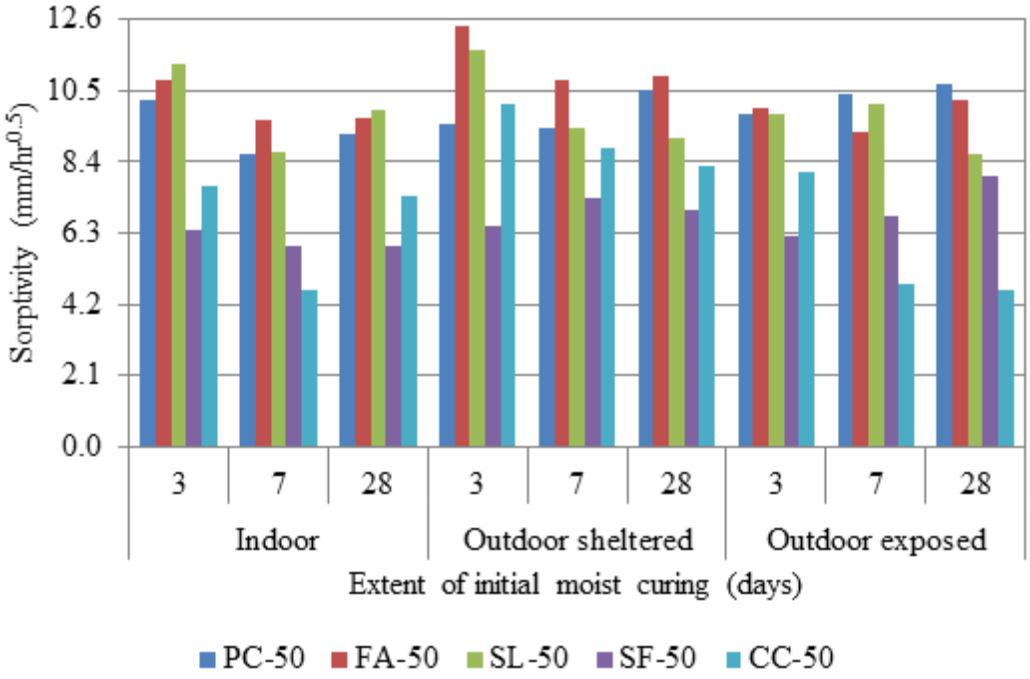


Figure 4.22: Concrete sorptivity measurement results after 6 months exposure to the inland environment

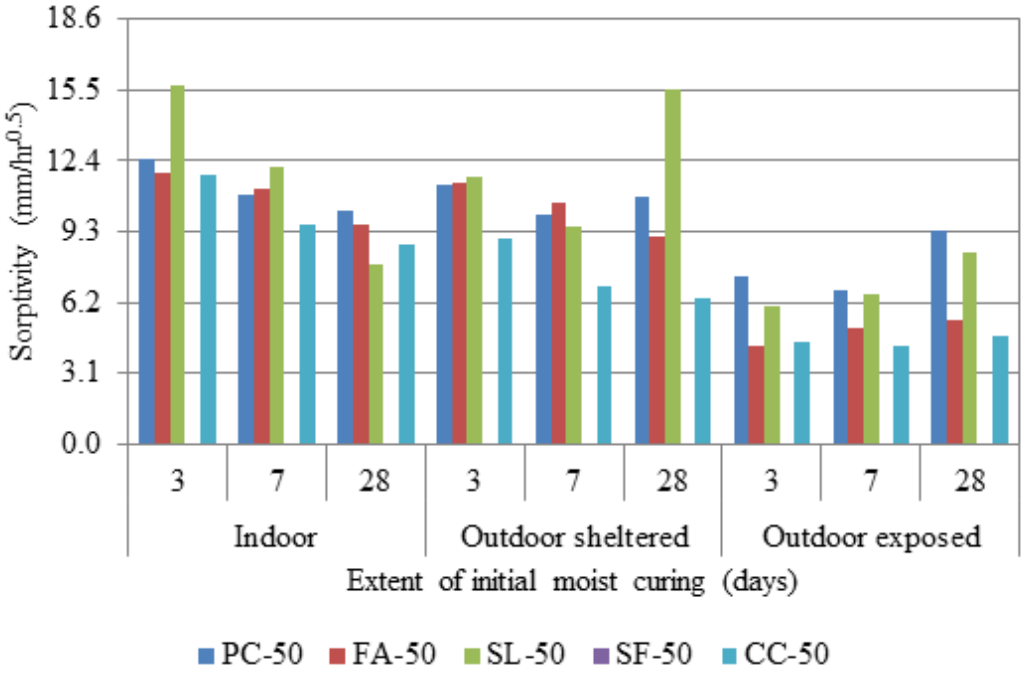


Figure 4.23: Concrete sorptivity measurement results after 12 months exposure to the inland environment

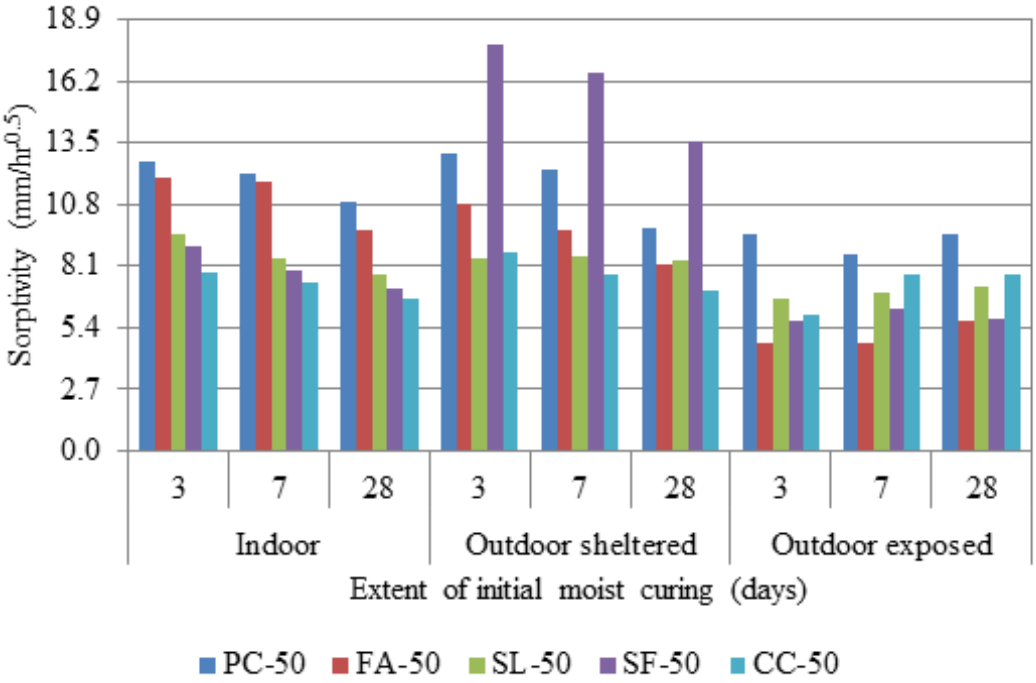


Figure 4.24: Concrete sorptivity measurement results after 18 months exposure to the inland environment

Figures 4.22 - 4.24 show the relationship between the medium-term sorptivity values of the concretes for the different inland environment investigated as well as the extent of the initial moist curing periods on the concrete sorptivity in the medium-term. Generally, it can be noted from the above figures that the relative effects of the extent of initial moist curing on the sorptivity values of the concretes are largely unchanged with time for the different exposure conditions investigated. However, this effect is less pronounced for the concrete samples exposed outdoor to rain and sun. Although companion concretes were tested at early-age (see section 4.4.1) direct comparison of the sorptivity results will not be made due to differences in the exposure conditions.

Figure 4.22 shows the 6 months water sorptivity test results of the concretes for the three exposure conditions investigated. It can be noted from the figure that the sorptivity values for all concretes on the different exposure sites reduces as the extent of initial moist curing periods increases. The improved sorptivity of all the concretes with initial curing time can be attributed to the reduction in the volume and size of the pores within the concrete microstructures due to improvement in hydration and/or carbonation (Khan & Lynsdale, 2002; Khan et al., 2001; Mehta & Manmohan, 1980). Similarly, blended concretes on the outdoor exposure sites showed lower sorptivity results than the *CEM I* concrete. This is probably due to either carbonation pollution or continued and better hydration of the blended concretes, since samples on this exposure site received moisture during the summer months. Concrete samples exposed outdoor to rain and sun generally presented better sorptivity values compared to the other exposure sites concretes after 6 months of exposure. Similar trends obtained for the 28 days water sorptivity test results in terms of binder types were still being maintained for the indoor and outdoor sheltered exposure sites concrete samples.

The 12 months water sorptivity test results of the concretes are presented in Figure 4.23. The trends obtained at 6 months were still being maintained. However, a notable reduction in the sorptivity values for all concretes is evident,

especially for the concrete samples exposed outdoors to rain and sun. Again similar trends observed at 12 months were still evident after 18 months of exposure as shown by the sorptivity plot in Figure 4.24. In this case, the sorptivity values between the concretes on the different exposure sites were very distinct, as well as the effect of the extent of initial moist curing periods. In addition, all the blended concretes showed lower sorptivity values compared to the *CEM I* concretes on all the exposure sites investigated. The reasons for the *CSF* concretes exposed outdoor but sheltered from rain and sun presenting higher sorptivity values in comparison with the *CEM I* concretes and equivalent *CSF* concretes exposed on the other exposure sites are unclear. The results seem anomalous and may need further investigation.

4.5 Results of Chemical Composition Tests

4.5.1 Calcium hydroxide content

The results of thermogravimetric analysis (*TGA*) test on specimens obtained from the concretes at 3, 7 and 28 days after casting are presented in Table 4.4. The calcium hydroxide ($Ca(OH)_2$) contents of the concretes are obtained from the *TG/DTG* plots following the procedure outlined in section 3.5.3. The individual *TG/DTG* plots for the concretes may be found in the file named "Early-age Thermogravimetric Test Results" in the attached CD.

The $Ca(OH)_2$ contents of the specimens are presented in percentages of the cement content in the specimen used for the thermal analysis. Expressing the $Ca(OH)_2$ contents of the specimen as a fraction of the cement content of the concrete allows comparisons of the chemical composition of the concretes across binder types. Furthermore, it allows a better estimate of when the pozzolanic reaction starts to deplete the $Ca(OH)_2$ content in the case of blended concretes.

Table 4.4: Calcium hydroxide content of the concretes

Binder type	Concrete mixture label	$Ca(OH)_2$ content in the concrete (% by mass of cement content)		
		3 days	7 days	28 days
100% CEM I	PC-40	17.9	21.3	23.8
	PC-50	15.5	19.0	22.5
	PC-60	14.7	17.3	21.3
	PC-75	13.1	14.9	18.2
70/30 CEM I-FA	FA-40	15.2	14.7	13.8
	FA-50	14.5	14.0	13.0
	FA-60	13.9	13.2	12.7
	FA-75	13.1	12.7	11.9
50/50 CEM I-GGBS	SL-40	15.1	12.4	11.9
	SL-50	14.0	10.5	9.5
	SL-60	13.8	9.6	8.7
	SL-75	13.1	9.2	8.0
90/10 CEM I-CSF	SF-40	13.4	12.7	11.2
	SF-50	12.7	11.8	10.4
	SF-60	11.8	11.3	9.3
	SF-75	10.5	10.7	8.7
100% CEM V	CC-40	13.9	10.1	9.3
	CC-50	13.5	9.0	8.0
	CC-60	12.3	8.2	7.8
	CC-75	11.7	7.7	7.1

The $Ca(OH)_2$ content of the concretes presented in Table 4.4 are shown graphically in Figures 4.25 - 29 which show the relationship between the $Ca(OH)_2$ content and w/b ratio for each concrete type at the different concrete ages considered. In order to allow comparison of the chemical composition of the concretes in terms of the $Ca(OH)_2$ content for the different concrete types tested across binder type, Figure 4.30 shows the $Ca(OH)_2$ content plotted against concrete ages after casting for the different w/b ratios investigated.

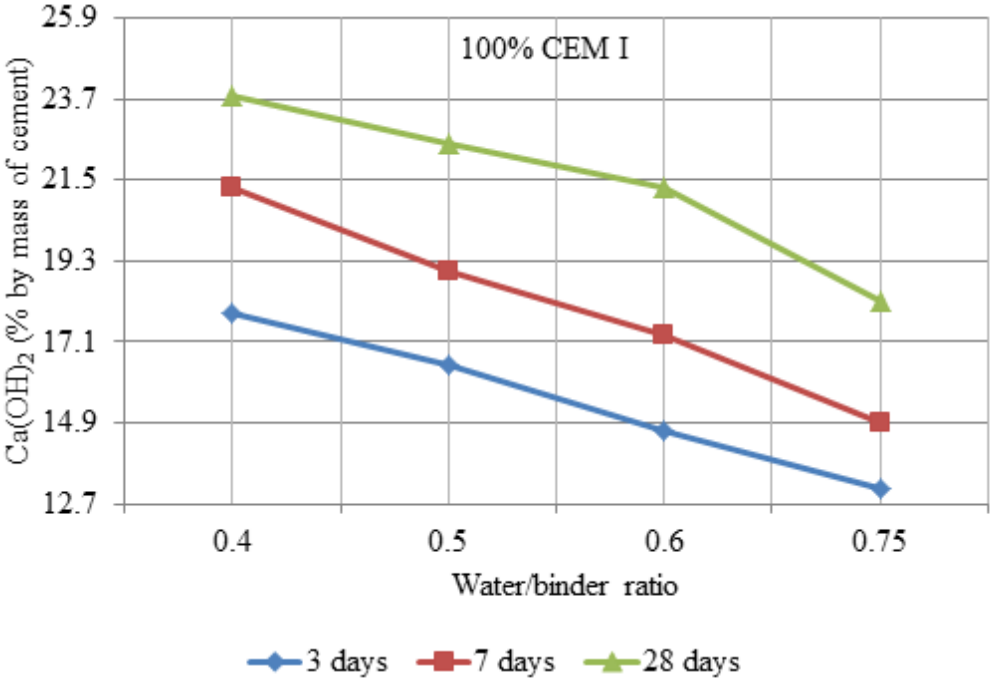


Figure 4.25: *Ca(OH)₂* content vs. Water/binder ratio for the 100% CEM I concretes

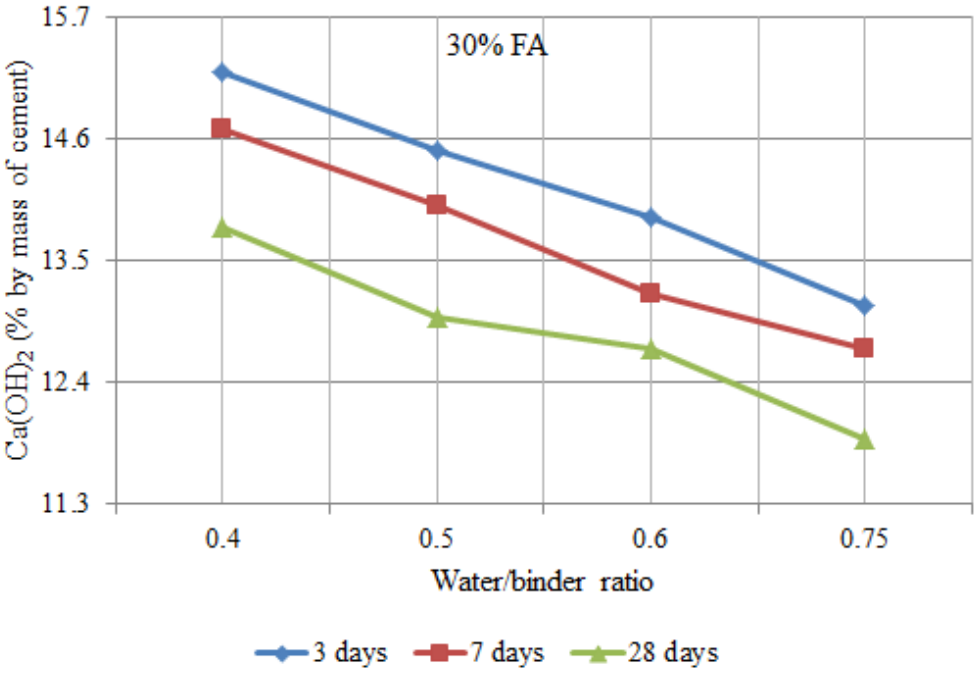


Figure 4.26: *Ca(OH)₂* content vs. Water/binder ratio for the 70/30 CEM I-FA concretes

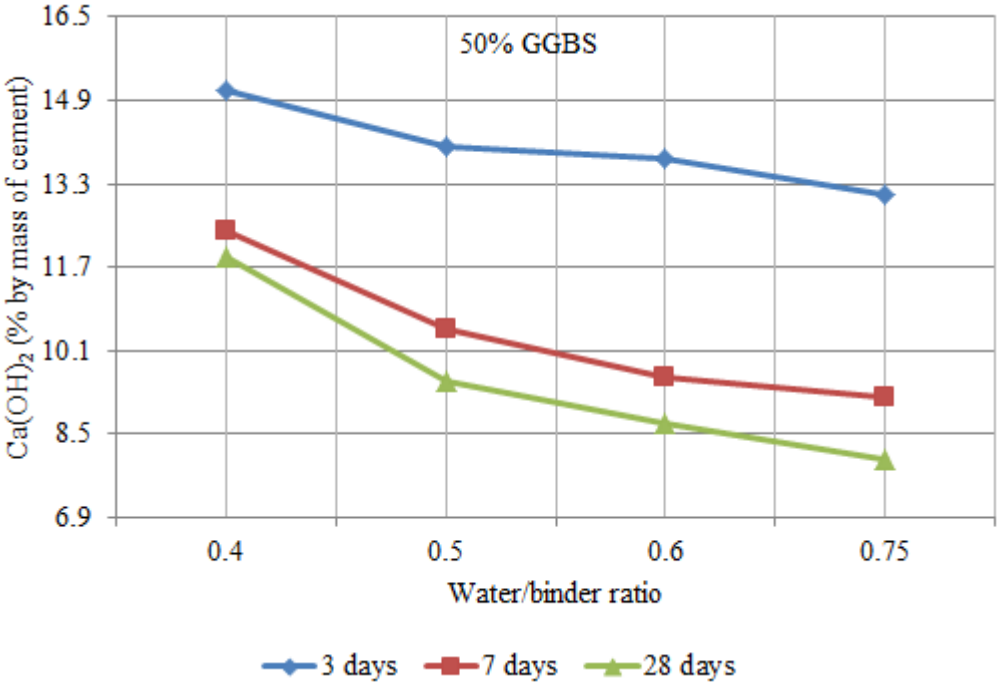


Figure 4.27: *Ca(OH)₂* content vs. Water/binder ratio for the 50/50 CEM I-GGBS concretes

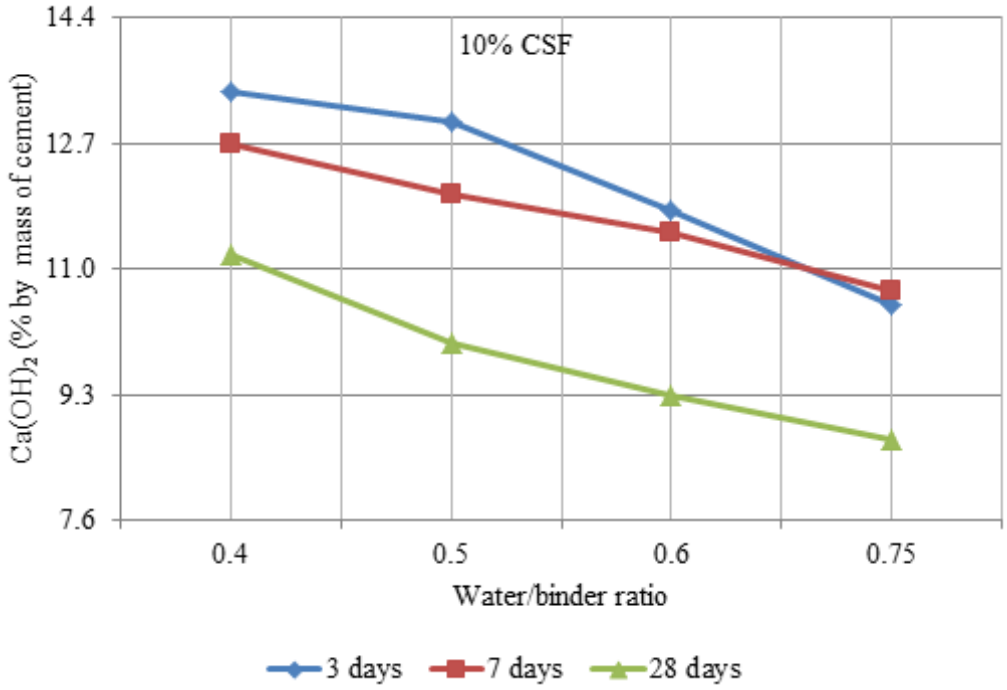


Figure 4.28: *Ca(OH)₂* content vs. Water/binder ratio for the 90/10 CEM I-CSF concretes

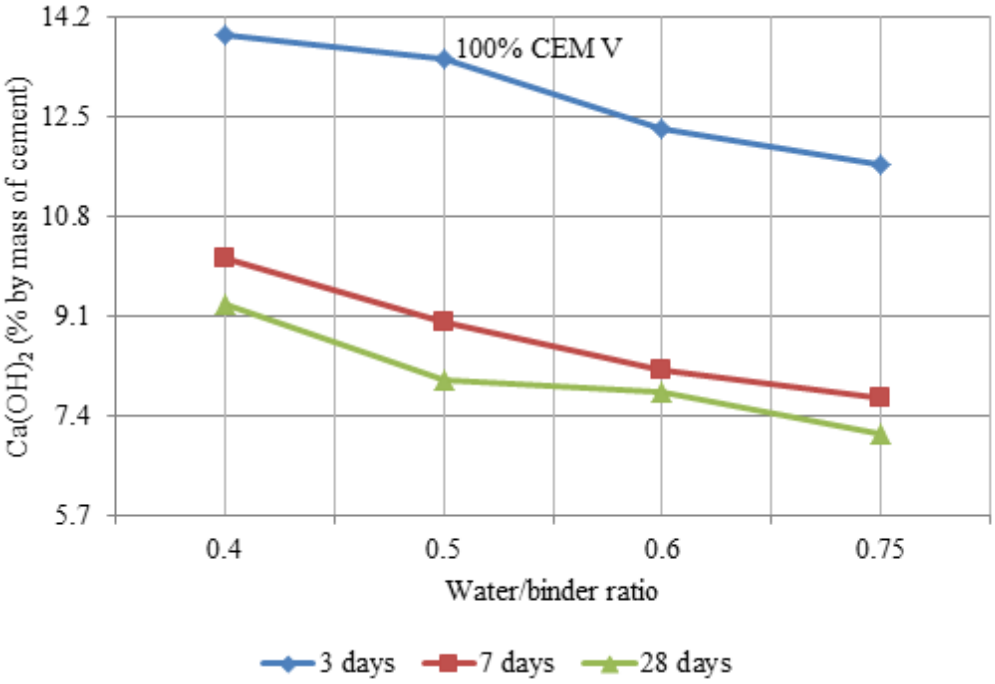


Figure 4.29: *Ca(OH)₂* content vs. Water/binder ratio for the 100% CEM V concretes

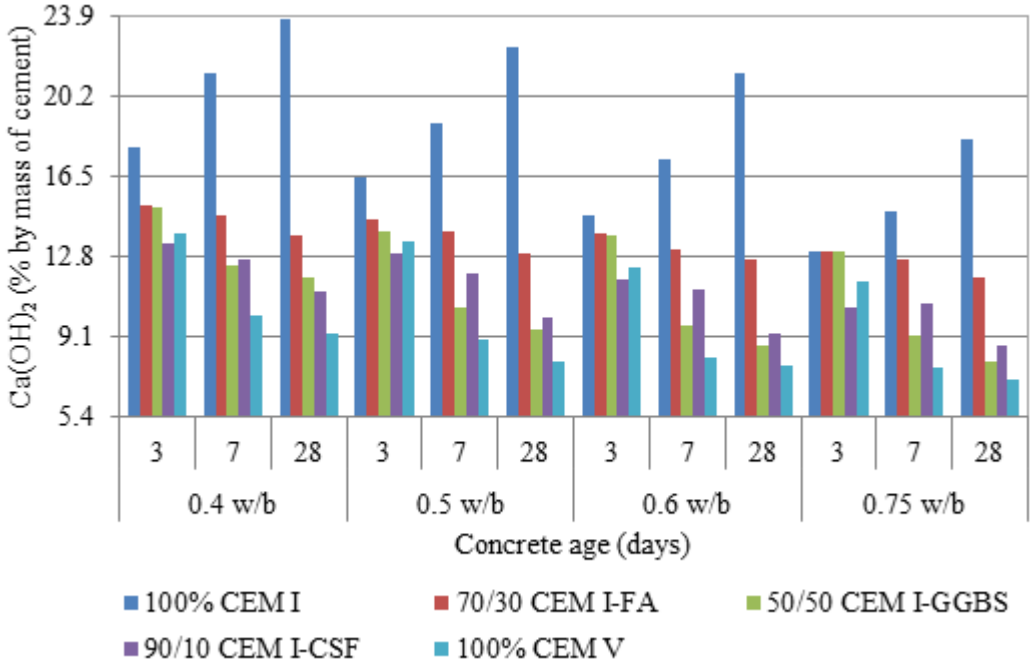


Figure 4.30: *Ca(OH)₂* content vs. Concrete age for all the concrete type studied

The use of different binder types influenced the $Ca(OH)_2$ content of the concretes, with increasing w/b ratios and decreasing binder contents resulting in decreased $Ca(OH)_2$ content for all the concrete types investigated. From the $Ca(OH)_2$ plots presented in Figures 4.25 - 29, it can be noted that the $Ca(OH)_2$ content increases as the concrete moist curing ages increases for the unblended concretes while it decreases for all the blended concretes for all the w/b ratios investigated. The reason for the increase in the unblended concretes is that, *CEM I* produces $Ca(OH)_2$ during hydration and its content increases with hydration time. While, the decrease in $Ca(OH)_2$ content for the blended concrete is as a result of $Ca(OH)_2$ consumption during the pozzolanic reaction between the produced $Ca(OH)_2$ and the *SCM*. As the pozzolanic reaction continues, the $Ca(OH)_2$ content from *CEM I* hydration is being depleted.

The variation in the $Ca(OH)_2$ contents for all the concrete types tested in relation to the w/b ratios and concrete ages are presented in Figure 4.30. From Figure 4.30, it can be noted that blended concretes presented lower $Ca(OH)_2$ contents in comparison to the *CEM I* concretes at all ages for the different w/b ratios investigated. The difference in $Ca(OH)_2$ content for the blended concretes are however lower at early-ages attributed to reduced pozzolanic reaction. Similar effects were found in paste and concretes systems published elsewhere (Franke & Sisomphon, 2004; Midgley, 1979).

It can also be noted from Figure 4.30 that the $Ca(OH)_2$ content for both the blended and unblended concretes are not significantly different at 3 and 7 days. This shows that the *SCM* have little effects on the normal hydration process of *CEM I* concretes at early ages. This behaviour is in agreement with earlier works by Marsh and Bonnery (1986) and Marsh and Day (1988), using *CEM I* and *FA* blended concretes, but it is however in conflict with the work of Dalziel (1986) as reported in Marsh and Day (1988).

Due to the inherently slower rate of hydration of *GGBS* and the higher replacement level of *SCM* in *CEM V*, the *CEM V* concretes presented the least $Ca(OH)_2$ content at all w/b ratios investigated especially at later ages in comparison to the other blended concretes. Generally, the higher the *SCM* content in a concrete mix for equal cement content, the lower will be the $Ca(OH)_2$ content. This can be attributed to both the high dilution effect related to the fact that $Ca(OH)_2$ results from cement hydration which in turn is directly related to the cement proportion in the mixture, as well as the pozzolanic reaction between $Ca(OH)_2$ and *SCM* which consumes some $Ca(OH)_2$, and may extend over a long time period.

From the presented $Ca(OH)_2$ results of the concretes obtained from the thermogravimetric analysis test in this study, for equal w/b ratio and concrete age under continuous moist curing the different concrete types can be ranked in terms of the $Ca(OH)_2$ content from the lowest as 100% *CEM V* concrete < 50% *GGBS* blended concrete < 10% *CSF* blended concrete < 30% *FA* blended concrete < 100% *CEM I* concrete. The ranking is generally true for all w/b ratios and concrete ages under continuous moist curing. The greatest improvement in buffering against CO_2 ingress into concrete can be achieved through the use of *CEM I* concrete. The *TGA* test result for all the concrete types investigated shows that the experimental work is of an acceptable quality, since results obtained follow expected trends and are comparable to results from other similar studies. Thus, the *TGA* test results of the concretes may be used in the development of carbonation prediction models.

4.5.2 Wet chemical analysis for calcium oxide content

Table 4.5 shows the results from the wet chemical analysis test (using the acid digestion method) carried out on specimens obtained from the concretes at 3, 7 and 28 days after casting. The calcium oxide (*CaO*) contents of the concretes are obtained from the test results following the procedure outlined in section 3.5.3.

Each value shown on Table 4.5 represents the average of two individual acid digestion tests. The *CaO* contents of the concretes are presented as a percentage of the cement content and are quoted to 2 significant figures.

Table 4.5: Calcium oxide results of the concretes

Binder type	Concrete mixture label	Average *CaO* content in the concretes (% by mass of cement content)		
		3 days	7 days	28 days
100% CEM I	PC-40	16.58	16.92	18.73
	PC-50	15.73	16.17	17.13
	PC-60	14.31	15.74	16.42
	PC-75	13.37	14.13	14.96
70/30 CEM I-FA	FA-40	16.58	15.59	15.10
	FA-50	15.73	14.87	14.29
	FA-60	14.31	13.17	12.46
	FA-75	13.37	12.49	11.77
50/50 CEM I-GGBS	SL-40	14.45	14.27	13.26
	SL-50	13.17	12.27	11.61
	SL-60	12.69	11.71	11.40
	SL-75	11.94	11.50	10.61
90/10 CEM I-CSF	SF-40	15.25	14.39	13.76
	SF-50	15.07	14.22	13.01
	SF-60	14.34	12.97	12.73
	SF-75	12.69	11.71	11.46
100% CEM V	CC-40	13.53	13.09	11.62
	CC-50	12.75	11.35	10.21
	CC-60	11.97	10.51	9.73
	CC-75	11.41	10.39	9.28

The wet chemical analysis results of the concretes presented in Table 4.5 are shown graphically in Figures 4.31 - 4.35, which show the relationship between the *CaO* content of the concretes and the w/b ratios for each concrete types at the different concrete ages considered. In order to allow comparison of the chemical composition of the concretes in terms of *CaO* content for the different concretes

tested across binder types, Figure 4.36 shows the *CaO* content plotted against concrete ages after casting the concretes for the different w/b ratios investigated.

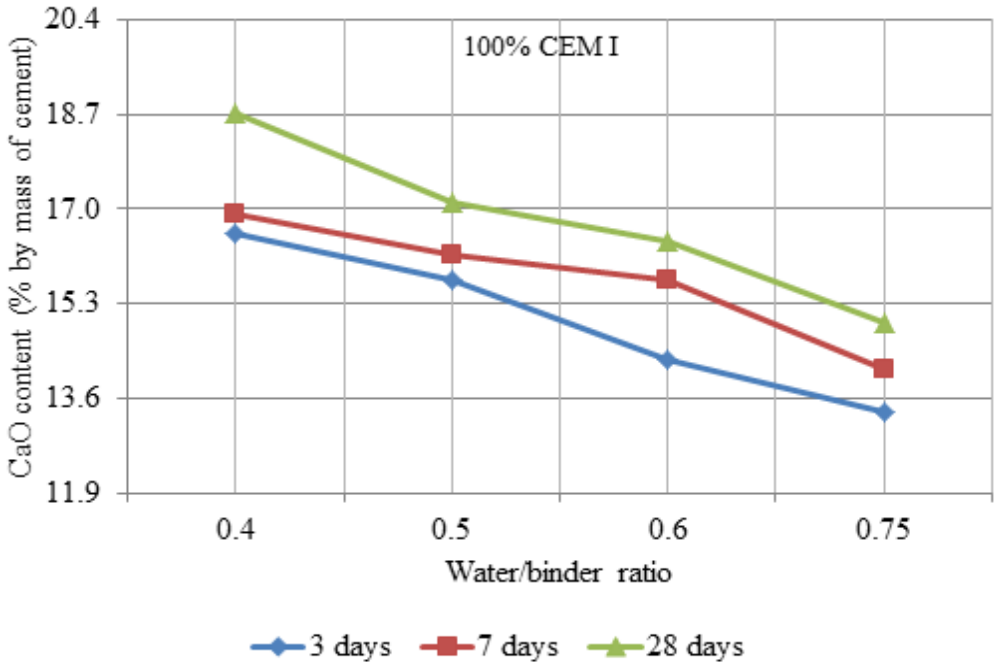


Figure 4.31: *CaO* content vs. Water/binder ratio for the 100% CEM I concretes

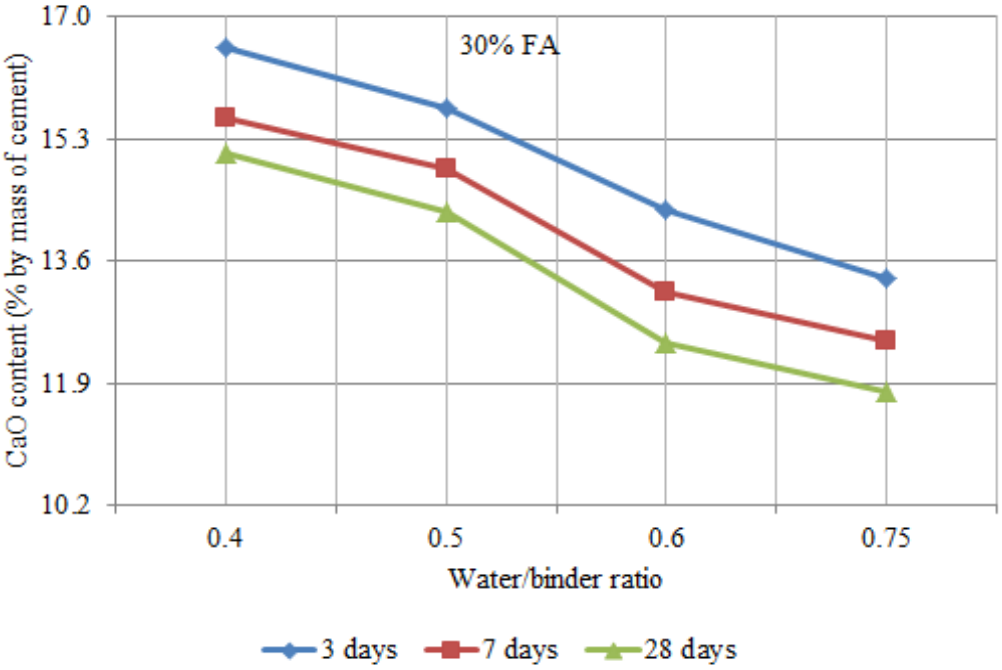


Figure 4.32: *CaO* content vs. Water/binder ratio for the 70/30 CEM I-FA concretes

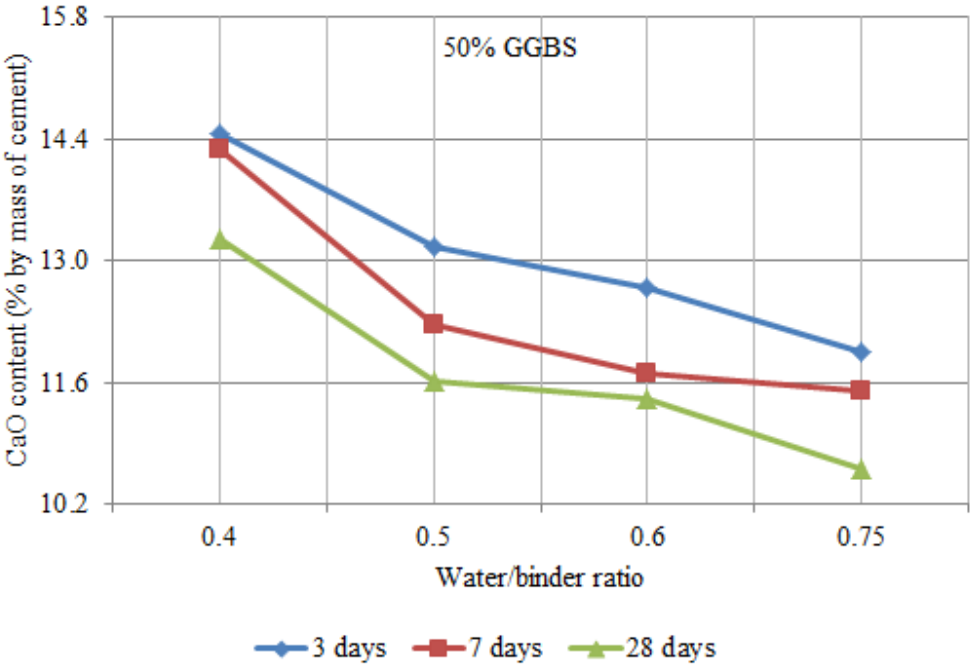


Figure 4.33: *CaO* content vs. Water/binder ratio for the 50/50 CEM I-GGBS concretes

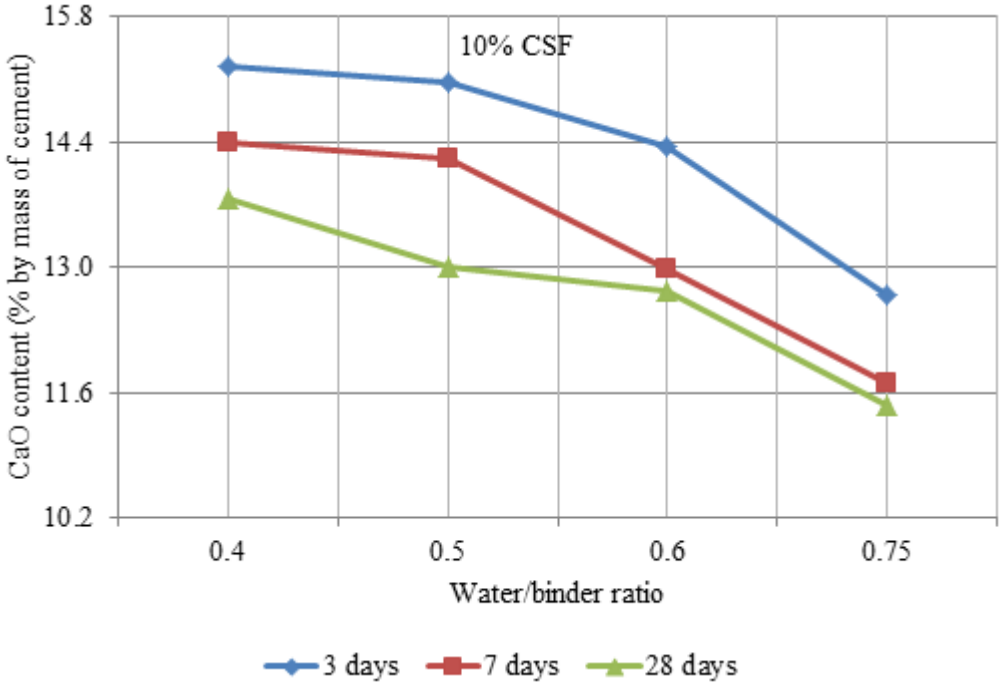


Figure 4.34: *CaO* content vs. Water/binder ratio for the 90/10 CEM I-CSF concretes

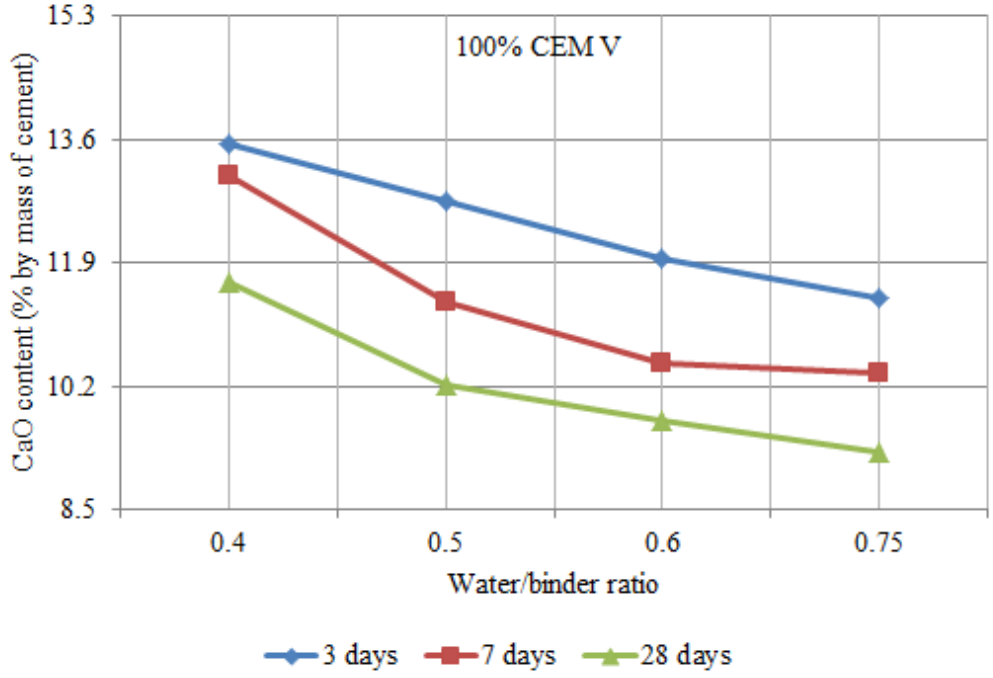


Figure 4.35: *CaO* content vs. Water/binder ratio for the 100% CEM V concretes

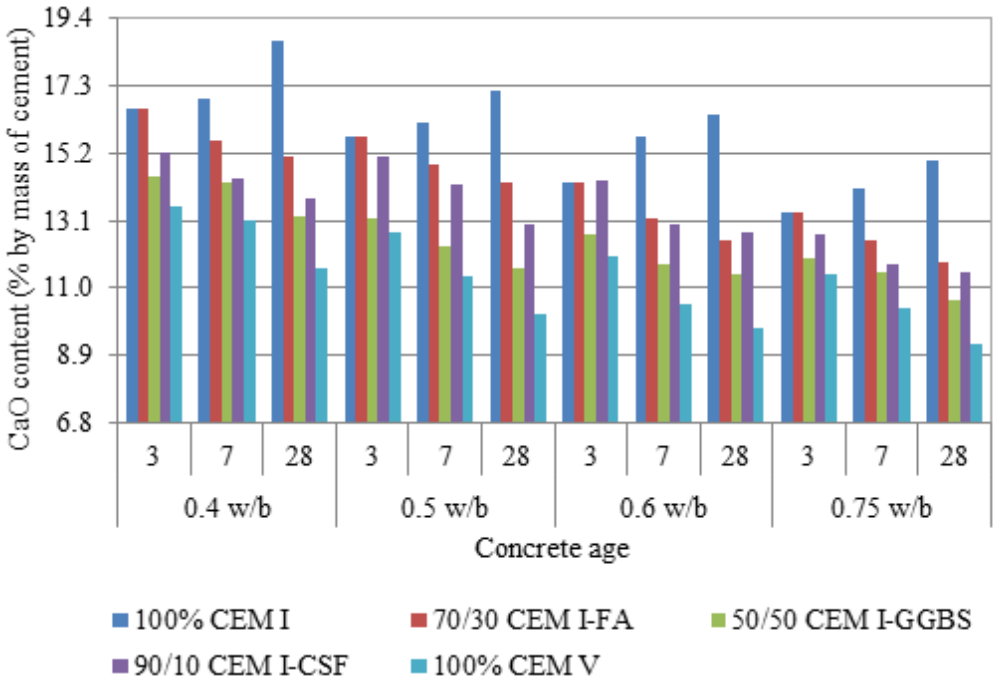


Figure 4.36: *CaO* content vs. Concrete age for all the concrete type studied

From the *CaO* content results of the concrete types presented in Figures 4.31 - 4.35, it is evident that the *CaO* content for the different concrete types investigated followed similar pattern to the $Ca(OH)_2$ content of the companion concretes in terms of trends obtained. However, differences in the chemical composition obtained for the concretes made from the same mixtures by the thermal and wet chemical analysis tests can be attributed to the fact that:

- thermal analysis test records the thermal and weight changes involved in the driving off of water in the course of the decomposition of calcium hydroxide between 400 - 500°C while;
- wet chemical analysis test measures the calcium ions that are taken into solutions. In addition to the calcium from $Ca(0H)_2$, calcium from other hydrated calcium bearing phases may also be extracted. Since the extraction is time dependent not all the $Ca(0H)_2$ may go into solution.

Thus, the variability in the chemical composition of the concretes can be attributed to the test methods employed and the component of the concrete chemistry they are quantifying. Therefore, similar reasoning is also applicable for the explanation of the *CaO* content of the different concrete types investigated as given for its $Ca(OH)_2$ content.

The differences in the chemical composition of the concretes obtained by the thermal and wet chemical tests noted in this study were also observed by Midgley (1979). Midgley (1979) in his study compares the chemical composition of concrete using five different test methods among which are the thermogravimetric and wet chemical analysis techniques. Based on his results which vary between the different test methods used, he concluded that in the determination of the chemical composition of set Portland cement, the thermal analysis test result are more reliable. However, in this study the intention is not to compare test methods used but rather to quantify the chemical composition of the concretes in terms of its $Ca(OH)_2$ and or *CaO* contents for possible use in carbonation modelling analysis, since these phases of concrete buffers CO_2 ingress.

The wet chemical analysis test results for all the concrete types tested clearly shows that the experimental work is of an acceptable quality, since results obtained follow expected trends and are comparable to results from other similar studies (Atis, 2003; Lampacher, 2000). Hence, the wet chemical analysis test results of the concretes can be used in the development of carbonation prediction models.

4.6 Micro-climate Variation at Exposure Sites

The annual micro-climatic variations for the exposure sites where the concrete samples were placed is presented in Table C1, in Appendix C. The variations in CO_2, *RH* and *temperature* are given as monthly minimum, maximum and mean values on the table. The monthly minimum and maximum values were obtained

from daily readings at intervals, while the monthly mean values are the average daily readings for a month. The micro-climate values were obtained from approximately 720 readings taken at 60 minute intervals continuously for any given month. The detailed monthly micro-climate readings for the exposure sites for a year may be found in the file named "Monthly Readings of Micro-Climates Data" in the accompanying CD. However, results of the mean monthly micro-climate results presented in Table C1, in Appendix C, are shown graphically in Figures 4.37 - 4.39 for the variations in CO_2, *RH* and *temperature* respectively.

4.6.1 Carbon dioxide variation

Figure 4.37 shows the average monthly CO_2 variation within a span of one year for the three exposure sites. From this figure it can be observed that the variability in CO_2 concentration between the exposure sites is not significant. However, slightly higher CO_2 values are observed for the indoor exposure site in most months and this can be attributed to the enclosed nature of the indoor site and the lack of free flow of air. Note also that the indoor exposure site is a basement parking garage and would be influenced by CO_2 from the exhaust fumes of cars. The outdoor exposed condition, unsheltered from rain and sun presented the least CO_2 concentration. This can be ascribed to its height above ground level and distance from sources of CO_2 pollution, since land use influences the CO_2 concentration.

Generally, based on the CO_2 variations presented in Figure 4.37 and all other factors being equal, concrete samples exposed to the indoor condition should have the highest carbonation rates while concretes exposed outdoor and unsheltered should present the least carbonation rates. This is based on the fact that the rate of diffusion of CO_2 into concrete increases with increase in CO_2 concentration between the internal and external environment of the concrete. The implication of the CO_2 variations for the durability performance and service life of concrete structures are that structural elements exposed to indoor conditions will be

exposed to higher carbonation rates and should therefore be more carefully designed and constructed if its design service life in terms of the initiation limit state (*ILS*) is to be achieved.

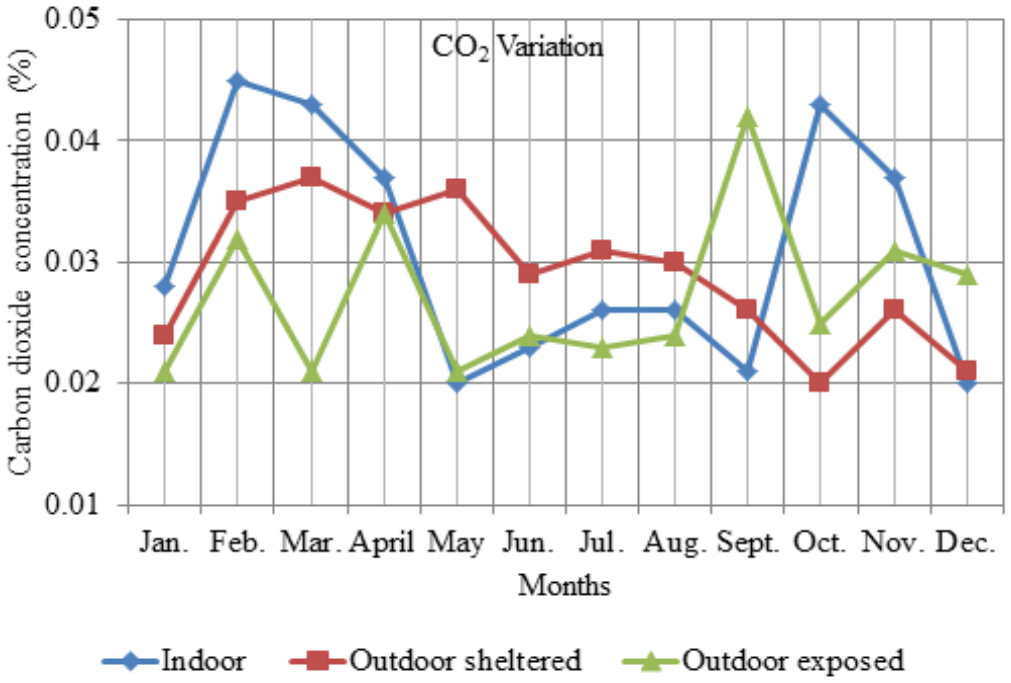


Figure 4.37: Average monthly carbon dioxide variations for the exposure sites

4.6.2 Relative humidity variation

The average monthly *RH* variation within a span of one year for the three exposure sites is shown in Figure 4.38. Based on the *RH* results for the exposure sites and since the external *RH* influences the internal humidity of the concrete, it is evident that concrete samples exposed indoors had the lowest internal moisture content. Concretes exposed outdoors but sheltered from rain and sun, had moderate internal humidity judging from the exposure site *RH* values presented in Figure 4.38. While the moisture content for concrete samples exposed outdoor to rain and sun had high for most part of the year as the average monthly *RH* for this site is higher compared to the other sites. Keeping other factors equal, the *RH* result presented shows that concrete cube samples exposed outdoor but sheltered

from rain and sun had the highest carbonation rates because this *RH* profile mostly lies in the zone of maximum carbonation rate.

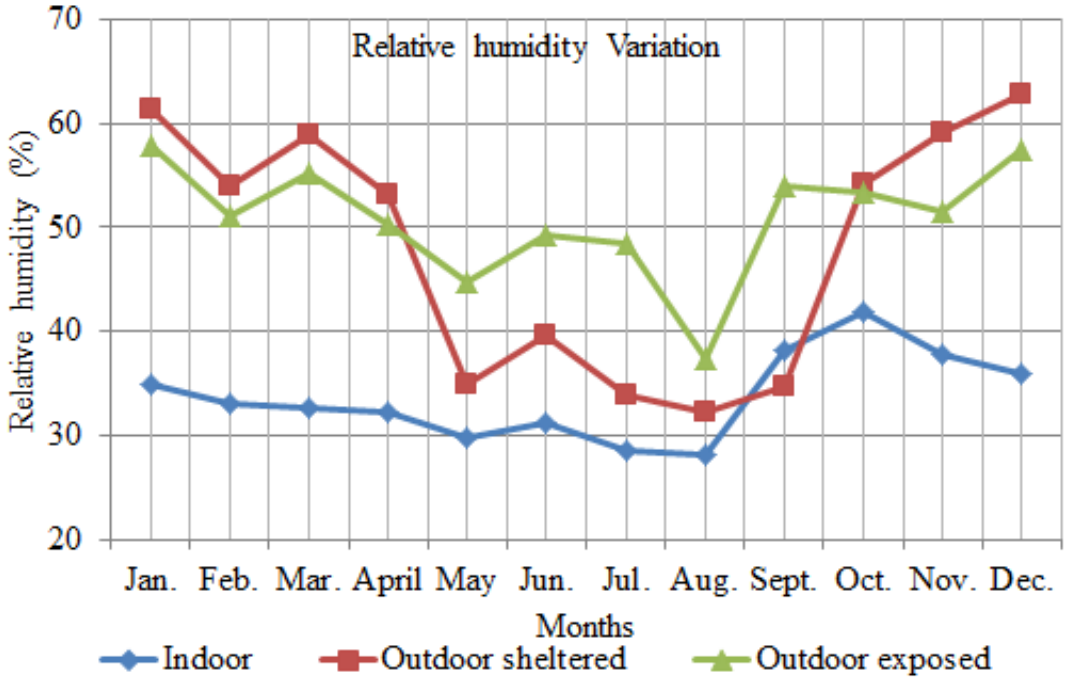


Figure 4.38: Average monthly relative humidity variations for the exposure sites

The implication of the *RH* results for durability performance and service life of reinforced concrete elements is that structural elements exposed outdoor but sheltered will present the highest carbonation rate. Thus, such elements should be more carefully designed and constructed if its design service life in terms of the *ILS* is to be achieved. It is also evident that concrete elements exposed outdoor to rain and sun are at risk of corrosion due to the high *RH* as a results of the occasional precipitation during summer months. Although the risk of carbonation may be very low for concrete elements exposed to the outdoor condition because of the low or high saturated pore structure which depend on the period of the year. The CO_2 ingress will be low during the summer months since pores will be saturated with moisture and the carbonation rate will be low during the winter months due to the fact that the pore structures will be dry.

4.6.3 Temperature variation

Figure 4.39 shows the average monthly temperature variation within a span of one year for the three exposure sites. From the temperature measurements recorded for these sites, it is evident that the indoor exposure site experienced warmer conditions for most part of the year while it was cooler for the outdoor sheltered and for the outdoor exposed sites during the winter months. Although, the influence of temperature variations is not very significant for carbonation in concrete (Da Silva, et al., 2009), results of the temperature variation shows that carbonation rates should be lower for concrete cube samples exposed indoors, while it may be similar for the other two exposure sites since their temperature profiles are similar.

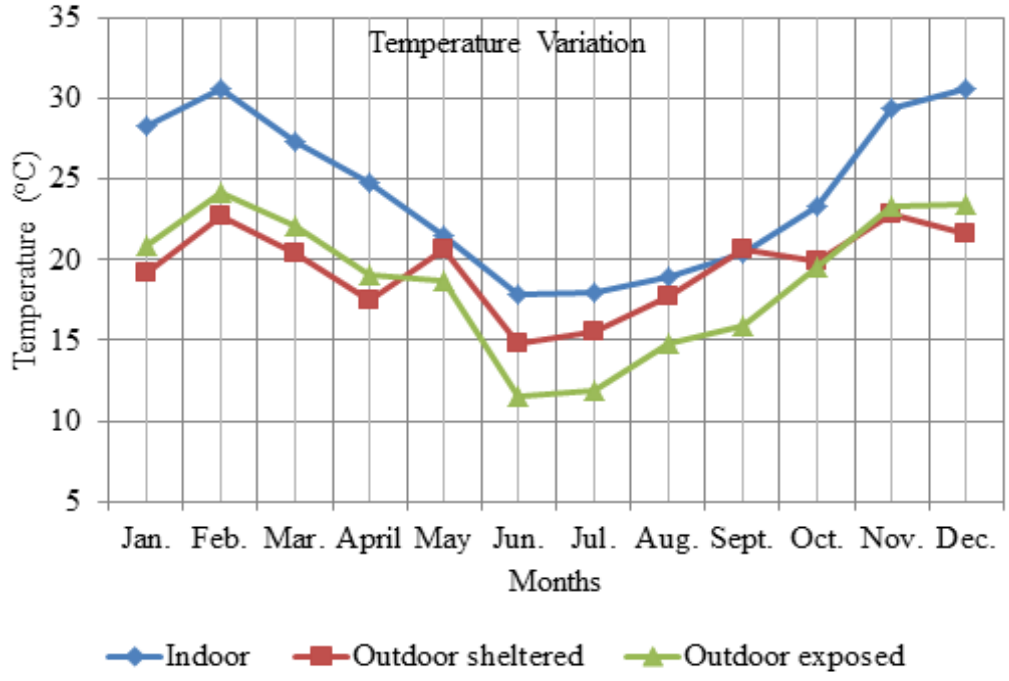


Figure 4.39: Average monthly temperature variations for the exposure sites

4.7 Concrete Carbonation Depth Results

The measured carbonation depth results from the carbonation tests on concrete samples exposed to the natural and accelerated environments are shown in Tables D1 to D4 in Appendix D. Each value shown in these tables represents the averages of six individual carbonation depth measurements on the two opposite side faces of the concrete cube samples. The carbonation depth results of the concrete samples exhibit a fairly wide scatter, not only because concrete itself is a variable material, but also due to the variable processing factors and and randomness of the micro-climatic conditions. The carbonation depth results presented in Tables D1 to D4 are shown graphically in Figures D1 to D60 in the file named "Concrete Carbonation Test Results Plots" in the accompanying CD. These figures show the relationship between the carbonation depth of the concrete and the exposure period for the different concrete types and w/b ratios considered. A typical carbonation depth versus exposure duration for the 100% *CEM I* concrete of different w/b ratios exposed indoor is shown in Figure 4.40

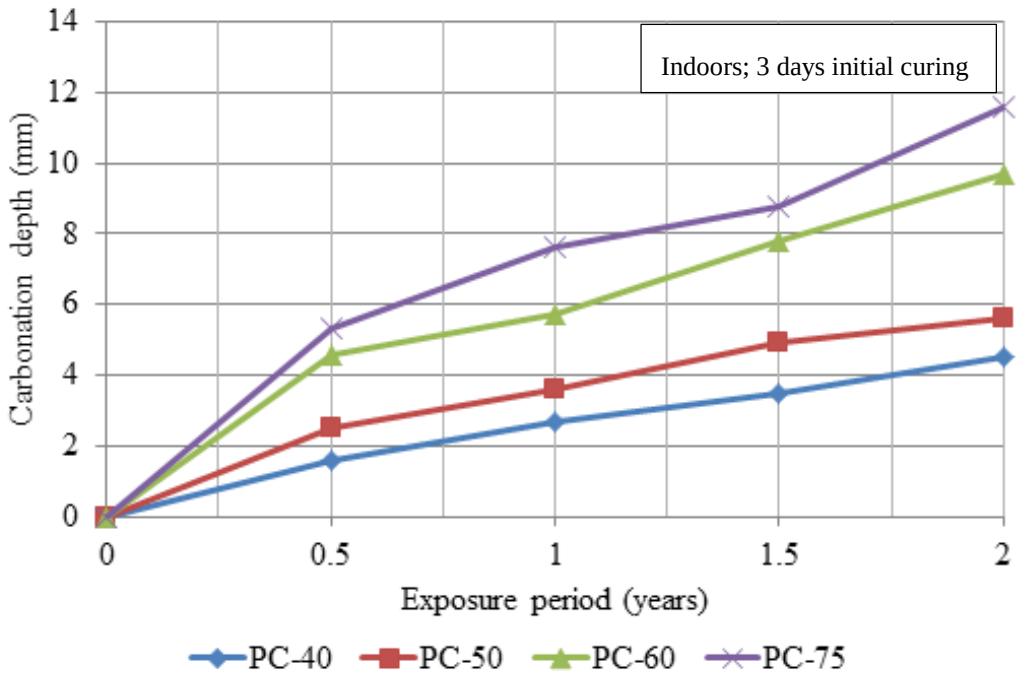


Figure 4.40: Carbonation depth vs. Exposure period

Figure 4.40 indicates that the carbonation depths increase at a decreasing rate with exposure period. Similar relationships were also observed for the other concrete types exposed to the different exposure conditions. The relationship observed for the carbonation depth plots in this study were also noted by other researchers (Sulapha et al., 2003).

From the carbonation depth results of the concretes observed in this study and for any given exposure condition investigated, the factors that influence the variability of the depth of carbonation of the concretes are the w/b ratio, binder types and contents, as well as the initial extent of moist curing of the concrete. Variability in the carbonation depth of the concretes across exposure conditions (sites) seems to be influenced also by the environmental conditions surrounding the concretes. Further explanation on these issues will be given at the end of the section.

4.7.1 Concrete carbonation rate

The results of the carbonation depths of the concrete presented on Tables D1 to D4 in Appendix D are plotted against their respective square root of exposure period. The plots of the carbonation depth versus square root of exposure period for the different concrete mixtures and exposure conditions investigated are shown in Figures D61 to D120 in the file named “Concrete Carbonation Rate Results Plots” in the accompanying CD. These figures show the relationship between the carbonation depth of the concrete and the square-root of the exposure period for the different concrete types and w/b ratios. A typical carbonation depth versus square-root of exposure period for the 100% *CEM I* concrete of different w/b ratios exposed to an indoor condition is shown in Figure 4.41.

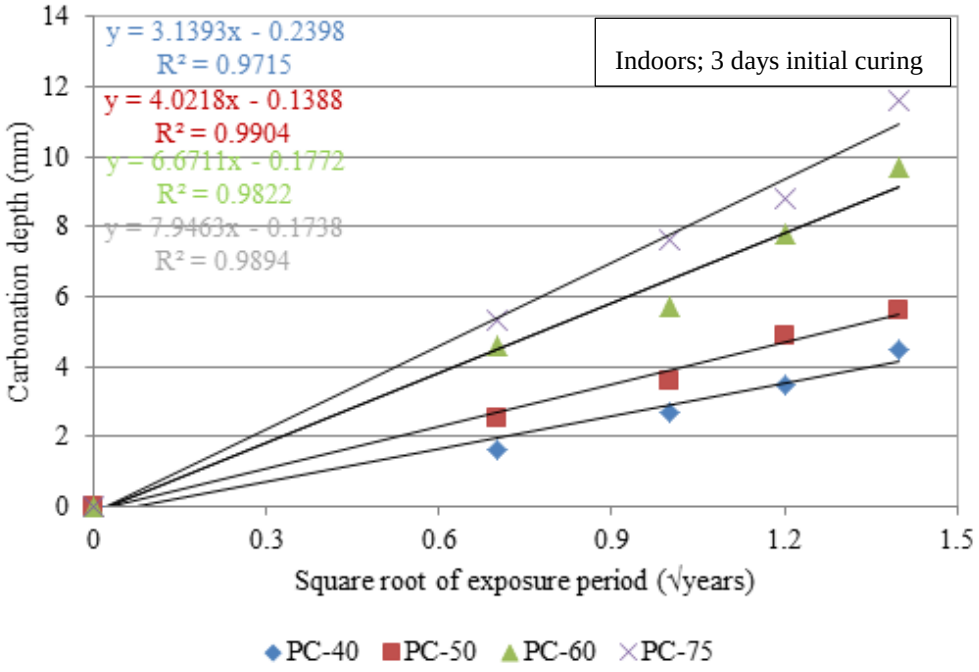


Figure 4.41: Carbonation depth vs. Square root of exposure period

Various forms of equation such as those represented by linear, square root, exponential and logarithm functions were fitted to the carbonation rate plots of the concrete. It is found that the relationship in Equation 4.1 gave the best correlation coefficient.

$$D = C\sqrt{t} + a \qquad 4.1$$

Where,

D = carbonation depth (mm)

C = carbonation rate (mm/√years or mm/√days)

t = exposure period (years or days)

a = empirical constant (mm)

The formulation of Equation 4.1 had been agreed upon by other researchers (Richardson, 1988; Tutti, 1982) especially when carbonation tests were performed under controlled indoor conditions. The values of C, a, and R^2 for all the concrete

types investigated are tabulated in Tables 4.6, 4.7, 4.8, and 4.9 for the indoor, outdoor sheltered, outdoor exposed and the accelerated exposures respectively. The values of "*a*" in equation 4.1 obtained for the different concrete mixtures were small compared to the measured carbonation depth *D*, therefore, they were discarded. This implies that Equation 4.1 can be simplified to $D = C\sqrt{t}$, which is similar to Fick's first law of diffusion that describes the carbonation process (Kropp, 1995). Since *C* is inversely proportional to the ability of concrete to resist the diffusion of CO_2, it becomes an important single parameter to directly compare and assess the resistance of the different mixtures (i.e. concrete types) to carbonation in this study. Additionally, *C* values for the individual concrete types allow variability to be quantified and trends to be established. Furthermore, the *C* values will also be useful for modelling analysis since it describes the concrete mixtures resistance to CO_2 ingress better than the carbonation depths.

Table 4.6: Regression parameters for the different concrete types exposed indoor

Concrete mixture label	Regression parameters								
	Extent of initial moist curing								
	3 days			7 days			28 days		
	C	*a*	R^2	*C*	*a*	R^2	*C*	*a*	R^2
PC-40	3.139	0.240	0.97	2.022	0.139	0.97	1.107	0.152	0.91
PC-50	4.022	0.139	0.99	2.923	0.094	0.99	1.831	0.114	0.97
PC-60	6.670	0.177	0.98	4.660	0.081	0.99	3.856	0.336	0.94
PC-75	7.945	0.174	0.989	5.983	0.286	0.98	4.948	0.415	0.95
FA-40	6.052	0.485	0.91	4.497	0.367	0.93	2.430	0.209	0.96
FA-50	7.628	0.600	0.94	6.574	0.474	0.95	4.636	0.407	0.95
FA-60	9.326	0.540	0.97	8.139	0.639	0.94	5.742	0.518	0.95
FA-75	13.698	0.440	0.99	10.720	0.350	0.99	8.091	0.738	0.95
SL-40	7.547	0.170	0.99	5.878	0.125	0.99	3.763	0.157	0.99
SL-50	9.300	0.282	0.99	7.545	0.031	0.99	5.589	0.305	0.95
SL-60	10.852	0.047	0.99	9.738	0.265	0.99	6.560	0.142	0.99
SL-75	15.745	0.299	0.99	12.880	0.442	0.99	9.992	0.207	0.99
SF-40	3.336	0.489	0.90	2.391	0.556	0.80	1.439	0.403	0.74
SF-50	4.483	0.736	0.87	3.609	0.444	0.93	2.233	0.461	0.83
SF-60	5.888	0.823	0.90	4.977	0.719	0.90	3.190	0.583	0.84
SF-75	7.374	0.842	0.90	6.582	0.681	0.93	4.337	0.630	0.91
CC-40	8.154	0.313	0.98	5.661	0.129	0.99	4.784	0.154	0.99
CC-50	9.699	0.182	0.99	8.233	0.061	0.99	5.606	0.261	0.98
CC-60	12.183	0.417	0.99	9.769	0.019	1.00	7.008	0.207	0.99
CC-75	13.893	0.248	0.99	12.700	0.182	0.99	9.371	0.259	0.99

Table 4.7: Regression parameters for the different concrete types exposed outdoor but sheltered

Concrete mix label	Regression parameters								
	Extent of initial moist curing								
	3 days			7 days			28 days		
	C	*a*	R^2	*C*	*a*	R^2	*C*	*a*	R^2
PC-40	2.936	0.175	0.89	2.287	0.086	0.99	1.349	0.120	0.96
PC-50	4.945	0.268	0.97	3.602	0.022	0.99	2.468	0.163	0.98
PC-60	7.161	0.022	0.99	5.649	0.338	0.97	4.310	0.467	0.91
PC-75	9.199	0.032	0.99	7.124	0.267	0.98	5.658	0.246	0.98
FA-40	6.503	0.133	0.99	5.054	0.526	0.91	2.958	0.264	0.94
FA-50	8.874	0.108	0.99	7.829	0.073	0.99	5.262	0.065	0.99
FA-60	11.097	0.596	0.97	9.209	0.180	0.99	7.987	0.569	0.95
FA-75	16.540	0.855	0.98	14.878	0.375	0.99	13.750	0.375	0.99
SL-40	7.371	0.141	0.99	6.054	0.074	0.99	3.685	0.009	0.99
SL-50	9.979	0.297	0.99	8.867	0.274	0.98	5.980	0.197	0.99
SL-60	12.617	0.149	0.99	11.948	0.385	0.99	7.242	0.068	0.99
SL-75	18.477	0.730	0.99	17.614	0.432	0.99	9.346	0.163	0.99
SF-40	2.646	0.456	0.86	1.787	0.437	0.76	1.659	0.487	0.69
SF-50	4.178	0.493	0.92	3.019	0.356	0.92	2.336	0.389	0.87
SF-60	7.319	0.974	0.92	5.339	0.572	0.93	4.129	0.591	0.88
SF-75	9.040	0.795	0.95	7.091	0.538	0.96	5.997	0.517	0.94
CC-40	8.675	0.360	0.99	7.493	0.284	0.98	6.060	0.092	0.99
CC-50	10.317	0.067	0.99	8.733	0.089	0.99	7.371	0.141	0.99
CC-60	11.909	0.138	0.99	10.243	0.191	0.99	8.470	0.004	0.99
CC-75	15.656	0.196	0.99	15.367	0.024	0.99	12.594	0.129	0.99

Table 4.8: Regression parameters for the different concrete types exposed outdoor but unsheltered

Concrete mix label	Regression parameters								
	Extent of initial moist curing								
	3 days			7 days			28 days		
	C	a	R^2	C	a	R^2	C	a	R^2
PC-40	1.555	0.018	0.98	0.901	0.055	0.98	0.554	0.076	0.91
PC-50	1.893	0.048	0.98	1.493	0.016	0.99	1.203	0.015	0.99
PC-60	3.198	0.109	0.99	2.493	0.016	0.99	2.206	0.003	0.99
PC-75	4.646	0.045	0.99	3.935	0.016	0.99	3.300	0.018	0.99
FA-40	3.315	0.009	0.99	2.450	0.107	0.99	1.681	0.126	0.97
FA-50	4.985	0.027	0.99	4.045	0.119	0.99	3.391	0.056	0.99
FA-60	6.813	0.100	0.99	5.809	0.176	0.99	5.274	0.156	0.99
FA-75	9.606	0.139	0.99	9.201	0.028	0.99	8.817	0.383	0.98
SL-40	3.888	0.023	0.99	3.510	0.199	0.98	1.998	0.159	0.95
SL-50	6.284	0.004	0.99	5.196	0.249	0.98	3.433	0.092	0.99
SL-60	8.136	0.057	0.99	6.441	0.199	0.99	4.393	0.098	0.99
SL-75	10.032	0.413	0.98	9.341	0.087	0.99	7.489	0.099	0.99
SF-40	1.267	0.389	0.63	0.920	0.311	0.56	0.772	0.264	0.52
SF-50	2.418	0.319	0.87	1.705	0.106	0.96	1.616	0.309	0.80
SF-60	3.503	0.433	0.86	2.520	0.140	0.96	2.123	0.225	0.90
SF-75	4.762	0.515	0.89	4.027	0.363	0.94	3.867	0.226	0.95
CC-40	5.329	0.223	0.99	4.379	0.066	0.99	3.654	0.063	0.99
CC-50	7.030	0.054	0.99	5.949	0.157	0.99	4.614	0.068	0.99
CC-60	8.739	0.076	0.99	6.799	0.127	0.99	5.519	0.006	0.99
CC-75	12.869	0.167	0.99	9.725	0.097	0.99	8.143	0.123	0.99

Table 4.9: Regression parameters for the different concrete types exposed to an accelerated condition

Concrete mix label	Regression parameters								
	Extent of initial moist curing								
	3 days			7 days			28 days		
	C	*a*	R^2	*C*	*a*	R^2	*C*	*a*	R^2
PC-40	0.776	0.155	0.98	0.417	0.152	0.92	0	-	-
PC-50	1.859	0.122	0.99	1.416	0.129	0.98	1.147	0.157	0.99
PC-60	2.607	0.126	0.99	2.459	0.113	0.99	2.114	0.069	0.99
PC-75	4.015	0.253	0.99	3.521	0.093	0.99	3.146	0.046	0.99
FA-40	1.951	0.099	0.99	1.586	0.021	0.98	1.281	0.13	0.99
FA-50	3.404	0.048	0.99	2.721	0.036	0.99	2.413	0.062	0.99
FA-60	5.414	0.259	0.99	4.402	0.239	0.99	4.049	0.121	0.99
FA-75	9.119	0.114	0.99	8.125	0.056	0.99	6.568	0.040	0.99
SL-40	2.778	0.200	0.99	2.299	0.028	0.99	1.724	0.113	0.99
SL-50	4.150	0.067	0.99	3.744	0.149	0.99	3.015	0.093	0.99
SL-60	6.079	0.263	0.99	5.025	0.139	0.99	3.931	0.043	0.99
SL-75	8.192	0.265	0.99	7.924	0.207	0.99	5.190	0.203	0.99
SF-40	1.041	0.206	0.99	0.607	0.127	0.95	0	-	-
SF-50	1.828	0.146	0.99	1.536	0.044	0.98	1.382	0.184	0.99
SF-60	2.966	0.232	0.99	2.758	0.223	0.99	2.510	0.053	0.99
SF-75	5.758	0.244	0.99	5.264	0.106	0.99	4.973	0.011	0.99
CC-40	4.082	0.055	0.99	3.195	0.129	0.99	2.576	0.107	0.97
CC-50	5.623	0.039	0.99	4.797	0.217	0.99	3.883	0.139	0.99
CC-60	9.00	0.336	0.99	6.743	0.094	0.99	5.520	0.011	1.00
CC-75	11.577	-	1.00	11.038	-	1.00	9.177	0.126	0.99

– Carbonation depth exceeds 50 mm.

The carbonation rate determinations of the concretes presented in Tables 4.6 to 4.9 are shown graphically in Figures 4.42 - 4.46, 4.48 - 4.52, 4.54 - 4.58 and 4.60 - 4.64 for the natural indoor, natural outdoor sheltered, natural outdoor exposed

and the accelerated exposure conditions respectively. These figures show the relationship between the carbonation rate of the concrete and the w/b ratio of each concrete type, for the different initial moist curing period considered. In order to allow comparison of the rates of carbonation in concrete across binder types for each exposure condition, Figures 4.47, 4.53, 4.59 and 4.65 show the carbonation rates versus the duration of initial moist curing before exposure for the different w/b ratios investigated. Similarly, in order to compare the rates of carbonation between the natural exposure conditions and since the carbonation rate trends are similar for the different w/b ratios investigated, the 0.5 w/b ratio concrete carbonation rates results were used in this comparison. Hence, Figure 4.66 shows the relationship between the carbonation rates of the concretes for the different natural exposure conditions investigated.

Carbonation rate plots for concrete cube samples exposed indoor

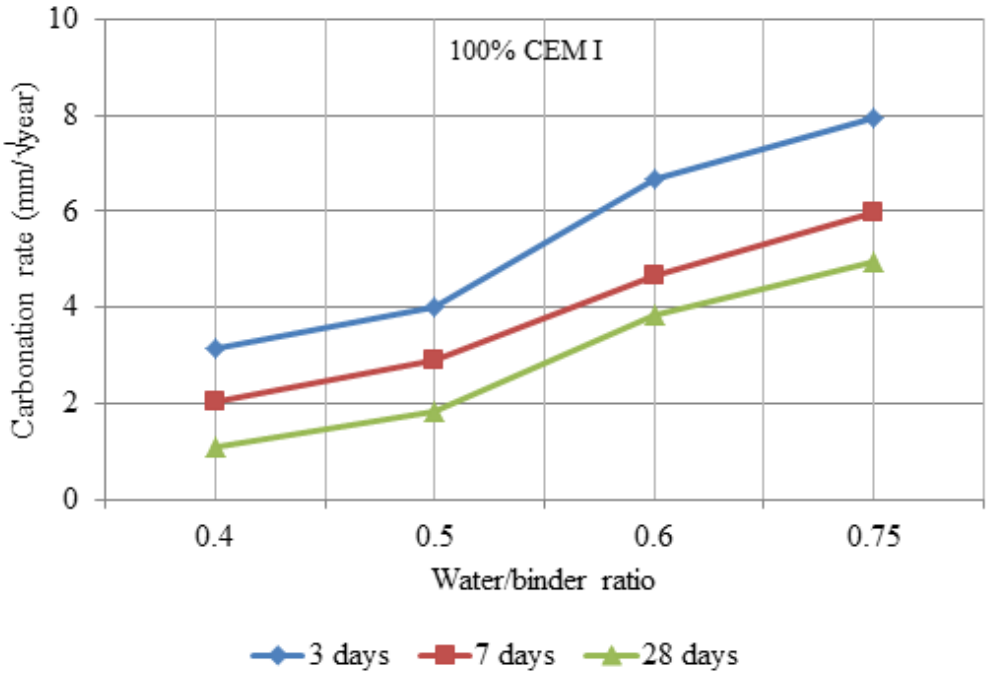


Figure 4.42: Carbonation rate vs. Water/binder ratio for the 100% CEM I concretes exposed indoors

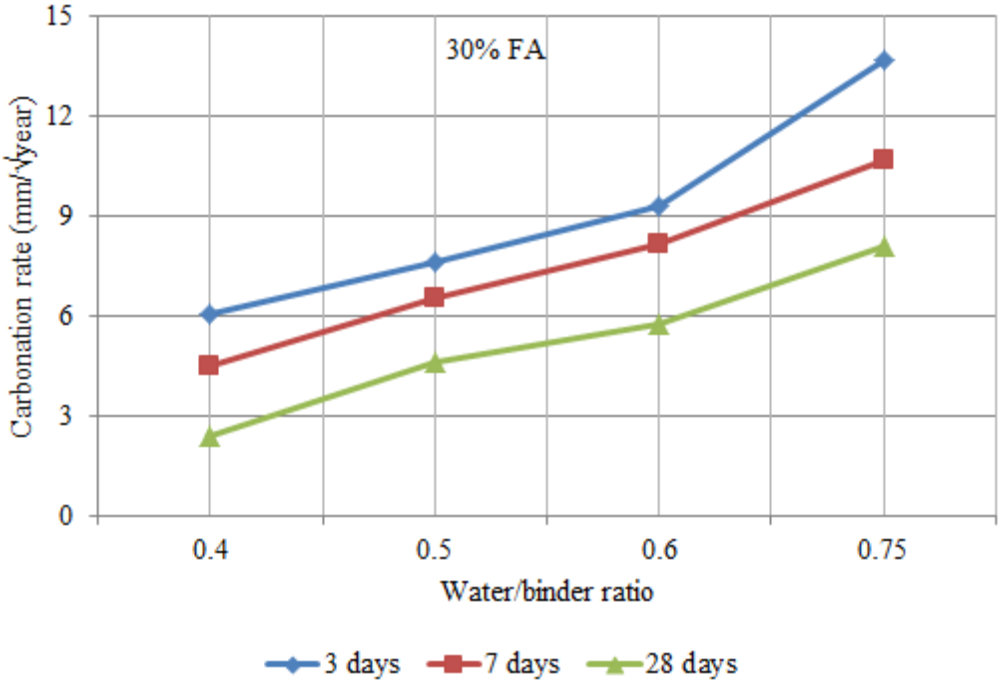


Figure 4.43: Carbonation rate vs. Water/binder ratio for the 70/30 CEM I-FA concretes exposed indoors

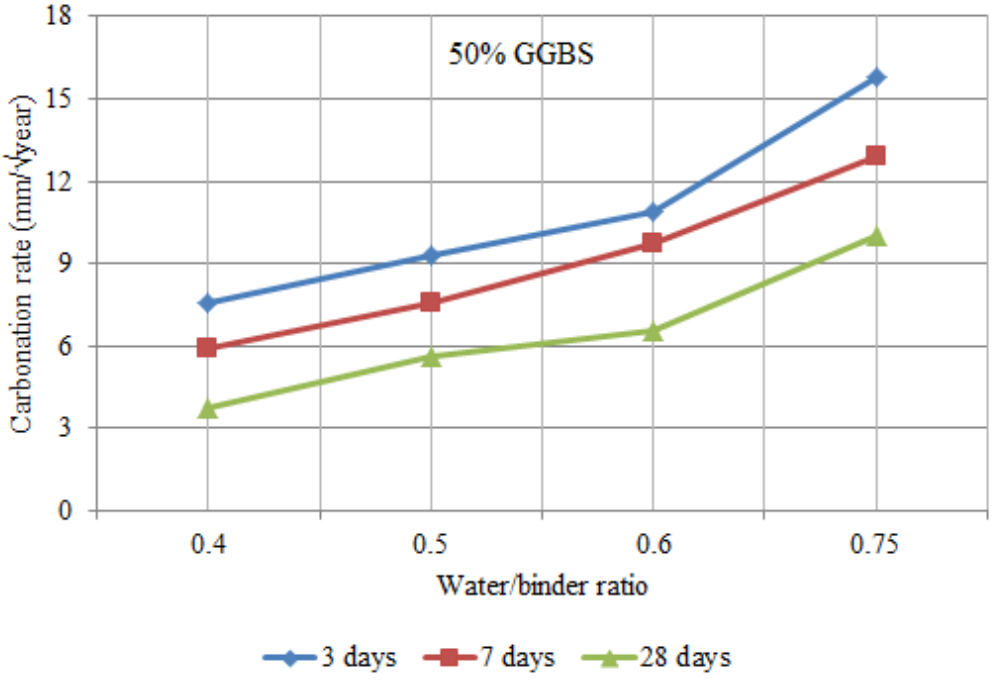


Figure 4.44: Carbonation rate vs. Water/binder ratio for the 50/50 CEM I-GGBS concretes exposed indoors

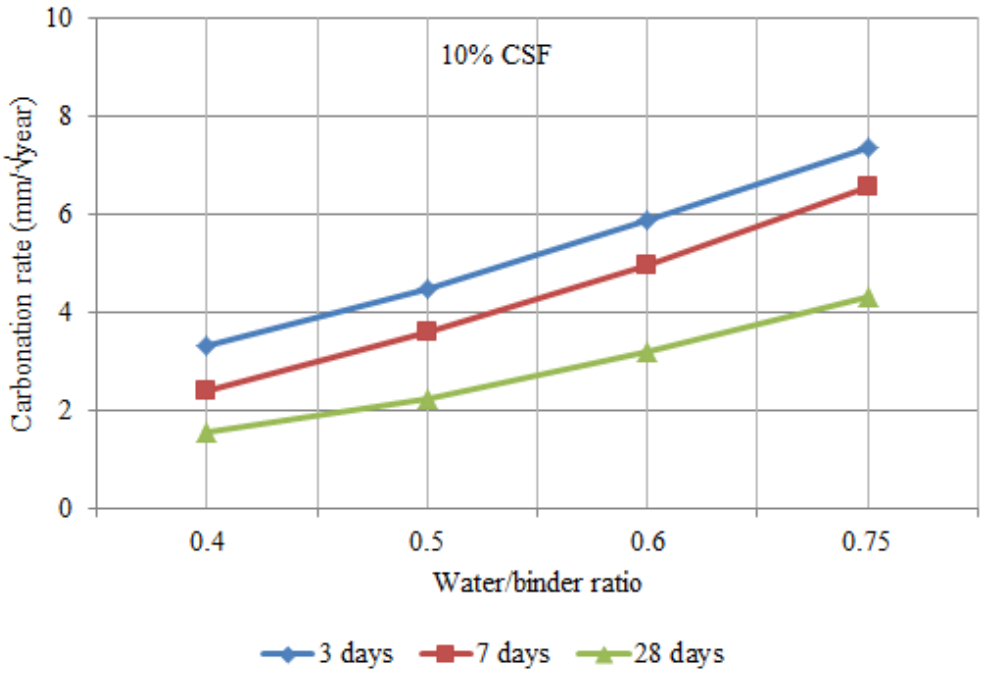


Figure 4.45: Carbonation rate vs. Water/binder ratio for the 90/10 CEM I-CSF concretes exposed indoors

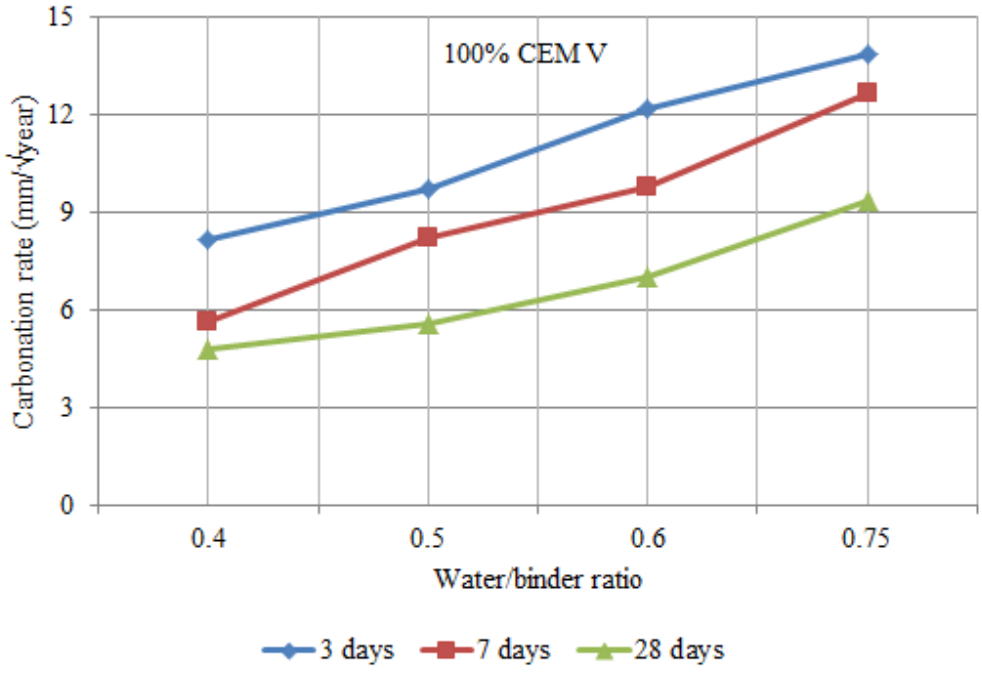


Figure 4.46: Carbonation rate vs. Water/binder ratio for the 100% CEM V concretes exposed indoors

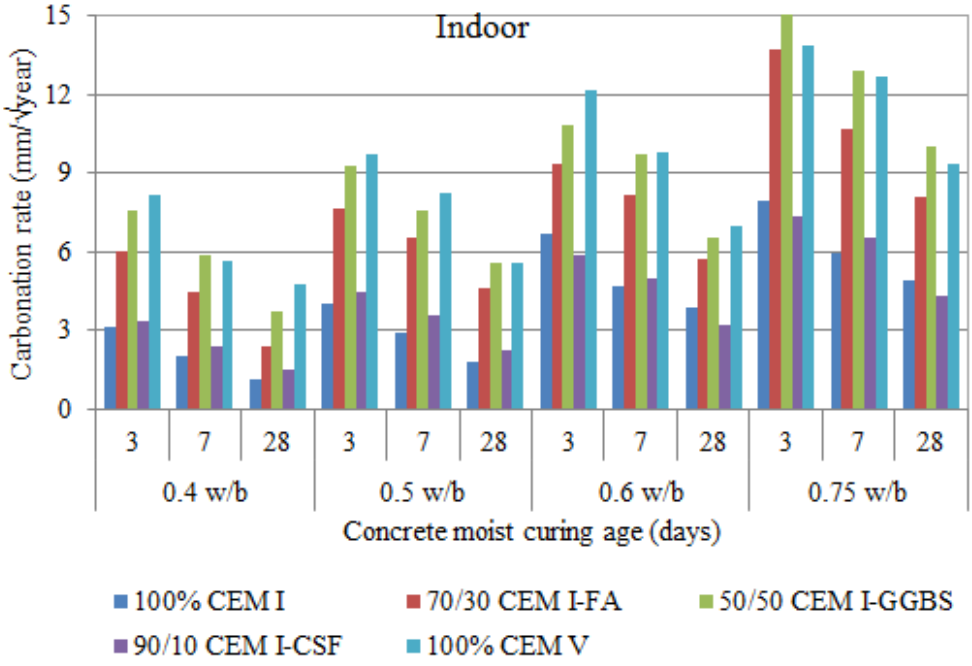


Figure 4.47: Carbonation rate vs. Concrete age for all the concrete types exposed indoors

Carbonation rate plots for concrete cube samples exposed outdoor but sheltered

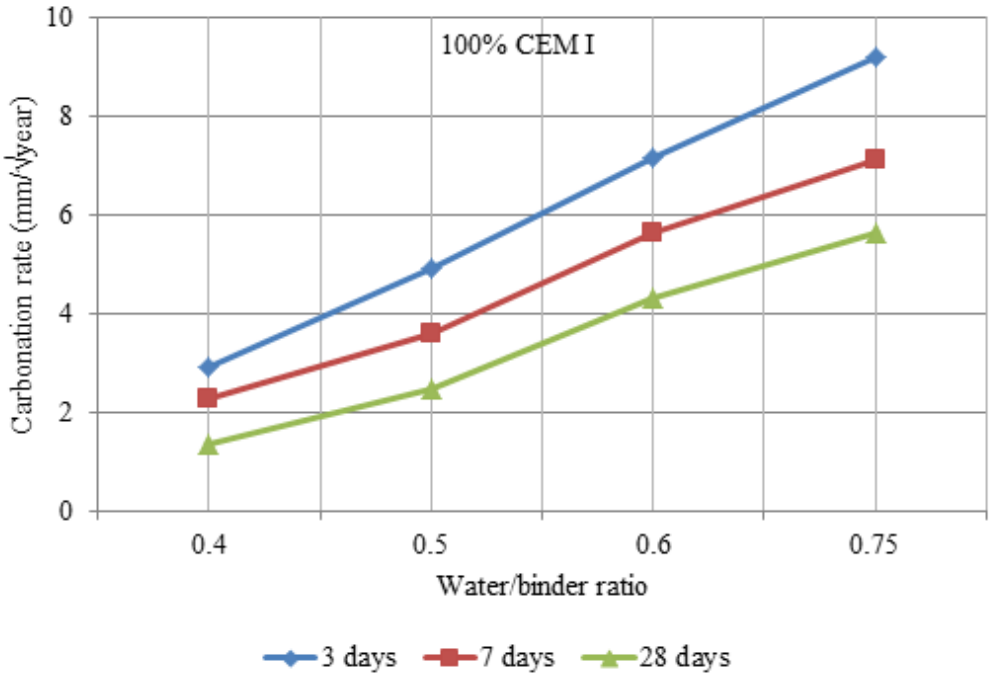


Figure 4.48: Carbonation rate vs. Water/binder ratio for the 100% CEM I concretes exposed outdoor sheltered

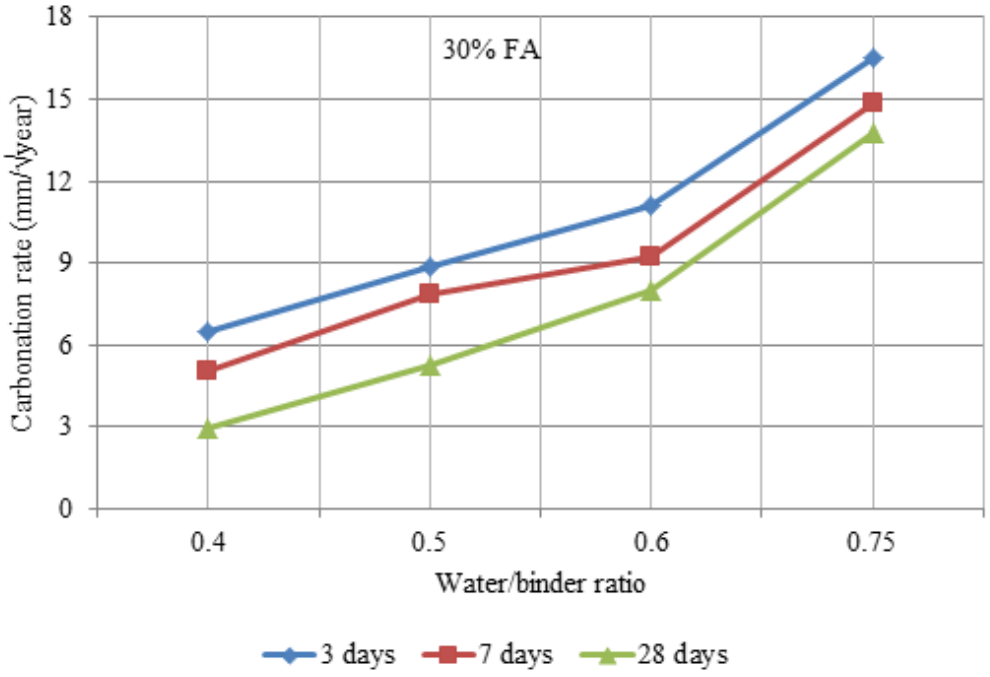


Figure 4.49: Carbonation rate vs. Water/binder ratio for the 70/30 CEM I-FA concretes exposed outdoor sheltered

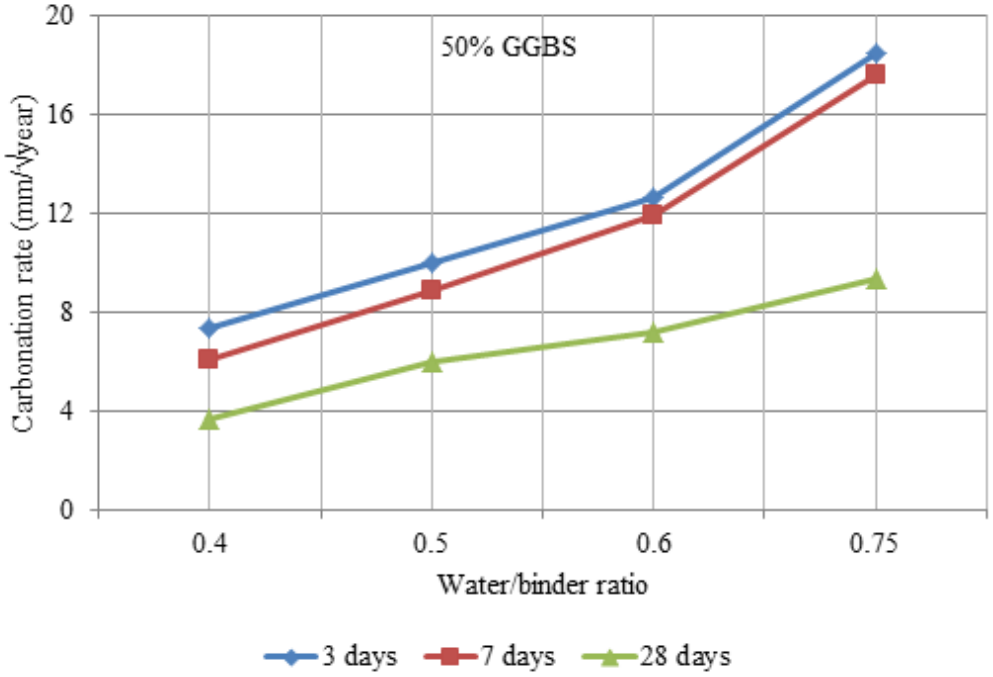


Figure 4.50: Carbonation rate vs. Water/binder ratio for the 50/50 CEM I-GGBS concretes exposed outdoor sheltered

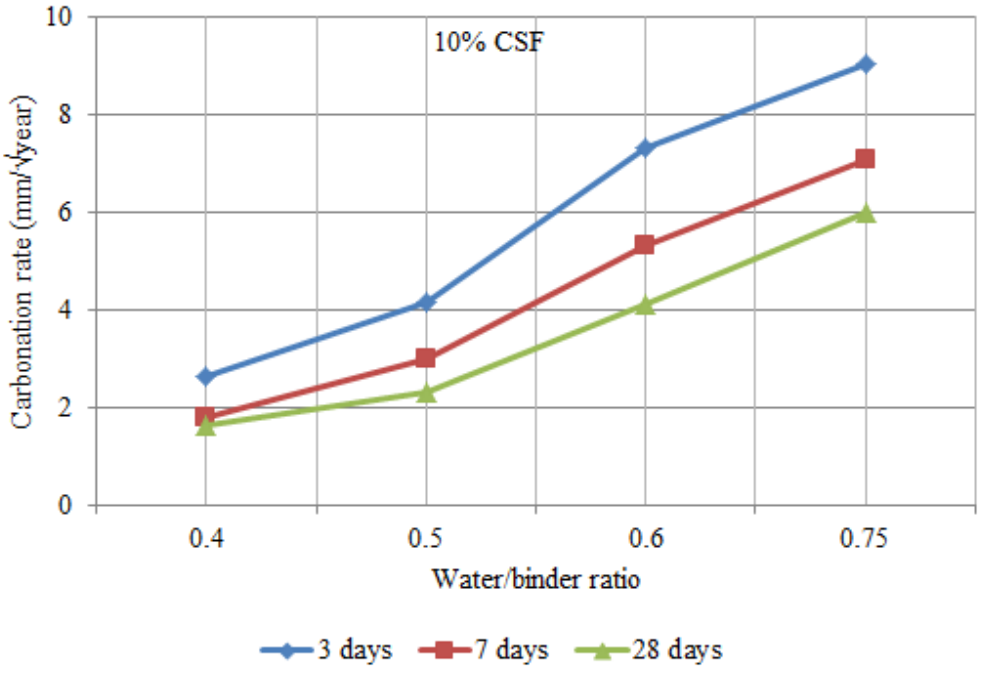


Figure 4.51: Carbonation rate vs. Water/binder ratio for the 90/10 CEM I-CSF concretes exposed outdoor sheltered

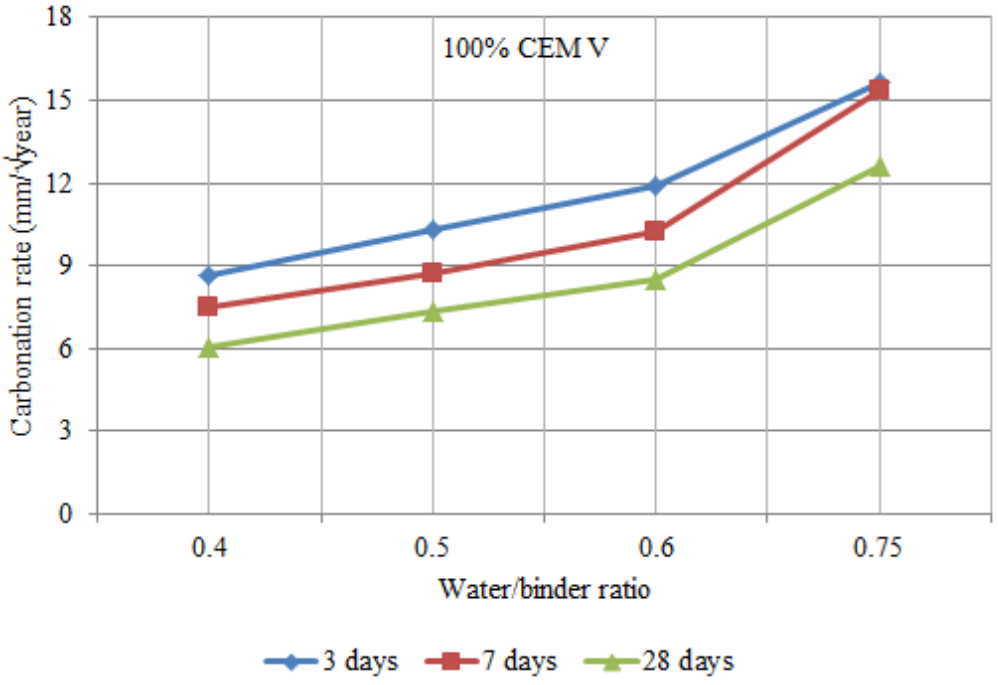


Figure 4.52: Carbonation rate vs. Water/binder ratio for the 100% CEM V concretes exposed outdoor sheltered

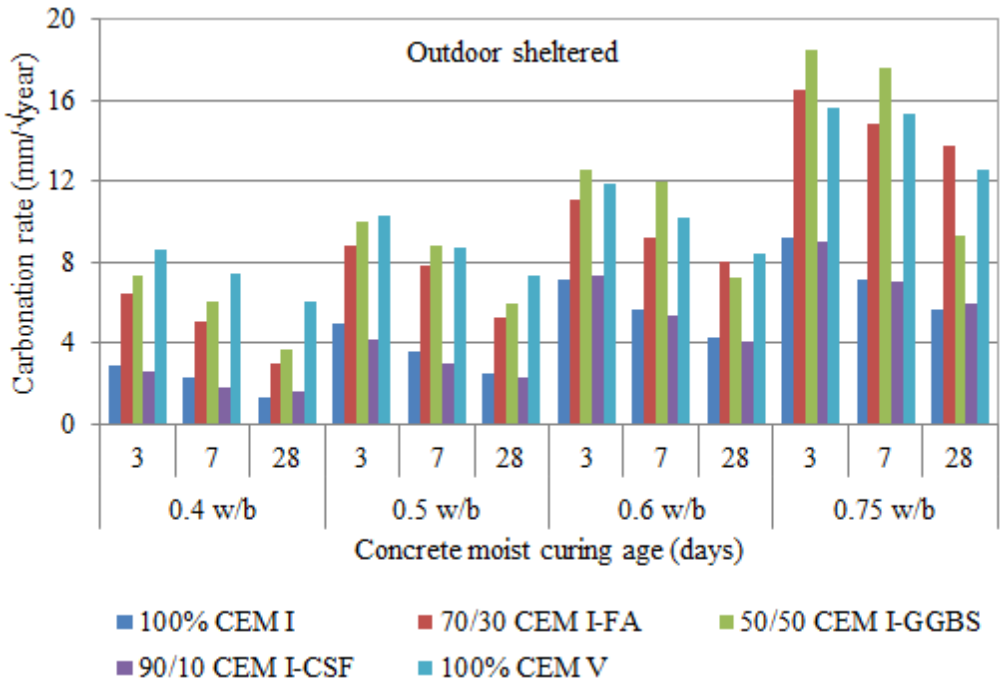


Figure 4.53: Carbonation rate vs. Concrete age for all the concrete types exposed outdoor sheltered

Carbonation rate plots for concrete cube samples exposed outdoor but not sheltered

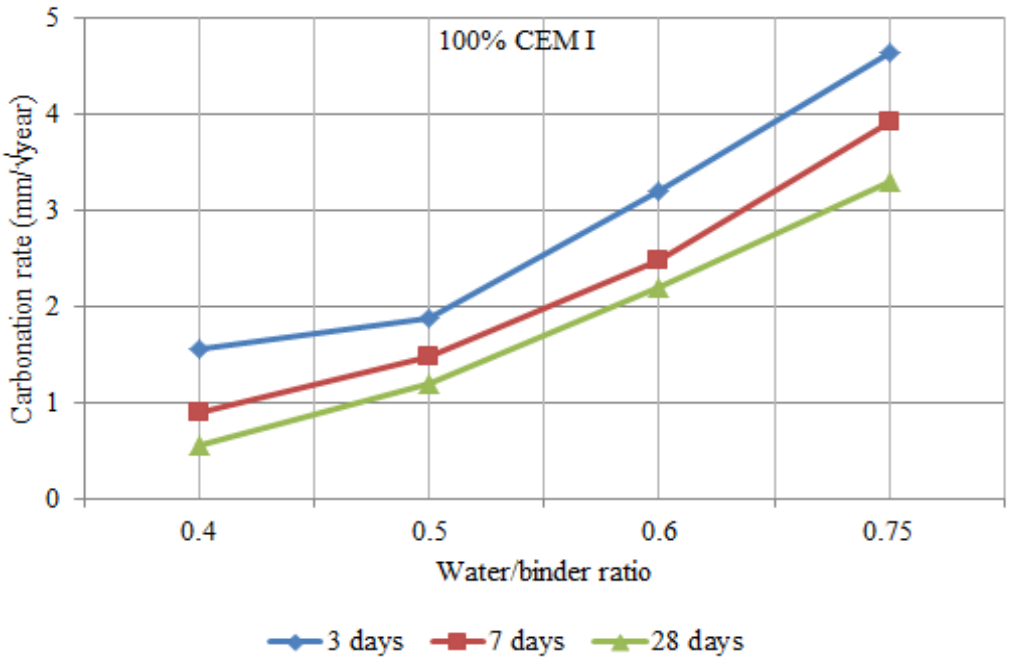


Figure 4.54: Carbonation rate vs. water/binder ratio for the 100% CEM I concretes exposed outdoors

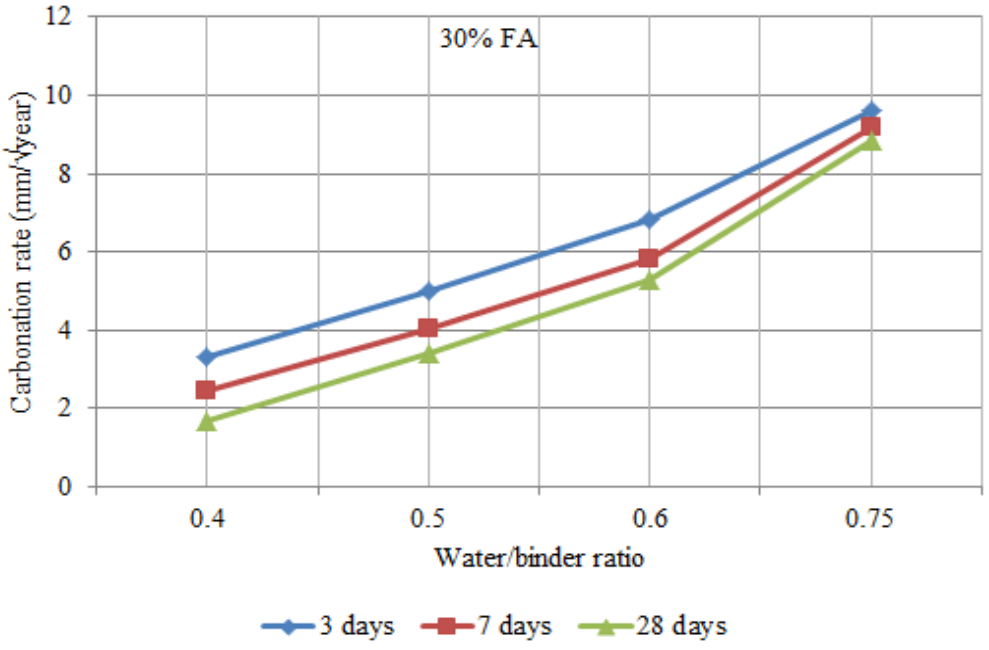


Figure 4.55: Carbonation rate vs. water/binder ratio for the 70/30 CEM I-FA concretes exposed outdoors

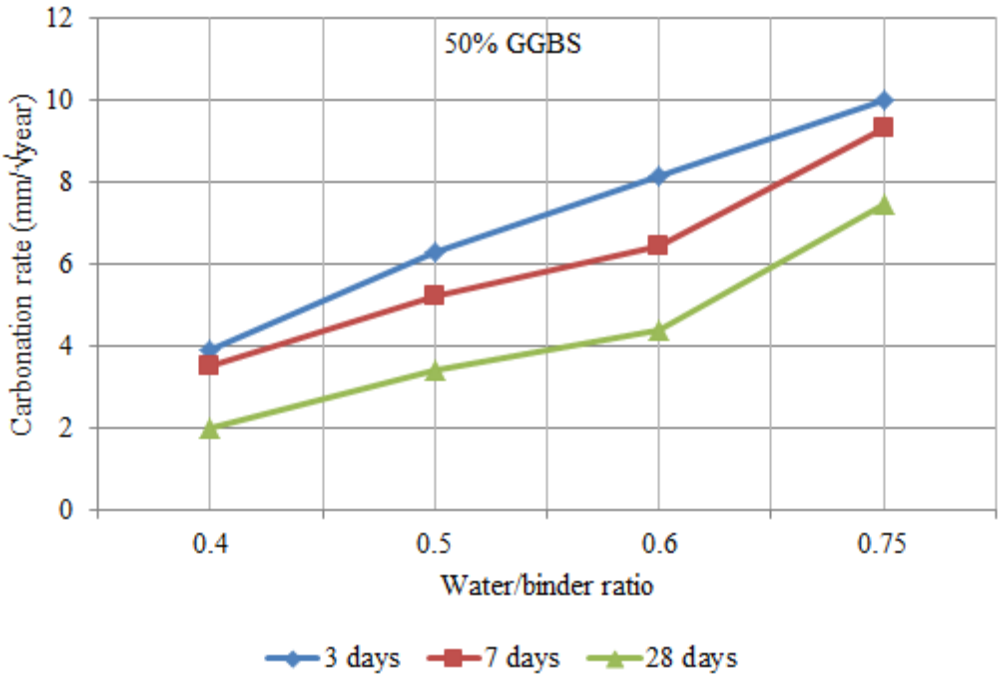


Figure 4.56: Carbonation rate vs. water/binder ratio for the 50/50 CEM I-GGBS concretes exposed outdoors

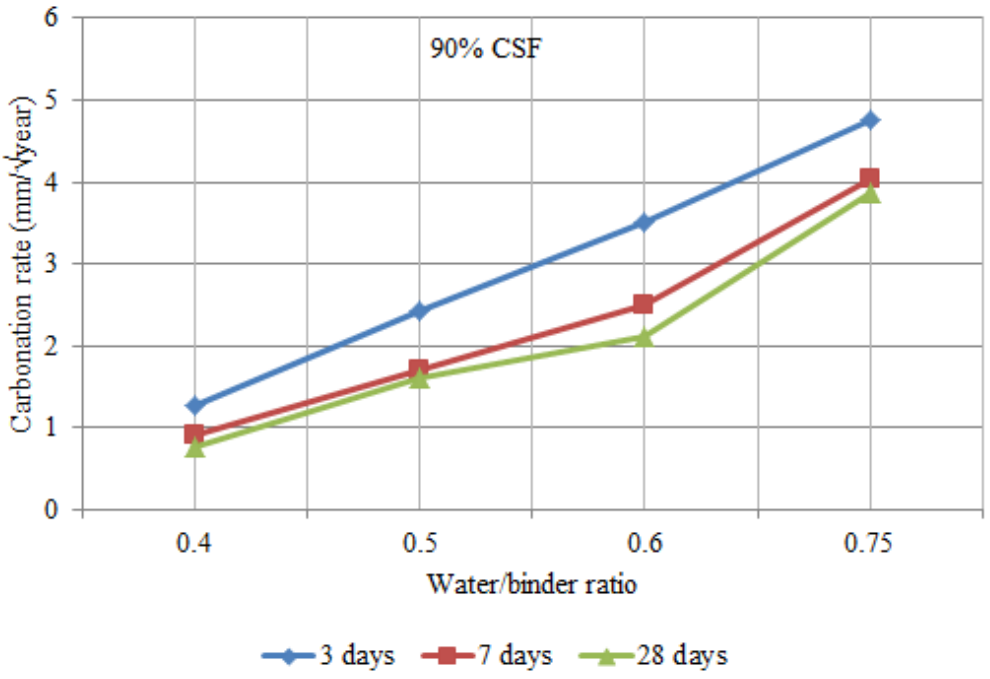


Figure 4.57: Carbonation rate vs. water/binder ratio for the 90/10 CEM I-CSF concretes exposed outdoors

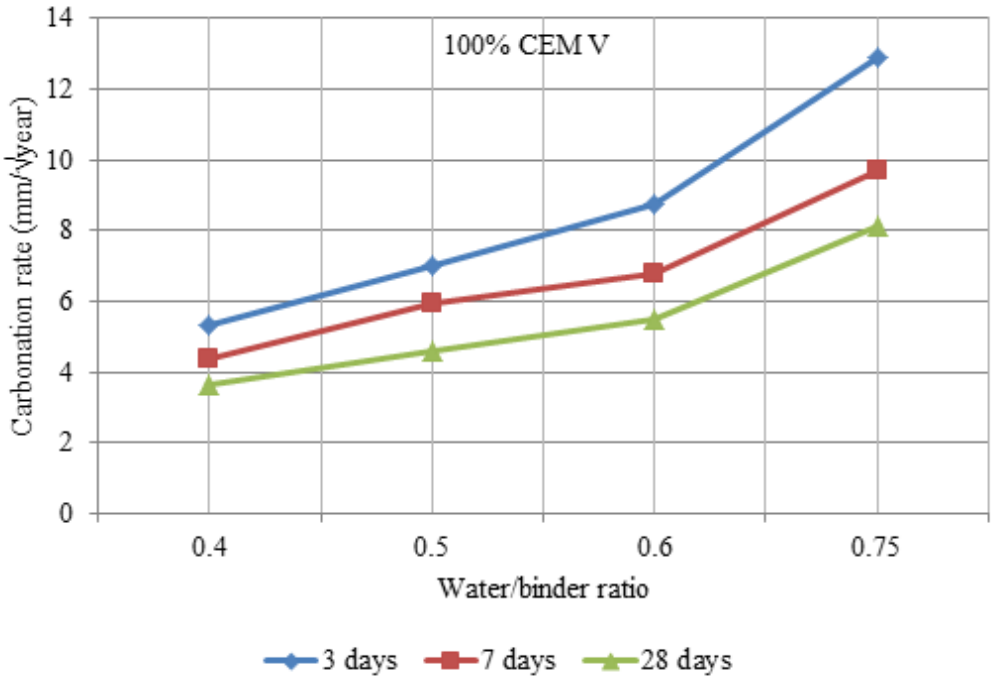


Figure 4.58: Carbonation rate vs. water/binder ratio for the 100% CEM V concretes exposed outdoors

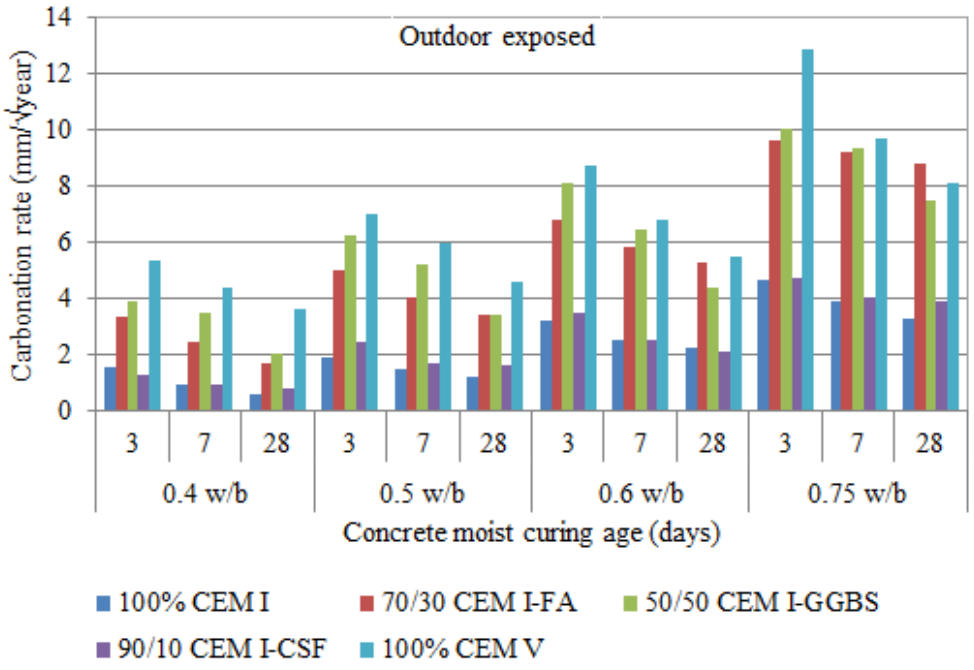


Figure 4.59: Carbonation rate vs. Concrete age for all the concrete types exposed outdoors

Carbonation rate plots for concrete cube samples exposed to an accelerated exposure

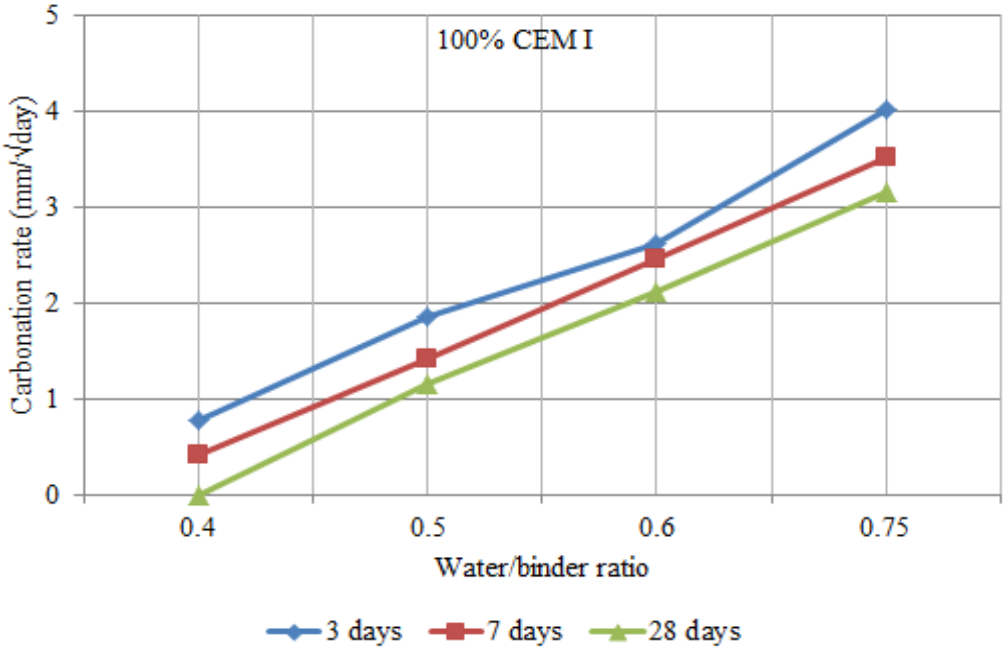


Figure 4.60: Carbonation rate vs. Water/binder ratio for the 100% CEM I concretes exposed to an accelerated condition

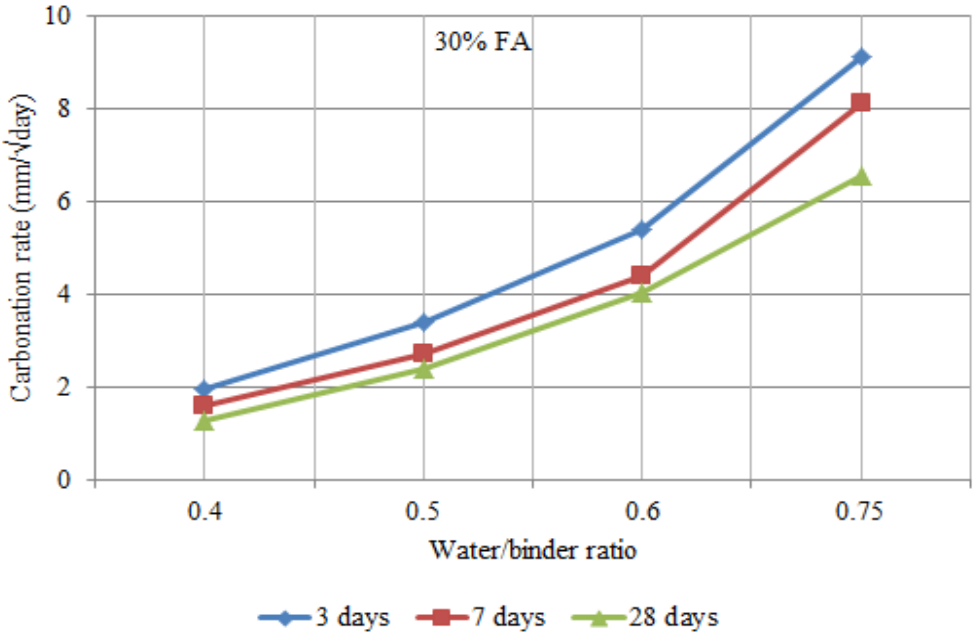


Figure 4.61: Carbonation rate vs. Water/binder ratio for the 70/30 CEM I-FA concretes exposed to an accelerated condition

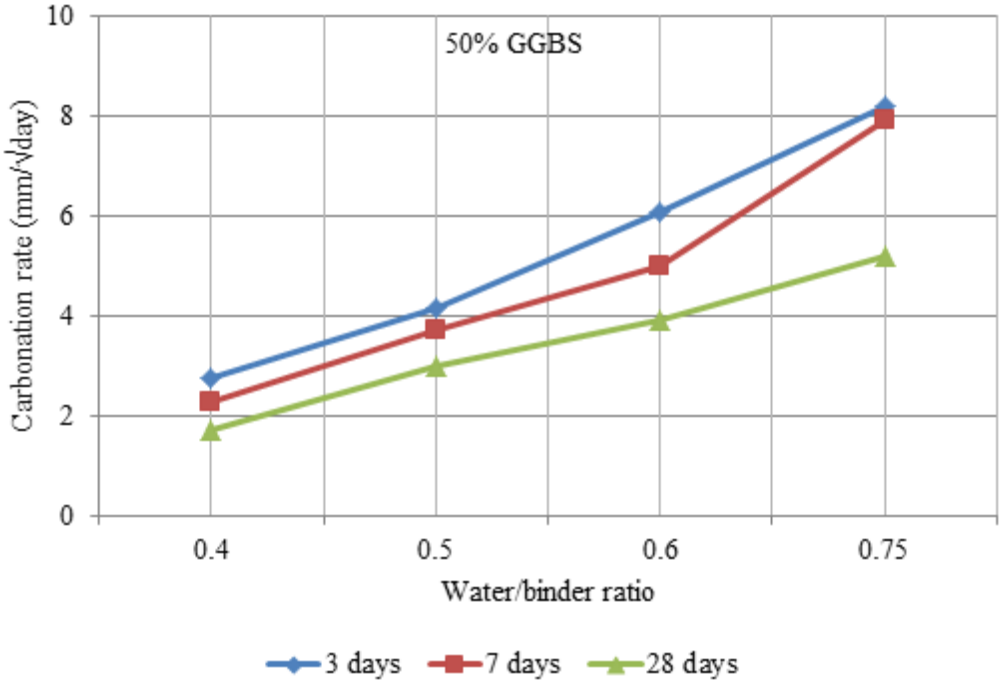


Figure 4.62: Carbonation rate vs. Water/binder ratio for the 50/50 CEM I-GGBS concretes exposed to an accelerated condition

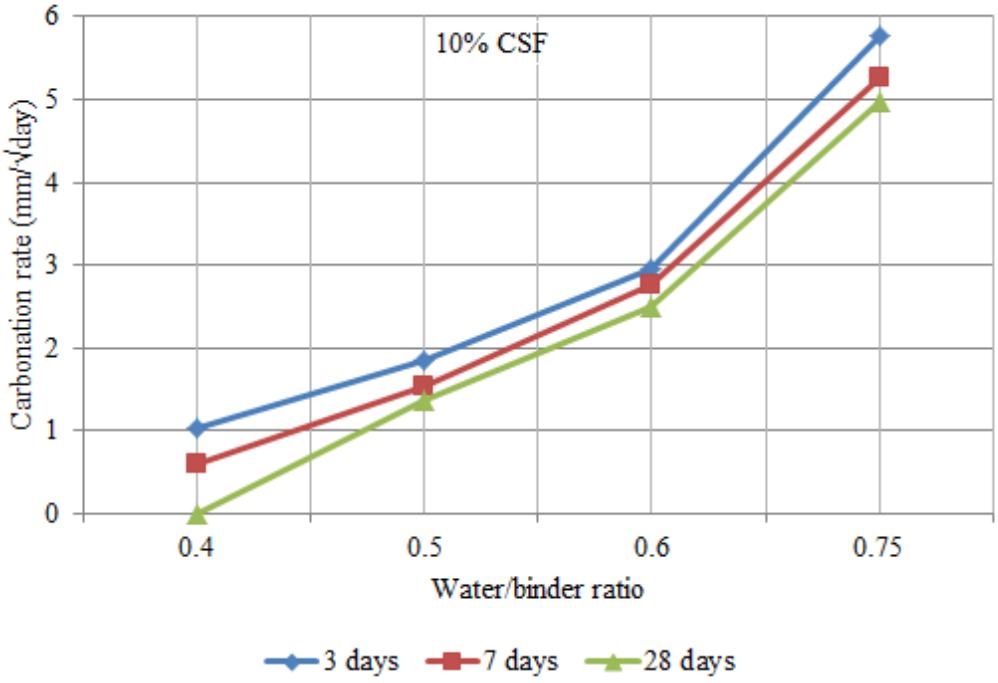


Figure 4.63: Carbonation rate vs. Water/binder ratio for the 90/10 CEM I-CSF concretes exposed to an accelerated condition

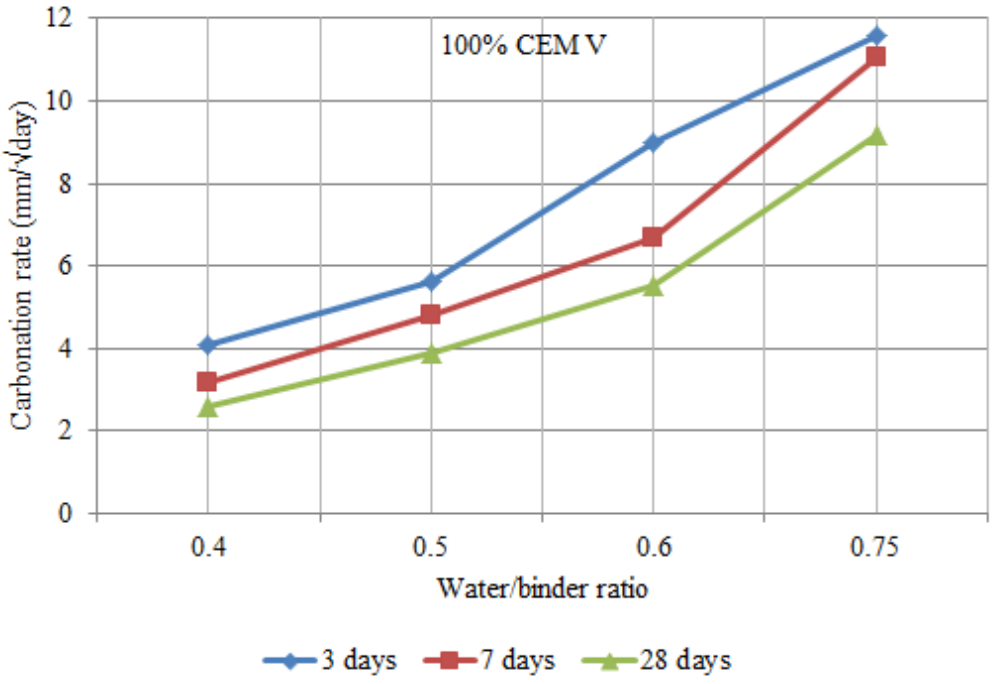


Figure 4.64: Carbonation rate vs. Water/binder ratio for the 100% CEM V concretes exposed to an accelerated condition

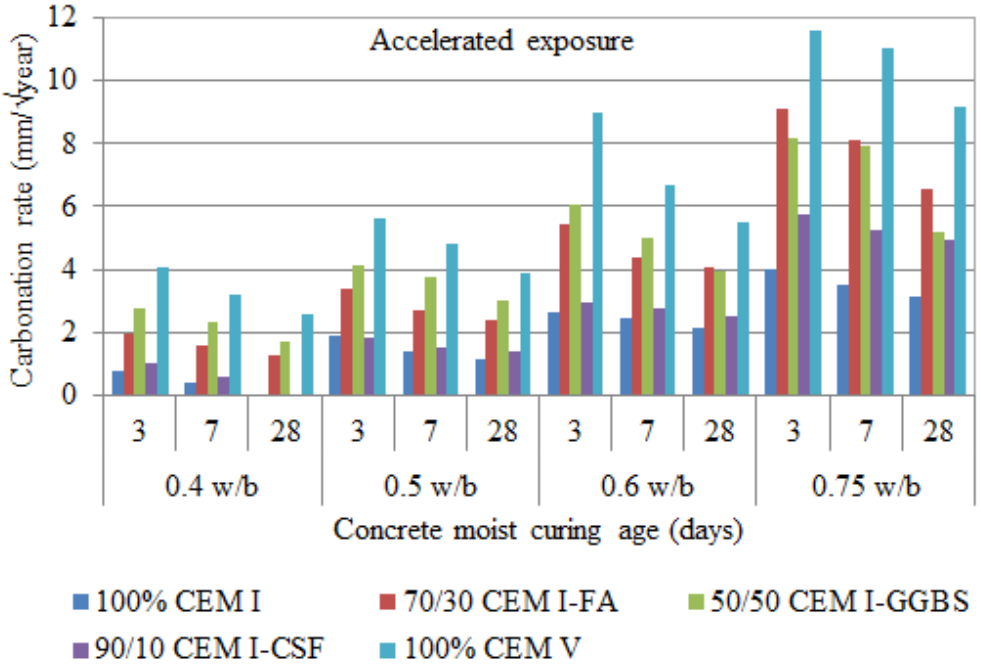


Figure 4.65: Carbonation rate vs. Concrete age for all the concrete types exposed to an accelerated condition

Carbonation rate plots for concrete cube samples exposed to the natural exposure sites

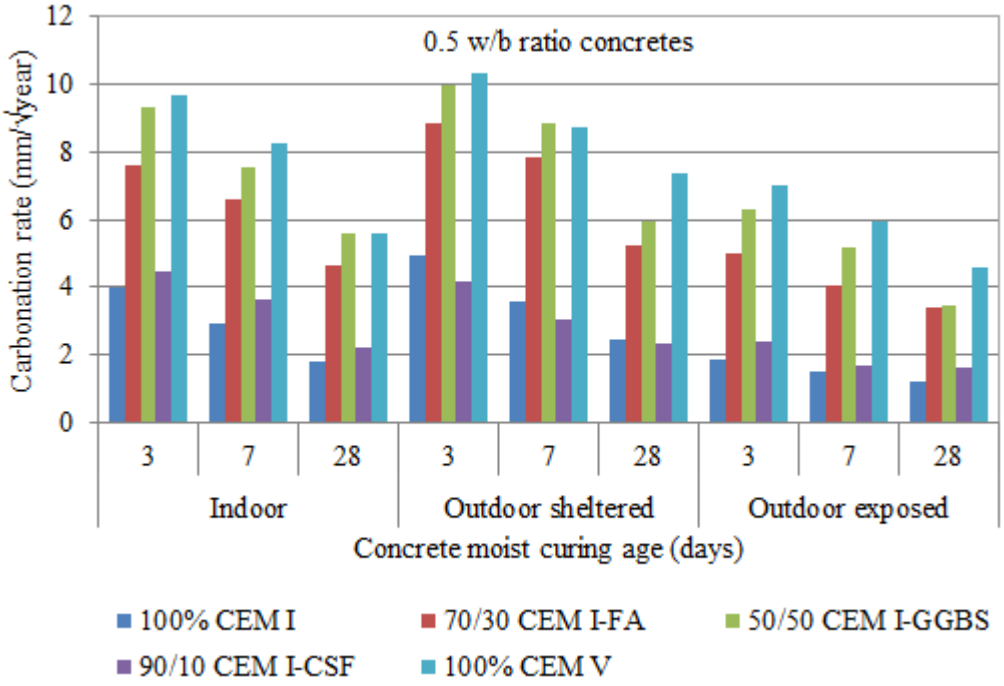


Figure 4.66: Carbonation rate vs. Exposure conditions for all the 0.5 w/b ratio concretes exposed to natural conditions

From the plots of carbonation coefficients versus w/b ratios presented in Figures 4.42 - 4.65 for the indoor, outdoor sheltered, outdoor exposed and accelerated exposures respectively, it is evident that the carbonation rate of the concretes followed similar pattern for the different exposure conditions investigated. Hence, a general explanation will be given for the trends observed in the concrete carbonation resistance results. The trends observed were distinctly influenced by the w/b ratio, *SCM* used and initial moist curing conditions of the concrete. Similarly, the rate of carbonation of the concretes also varies across the different exposure conditions, influenced by the micro-climates of the exposure conditions. Thus, variations of the carbonation rates for the concretes will be explained in relation to each of these influencing factors.

Effect of w/b ratio on carbonation rate of concrete

From the carbonation rate plots for all the concrete types presented in Figures 4.42 - 4.46, 4.48 - 4.52, 4.54 - 4.58 and 4.60 - 4.64 for the different exposure conditions investigated, it can be noted that the carbonation rate increases with an increase in w/b ratio irrespective of the concretes' initial moist curing periods and binder types. It is also evident from Figures 4.47, 4.53, 4.59 and 4.65, that the effect of w/b ratio is more significant than the moist curing duration effect as the carbonation rates increases significantly as w/b ratio varies. This is attributed to increased pore connectivity of the concrete since w/b ratio primarily determines the gel/space ratio, the capillary porosity and thus the permeability of the concrete.

Concretes of lower w/b ratio had better resistance against the diffusion of CO_2, possibly due to the denser pore structure and higher $Ca(OH)_2$ content. Similar findings in relation to the effect of w/b ratio on carbonation have also been reported in the literature (Houst & Wittmann, 1994; Sulapha et al., 2003; Wee et al., 1999). The decrease in the carbonation rates of the concretes at lower w/b ratio can be attributed to the fact that the cumulative pore volume and the amount of pores are lower compared to a higher w/b ratio concrete. This fact was also evident from the permeation test results of the concretes. Hence, the lower w/b ratio concretes, either blended or unblended showed superior resistance against carbonation.

Effect of SCM on carbonation rate of concrete

The effects of *SCM* on the carbonation rate of concretes can be seen in Figures 4.47, 4.53, 4.59 and 4.65 for the different exposure conditions investigated. At all w/b ratios for the different exposure conditions, *SCM* blended concretes presented higher carbonation rates irrespective of the initial moist curing period and w/b ratio. However, the *CSF* blended concretes are an exception. This observation is consistent with the trend noted by other researchers (Ananmalay,

1996; Ohga & Nagataki, 1989; Osborne, 1999; Papadakis, 2000; Simões et al., 1995).

Although the pore structure of blended concretes is denser as a result of the finer particle size and filler effects of *SCM*, the carbonation rates of blended concretes are higher. This suggests that pore structure is not the only parameter that controls the rate of carbonation in concretes, but also the amount of $Ca(OH)_2$ present within the hydrated cement paste of the concretes. The presence of $Ca(OH)_2$ in concrete results from the hydration reaction of C_2S and C_3S, which are the main components of cement. In the presence of *SCM*, the amount of $Ca(OH)_2$ available to react with CO_2 is lower, for two reasons; firstly, less CaO is added to the concretes and secondly, some of the $Ca(OH)_2$ produced reacts with the *SCM* present.

Effect of initial water curing period of the concrete on its carbonation rate

The effects of the initial water curing duration of the concrete on its carbonation rates can also be observed in Figures 4.47, 4.53, 4.59 and 4.65. It can be noted from the figures that a longer initial moist curing duration generally resulted in a lower carbonation rate. This is attributed to the fact that as curing increases hydration in concrete, the pore spaces in concrete reduces, particularly in the near surface zone. Additionally, curing influences the chemical properties of the concrete, for instance in unblended concrete it increase the $Ca(OH)_2$ content of the concrete thereby improving its buffering effect against CO_2. Curing, however reduces the $Ca(OH)_2$ content in blended concretes but improves the concrete microstructure. For example, in plain concretes, the carbonation rate decreased significantly with curing age within the first seven days. In the case of concrete containing *SCM*, the carbonation rate continued to decrease even after 7 days of curing again pointing to the later hydration effect of these *SCM*.

Effect of natural exposure condition on carbonation rate of concrete

The influence of the different natural exposure conditions investigated on the rate of concrete carbonation is shown in Figure 4.66. From the figure, concrete cube samples exposed to the outdoor sheltered conditions presented the highest carbonation rate while the lowest carbonation rates were observed in the concrete cube samples at the outdoor exposed site. The wetting and drying period experienced by samples on the exposed site is probably the reason for the reduced carbonation rate, since both the outdoor sheltered and unsheltered exposure conditions have similar micro-climates in terms of CO_2 content, *RH* and temperature as noted in section 4.6. In addition, concrete cube samples exposed outdoor to rain and sun have higher internal humidity during the summer months from precipitation effects, thus reducing CO_2 ingress during this period. Furthermore, these concretes had improved pore structures from rapid hydration effects as a result of its high internal moisture content during the summer months.

The micro-climate factors known to influence the carbonation rate of concretes are the CO_2 concentration, *RH* and temperature with the most important being *RH*. The *RH* surrounding the concrete influences the concretes internal humidity which then affects the ingress of CO_2. For instance, Loo et al. (1994) noted an insignificant effect on concrete carbonation rate for specimen with compressive strength less than or equal to 40 MPa when the CO_2 concentrations were varied between 7% and 18%. While for concretes with strength higher than 40 MPa, variation of a greater order of magnitude in CO_2 concentration may be required to show any significant effect on the carbonation rate. The rate of carbonation in concrete is also weakly sensitive to temperature within the range 20-40 ^{o}C (Papadaki et al., 1991). A similar observation regarding the insensitivity of temperature to the rate of carbonation in concrete was also noted by Loo et al., (1994) in their work.

This chapter has presented, analysed and discussed the results obtained from the experimental work described in Chapter 3. The influence of the materials used,

processing and environmental conditions on the carbonation rate of the concretes and hence their potential durability performance and service life was also discussed in this chapter. In the next chapter, the results of the statistical analysis performed on the results obtained from this chapter with the intention of developing prediction models for carbonation rate of concretes will be presented. Results of the multiple linear regression analyses between the natural carbonation rates of the concretes (as the response variable) and the concrete mixture design and the early-age characterisation parameters (as the predictor variables) will be presented and discussed.

Chapter References

ACI, C. (1987). *Silica fume in concrete* (pp. pp 158-166). ACI Materials Journal.

Alexander, M., & Magee, B. (1999). *Durability performance of concrete containing condensed silica fume*. Cement and Concrete Research, 29(6), *917-922.*

Alexander, M., & Moyo, P. (2012). *Durability performance of a range of marine concretes and the applicability of the South African Service Life Prediction Model.* Materials and structures, 45(1-2), 185-198.

Alexander, M. G., Ballim, Y., & Mackechnie, J. R. (1999). *Concrete durability index testing manual*. Research monograph, No. 4.

Ananmalay, N. (1996). *Characterising the strength and durability performance of South African silica fume concretes.* MSc Dissertation University of the Witwatersrand, Johannesburg.

Ballim, Y. (1994). *Curing and the durability of concrete. PhD Thesis,* University of the Witwatersrand.

Berry, E., & Malhotra, V. (1987). Supplementary Cementing Materials for Concrete. *VM Malhotra, CANMET, Ottawa, Canada*, 37-163.

Bertolini, L., Elsener, B., Pedeferri, P., Redaelli, E., & Polder, R. B. (2013). *Corrosion of steel in concrete: prevention, diagnosis, repair*: Wiley. com.

Blight, G. (1991). *A study of four waterproofing systems for concrete*. Magazine of Concrete Research, 43(156), 197-203.

Bonen, D., & Khayat, K. H. (1995). *Characterization and pozzolanic properties of silica fume stored in an open pond.* Cement and Concrete Research, 25(2), 395-407.

Bruno, S. (2010). *Modelling the carbonation of concrete usinf early age oxygen permeability index tests.* MSc University of Cape Town.

Collins, F., & Sanjayan, J. (1999). *Effects of ultra-fine materials on workability and strength of concrete containing alkali-activated slag as the binder*. Cement and Concrete Research, 29(3), 459-462.

Da Silva, F., Helene, P., Castro-Borges, P., & Liborio, J. (2009). *Sources of variations when comparing concrete carbonation results.* Journal of Materials in Civil Engineering, 21(7), 333-342.

Goldman, A., & Bentur, A. (1993). The influence of microfillers on enhancement of concrete strength. *Cement and Concrete Research, 23*(4), 962-972.

Detwiler, R. J., & Mehta, P. K. (1989). Chemical and physical effects of silica fume on the mechanical behaviour of concrete. *ACI Materials Journal, Vol. 86, No. 6, November - December 1989,* pp 609-614.

Franke, L., & Sisomphon, K. (2004). *A new chemical method for analyzing free calcium hydroxide content in cementing material*. Cement and Concrete Research, 34(7), 1161-1165.

Gräf, H., & Grube, H. (1986). *Experimental testing method of water and gas permeability of mortar and concrete*: Part 1. Beton, *36*(5), 184-187.

Goldman, A., & Bentur, A. (1993). The influence of microfillers on enhancement of concrete strength. *Cement and Concrete Research, 23*(4), 962-972.

Henry, R., & Kurtz, G. (1963). *Water vapor transmission of concrete and of aggregates*: DTIC Document.

Houst, Y. F., & Wittmann, F. H. (1994). *Influence of porosity and water content on the diffusivity of CO< sub> 2</sub> and O< sub> 2</sub> through hydrated cement paste.* Cement and Concrete Research, 24(6), 1165-1176.

Khan, M., & Lynsdale, C. (2002). *Strength, permeability, and carbonation of high-performance concrete.* Cement and Concrete Research, 32(1), 123-131.

Khan, M., Lynsdale, C., & Choo, B. (2001). *Pore structure of high strength cement mortar containing fly ash and microsilica.* Paper presented at the Supplementary Proceedings of the ACI/CANMET International Symposium on Sustainable Development of Cement and Concrete.

Khan, M., Lynsdale, C., & Waldron, P. (2000). *Porosity and strength of PFA/SF/OPC ternary blended paste.* Cement and Concrete Research, 30(8), 1225-1229.

Kropp, J. (1995). *Relations between transport characteristics and durability*. Performance criteria for concrete durability, RILEM Report, 12, 97-137.

Lagerblad, B., Utkin, P., & Betonginstitutet, C. (1993). *Silica Granulates in Concrete: Dispersion and Durability Aspects:* Swedish Cement and Concrete Research Institute.

Lampacher, B. J. (2000). *Durability of concrete structures.* PhD Thesis, University of the Witwatersrand, Johannessburg.

Larbi, J., & Bijen, J. (1990). *Orientation of calcium hydroxide at the Portland cement paste-aggregate interface in mortars in the presence of silica fume: a contribution.* Cement and Concrete Research, 20(3), 461-470.

Loo, Y., Chin, M., Tam, C., & Ong, K. (1994). *A carbonation prediction model for accelerated carbonation testing of concrete.* Magazine of Concrete Research, 46(168), 191-200.

Mackechnie, J., & Alexander, M. (2002). *Durability predictions using early-age durability index testing.* Paper presented at the Proc. Ninth Durability and Building Materials Conference, Australian Corrosion Association, Brisbane, Australia.

Mackechnie, J. R. (1996). *Predictions of reinforced concrete durability in the marine environment.* PhD thesis, University of Cape Town.

Manmohan, D., Metha, P.K. (1981). *Influence of pozzolanic, slag and chemical admixtures on pore size distribution and permeability of hardened cement paste,* Cement, Concrete and Aggregates, 3 (1981) 63-67.

Marsh, B., Day, R., & Bonnery, D. (1986). *Strength gain and calcium hydroxide depletion in hardened cement pastes containing fly ash*. Magazine of Concrete Research, 38(134), 23-29.

Marsh, B. K., & Day, R. L. (1988*). Pozzolanic and cementitious reactions of fly ash in blended cement pastes.* Cement and Concrete Research, 18(2), 301-310.

Mehta, P., & Gjørv, O. (1982). *Properties of Portland cement concrete containing fly ash and condensed silica-fume.* Cement and Concrete Research, 12(5), 587-595.

Mehta, P., & Manmohan, D. (1980). *Pore size distribution and permeability of hardened cement pastes, 7th Int*. Conge. Chem. Cem.

Mehta, P. K. (1983). *Pozzolanic and cementitious byproducts as mineral admixtures for concrete-a critical review*. ACI Special Publication, 79.

Midgley, H. (1979). *The determination of calcium hydroxide in set Portland cements.* Cement and Concrete Research, 9(1), 77-82.

Mitchell, D., Hinczak, I., & Day, R. (1998). *Interaction of silica fume with calcium hydroxide solutions and hydrated cement pastes*. Cement and Concrete Research, 28(11), 1571-1584.

Neville, A. (1981). *Properties of Concrete (3rd edn.) Pitman*. London, UK.

Neville, A. M. (1997). *Properties of concrete. 4th and final ed*. Harlow, UK: Pearson Education Limited.

Ohga, H., & Nagataki, S. (1989). *Prediction and evaluation of the depth of carbonation of concrete by accelerated test*. Concrete Library of JSCE, 7, 93-106.

Osborne, G. (1999). *Durability of Portland blast-furnace slag cement concrete*. Cement and Concrete Composites, 21(1), 11-21.

Papadakis, V. G. (2000). *Effect of supplementary cementing materials on concrete resistance against carbonation and chloride ingress*. Cement and Concrete Research, 30(2), 291-299.

Papadakis, V.G., Vayenas, C.G. & Fardis, M.N. (1991). Fundamental modelling and experimental investigation of concrete carbonation. *American Concrete Institute Materials Journal.* 88(4): 363-373.

Richardson, M. G. (1988). *Carbonation of reinforced concrete: Its causes and management:* Citis.

Roy, D. M. (1999). *Alkali-activated cements opportunities and challenges.* Cement and Concrete Research, 29(2), 249-254.

Shah, S., & Slate, F. (1968). *Internal microcracking, mortar-aggregate bond and the stress-strain curve of concrete.*

Simões, A., Ferreira, M. G., Montemor, M., & Salta, M. M. (1995). *Carbonation of flyash-containing concrete: electrochemical studies.* Paper presented at the Materials Science Forum.

Sulapha, P., Wong, S., Wee, T., & Swaddiwudhipong, S. (2003). *Carbonation of concrete containing mineral admixtures.* Journal of materials in civil engineering, 15(2), 134-143.

Tutti, K. (1982). *Corrosion of steel in concrete*. Swedish Cement and Concrete Institute: CIB, Research Report.

Verbeck, G. (1958). *Carbonation of hydrated Portland cement*. Cement and Concrete, 17-36.

Wee, T., Suryavanshi, A., & Logendran, D. (1999). *Pore structure controlling the carbonation of a hardened cement matrix blended with mineral admixture*. Advances in cement research, 11(2), 81-95.

CHAPTER 5

MODELLING THE CARBONATION RATE OF CONCRETE

5.1 Introduction

The results presented in Chapter 4 were used as the basis for developing statistically defensible carbonation prediction models for the inland environment. The analyses, results and interpretations of the multiple linear regressions are presented in this chapter. The dependent (response) variable (natural carbonation rate of the concrete) is modelled in terms of the independent (predictor) variables which describe the concrete mixture design and the concrete early-age characterisation parameters by multiple linear regression. Also included in the predictor variables are three variables (binder types, curing periods and exposure conditions) known to influence the response variable.

Firstly, a formulation of the prediction model and review of the regression analysis method to be used are outlined. Then the description and preparation of both the response and the predictor variables for correlation and regression analysis are presented. Thereafter, the grouping of the predictor variables into meaningful sets in order to avoid multi-collinearity was performed. The grouping was based on the results from the bivariate correlation and analysis of the association between the predictor variables and or the response variable as well as on the mechanisms of carbonation process in concrete and some measure of engineering judgment.

The outcomes of the multiple linear regression analyses are presented after performing detailed diagnostic checks for any violation of the standard linear regression assumptions and corrections or eliminations where necessary. The models are then described and interpreted in terms of their range of applicability

and estimated coefficients in the prediction of the natural carbonation rate of concretes.

5.2 Formulation of a Prediction Model for the Carbonation Rate of Concrete

Regression analysis is a method for investigating functional relationships that may exist among variables (Chatterjee & Hadi, 2009, 2013). The relationship is expressed in the form of an equation or a model connecting the response variable(s) and one or more predictor variables. This approach has been used in a variety of applications (Alexander et al., 2007; Gaylard et al., 2013; Gaylard, 2011; Dhir et al., 1994; Jean-Marie, 2011; Mackechnie, 1996; Parrott, 1994; Wierig, 1984).

The carbonation process of concrete is known to be influenced by the concrete making materials and processes, as well as the environmental conditions surrounding concrete (Bertolini, 2008; Tutti, 1982). The above mentioned factors affect the rate of concrete carbonation directly. The relationship between the carbonation rate of concrete and the factors that influence it have generally been assumed to be linear (Ballim, 1994; Mackechnie, 1996; Parrott, 1987; Wierig, 1984). Thus, developing this relationship using a linear regression model is appropriate. Since the predictor variables are linearly related to the response variable and the predictor variables are more than two and only one response variable, the form of the regression model to be used in modelling the relationship is the multiple linear regression (Chatterjee & Hadi, 2013).

In this study, the data set modelled consists of one response variable (the natural carbonation rate values of the concrete (K_{nat})) and eleven quantitative predictor variables. The quantitative predictor variables consist of the:

a. concrete mixture design parameters:
    - water/binder ratio (w/b);

- water content (*W*);
- binder content (*B*);
- cement content (*C*);
- supplementary cementitious materials content (*SCM*);

b. concrete early-age (28 days) characterisation parameters:
    - compressive strength (f_c);
    - oxygen permeability index (*OPI*);
    - water sorptivity (*WS*);
    - calcium hydroxide (*CH*) content;
    - calcium oxide (*CaO*) content;
    - accelerated carbonation rate (K_{acc})

The binder types used in making concretes, the concrete curing duration as well as the micro-climatic variations (carbon dioxide, relative humidity and temperature) of the exposure condition surrounding concretes are also known to influence the depths and rates of concrete carbonation (Alexander et al., 2007; Ballim, 1994; Mackechnie, 1996; Parrott, 1987; Wierig, 1984; Dhir et al., 1994). The binder types used in making the concretes *are CEM I*, *CEM I/FA*, *CEM I/GGBS*, *CEM I/CSF* and *CEM V*, the water curing durations concretes were exposed to are 3, 7 and 28 days while the micro-climatic variations surrounding the concretes were grouped into the different exposure sites concretes samples were place as indoor, outdoor sheltered and outdoor exposed conditions. These qualitative (categorical) variables were also included among the predictor variables as indicator (dummy) variables during model development.

Apart from the fact that the categorical variables influence the rates of carbonation in concrete, preliminary analysis performed on the relationship between the response and predictor variables show five banded pattern or relationship for the binder types, and three for the curing duration for each of the exposure conditions studied. Similar results were also obtained by Dhir et al. (1994) and Parrott (1987)

in their study. Dhir et al., (1994) noted banded relationship for the binder types used in making the concrete when regression analyses were performed between 30-weeks carbonation depths of concrete and the permeation properties of the companion concretes. Dhir et al., (1994) thus concluded that the resistance of concrete to carbonation is affected by the concrete pore structure and binder chemistry, other parameters relating to the binder types and content, curing periods as well as the exposure condition. These variables need to be considered in order to establish usable predictive relationship hence raising the confidence and reliability of durability prediction

The processes or stages involved in the regression analysis or in developing a relationship between the response and predictor variables are presented in a flow diagram as shown in Figure 5.1 - illustrating the iterative process in the regression analysis modelling. With the identification of the appropriate predictor variables that best describes the response variable based on the process of carbonation, engineering judgment and results from statistical analysis between the variables, a form of model is chosen that best represents the response variable in terms of goodness of fit measures.

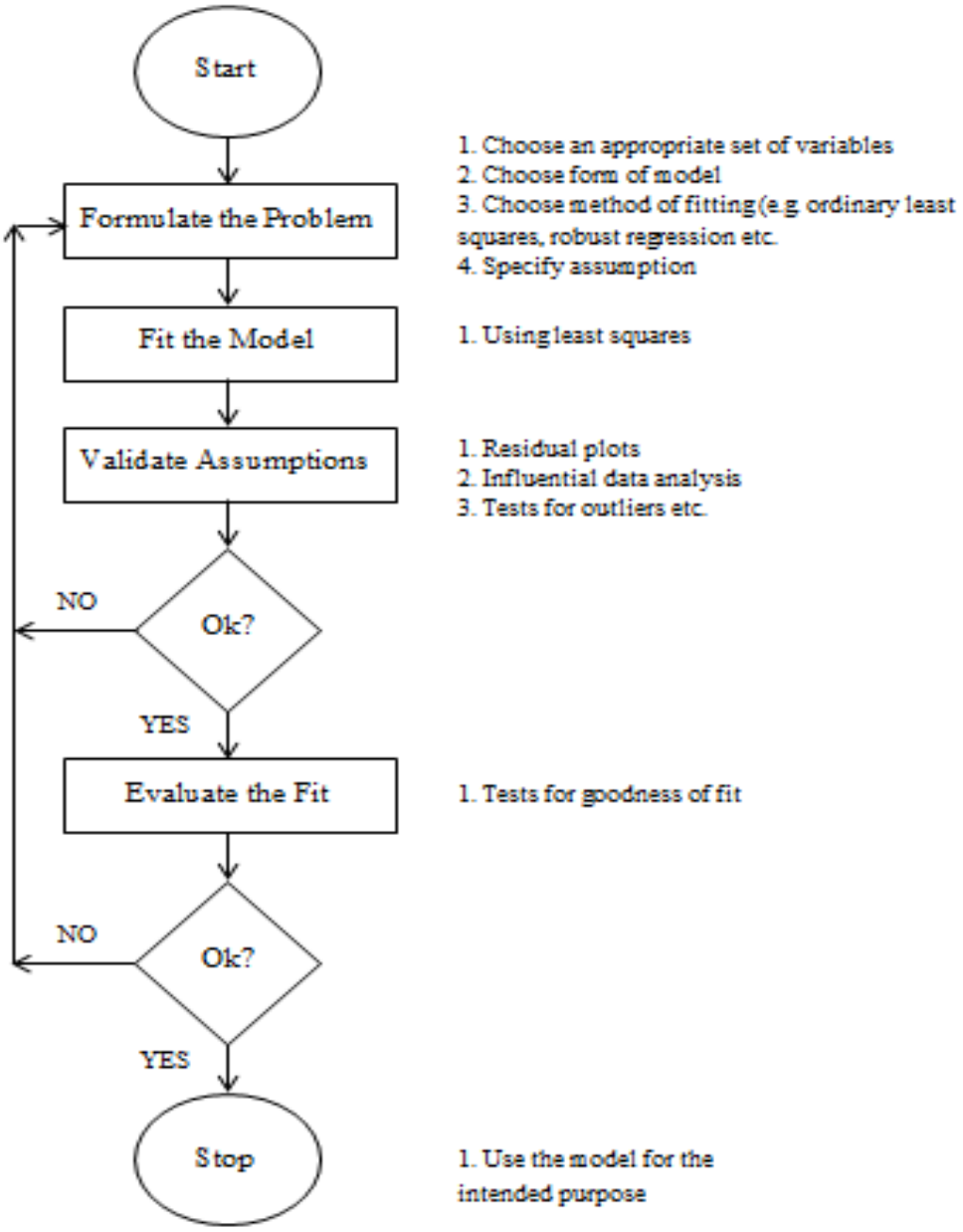


Figure 5.1: A flow diagram illustrating the iterative regression process (Chatterjee & Hadi, 2009)

5.3 Multiple Linear Regression: A Review

In this section, the general multiple linear regression model is presented. Key theoretical results are given without mathematical derivations. Mathematical derivation for a formal development of multiple linear regression theory, in which

the results are developed using relatively simple algebra can be found in Chatterjee & Hadi (2013); Cohen & Cohen (1975); Fox (1984) and Kmenta (1971).

Multiple linear regression considers the relationship between several predictor variables and one response variable (Chatterjee & Hadi, 2013). This relationship is however governed by assumptions for its mathematical development (Cohen & Cohen, 1975). In the general form of the multiple linear regression model, the response variable, *Y*, is assumed to be a function of a set of *n* predictor variables, – X_1, X_2, X_3, …, X_n. To express the model in equation form, let X_{ij} denote the value of the jth experiment (observation) of the variable X_i. The linear regression model assumes that for each set of the values for the *n* predictor variables $(X_{1j}, X_{2j}, X_{3j}, \ldots, X_{nj})$ there is a distribution of Y_j values such that the mean of the distribution is on the surface (plane) represented by Equation 5.1 (Berry & Feldman, 1985). Each individual observation of Y_j is assumed to be determined by an equation containing an error term, ε_j .

$$Y_j = \beta_o + \beta_1 X_{1j} + \beta_2 X_{2j} + \cdots + \beta_n X_{nj} \qquad 5.1$$

Where,

Y_j = the value of the response variable for the jth observation ($j=1, 2, \ldots, m$).

X_{ij} = the value of the ith predictor variable ($i=1, 2, \ldots, n$) for the jth observation.

β_o = a parameter that represents the population regression intercept, or β_o is the mean of *Y* when the values for $X_1, X_2 \ldots, X_n,$ are all equal to zero.

β_j = the parameter that represents the slope of the population regression surface with respect to the jth predictor variable, or β_j indicates the change in the mean value of *Y* for a unit change in the predictor variables X_i, when all other predictor variables in the model are held constant.

ε_j = the value of a random fluctuation or error for the jth observation.

Hence, it is assumed that for any set of fixed values of X_1, X_2, X_3,..., X_n that fall within the range of the data, the linear equation (Equation 5.1) provides an acceptable approximation of the true relationship between *Y* and the *X* values. Stated differently, *Y* is approximately a linear function of *X* and ε_j measures the discrepancy in that approximation. In particular, ε_j contains no systematic information for determining *Y* that is not already captured by the *X* values.

The error term, ε_j is the deviation of the value of Y_j from the mean value of the distribution obtained by repeated observation of *Y* values for *n* cases, each with fixed values for each of the predictor variables. This error term represents the effects on *Y* of variables not explicitly included in the equation as well as a residual random element in the response variable. The least squares method is used for estimating the parameters $\beta_o, \beta_1, \beta_2, \ldots, \beta_n$ in Equation 5.1. This method minimizes the sum of squares of the errors in the regression equation. This system of equations is solvable and produces a unique solution.

The relation between *Y* and each X_i is assumed to be linear as stated and the effects of the *n* predictor variables are additive. In addition, several other assumptions must be made to be able to appropriately estimate the regression parameters and conduct tests of statistical significance. The assumptions are as follows (Berry & Feldman, 1985):

- All variables are measured at the intervals determined and without error;
- For each set of values for the n predictor variables, the expected error term is equal to zero;
- For each set of values for the n predictor variables, the variance of the error term is constant;
- For any two sets of values for the n predictor variables, the error terms are uncorrelated;

- The predictor variables are un-correlated with the error term;
- No predictor variable is linearly related to one or more of the other predictor variables in the model;
- For each set of values for the n predictor variables, the error term is normally distributed.

Violation of the above assumptions may lead to bias in the estimation of the regression coefficients, thus the true value of the coefficients will not be obtained. In addition, the estimates of the regression coefficients, R^2, significance tests and confidence intervals may not be correct. Furthermore, the estimate of the standard error of the regression coefficients may be biased. Problems in the data set, the use of an incorrect regression model or both are the possible ways of violating these assumptions.

5.4 Description of the Response and Predictor Variables

The variables to be modelled using multiple linear regression as stated before are the natural carbonation rate of the concrete as the response variable and the concrete mixture design parameters and the concrete early-age characterisation parameters as the predictor variables. In addition, the dummy variables for the binder type used in making the concretes, the curing durations given to the concretes and the exposure conditions are also included as predictor variables. Table 5.1 presents the variables to be used in the regression analysis. This table gives a detailed description of the response and predictor variables as well as the range/category and the variable type.

Table 5.1: Description of the response and predictor variables

Variable	Interpretation	Range / Category	Variable type
Response variable			
Natural carbonation rate (K_{nat})	The K_{nat} in mm/√year of the concrete, derived from the slope of a plot of carbonation depths in mm versus the square root of the individual exposure duration in years.	0.55 - 18.48 mm/√years	Continuous
Predictor variables:- Mixture design parameters			
Water/binder (*w/b*) ratio	The mass ratio of water to (cement + supplementary cementitious materials) in the concrete mix.	0.40 - 0.75	Continuous
Water content (*W*)	Mass of water required for 1 m^3 of the concrete mix.	190 - 210 kg/m^3	Continuous
Binder content (*B*)	Mass of cement or (cement + supplementary cementitious materials) required for 1 m^3 of the concrete mix.	300 - 450 kg/m^3	Continuous
Cement content (*C*)	Mass of cement required for 1 m^3 of the concrete mix.	150 - 450 kg/m^3	Continuous
Supplementary cementitious material content (*SCM*)	Mass of supplementary cementitious materials (*FA*, *GGBS*, and *CSF*) required for 1 m^3 of the concrete mix.	30 - 225 kg/m^3	Continuous
Predictor variables:- Concrete early-age characterisation parameters			
Compressive strength (f_c)	The f_c of the concrete measured at 3, 7 and 28 days after casting (averages of three test results).	8.73 - 91.40 MPa	Continuous

Table 5.1: Description of the response and predictor variables (Continued)

Variable	Interpretation	Range / Category	Variable type
Predictor variables:- Concrete early-age characterisation parameters			
Oxygen permeability index (*OPI*)	The *OPI* of the concrete measured at between 28 - 32 days after casting (averages of four test results).	8.2 - 10.4	Continuous
Water sorptivity (*WS*)	The *WS* of the concrete measured at between 28 - 32 days after casting (averages of four test results).	3.4 - 20.0 mm√hr	Continuous
Calcium hydroxide (*CH*) content	The *CH* content of the concrete measured at 3, 7 and 28 days after casting	9.28 - 18.73 % by mass of cement	Continuous
Calcium oxide (*CaO*) content	The *CaO* content of the concrete measured at 3, 7 and 28 days after casting (averages of two test results).	6.5 - 16.4 % by mass of cement	Continuous
Accelerated carbonation rate (K_{acc})	The K_{acc} in mm/√day of the concrete, derived from the slope of a plot of accelerated carbonation depths in mm versus the square root of the individual exposure duration in days.	0 - 9.27 mm/√day	Continuous
Predictor variables –dummy variables			
Binder type (*BT*)	The different binder types used in the concrete.	5 categories (CEM I, CEM I/FA, CEM I/GGBS, CEM I/ CSF and CEM V).	Categorical (Nominal)
Curing period (*CP*)	The different curing periods to which the concrete were exposed.	3 categories (3 days, 7 days and 28 days)	Categorical (Nominal)
Exposure condition (*EC*)	The different conditions to which the concrete were exposed.	3 categories (Indoor, Outdoor sheltered and Outdoor exposed).	Categorical (Nominal)

5.5 Preparation of the Response and Predictor Variables

5.5.1 Univariate analysis of the response and predictor variables

Data analysis often begins with the examination of each individual variable in isolation. The purpose is to have a general idea about the distribution of each individual variable, whether symmetric or skewed, and to identify possible outliers. Ideally, the distribution of the values of the variables should not be too skewed nor the range of the values very large. Before using the variables (response and predictors) described in the modelling analysis, univariate analysis was performed on the variables.

Univariate analysis provides an idea of the distribution (normal, bimodal, or skewed), central tendency (mean, median and mode) and dispersion (standard deviation, variance, range and quartiles) of the variables as well as identification of the presence of outliers (extreme values). The univariate analysis illuminates the individual variables before they are modelled, making the eventual interpretation of the output from further analysis easier. It also informs of any need for transformation of variables before being used in modelling (Chatterjee & Hadi, 2013; Fox, 1990; Lee & Tu, 1997).

Specifically, the outcomes of the univariate analysis are useful in the data checking and model formulation steps. Not performing univariate analysis on variables before modelling may restrict the usefulness of further procedures like the correlation and regression analysis. This is because the interpretation of the output from the correlation and regression analysis will be difficult because of an inadequate understanding of how the variables behaved individually.

The key results of the univariate analysis of the response variable are given in Table 5.2. The distribution of the response variable and its normal probability plot are shown in Figures 5.2 and 5.3 respectively. While the univariate statistics for

the predictor variables are presented in Table 5.3 and the histograms and normal probability plots for the individual predictor variables are shown in Figures 5.4 and 5.5 respectively.

Table 5.2: Univariate statistics for the response variable

Statistic	Response variable
	Natural carbonation rate of concrete (mm/√years)
Number of observations	180
Mean	6.32
Median	5.78
Mode	7.37
Standard deviation	3.73
Skewness	0.84
Kurtosis	0.47
Range	0.55 - 18.48
Inter quartile range	3.45 - 8.72

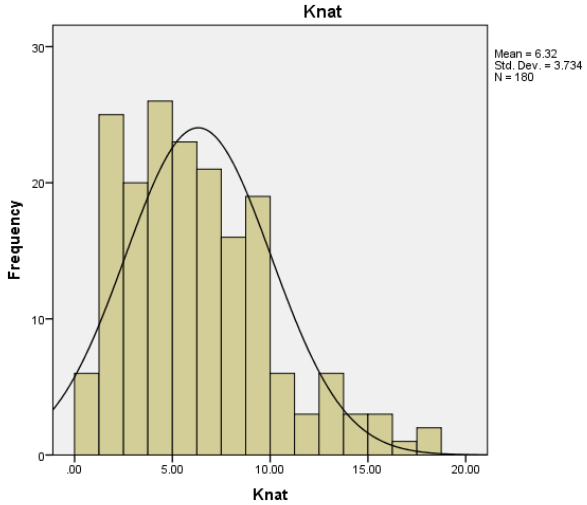


Figure 5.2: Histogram showing the distribution of the response variable

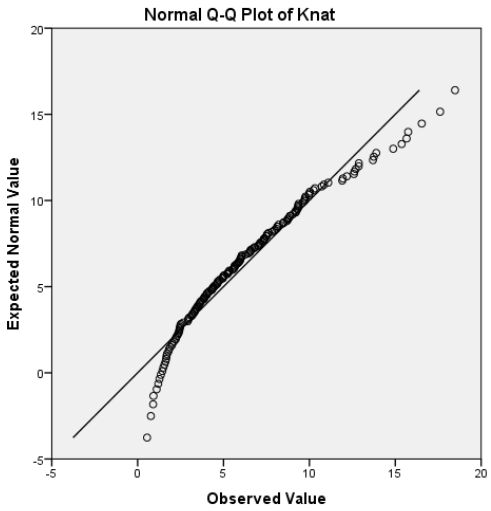
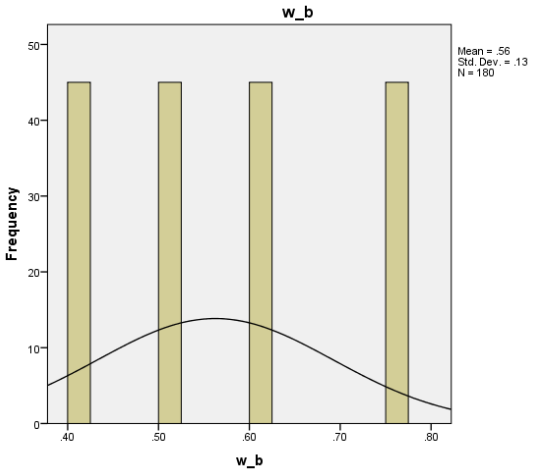


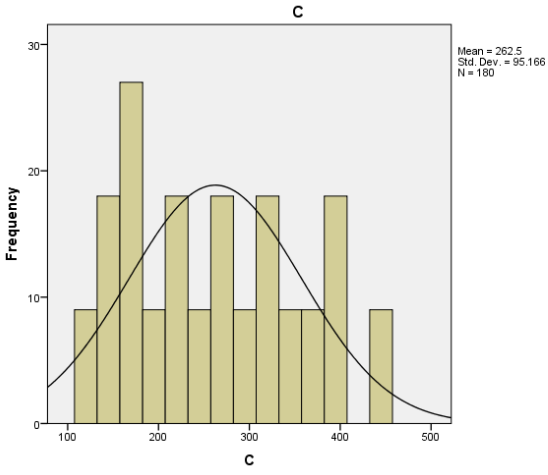
Figure 5.3: P - P plot for the response variable

Table 5.3: Univariate statistics for the predictor (continuous) variables

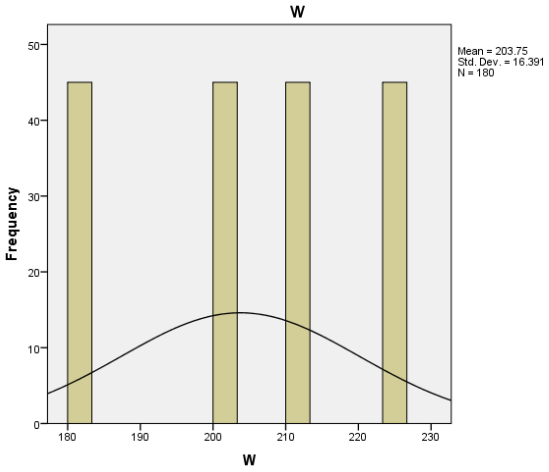
Statistics	Predictor (continuous) variables										
	w/b	*W*	*B*	*C*	*SCM*	f_c	*OPI*	*WS*	*CH*	*CaO*	K_{acc}
Number of observations	180	180	180	180	180	180	180	180	180	180	180
Mean	0.56	203.75	375.00	262.50	112.50	35.89	9.63	10.03	13.44	12.85	3.94
Median	0.55	205.00	375.00	257.50	112.50	31.14	9.65	8.85	13.22	12.70	3.30
Standard deviation	0.13	16.39	56.06	95.17	88.32	18.57	0.40	3.89	2.02	3.69	2.69
Skewness	0.25	-0.21	0.00	0.30	0.16	0.87	-0.97	0.95	0.23	0.95	0.94
Kurtosis	-1.26	-1.17	-1.36	-1.02	-1.34	0.22	1.60	0.39	-0.39	0.94	0.43
Range	0.40-0.75	190-210	300-450	150-450	30-225	8.73-91.40	8.2-10.4	3.4-20.0	9.28-18.73	6.5-16.4	0-9.27
Inter quartile range	0.43-0.71	185.00-221.25	312.50-437.50	176.25-341.25	31.25-195.00	22.30-48.28	9.33-9.90	7.55-12.30	11.73-14.94	10.18-14.38	1.88-5.37



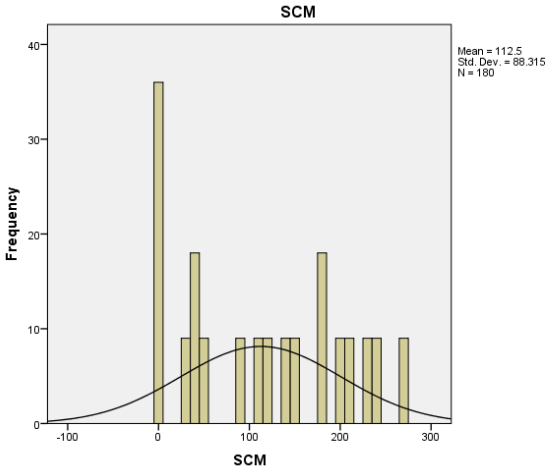
(I) *w/b*



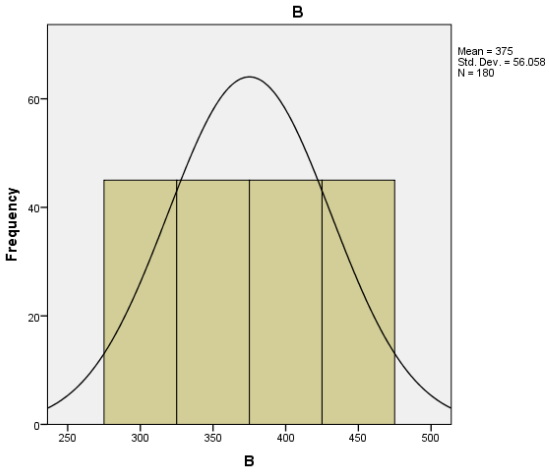
(IV) *C*



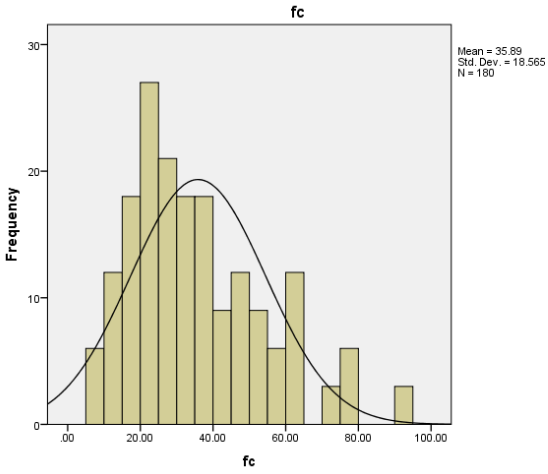
(II) *W*



(V) *SCM*

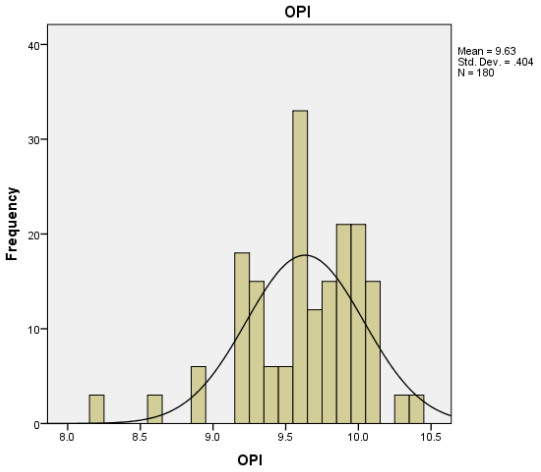


(III) *B*

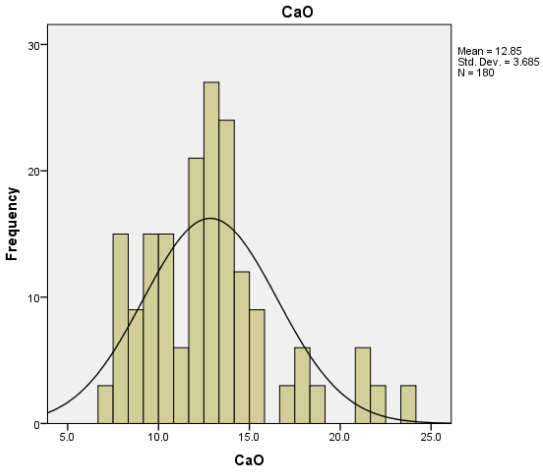


(VI) f_c

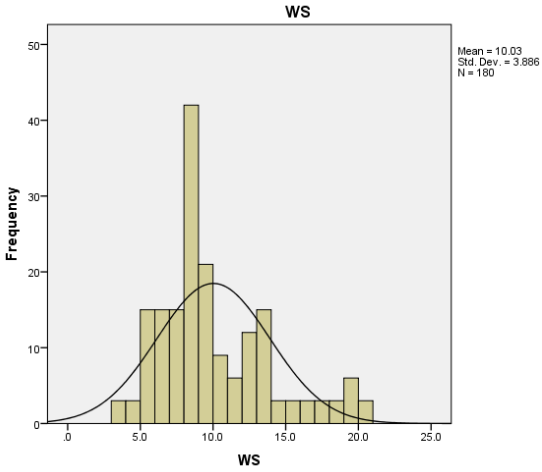
Figure 5.4: Histograms showing the distribution of the predictor variable



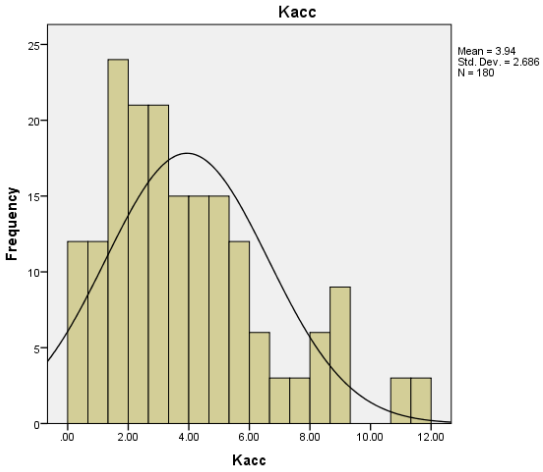
(VII) *OPI*



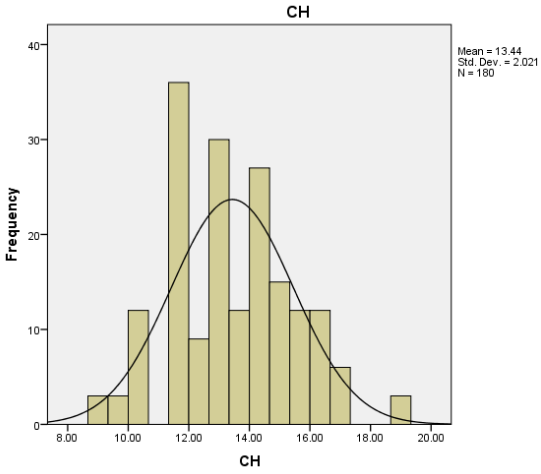
(X) *CaO*



(VIII) *WS*

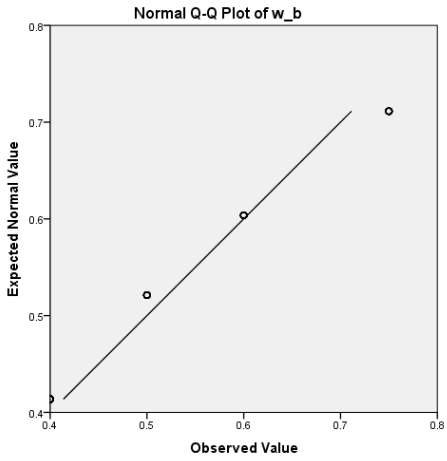


(XI) K_{acc}

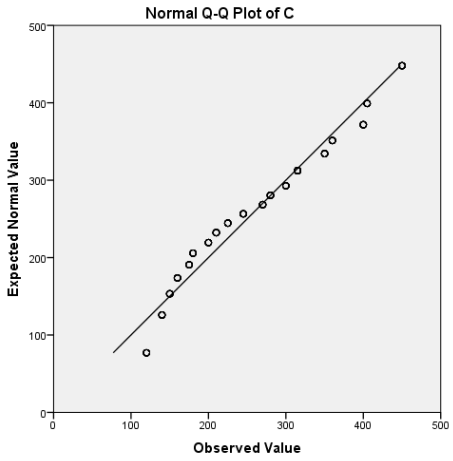


(IX) *CH*

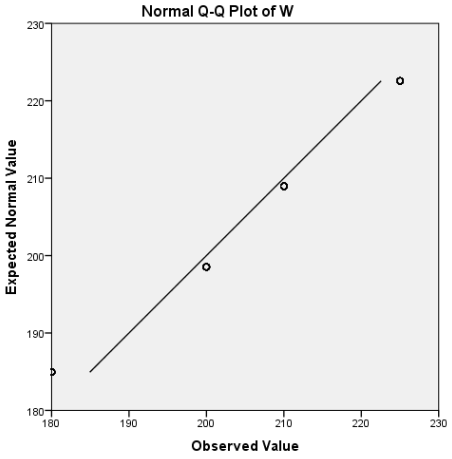
Figure 5.4: Histograms showing the distribution of the predictor variable (Continued)



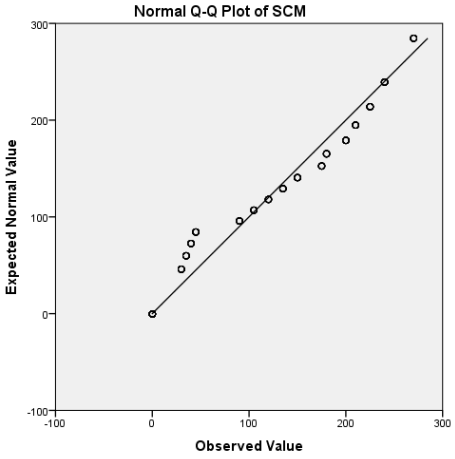
(I) *w/b*



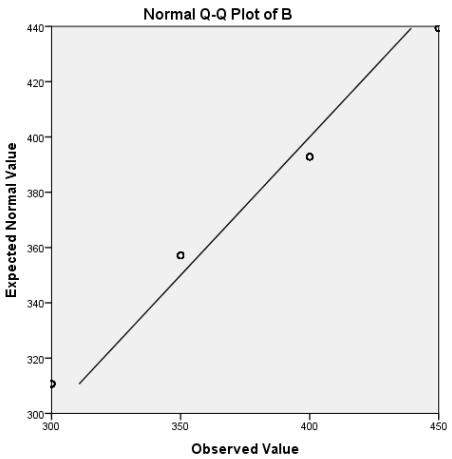
(IV) *C*



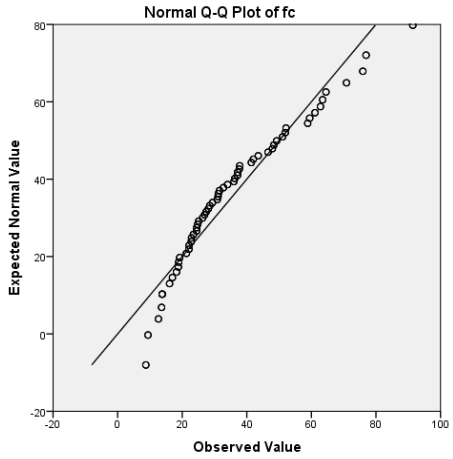
(II) *W*



(V) *SCM*

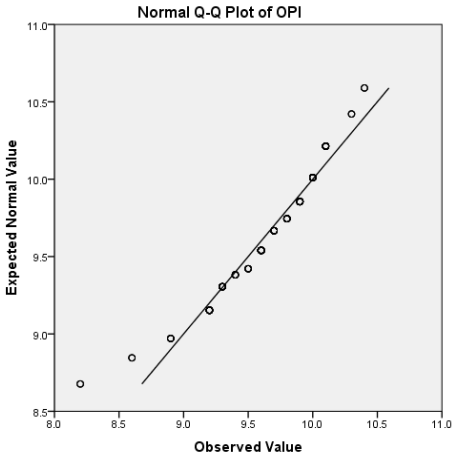


(III) *B*

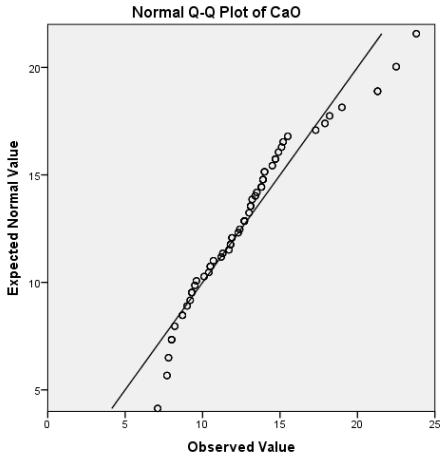


(VI) f_c

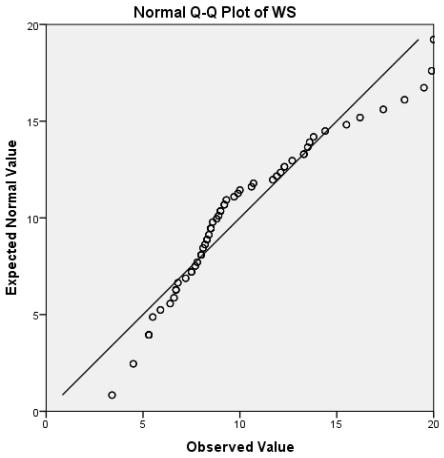
Figure 5.5: P - P plots for the predictor variables



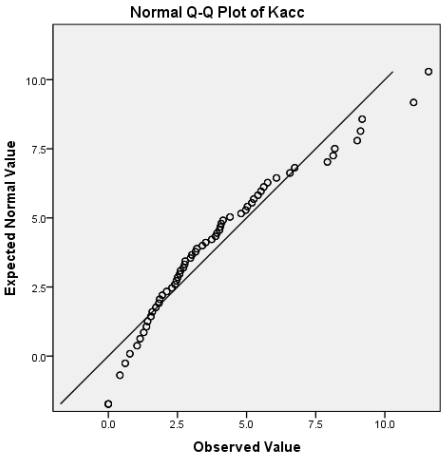
(VII) *OPI*



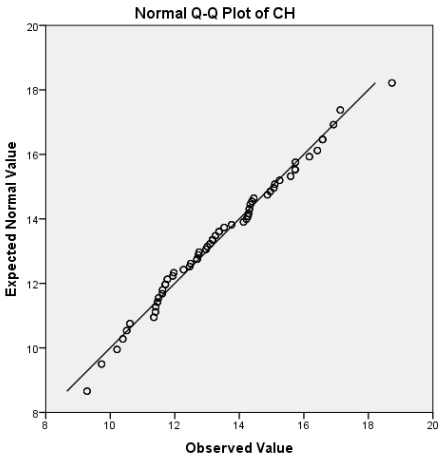
(X) *CaO*



(VIII) *WS*



(XI) K_{acc}



(IX) *CH*

Figure 5.5: P - P plots for the predictor variables (Continued)

The mean value of a distribution is the averages of all the values while the median value is the middle value when the values are arranged in ascending or descending order. The mode is the most frequently occurring value. From the univariate statistics of the natural carbonation rate values of the concrete (response variable) presented in Table 5.2, the mean and median values are similar but some positive skewness is noted in the histogram in Figure 5.2. The natural carbonation rates do not appear to contain outliers.

Skewness is a measure of the degree of symmetry in a distribution, with skewness values between -0.5 and 0.5 indicating an approximately symmetrical distribution. The distribution of the natural carbonation rate of the concrete is moderately positively skew (skewness = 0.84). Kurtosis measures the degree to which the data is distributed closer to the mean or closer to the extremes. A normal distribution has a kurtosis of 0. The response variable is slightly leptokurtic.

A further inspection of the normality of the natural carbonation rate of the concretes can be made using the P-P plot presented in Figure 5.3. This plot is used to make a more confident statement about the distribution of the response variable or of the histogram. However, it is clear from the histogram that the natural carbonation rate of the concrete is not normally distributed, it is positively skewed. Note that the smaller the gap between the line of equality and the dotted curve on the p-p plot, the higher will be the chance of the distribution of the variable being the same as the “Test Distribution” which, in this case, is the normal distribution. The P-P plot also tests whether the quartiles of the variable distribution match the quartiles that would indicate that the distribution is of the type being compared.

Interpretation of the univariate analysis results for the predictor variables was carried out similarly to that for the response variable. The values of the mean and median are similar for each of the predictor variables. Additionally, none of these

variables contain obvious outliers. Generally, from the univariate analysis of the predictor variables, the *OPI* values is highly negatively skewed; f_c, *WS, CH, CaO*, K_{acc} are moderately positively skewed. Further, *w/b, W, B, C, SCM* are platykurtic, or presumably because of the choice of experimental design values for these variables. The univariate statistics for the predictor variables showed nothing untoward, particularly no outliers which needed to be investigated.

The next step in the analysis process (preparation of variables), namely the investigation of bivariate relationships between the predictor variables themselves, and between the predictors and response variables, could thus be carried out. The values of the response and predictor variables that was subjected to the bivariate correlation analysis can be found in the excel spread sheet named "Correlation and Multiple Regression Data" on the accompanying CD.

5.5.2 Relationship between the response and predictor variables

Bivariate analysis of the response and predictor variables

Correlation between response and predictor variables, or between two predictor variables, indicates the suitability of an assumed functional relationship. The value of the correlation coefficients informs on the direction and strength of the relationship as well as the significance of the correlation. Bivariate correlation estimates the correlation coefficients between two continuous variables at a time, ignoring the effect of all other variables. The bivariate characteristics of the response and predictor variables as well as between the predictor variables were assessed and the result of this analysis is presented in Table 5.4, while the detailed analysis of the results can be found in Table E1, Appendix E. Table 5.4 shows the correlation coefficients as well as their significance for the linear relationship between the response variable and each predictor variable as well as correlation coefficients for the linear relationships between the predictor variables. Although correlation coefficients as low as ± 0.37 were found to be statistically significant

at the 5% level, absolute values of correlation coefficient greater than 0.75 were considered to be practically significant.

Table 5.4: Bivariate correlation coefficients between the variables

Variables	Variables											
	K_{nat}	*w/b*	*W*	*B*	*C*	*SCM*	f_c	*OPI*	*WS*	*CH*	*CaO*	K_{acc}
K_{nat}	1											
w/b	**0.591****	1										
W	0.576**	0.983**	1									
B	-0.584**	-0.994**	-0.992**	1								
C	**-0.735****	-0.410**	-0.409**	0.412**	1							
SCM	0.421**	-0.189*	-0.189*	0.190*	-0.816**	1						
f_c	**-0.777****	-0.600**	-0.606**	0.608**	0.647**	-0.312**	1					
OPI	**-0.738****	-0.823**	-0.800**	0.817**	0.585**	-0.112	0.742**	1				
WS	**0.747****	0.759**	0.735**	-0.751**	-0.517**	0.080	-0.718**	-0.855**	1			
CH	**-0.744****	-0.511**	-0.513**	0.515**	0.834**	-0.571**	0.723**	0.660**	-0.572**	1		
CaO	-0.374**	-0.302**	-0.306**	0.305**	0.677**	-0.532**	0.262**	0.270**	-0.115	0.690**	1	
K_{acc}	**0.857****	0.734**	0.713**	-0.725**	-0.790**	0.391**	-0.761**	-0.871**	0.858**	-0.828**	-0.475**	1

** Correlation is significant at the 0.01 level (2-tailed)
* Correlation is significant at the 0.05 level (2-tailed)

From Table 5.4, it can be noted that all the predictor variables exhibit good correlations with the response variable and these correlations are significant at the 5% level. The strongest correlation was observed between the K_{nat} and the K_{acc} of the concrete ($r = 0.86$), while the weakest was between the K_{nat} and the *CaO* content ($r = -0.37$).

As expected, the data set contained a number of highly correlated predictor variables as evident from the correlation coefficients (see Table 5.4), arising from the fact that the variables describe similar parameters of the mixture design or that the variables quantify related early-age parameters of the concrete properties. Thus, it is necessary to specify sets of predictor variables for multiple linear regression for the prediction of the response variable in order to eliminate the problem of multi-collinearity. This is a situation where two or more variables have a similar effect in predicting the response variable, making one or more of the variables redundant. Multi-collinearity arises when absolute correlation coefficients value between two predictor variables is greater than 0.75 (Chatterjee & Hadi, 2009).

As a first step, the correlation coefficients between the response and predictor variables were used to identify highly correlated relationships. Considerations were then given to the physical and chemical properties of the concrete, the mechanism of carbonation process in concrete as well as some measure of engineering judgment in the final grouping of the predictor variables for regression analysis. The approach used in developing the model was therefore to overlay the characteristics and responses of the concrete material variables onto the statistical analysis, in a manner that allowed a material – based interpretation of the correlation data.

The mixture design parameters were correlated to K_{nat} except for the *SCM* variable. However the correlation coefficient for this variable is significant at the

5% level. Among the mixture design variables, the w/b ratio, water content and binder content are highly correlated to each other. The correlation coefficient between w/b ratio and water content is 0.98, w/b and binder content is -0.99 and between water content and binder content is -0.99. This high correlation is expected since these variables all describe similar mixture design parameters of the concrete. In addition, these variables also influence the physical properties of the concrete in terms of the concrete microstructure development and characteristics.

The high correlation coefficients among the w/b, water content and binder content variables suggest that they all have similar influence or effect in predicting the response variable. Therefore, only one of these variables should be used in the modelling analysis if multi-collinearity is to be avoided. Since the three variables are correlated with the natural carbonation rate of the concrete, it is natural to pick the variable with the highest correlation coefficient (which is *w/b* ratio, $r = 0.59$). Additionally, this variable has greater practical importance and is more commonly used in the description of concrete mixture proportions than the other two variables.

The carbonation process in concrete is a physical and chemical process (Papadakis et al., 1991), hence the need to include the chemical aspect in a reliable prediction of the natural carbonation rate of concrete. The cement, binder and *SCM* content of the mixture design parameters dictates to a large extent the chemical composition of the concrete. From the correlation coefficient between the cement, binder and *SCM* contents and the K_{nat} of the concrete ($r = -0.74, -0.58$ and 0.42 respectively) coupled with the high correlation of cement content to *SCM* content ($r = 0.82$), the best variable to describe or represent the chemical composition of the concrete is the cement content. However, the cement content and *SCM* content cannot be in the same variable sets for the prediction of K_{nat}, to avoid multi-collinearity as stated before.

In general, the mixture design parameters that best influence the K_{nat} of the concrete based on the correlation coefficient results, knowledge of the mechanism of carbonation process in concrete and some measure of engineering judgment, are the w/b ratio and cement content.

Early-age concrete characterisation parameters that are known to influence the K_{nat} of the concrete are f_c, *OPI, WS, CH, CaO and* K_{acc} (Bertolini et al., 2013; Tutti, 1982; Wierig, 1984). While the *OPI* and *WS* variables measure the physical properties of concrete and, at the same time, quantify or describe the physical aspect of concrete carbonation, the *CH* and *CaO* content of the concrete quantify the chemical composition of the concrete and thus describe the chemical aspect of carbonation in concrete. The K_{acc} of the concrete covers both the physical and chemical processes of carbonation in concrete and is also influenced by the physical and chemical properties of the concrete.

Although the compressive strength of concrete quantifies the physical property of concrete, it may not be a good indicator for the rate of carbonation. It is nevertheless a factor that concrete designers would commonly take into consideration when designing concrete structures for resisting applied loads and possibly where carbonation-induced corrosion is the main deterioration mechanism. Additionally, compressive strength will probably be the only known design parameter for many existing concrete structures. Furthermore, in the consideration of comparative analysis (validation) between carbonation prediction by the proposed models and historically measured carbonation, the inclusion of this parameter in the modelling analysis will be important.

Thus, drawing from the above reasoning, the early-age concrete characterisation parameters can be grouped in accordance with the mechanism of carbonation process and the properties of concrete that these early-age parameters are measuring. Similarly, the results of the correlation coefficients of the response and

predictor variables and between the predictor variables have to be taken into consideration in the final grouping of the early-age characterisation parameters.

From the correlation coefficient results, the *OPI* and *WS* are highly correlated with K_{nat} of the concrete (r = *-0.74*, *0.75* respectively). These variables are also correlated with each other (*OPI* and *WS*, r = *-0.85*), attesting to the fact that these variables describe similar physical parameters of the concrete. Therefore, the variables *OPI* and *WS* cannot be in the same variable set for the prediction of K_{nat} based on the process of carbonation and engineering judgment.

The *CH* content is more highly correlated to K_{nat} than *CaO* content (r = *-0.74* and *-0.37* for *CH* and *CaO* contents respectively). And since the *CH* variable is correlated with the *CaO* content (r = *0.69*), both variables cannot represent the concrete chemical composition if multi-collinearity is to be avoided. Therefore, the *CH* variable was used to represent the chemical properties of the concrete as well as the chemical aspect of the carbonation process of concrete based on the high correlation coefficients with K_{nat}.

As stated before, the K_{acc} describes both the physical and chemical aspects of the carbonation process, and is influenced by both the physical and chemical properties of the concrete, as with K_{nat}. This is the reason for the high correlation coefficient observed between the two variables (r = *0.86*). Thus, the K_{acc} will be in its own variable set. Similarly, and based on engineering reasoning as given above, the f_c of the concrete will be in its own variable set as well as in combination with the other physical and or chemical parameter of the concrete.

For the correlation coefficient between variables to be valid there must be a linear relationship between the variables. Thus, the validity of the correlation coefficients between the variables as given above was examined by means of scatter plots. The scatter plots between the response and predictor variables and

between the predictor variables themselves were investigated and the results are given in Figure E1, Appendix E. From the results of the scatter plots obtained, linear relationships were noted for all the plots except for those plots that involves the *w/b* ratio, *W* content and or *B* content variables. The reasons for these plots not presenting linear relationships is as a result of the nature of the values of the variables which stem from the experimental design.

Association between the response and predictor variables

In the final grouping of the predictor variables for regression analysis, the association between the categorical variables as well as between each categorical and continuous variable needs to be investigated. While the Chi-square test was used to investigate association between categorical variables, the ANOVA test was used to identify association between categorical and continuous variables. The detailed results for these analyses are given in Tables E2 and E3, Appendix E, while Table 5.5 gives the specific association and its significance between the variables. Thus, Table 5.5 in conjunction with Table 5.4 was used in the final selection of variable sets for regression.

Table 5.5: Table of association between the variables

Variables	Variables														
	K_{nat}	*w/b*	*W*	*B*	*C*	*SCM*	f_c	*OPI*	*WS*	*CH*	*CaO*	K_{acc}	*BT*	*CP*	*EC*
K_{nat}															
w/b															
W															
B															
C															
SCM															
f_c															
OPI															
WS															
CH															
CaO															
K_{acc}															
BT	η^2=0.342 P<0.05	η^2=0 P=1.0	η^2=0 P=1.0	η^2=0 P=1.0	η^2=0.812 P<0.05	η^2=0.943 P<0.05	η^2=0.229 P<0.05	η^2=0.149 P<0.05	η^2=0.191 P<0.05	η^2=0.584 P<0.05	η^2=0.651 P<0.05	η^2=0.348 P<0.05	1		
CP	**η^2=0.101 P<0.05**	η^2=0 P=1.0	η^2=0 P=1.0	η^2=0 P=1.0	η^2=0 P=1.0	η^2=0 P=1.0	η^2=0.340 P<0.05	η^2=0.048 P=0.012	η^2=0.094 P<0.05	η^2=0120 P<0.05	η^2=0.026 P=0.097	η^2=0.044 P=0.018	η^2=0 P=1.0	1	
EC	**η^2=0.122 P<0.05**	η^2=0 P=1.0	η^2=0 P=1.0	η^2=0 P=1.0	η^2=0 P=1.0	η^2=0 P=1.0	η^2=0 P=1.0	η^2=0 P=1.0	η^2=0 P=1.0	η^2=0 P=1.0	η^2=0 P=1.0	η^2=0 P=1.0	η^2=0 P=1.0	η^2=0 P=1.0	1

From the tables of correlation and association given above, considering that strong correlation and or associations are defined by an absolute correlation coefficient ≥ *0.75*, or an ANOVA $\eta^2 > 0.14$. Relationship exists between *w/b* ratio, *W* and *B*; *C* and *SCM; BT, C* and *SCM*. Thus, for the mixture design variables, the possible input variables are *EC, CP, w/b, C* and or *BT* while for the early-age parameters, strong relationships exist between *OPI* and *WS;* $K_{acc,}$ f_c, *OPI, WS* and *CH; BT* and all the early-age parameters. The early-age properties of the concrete describe the difference between the binder types. Hence, early-age concrete properties did not need the inclusion of binder type in any variables set that have any of the early-age property. Thus, the possible variables are *EC, CP*, and or K_{acc}, *CH*, f_c, *OPI*, *WS*. Additionally, based on engineering judgment and some statistical reasoning, the mixture design and early-age parameters can be combined to give a more complex variable subsets for the prediction of the response variables.

The predictor variables were then grouped into subsets for evaluation by multiple linear regression for the prediction of the response variables. The sets were constructed based on the results of the bivariate correlation between the continuous variables (see Table 5.4), and the association between the categorical variables as well as the association between the categorical variables and each continuous variable (see Table 5.5), the mechanism of carbonation in concrete and some measure of engineering judgment. Based on the above analysis, the construction of the predictor variable subsets is given in Table 5.6.

Table 5.6: Predictor variable subsets for the prediction of K_{nat}

Sets	Predictor variables
Set 1	w/b, C, CP, EC
Set 2	w/b, BT, CP, EC
Set 3	fc, EC
Set 4	fc, CP, EC
Set 5	OPI, EC
Set 6	WS, EC
Set 7	fc, OPI, EC
Set 8	fc, WS, EC
Set 9	OPI, CH, EC
Set 10	WS, CH, EC
Set 11	fc, OPI, CH, EC
Set 12	fc, WS, CH, EC
Set 13	Kacc, EC
Set 14	Kacc, CP, EC

The last step in the preparation of the predictor variables was the coding of the categorical variables. The categorical variables were coded as indicator (dummy) variables, relative to a reference category (coded as 0) (Cohen & Cohen, 1975; Douglas et al., 2012). The levels of the categorical variables for the binder types are given in Table 5.7 with *CEM I* as the reference category. The levels of the categorical variables for the curing duration are given in Table 5.8 with the 28 days moist curing period as the reference category. While the levels of the categorical variables for the exposure conditions are given in Table 5.9 with the indoor exposure condition as the reference category.

Table 5.7: Dummy variable coding for binder types

Types of binder used in concrete	X1	X2	X3	X4	Identification
CEM I	0	0	0	0	If CEM I is used in the concrete
CEM I/FA	1	0	0	0	If CEM I/FA is used in the concrete
CEM I/GGBS	0	1	0	0	If CEM I/GGBS is used in the concrete
CEM I/CSF	0	0	1	0	If CEM I/CSF is used in the concrete
CEM V	0	0	0	1	If CEM V is used in the concrete

Table 5.8: Dummy variable coding for curing periods

Types of moist curing condition concrete is given	X1	X2	Identification
28 days	0	0	If concrete is placed in water for 28 days
7 days	1	0	If concrete is placed in water for 7 days
3 days	0	1	If concrete is placed in water for 3 days

Table 5.9: Dummy variable coding for exposure conditions

Types of exposure condition concrete is placed	X1	X2	Identification
Indoor	0	0	If concrete is placed in an indoor condition
Outdoor sheltered	1	0	If concrete is placed in an outdoor sheltered condition
Outdoor exposed	0	1	If the concrete is placed in an outdoor exposed condition

From the individual predictor variable subsets given in Table 5.6 above for the prediction of K_{nat}, with the inclusion of the relevant dummy variable sets shown in Tables 5.7, 5.8 and 5.9, Equation 5.1 was fitted individually using multiple linear

regression analysis. The unknown coefficients (β_0, β_1, β_2,…, β_n) in the equation were estimated from the regression analysis. The values of the response and predictor variables that were used for the regression analysis can be found in the excel spread sheet named "Correlation and Multiple Regression Data" on the accompanying CD.

5.6 Regression Analysis between the Response and Predictor Variables

Multiple linear regression analysis was performed in the Statistical Package of Social Science (SPSS) 20 software. The method of analysis was based on the Ordinary Least Squares (*OLS*) procedure to estimate the regression parameters (coefficients). The values of the predictor variable subsets presented in Table 5.10 with the inclusion of the dummy variables for each categorical variable were used in the regression analysis. Table 5.10 also introduces simpler referencing of the models which will be used henceforth.

Table 5.10: Predictor variables subsets for the prediction of K_{nat}

Model	Predictor variables subsets
Model 1	w/b, C, CP, EC
Model 2	w/b, BT, CP, EC
Model 3	f_c, EC
Model 4	f_c, CP, EC
Model 5	OPI, EC
Model 6	WS, EC
Model 7	f_c, OPI, EC
Model 8	f_c, WS, EC
Model 9	OPI, CH, EC
Model 10	WS, CH, EC
Model 11	f_c, OPI, CH, EC
Model 12	f_c, WS, CH, EC
Model 13	K_{acc}, EC
Model 14	K_{acc}, CP, EC

The values of the predictor variable sets shown in Table 5.10 were used in the multiple linear regression analysis in turn with the values of the natural carbonation rate of the concrete as response variable. The dummy variables for each of the categorical variables were transformed by recording into the indicator variables (0 and 1) before use in the regression analysis. The detailed regression analysis outcomes for each of the model can be obtained in the file named "Regression Analysis Main Modelling Results" in the accompanying CD, while key regression results for the individual models are given in Model 1 to Model 14 in Appendix F. Table 5.11 presents the analysis of the regression outcomes as well as key diagnostics checks of the results in Appendix F for the individual model regression analysis. These diagnostics are similar to those used in the univariate analysis and comprised (Chatterjee & Hadi, 2009, 2013):

- Examination of the model summary collinearity and collinearity diagnostics table for the R-square value and T-values: Collinearity is

indicated if the R-square is high ($R^2 > 0.75$) and only a few T-values are significant. Additionally, significant collinearity is present if the condition index is > 10.

- Check for mis-specification like incorrect functional form and omission of a relevant predictor variable: Any pattern in the plot ZPRED and Y-PRED implies mis-specification and/or heteroskedasticity. Additionally, the T-statistics should be significant at the 10% level.
- Examination of the regression variate: Plot of standard normal predicted variable versus standard normal of the regression residual (scatter plot) and plots of the predicted response variables and residual (partial plots) should all be evenly dispersed and may show no obvious patterns.
- Check of the assumed linearity of the overall relationship: The plot of residuals versus the predicted dependent variable should not show obvious patterns. Partial regression plots for the residuals versus each predictor variable should not exhibit any relationship or outliers.
- Check of the assumption of homoscedasticity: The plot of residuals versus the predicted response variable should not fan out.
- Check of the assumption of the normality of the error term distribution: The residuals should be approximately normally distributed and the normal probability plots of the residuals should be approximately linear.
- Examination for outliers and influential points**:** Outliers were identified by means of large standardised residuals and also from the partial regression plots.

Table 5.11: Results of the multiple linear regression analysis

Statistics	Model 1	Model 2	Model 3	Model 4	Model 5
Sig.-F (in the ANOVA table)	Sig. F < 0.05, significantly fit data	Sig. F < 0.05, significantly fit data	Sig. F < 0.05, significantly fit data	Sig. F < 0.05, significantly fit data	Sig. F < 0.05, significantly fit data
R^2 (in the Model Summary table)	$R^2 = 0.86$	$R^2 = 0.92$	$R^2 = 0.73$	$R^2 = 0.76$	$R^2 = 0.67$
Adjusted R^2 (in the Model Summary table)	Adj. $R^2 = 0.86$	Adj. $R^2 = 0.91$	Adj. $R^2 = 0.72$	Adj. $R^2 = 0.75$	Adj. $R^2 = 0.66$
T-Ratios (in the Coefficients table)	Ok for all the variables	Ok for all variables except CEMI/CSF	Ok for all variables	Ok for all variables	Ok for all variables
Distribution of residual (Histogram)	No outliers, normal distribution	No outliers, normal distribution	No outliers, normal distribution	No outliers, normal distribution	No outliers, normal distribution
Normal probability plot (P-P Plot)	Confirms normality	Confirms normality	Confirms normality	Confirms normality	Confirms normality
Regression standardized predicted vs. standardized residual (Scatter plot)	No pattern observed	No pattern observed	No pattern observed	No pattern observed	No pattern observed
Regression residual vs. predictors in model (Partial plots)	No pattern observed for all plots	Pattern observed for some plots	Pattern observed for some plots	Pattern observed for some plots	Pattern observed for some plots
Variance Inflation Factor (VIF) (in the Coefficients table)	All variables VIF < 10, fine	All variables VIF < 10, fine	All variables VIF < 10, fine	All variables VIF < 10, fine	All variables VIF < 10, fine

Table 5.11: Results of the multiple linear regression analysis (Continued)

Statistics	Model 6	Model 7	Model 8	Model 9	Model 10
Sig.-F (in the ANOVA table)	Sig. F < 0.05, significantly fit data	Sig. F < 0.05, significantly fit data	Sig. F < 0.05, significantly fit data	Sig. F < 0.05, significantly fit data	Sig. F < 0.05, significantly fit data
R^2 (in the Model Summary table)	$R^2 = 0.68$	$R^2 = 0.78$	$R^2 = 0.80$	$R^2 = 0.78$	$R^2 = 0.83$
Adjusted R^2 (in the Model Summary table)	Adj. $R^2 = 0.67$	Adj. $R^2 = 0.78$	Adj. $R^2 = 0.80$	Adj. $R^2 = 0.78$	Adj. $R^2 = 0.83$
T-Ratios (in the Coefficients table)	Not ok for the intercept	Ok for all variables	Ok for all variables	Ok for all variables	Ok for all variables
Distribution of residual (Histogram)	No outliers, normal distribution	No outliers, normal distribution	No outliers, normal distribution	No outliers, normal distribution	No outliers, normal distribution
Normal probability plot (P-P Plot)	Confirms normality	Confirms normality	Confirms normality	Confirms normality	Confirms normality
Regression standardized predicted vs. standardized residual (Scatter plot)	No pattern observed	No pattern observed	No pattern observed	No pattern observed	No pattern observed
Regression residual vs. predictors in model (Partial plots)	Pattern observed for some plots	Pattern observed for some plots	Pattern observed for some plots	Pattern observed for some plots	Pattern observed for some plots
Variance Inflation Factor (VIF) (in the Coefficients table)	All variables VIF < 10, fine	All variables VIF < 10, fine	All variables VIF < 10, fine	All variables VIF < 10, fine	All variables VIF < 10, fine

Table 5.11: Results of the multiple linear regression analysis (Continued)

Statistics	Model 11	Model 12	Model 13	Model 14
Sig.-F (in the ANOVA table)	Sig. F < 0.05, significantly fit data	Sig. F < 0.05, significantly fit data	Sig. F < 0.05, significantly fit data	Sig. F < 0.05, significantly fit data
R^2 (in the Model Summary table)	$R^2 = 0.83$	$R^2 = 0.86$	$R^2 = 0.86$	$R^2 = 0.88$
Adjusted R^2 (in the Model Summary table)	Adj. $R^2 = 0.82$	Adj. $R^2 = 0.85$	Adj. $R^2 = 0.85$	Adj. $R^2 = 0.87$
T-Ratios (in the Coefficients table)	Ok for all variables	Ok for all variables	Ok for all variables	Ok for all variables
Distribution of residual (Histogram)	No outliers, normal distribution	No outliers, normal distribution	No outliers, normal distribution	No outliers, normal distribution
Normal probability plot (P-P Plot)	Confirms normality	Confirms normality	Confirms normality	Confirms normality
Regression standardized predicted vs. standardized residual (Scatter plot)	No pattern observed	No pattern observed	No pattern observed	No pattern observed
Regression residual vs. predictors in model (Partial plots)	Pattern observed for some plots	Pattern observed for some plots	Pattern observed for some plots	Pattern observed for some plots
Variance Inflation Factor (VIF) (in the Coefficients table)	All variables VIF < 10, fine	All variables VIF < 10, fine	All variables VIF < 10, fine	All variables VIF < 10, fine

The findings of the diagnostics for the 14 models were very similar, and are thus discussed in general terms. All model terms are significant at the 5% level with the R^2 and adjusted R^2 values greater than *0.66*. The T-Ratios of the variables for all the models are also significant for all the variables except for Model 2, while for Model 6 the value of the intercept was not significant. The proportion of the variation in response variable that could be explained by the variation in the predictor for the models ranged between *0.67* to *0.92*, while the proportion of the variance in the response variable that was explained by variations in the predictor variables ranged between *0.66* and *0.91*.

Most of the estimated coefficients are significant at the 5% level, especially for the variables. This means that the dispersion/variance is not high and the estimated coefficients are reliable. Plots of residuals versus the predicted dependent variable as well as the partial regression plots for the residuals versus each predictor variable show no outliers and obvious patterns. Outliers were also not observed in the plots of the studentised residuals versus the observed dependent variables. Overall shapes of the residual plots indicated that there was no heteroskedasticity of errors, which was confirmed by the distribution of the studentised residuals as well as their normal probability plots. Plots of the residual versus predictors were all acceptable.

Whilst care had been taken to exclude multi-collinear predictor variables from the variable subsets, each model output were again examined for multi-collinearity by inspecting the Variance Inflation Factors (*VIF*) of the model terms. *VIF* values greater than 10 were considered significant (Douglas et al., 2012), meaning that the models regression coefficients are poorly estimated. It was found that all the models have *VIF* values that are less than 5. High multi-collinearity results in difficulties in the correct estimation of regression coefficients by the variables (coefficients may have an incorrect sign and magnitude at high collinearity) as well as in separating the contribution of each predictor.

The detailed description and ranges of applicability of the developed models are given in Table 5.1 above as well as in Table 5.12, while the estimated model coefficients are presented in Tables 5.12. The ranges of applicability covered by the models are limited to the concrete mixture design and early-age characterisation parameters covered by the 180 carbonation profiles that were used in the multiple linear regression analysis. In addition, the models are limited to the different binder types used in making the concrete, moist cured duration as well as the micro-climatic variations of the exposure conditions investigated.

Table 5.12: Estimated model coefficients

Variables	Range	Units	Estimated Coefficients				
			Model 1	Model 2	Model 3	Model 4	Model 5
Intercept	-	-	+5.63	-7.03	+12.27	+14.26	+72.32
w/b	0.40-0.75	-	+10.01	+17.01	-	-	-
C	150-450	Kg/m^3	-0.02	-	-	-	-
f_c	8.73-91.40	MPa	-	-	-0.16	-0.18	-
OPI	8.2-10.4	-	-	-	-	-	-6.82
WS	3.4-20.0	mm/√hr.	-	-	-	-	-
CH	9.28-18.73	% by mass of cement	-	-	-	-	-
K_{acc}	0-9.27	mm/√day	-	-	-	-	-
CEM I	0-1	-	-	0	-	-	-
CEM I/FA	0-1	-	-	+3.60	-	-	-
CEM I/GGBS	0-1	-	-	+4.49	-	-	-
CEM I/CSF	0-1	-	-	+0.02	-	-	-
CEM V	0-1	-	-	+5.00	-	-	-
28 days	0-1	-	0	0	-	0	-
7 days	0-1	-	+1.61	+1.61	-	-1.56	-
3 days	0-1	-	+2.90	+2.90	-	-1.79	-
Indoor (In)	0-1	-	0	0	0	0	0
Outdoor sheltered (Os)	0-1	-	+1.07	+1.07	+1.07	+1.07	+1.07
Outdoor exposed (Oe)	0-1	-	-2.07	-2.07	-2.07	-2.07	-2.07

Table 5.12: Estimated model coefficients (Continued)

Variables	Range	Units	Estimated Coefficients				
			Model 6	Model 7	Model 8	Model 9	Model 10
Intercept	-	-	-0.54	+42.29	+6.49	+56.89	+13.74
w/b	0.40-0.75	-	-	-	-	-	-
C	150-450	Kg/m^3	-	-	-	-	-
f_c	8.73-91.40	MPa	-	-0.10	-0.10	-	-
OPI	8.2-10.4	-	-	-3.32	-	-4.04	-
WS	3.4-20.0	mm/√hr.	+0.72	-	+0.37	-	+0.46
CH	9.28-18.73	% by mass of cement	-	-	-	-0.84	-0.87
K_{acc}	0-9.27	mm/√day	-	-	-	-	-
CEM I	0-1	-	-	-	-	-	-
CEM I/FA	0-1	-	-	-	-	-	-
CEM I/GGBS	0-1	-	-	-	-	-	-
CEM I/CSF	0-1	-	-	-	-	-	-
CEM V	0-1	-	-	-	-	-	-
28 days	0-1	-	-	-	-	-	-
7 days	0-1	-	-	-	-	-	-
3 days	0-1	-	-	-	-	-	-
Indoor (In)	0-1	-	0	0	0	0	0
Outdoor sheltered (Os)	0-1	-	+1.07	+1.07	+1.07	+1.07	+1.07
Outdoor exposed (Oe)	0-1	-	-2.07	-2.07	-2.07	-2.07	-2.07

Table 5.12: Estimated model coefficients (Continued)

Variables	Range	Units	Estimated Coefficients			
			Model 11	Model 12	Model 13	Model 14
Intercept	-	-	+41.24	+13.75	+1.96	+1.44
w/b	0.40-0.75	-	-	-	-	-
C	150-450	Kg/m^3	-	-	-	-
f_c	8.73-91.40	MPa	-0.07	-0.06	-	-
OPI	8.2-10.4	-	-2.53	-	-	-
WS	3.4-20.0	mm/√hr.	-	+0.34	-	-
CH	9.28-18.73	% by mass of cement	-0.57	-0.63	-	-
K_{acc}	0-9.27	mm/√day	-	-	+1.19	+1.15
CEM I	0-1	-	-	-	-	-
CEM I/FA	0-1	-	-	-	-	-
CEM I/GGBS	0-1	-	-	-	-	-
CEM I/CSF	0-1	-	-	-	-	-
CEM V	0-1	-	-	-	-	-
28 days	0-1	-	-	-	-	0
7 days	0-1	-	-	-	-	+0.74
3 days	0-1	-	-	-	-	+1.31
Indoor (In)	0-1	-	0	0	0	0
Outdoor sheltered (Os)	0-1	-	+1.07	+1.07	+1.07	+1.07
Outdoor exposed (Oe)	0-1	-	-2.07	-2.07	-2.07	-2.07

5.6.1 Developed carbonation prediction models

The individual models for the prediction of the natural carbonation rate of concrete in the inland environment are presented in Equations 5.2 to 5.15. These models are obtained from Equation 5.1 by inserting the estimated coefficients obtained from the regression analysis and as presented in Table 5.12 above.

Model 1

$$K_{nat.} = 5.63 + 10.01\,(w/b) - 0.02(C) + \alpha_1 + \beta \quad 5.2$$

Model 2

$$K_{nat.} = -7.03 + 17.01(w/b) + \gamma + \alpha_1 + \beta \quad 5.3$$

Model 3

$$K_{nat.} = 12.27 - 0.16(f_c) + \beta \quad 5.4$$

Model 4

$$K_{nat.} = 14.26 - 0.18(f_c) + \alpha_2 + \beta \quad 5.5$$

Model 5

$$K_{nat.} = 72.32 - 6.82(OPI) + \beta \quad 5.6$$

Model 6

$$K_{nat.} = -0.54 + 0.72(WS) + \beta \quad 5.7$$

Model 7

$$K_{nat.} = 42.29 - 0.10(f_c) - 3.32(OPI) + \beta \quad 5.8$$

Model 8

$$K_{nat.} = 6.49 - 0.10(f_c) + 0.37(WS) + \beta \quad 5.9$$

Model 9

$$K_{nat.} = 56.89 - 4.04(OPI) - 0.84(CH) + \beta \quad 5.10$$

Model 10

$$K_{nat.} = 13.74 + 0.46(WS) - 0.87(CH) + \beta \quad 5.11$$

Model 11

$$K_{nat.} = 41.24 - 0.07(f_c) - 2.53(OPI) - 0.57(CH) + \beta \quad 5.12$$

Model 12

$$K_{nat.} = 13.75 - 0.06(f_c) + 0.34(WS) - 0.63(CH) + \beta \quad 5.13$$

Model 13

$$K_{nat.} = 1.96 + 1.19(K_{acc.}) + \beta \quad 5.14$$

Model 14

$$K_{nat.} = 1.44 + 1.15(K_{acc.}) + \alpha_3 + \beta \quad 5.15$$

Where,

K_{nat} = natural carbonation rate, in mm/√years;

w/b = water/binder ratio;

C = cement content, in kg/m^3;

f_c = 28 day compressive strength of concrete, in MPa;

OPI = 28 day oxygen permeability index of concrete;

WS = 28 day water sorptivity of the concrete in mm√hour;

CH = 28 day calcium hydroxide content of the concrete;

K_{acc} = 28 day accelerated carbonation rate of the concrete in mm/√day;

γ = binder type used in concrete and obtained from Table 5.13.

$\alpha_{1,2,3,4}$ = curing duration given to concrete and obtained from Table 5.14.

β = exposure condition of the concrete and obtained from Table 5.15

Table 5.13: Model coefficients for binder types

Binder type	γ
CEM I	0
CEM I/FA	+3.60
CEM I/GGBS	+4.49
CEM I/CSF	+0.02
CEM V	+5.00

Table 5.14: Model coefficients for curing durations

Curing duration	α_1	α_2	α_3
28 days	0	0	0
7 days	+1.61	-1.56	+0.74
3 days	+2.90	-1.79	+1.31

Table 5.15: Model coefficients for exposure conditions

Exposure condition	β
Indoor	0
Outdoor sheltered	+1.07
Outdoor exposed	+-2.07

The developed carbonation rate prediction models (Equations 5.2 to 5.15) for concrete structures in the inland environment were for use at different stages of the concrete construction project. These models can be applicable at three different levels, depending on the type and quality of information available. Thus, the models can be applicable at the planning, design and/or construction stage of proposed concrete structures as well as for maintenance and repair schedules for existing structures.

The first level model (Models 1 and 2) is the mixture design model to be used at the planning stage, where only basic information on the mixture proportions of the concrete to be used is known. Also known are the binder types used in the concrete, the likely curing duration and the exposure condition. This level of model is able to estimate the rate and thus depth of carbonation given the mixture proportion, curing duration and the nature of exposure. The outcome of this model will assist the designer/contractor with the steel reinforcement cover depth determination for the proposed reinforced concrete structures for a given design service life.

The second level model (Models 3 to 12), which are build up on the first level model is for use at the planning stage for estimation of the concrete physical and/or chemical parameters, given the concrete depth of carbonation and design service life. Similarly, the second level models can be used for maintenance and repair scheduling or for the estimation of the concrete residual service life given its physical and/or chemical parameters. The third level model (Models 13 and 14)

is similar in application to the second level model and consists of the concrete accelerated carbonation characteristics and/or chemical parameters as input variables. The developed models in this study can also be used for quality control of concrete on construction sites.

This chapter has analysed, discussed and presented the results of the multiple linear regression analysis between the natural carbonation rate of the concretes (as the response variable) and the concrete mixture design parameters and the early-age characterisation parameters (as the predictor variables). Included in the predictor variables are the dummy variables for the binder types used in making the concrete, curing duration of the concrete as well as the concrete exposure conditions. These variables help improve the predictability and reliability of the natural carbonation rate models. The individual carbonation rate prediction models were presented and their range of applicability was described. In the next chapter, the predicted carbonation from the developed prediction models will be assessed by comparisons with historically measured carbonation from carbonation studies obtained from the literature.

Chapter References

Alexander, M., Mackechnie, J., & Yam, W. (2007). *Carbonation of concrete bridge structures in three South African localities*. Cement and Concrete Composites, 2*9*(10), 750-759.

Ballim, Y. (1994). *Curing and the durability of concrete.* PhD Thesis, University of the Witwatersrand, Johannesburg.

Berry, W. D., & Feldman, S. (1985). *Multiple regression in practice*: Sage.

Bertolini, L. (2008). *Steel corrosion and service life of reinforced concrete structures.* Structure and Infrastructure Engineering, 4(2), 123-137.

Bertolini, L., Elsener, B., Pedeferri, P., Redaelli, E., & Polder, R. B. (2013). *Corrosion of steel in concrete: prevention, diagnosis, repair*: Wiley. com.

Bruno, S. (2010). *Modelling the carbonation of concrete usinf early age oxygen permeability index tests.* MSc University of Cape Town, Cape Town.

Chatterjee, S., & Hadi, A. S. (2009). *Sensitivity analysis in linear regression* (Vol. 327): Wiley. com.

Chatterjee, S., & Hadi, A. S. (2013). *Regression analysis by example*: John Wiley & Sons.

Cohen, J., & Cohen, P. (1975). *Applied multiple regression/correlation analysis for the behavioral sciences*: Lawrence Erlbaum.

Dhir, R. K., Hewlett, P. C., Byars, E. A., & Bai, J. P. (1994). *Estimating the durability of concrete in structures*. Concretes Society, London, Vol. 28, No. 6, pp. 25-30.

Douglas, M. C., Peck, E. A., & Vining, G. G. (2012). *Introduction to linear regression analysis* (Vol. 821): John Wiley & Sons.

Fox, J. (1984). *Linear statistical models and related methods: With applications to social research*: Wiley New York.

Fox, J. (1990). *Describing univariate distributions, Modern Methods of Data Analysis*, (Newbury Park, CA: Sage Publications, 1990), 58-125.

Gaylard, P., Ballim, Y., & Fatti, L. (2013). *A model for the drying shrinkage of South African concretes*. Journal of the South African Institution of Civil Engineering, *55*(1), 45-59.

Gaylard, P. C. (2011). *Statistical modelling of the shrinkage behaviour of South African concretes.* Faculty of Science, University of the Witwatersrand, Johannesbourg.

Jean-Marie, K. O. (2011). *Landuse Impacts on Water Resources Management in a Data-Scarce Watershed of the Equatorial Nile: Case Study of the Semliki.* PhD Thesis, University of the Witwatersrand, Johannesburg.

Kmenta, J. (1971). *Elements of econometrics*: Macmillan New York.

Lee, J. J., & Tu, Z. N. (1997). *A versatile one-dimensional distribution plot: the BLiP plot*. The American Statistician, *51*(4), 353-358.

Mackechnie, J. R. (1996). *Predictions of reinforced concrete durability in the marine environment.* PhD thesis, University of Cape Town, Cape Town.

Papadakis, V. G., Vayenas, C. G., & Fardis, M. N. (1991). *Experimental investigation and mathematical modeling of the concrete carbonation problem*. Chemical Engineering Science, 46(5), 1333-1338.

Parrott, L. (1987). *A review of carbonation in reinforced concrete*.

Parrott, L. J. (1994). *Design for avoiding damage due to carbonation-induced corrosion*, Durability of Concrete- 3rd International Conference, Nice, France 1994, pp.283-298.

Snedecor, G. WG COCHRAN., (1980). *Statistical Methods*: The Iowa State University Press, Ames.

Tutti, K. (1982). *Corrosion of steel in concrete*. Swedish Cement and Concrete Institute: CIB, Research Report.

Wierig, H. (1984). *Longtime studies on the carbonation of concrete under normal outdoor exposure.* Proceedings of the RILEM, Hannover University, 239-249.

CHAPTER 6

COMPARISON OF CARBONATION PREDICTIONS FROM DEVELOPED MODELS WITH HISTORICALLY MEASURED CARBONATION

6.1 Introduction

The carbonation predictions from the developed models in Chapter 5 were compared with historically measured carbonation data, in this chapter. The historical carbonation data obtained from the literature consisted of carbonation depth measurements and rate determinations from carbonation studies of concrete exposed to an inland environment. The comparison process was hence completely independent of the model formulation, since the data used were obtained from carbonation studies with different concrete making materials and processes as well as mixture proportions. The environmental exposure conditions are however similar, since the studies were carried out in the same inland environment used in the development of the models. Thus, the comparison can be made on the basis of material and processing influence on the rate of carbonation.

The carbonation data obtained from the literature were however limited to the physical characterisation (compressive strength, oxygen permeability index, water sorptivity and accelerated carbonation rate) of the concretes as most of the carbonation studies do not report the concrete chemical composition or the mixture design parameters. Variability and randomness in the test conditions for laboratory studies as well as in the processing and environmental exposure conditions for data obtained from laboratory or existing structures pose challenges to the process in terms of realistic and direct comparison of the measured and predicted carbonation. With the above mentioned limitations in the obtained data, comparative analyses for some of the developed models, which require the mixture design and or chemical composition of the concrete at early-ages, could

not be performed. However, the comparison was useful in terms of the reliability and confidence of the predictions from the developed models. This chapter then concludes with the possible reasons for differences noted in the measured and predicted carbonation.

6.2 Comparison of Carbonation Predictions from Developed Models and Measured Carbonation

Numerous carbonation studies on concrete in the medium- and long-term have been conducted for both inland and marine exposure conditions in South Africa (see Section 2.4.3). These studies were either on laboratory concrete samples or on existing concrete structures. However, only studies that were relevant to the developed models in terms of the concrete making materials, and processing as well as the environmental exposure conditions were assessed. Among these were studies by Ballim, (1994); Ananmalay, (1996); Ballim and Lampacher, (1996); Lampacher, (2000) and Yam, (2004). While carbonation studies by Ballim and Ananmalay were on laboratory made concrete samples exposed to the inland environment of South Africa, similar studies by Ballim and Lampacher, Lampacher and Yam were on existing concrete structures in the inland environment of South Africa.

These carbonation studies are presented in terms of their mixture design parameters, early-age characterisation parameters and the medium - and/or long - term durability performance in terms of the rate or depth of carbonation in concrete. The carbonation results obtained from the above studies that are similar in terms of concrete making materials, processing and exposure conditions are compared to the predicted results obtained from the developed models on the basis of the rate or depth of carbonation in order to estimate the reliability and confidence of the developed models.

6.2.1 Ballim's data

Ballim (1994), in his carbonation study, produced concretes with different binder types and w/b ratios, and exposed them to varying initial water curing periods. The objective of the investigation among others was to quantify the effect of early-age curing on the durability performance of different concrete strength grades. Thus, the oxygen permeability, and water sorptivity of the concretes were measured after the initial moist curing periods at 28 days and again at 10 months after casting with the intention of monitoring the potential durability of the concrete while the compressive strength was assessed at only 28 days.

The carbonation depths of companion concretes were measured after 10 and 20 months of exposure to a controlled laboratory condition in the inland environment of Johannesburg, with the aim of quantifying the durability performance of the concretes. Presented in Table 6.1 are the mixture design and early-age characterisation parameters taken from Ballim's study, while Table 6.2 shows the carbonation depth data and the corresponding carbonation rates (based on a square-root relationship) of companion concretes exposed to the controlled laboratory conditions. Although, the exposure condition was controlled, the results from Ballim's study are relevant for comparison to the predictions made by the relevant models developed in this study.

Table 6.1: Mixture design and early-age characterisation parameters of concretes (taken from Ballim, 1994)

Binder types	Mixtures design parameters		28 days early-age characterisation parameters			
	w/b	Cement content (kg/m^3)	f_c (MPa)	Oxygen permeability		*WS* ($mm/hr^{0.5}$)
				Measured *K* ($x10^{-10}$ m/s)	Calculated *OPI*	
100% CEM I	0.67	308	39.6	0.74	10.1	10.1
	0.56	378	47.7	0.73	10.1	9.3
	0.47	441	59.4	0.60	10.2	8.5
70/30 CEM I /FA	0.59	230	30.3	4.50	9.3	11.7
	0.49	273	45.3	0.39	10.4	7.9
	0.41	316	58.6	0.29	10.5	7.4
50/50 CEM I /GGBS	0.63	164	37.1	3.90	9.4	7.7
	0.51	197	39.4	0.59	10.2	5.5
	0.43	230	53.2	2.20	**9.4***	**6.7***

* Value did not follow trend

Table 6.2: Companion concrete carbonation depths and rates (taken from Ballim, 1994)

Binder type	*w/b*	Moist curing period (day)	Carbonation depth/rate for the concretes			
			Depth at 10 months (mm)	Rate at 10 months (mm/√mths.)	Depth at 20 months (mm)	Rate at 20 months (mm/√mths.)
100% CEM I	0.67	1	13.5	4.24	-	-
		3	10.5	3.32	-	-
		7	7.0	2.25	-	-
		28	5.0	1.61	-	-
	0.56	1	9.5	3.07	-	-
		3	7.0	2.18	-	-
		7	3.0	1.01	-	-
		28	2.0	0.63	-	-
	0.47	1	7.0	2.21	-	-
		3	5.5	1.68	-	-
		7	3.0	0.92	-	-
		28	1.5	0.41	-	-
70/30 CEM I /FA	0.59	1	13.5	4.27	-	-
		3	11.5	3.64	-	-
		7	10.5	3.32	-	-
		28	6.50	2.06	-	-
	0.49	1	11.5	3.64	20.5	4.63
		3	7.0	2.21	14.0	3.13
		7	5.0	1.58	12.5	2.84
		28	4.0	1.20	10.0	2.24
	0.41	1	10.5	3.29	19.0	4.24
		3	7.0	2.18	13.0	2.91
		7	5.5	1.68	9.5	2.17
		28	2.5	0.79	6.0	1.34
50/50 CEM I /GGBS	0.63	1	18.5	5.79	28.0	6.26
		3	14.0	4.36	23.5	5.30
		7	10.5	3.32	19.0	4.25
		28	6.0	1.96	10.0	2.24
	0.51	1	13.5	4.30	26.5	5.97
		3	9.5	3.04	17.0	3.80
		7	7.5	2.31	14.0	3.11
		28	4.5	1.49	7.0	1.56
	0.43	1	12.0	3.79	21.5	4.76
		3	8.0	2.53	11.5	2.52
		7	4.0	1.26	7.5	1.72
		28	1.5	0.47	6.5	1.50

- No measurement available

From the presented carbonation results in Tables 6.1 and 6.2, it is evident that only Models 1, 4, 7, and 8 can be assessed using the measured and calculated carbonation depths and rates from Ballim's study. This is because the input parameters for these models are mixture design, and early-age compressive strength, oxygen permeability index and water sorptivity values respectively. The comparison will however be made for the different concrete types (*CEM I, CEM I/FA* and *CEM I/GGBS* concretes) and curing periods (1, 3, 7 and 28 days) but for the 0.56, 0.49 and 0.51 w/b ratios respectively. The prediction models mentioned above were then evaluated on the basis of input parameters in Table 6.1, 7 days moist curing period and an indoor exposure conditions. Table 6.3 presents the relevant measured depths/rates of carbonation taken from Ballim's study and the equivalent predicted rates and depths of carbonation by the developed models as stated above.

Table 6.3: Comparison of measured and calculated depths and rates and predicted rates/depths by the developed models

Binder type	*w/b*	Curing period (days)	Measured depth and rate of carbonation taken from Ballim's study				Predicted rate (mm/√yrs.) and depth (mm) of carbonation by the developed models							
			Depth, mm at 10mths	Rate, mm/√mths. At 10mths	Depth, mm at 20mths	Rate, mm/√mths. At 20mths	Model 1		Model 4		Model 7		Model 8	
							Rate	Depth	Rate	Depth	Rate	Depth	Rate	Depth
100% CEM I	0.56	1	9.5	3.07	-	-	**5.3**	10 month =16.8 20 month =23.7	**4.1**	10 month =13.0 20 month =18.3	**4.0**	10 month =12.6 20 month =17.9	**5.2**	10 month =16.4 20 month =23.3
		3	7.0	2.18	-	-								
		7	**3.0**	**1.01**	-	-								
		28	2.0	0.63	-	-								
70/30 CEM I /FA	0.49	1	11.5	3.64	20.5	4.63	**6.7**	10 month =21.2 20 month =30.0	**4.5**	10 month =14.2 20 month =20.1	**3.2**	10 month =10.1 20 month =14.3	**4.9**	10 month =15.5 20 month =21.9
		3	7.0	2.21	14.0	3.13								
		7	**5.0**	**1.58**	**12.5**	**2.84**								
		28	4.0	1.20	10.0	2.24								
50/50 CEM I /GGBS	0.51	1	13.5	4.30	26.5	5.97	**8.4**	10 month =26.6 20 Month =37.6	**5.6**	10 month =17.7 20 month =25.0	**4.5**	10 month =14.2 20 month =20.1	**4.6**	10 month =14.5 20 month =20.6
		3	9.5	3.04	17.0	3.80								
		7	**7.5**	**2.31**	**14.0**	**3.11**								
		28	4.5	1.49	7.0	1.56								

- No measurement available

Although the exposure conditions for the two studies are similar, the carbonation result comparisons presented in Table 6.3 show that the developed models generally overestimated the carbonation rates and depths for all the concrete types (see Figures in bold). However, the trends in the carbonation data are similar in both studies, with the order of performance being: - *CEM I* < *CEM I/FA* < *CEM I/GGBS*. The predictions from the developed models however agree well with one another, with the mixture design model (Model 1) showing greater over-estimation for blended concretes.

The reasons for the similarity in the prediction by the developed models is probably due to the fact that they are all based on similar early-age characteristics of the concretes. A discussion on the possible reasons for the differences in the measured carbonation from Ballim's study and the predicted carbonation by the developed models will be provided in the section analysing the differences in the measured and model predicted carbonations.

6.2.2 Ananmalay's data

Ananmalay (1996) compared the strength and durability performance of concrete made with 100% *CEM I* and 90/10 *CEM I/CSF* binders, different w/b ratios and cement content. The concretes were treated to varying initial water curing periods (1, 3, 7 and 28 days) and characterised in terms of compressive strength, oxygen permeability and water sorptivity at 28 days. Companion concretes were exposed to accelerated carbonation, controlled indoor and natural outdoor conditions in the inland environment of South Africa after each initial moist cured period. The durability performances of the exposed concretes in terms of depth of carbonation were obtained at different time interval. Presented in Table 6.4 is the mixture design and early-age characterisation parameters taken from Ananmalay's study, while Table 6.5 shows the carbonation depth data for all the studied exposure conditions.

Table 6.4: Mixture design and early-age characterisation parameters of concretes (taken from Ananmalay, 1996)

Binder types	Mixture design parameters		28 days early age characterisation parameters			
	w/b	Cement content (kg/m^3)	f_c (MPa)	Permeability		*WS* ($mm/hr^{0.5}$)
				Measured *K* ($x10^{-10}$ m/s)	Calculated *OPI*	
100% CEM I	0.80	256	21.2	1.34	9.9	10.98
	0.53	390	47.8	0.44	10.4	8.44
	0.36	574	69.8	**0.49***	**10.3***	**9.45***
90/10 CEM I/CSF	0.91	203	23.1	3.99	9.4	10.88
	0.59	314	44.6	2.72	9.6	8.25
	0.43	424	74.6	0.46	10.3	**8.67***

*Value did not follow trend

Table 6.5: Companion carbonation depth results for concrete made with properties shown in Table 6.4 (taken from Ananmalay, 1996)

Binder type	*w/b*	Moist curing period (day)	Carbonation depth for the concretes (mm)						
			Accelerated exposure (days)	Controlled indoor exposure (days)				Natural outdoor exposure (days)	
			7	80	210	365	1095	365	1095
100% CEM I	0.80	1	26	10	12	18	25	-	-
		3	22	7	10	15	18	7	12
		7	18	6	9	13	16	-	-
		28	14	3	6	10	14	-	-
	0.53	1	14	6	7	*	12	-	-
		3	13	4	6	*	10	2	4
		7	11	3	4	**1****	**10****	-	-
		28	9	1	3	*	6	-	-
	0.36	1	7	4	5	**5****	7	-	-
		3	5	2	3	*	5	1	**1****
		7	3	1	2	2**	3	-	-
		28	1	**1****	**2****	*	**3****	-	-
90/10 CEM I /CSF	0.91	1	28	10	18	*	28	-	-
		3	25	9	15	17	25	9	16
		7	23	7	12	*	**26****	-	-
		28	16	4	7	9	17	-	-
	0.59	1	13	9	*	*	14	-	-
		3	**13****	5	7	**7****	11	4	8
		7	12	4	6	7	10	-	-
		28	9	2	4	5	9	-	-
	0.43	1	12	4	7	*	12	-	-
		3	7	2	3	**3****	6	1	5
		7	5	1	2	*	5	-	-
		28	3	0	1	**1****	**6****	-	-

* Results discarded by author

- No measurement available

** Values did not follow trend

From the presented carbonation results in Table 6.4 and 6.5, it is evident that only carbonation predictions from Model 1, 4, 7, 8 and 14 can be assessed using the measured carbonation depths results from Ananmalay's study. This is because the input parameters for these models are mixture design, early-age compressive strength, oxygen permeability index, water sorptivity and accelerated carbonation depth values respectively. Although the results for the controlled indoor exposure given in Table 6.5 contains many anomalous results the comparison will still be made for the *CEM I* and *CEM I/CSF* concrete types and curing periods (1, 3, 7 and 28 days) but only for the 0.53 and 0.59 w/b ratios concretes respectively. This will provide a useful idea of the material and processing effects on the rate of carbonation.

The relevant carbonation depth results for the controlled indoor exposure for *CEM I* and *CEM I/CSF* concretes shown in Table 6.5 are presented graphically in Figures G1 to G8 in Appendix G. These plots show the relationship between the carbonation depth of the concrete and the equivalent square root of exposure period. As stated in Section 4.7.1 in Chapter 4 and in agreement to study by Yam, (2004) and Alexander et al., (2007), the formulation of Equation 4.1 in Chapter 4 was applied to Figures G1 to G8 in order to determine the rate of carbonation for the different concrete types. Similarly, Equation 4.1 was applied to the accelerated carbonation depth for the quantification of the accelerated carbonation rate of the concretes.

Table 6.6 presents the calculated rate of carbonation for the controlled indoor exposure from the measured carbonation depth given in Table 6.5 as obtained from Figures G1 to G8. Also shown on the table are the predicted rates of carbonation by the relevant developed models using the information given in Table 6.4, 7 day moist curing period as well as an indoor exposure condition.

Table 6.6: Comparison of calculated rate of carbonation for the controlled indoor exposure and predicted rate of carbonation by the developed models

Binder type	*w/b*	Moist curing period (day)	Calculated rate of carbona-tion (mm/ √yrs.)	Predicted rate of carbonation by the developed models (mm/√yrs.)				
				Model 1	Model 4	Model 7	Model 8	Model 14
100% CEM I	0.53	1	5.1	**4.7**	**4.1**	**3.0**	**4.8**	**2.4**
		3	4.9					
		7	**6.0***					
		28	4.0					
90/10 CEM I /CSF	0.59	1	4.2*	**6.9**	**4.7**	**6.0**	**5.1**	**2.4**
		3	4.9*					
		7	**4.9***					
		28	5.8*					

* Results seem anomalous

Table 6.7 presents the rate of carbonation for outdoor exposed condition as predicted by the developed models using Ananmalay's mixtures design and early-age characterisation parameters. The rates of carbonation presented in Table 6.7 were used for calculating the depth of carbonation at 1 and 3 years, as given on Table 6.8. Table 6.8 also, shows comparisons of the measured depth of carbonation obtained from Ananmalay's study for the outdoor condition and the predicted depths of carbonation by the models developed in this study.

Table 6.7: Predicted rate of carbonation by the developed models for the outdoor exposed conditions

Binder type	*w/b*	Predicted rate of carbonation (mm/√yrs.) by the developed models using Ananmalay's data's				
		Model 1	Model 4	Model 7	Model 8	Model 14
100% CEM I	0.53	2.7	2.0	0.9	2.8	0.4
90/10 CEM I /CSF	0.59	4.8	2.6	3.9	3.0	0.4

Table 6.8: Comparison of measured depth of carbonation for outdoor exposed concretes and predicted depths of carbonation for outdoor exposed condition by the developed models

Binder type	*w/b*	Moist curing period (day)	Measured depth of carbonation (mm)		Predicted depth of carbonation (mm) by the developed models									
			1 year	3 years	Model 1		Model 4		Model 7		Model 8		Model 14	
					1 yrs.	3 yrs.	1 yrs.	3 yrs.	1 yrs.	3 yrs.	1 yrs.	3 yrs.	1 yrs.	3 yrs.
100% CEM I	0.53	3	**2**	4	**2.7**	4.6	**2.0**	3.4	**0.9**	1.6	**2.8**	4.8	**0.4**	0.7
90/10 CEM I /CSF	0.59	3	**4**	8	**4.8**	8.3	**2.6**	4.5	**3.9**	6.8	**3.0**	5.2	**0.4**	0.7

Despite the fact that the indoor exposure condition used by Ananmalay is conducive for greater carbonation, the carbonation predictions from the developed models are within a similar range as Ananmalay's study. However, the developed models mostly overestimate the extent of carbonation. The accelerated carbonation model (Model 14) underestimates the carbonation for all concrete types while the permeability model (Model 7) underestimate the carbonation for the plain concrete only. Importantly, the trends in the carbonation data in both studies are similar in the order of performance - *CEM I* < *CEM I/CSF*.

Comparing the predicted rate of carbonation results from the developed models presented in Table 6.7, the accelerated carbonation model (Model 14) presented the lowest rate of carbonation for the outdoor exposure condition as did the permeability model (Model 7) for the plain concrete only. The reasons for the similarity in the carbonation prediction across the developed Models 1, 4, 7, and 8 could be due to the fact that they are all based on similar early-age characteristics of the concretes. The probable reason for the under-estimation by the accelerated carbonation model can be attributed to the fact that the input parameter used was the accelerated carbonation rate obtained from the 7 days accelerated carbonation depth whereas the developed model was based on accelerated carbonation depth at 28 days.

The comparison of the measured and predicted depth of concrete carbonation for the outdoor exposure condition given in Table 6.8 shows that the predictions by the developed models, in most cases, over-estimate the depth of carbonation for all concrete types except for the accelerated carbonation model (Model 14) prediction. Carbonation predictions from the permeability model (Model 7) for plain concrete underestimate the carbonation greatly. The reason for this consistent under estimation by the permeability model is not clear at this point and will require further investigation. A discussion of the reasons for the difference in the measured carbonation from Ananmalay's study and the carbonation prediction

from the developed models will be provided in the section analyzing the differences in the measured carbonation and the model predicted carbonation.

6.2.3 Ballim and Lampacher's data

Ballim and Lampacher (1996) investigated the long-term effects of carbonation on 10 major bridge structures situated in the inland environment of Johannesburg, South Africa. The purpose of the investigation was to quantify the extent of carbonation of the concrete structures in order to estimate the corrosion initiation time. The possibility of a relationship between the permeation properties of the concrete and the depth of carbonation was also assessed by the authors. Cores were obtained from the selected concrete structures and tested for carbonation depth, oxygen permeability and water sorptivity. However, only the depth of carbonation values and the respective rates of carbonation were presented for each structure by the authors as reproduced in Table 6.9.

Table 6.9: Carbonation depths/rates results for the concrete cores obtained from the bridge structures (taken from Ballim and Lampacher, 1996)

Structure (Year of construction)	Exposure condition	Carbonation depth (mm)	Carbonation rate (mm/√year)
Harrow/Saratoga Bridge (1962)	Exposed/sheltered	15 34 >35 18	2.7 6.2 >6.4 3.3
Goch St South Bridge (1965)	Exposed	14 10 18 **2***	2.7 2.0 3.5 0.4
Goch St North Bridge(1966)	Exposed	20 **28*** 14 **10*** 16 15	4.0 5.5 2.7 2.0 3.3 2.9
Empire Rd Bridge (1968)	Sheltered	9 11 12 11 12	1.8 2.2 2.6 2.4 2.6
St Andrews Rd Bridge (1968)	Sheltered/exposed	2 15 4 3	0.4 2.9 0.9 0.5
Rissik St Off/R M2E Bridge (1968)	Exposed	20 30 **41*** 35 >20 >20	>4.2 6.2 8.4 7.1 >4.2 >4.2
M2 E/W Bridge (Loveday St) (1968)	Sheltered	35 25 20 19	7.1 5.1 4.2 4.0
1st Ave Bridge (1971)	Exposed/sheltered	13 17 20 15	2.9 3.7 4.4 3.3
Corlett Drive Bridge (1972)	Exposed/ sheltered	8 20 24 23	1.6 4.6 5.3 5.3
Booysens Rd On/Off Ramp/Bridge (1973)	Exposed	**30*** 19 19 17	6.9 4.4 4.4 3.8

*Values did not follow trend

Statistical analysis of the data on Table 6.9 by the authors gives an average carbonation rate of 3.76 mm/√year Thus, Equation 6.1 shows the proposed prediction model by Ballim and Lampacher.

$$d_c = 3.76\sqrt{t} \qquad 6.1$$

Where,

d_c = depth of carbonation (mm)

3.76 = carbonation rate (mm/√year)

t = exposure time (year)

Of note is the fact that the proposed model makes no distinction of exposure condition and also the carbonation depth data given in Table 6.9 shows a wide scatter. The wide scatter arises not only from the fact that concrete itself is a variable material but also from the variability and randomness of micro-climate surrounding the concrete structures as well as the exposure conditions of the locations where cores were obtained. However, some of the measured depth of carbonation can be considered anomalous (as indicated with an asterisk) and an outlier and was neglected for the purpose of this comparison.

Based on historical records (bridge drawings), the authors state that the compressive strength for the bridge structures ranged between 20 MPa and 40 MPa, and that the minimum observed depth of cover was 25 mm for the structures. Mixture design and early-age characterisation parameters in terms of the permeation properties were however not presented by the authors for the investigated structures. Two exposure conditions were used in the description of the test area where the concretes cores were obtained– exposed to sun, rain and wind and sheltered from sun and rain. The binder type used in the bridge structures was assumed to be plain Portland cement.

Clearly for this study and in consideration of the available data, only the developed Models 3 and 4 with compressive strength of concrete as input parameter can be compared with the carbonation depth data from the Ballim and Lampacher study. Thus, in the calculation of the rate of carbonation by the developed carbonation models, 7 days moist curing periods was used as the probable curing duration as well as outdoor sheltered and exposed conditions. An average strength of 30 MPa was used based on the given compressive strength of the structures (20 – 40 MPa) and since in construction, the mean concrete strength would be between 5 and 10 MPa higher than the specified strength. The curing period was assumed to be 7 days since this is a "best" case curing period for most existing structures.

Applying the above information to the developed carbonation models, a rate of carbonation of 8.2 and 5.1 mm/√year was obtained from Model 3 for the outdoor sheltered and exposed conditions respectively. While for Model 4, rates of carbonation of 8.4 and 5.2 mm/√year were obtained for the outdoor sheltered and exposed conditions respectively. To compare the predictive ability of the developed models, the obtained rates of carbonation were fitted to the square root equation as shown in Equations 6.2 to 6.5. And in order to assess and compare the predicted depth of carbonation at various exposure times with carbonation prediction from Ballim and Lampacher model, Figures 6.1 and 6.2 presents the carbonation predictions by the models.

$D = 8.2\sqrt{t}$ (Model 3, outdoor sheltered) 6.2

$D = 5.1\sqrt{t}$ (Model 3, outdoor exposed) 6.3

$D = 8.4\sqrt{t}$ (Model 4, outdoor sheltered) 6.4

$D = 5.2\sqrt{t}$ (Model 4, outdoor exposed) 6.5

Table 6.10 presents comparison between measured depth of carbonation for some selected concrete structures taken from the Ballim and Lampacher study and the equivalent predicted depths of carbonation by the Model 3 and 4.

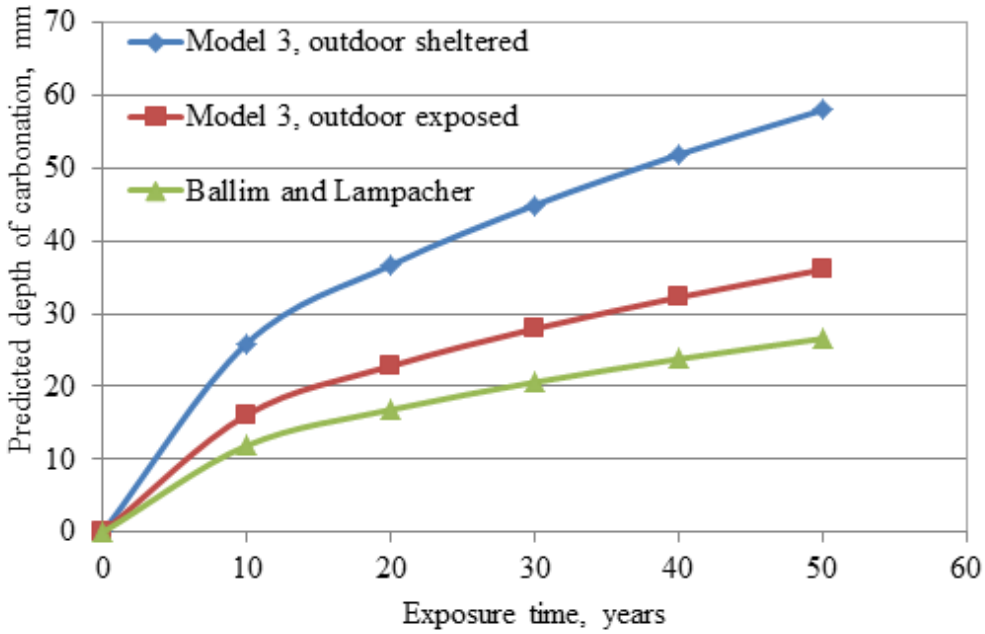


Figure 6.1: Comparison of predicted carbonation of Model 3 (outdoor sheltered and exposed) and measured carbonation

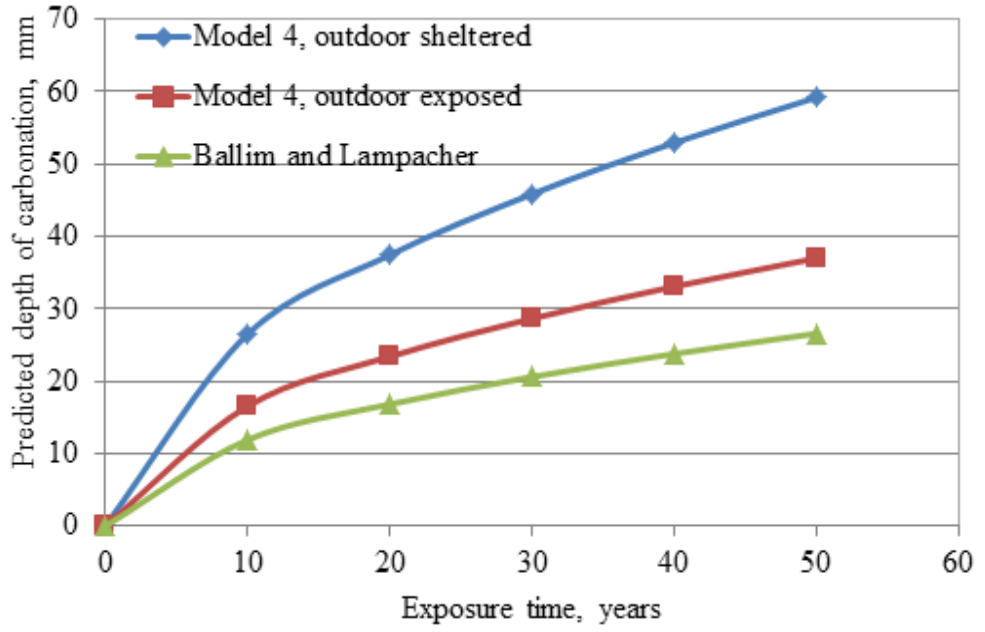


Figure 6.2: Comparison of predicted carbonation of Model 4 (outdoor sheltered and exposed) and measured carbonation

Table 6.10: Comparison of measured depths of carbonation and predicted depth of carbonation by the developed models

Structure/year of construction/exposure condition	Age in 1996	Measured carbonation depth (mm) as at 1996	Predicted carbonation depth (mm) using the ages given in column two			
			Model 3		Model 4	
			Outdoor sheltered	Outdoor exposed	Outdoor sheltered	Outdoor exposed
Goch St South Bridge (1965) Exposed	31	14 10 18 2*	46	28	47	29
Rissik St Off/R M2E Bridge (1968) Exposed	28	20 30 41* 35 >20 >20	43	27	44	28
Booysens Rd On/Off Ramp/Bridge (1973) Exposed	23	30* 19 19 17	39	24	40	25
Empire Rd Bridge (1968) Sheltered	28	9 11 12 11 12	43	27	44	28
Harrow/Saratoga Bridge (1962) Exposed/sheltered	34	15 34 >35 18	48	30	49	30

*Values did not follow trend

From Figures 6.1 and 6.2, it can be noted that both the developed models overestimate the depth of carbonation, with the overestimation being more for the outdoor sheltered condition. This is probably due to the fact that the carbonation data used in the derivation of their model were obtained from exposed locations as can be noted in Table 6.9. A similar trend was also observed between the predicted and measured depth of carbonation as presented in Table 6.10. A discussion on the possible reasons for the overestimation of the carbonation by the developed models will be provided in the section analysing the differences in the predictions in measured and model predicted carbonation.

6.2.4 Lampacher's data

In a similar investigation to Ballim and Lampacher study, Lampacher (2000) carried out more comprehensive investigation on the carbonation of existing concrete structures (buildings and bridges) in Johannesburg, South Africa. In his study, 15 major concrete structures ranging from 19 to 70 years in age were characterised for permeation, chemical and mechanical properties. The durability performances of these structures in terms of their depth of carbonation were also quantified. The intention of Lampacher's study was to assess the durability performance of these existing concrete structures in the inland environment with the aim of predicting their residual service life, in order that maintenance, rehabilitation and replacement programs can be planned and the associated cost implications optimized.

Compressive strength, oxygen permeability, water sorptivity, covercrete absorption, static elastic modulus and dynamic elastic modulus tests were performed on cores obtained from the structures as well as on the structures themselves. Also measured was the cement content of the core samples and their depths of carbonation. Presented in Table 6.11 are the obtained results from Lampacher's study. The compressive strength results presented is however the normalized 28 days strength.

Table 6.11: Concrete characterisation results (taken from Lampacher, 2000)

Structure	Age (Yrs.)	Binder types	C (kg/m^3)	f_c (MPa)	K (x10^{-10})	WS (mm/ hr$^{0.5}$)	Measured carbonation rate (mm/√yr.)
Yale Telescope	70	OPC	312	35.3	2.00E-09	2.33	1.91
Harrow/ Saratoga	30	OPC	299	29.1	1.00E-09	4.44	4.65
Goch South	27	OPC	330	44.1	3.00E-10	2.37	2.15
Goch North	26	OPC	326	47.7	3.00E-10	5.48	3.40
N4 Witbank	27	OPC/ Slag		43.8	1.00E-10	13.58	3.59
Empire	24	OPC	407	61.2	2.00E-09	6.47	2.32
St Andrew	24	OPC	332	53.4	5.00E-10	3.38	1.18
Rissik	24	OPC	279	35.8	7.00E-09	8.21	5.72
M2 E/W	24	OPC	306	20.4	7.00E-10	8.22	5.10
Ponte	23	OPC/ Slag		52.7	3.00E-09	9.64	1.40
1st Ave	21	OPC	375	36.9	2.00E-10	4.64	3.58
Diepsloot 2	20	OPC	350	43.8	2.00E-10	3.53	3.27
Diepsloot 3	20	OPC	343	54.4	1.00E-10	2.64	2.18
Corlett	20	OPC	455	37.2	1.00E-09	4.45	4.20
Booysens	19	OPC	306	38.7	6.00E-10	3.79	4.88

Statistical analysis of the obtained carbonation depth data by the author gives an average carbonation rate of 3.16 mm/√years. Fitting this rate of carbonation into the square-root of time relationship gives the prediction model proposed by Lampacher as shown in Equation 6.6.

$$d_c = 3.16\sqrt{t} \qquad 6.6$$

Where,

d_c = depth of carbonation (mm)

3.16 = carbonation rate (mm/√years)

t = exposure time (years)

From the carbonation results obtained from Lampacher's study, only the developed Models 3 and 4 that require compressive strength as input, can be assessed. The calculated average 28 days compressive strength for the concrete structures investigated by Lampacher is 42.3 MPa. As stated before, since in construction, mean concrete strength would be 5 to 10 MPa higher than specified strength, a concrete compressive strength of 32 MPa was used as input in Models 3 and 4. For exposure and curing duration, an outdoor exposed condition was used since it is the worst case for carbonation-induced reinforcement corrosion while 7 days moist curing was used for the curing period as most structures in practice are rarely given more than 7 days curing. Thus, 7 days curing duration is a "best" case for most existing concrete structures.

Applying the above details to Models 3 and 4, rates of carbonation of 5.1 and 5.2 mm/√year were respectively obtained for the outdoor exposed conditions. In order to compare the predictive ability of the developed models, the rate of carbonation from this study were fitted to the square-root of time equation as shown in Equations 6.7 and 6.8. And to compare the predicted depth of carbonation at various exposure times with that obtained from Lampacher's model, Figure 6.3 presents this comparison.

$D = 4.8\sqrt{t}$ (Model 3, outdoor exposed condition) 6.7

$D = 4.9\sqrt{t}$ (Model 4, outdoor exposed condition) 6.8

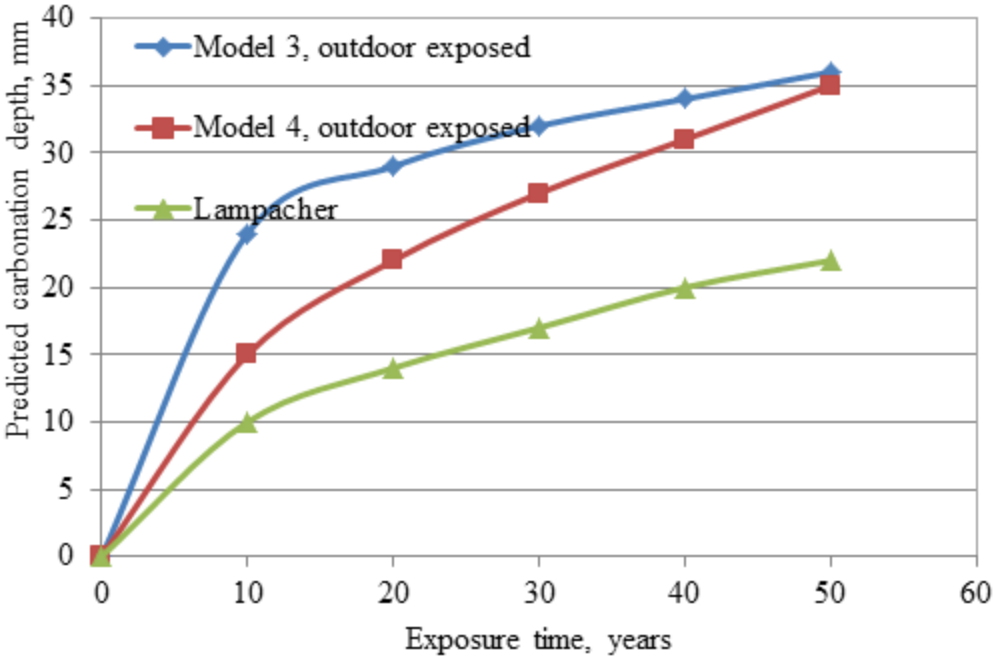


Figure 6.3: Comparison of predicted carbonation of Models 3 and 4 (outdoor exposed) and measured carbonation

From Figure 6.3, it can be noted that the developed models both overestimated the depth of carbonation, as was also noted in Ballim and Lampacher results. Again, a discussion on the possible reasons for the overestimation of the carbonation by the developed models will be provided in the section analysing the differences in the predictions in measured and developed model predicted carbonation.

6.2.5 Yam's data

In a more thorough carbonation study on existing concrete structures, Yam (2004) investigated the rates of carbonation of reinforced concrete bridges in three localities in South Africa. The aim of his study was to develop prediction models for use in maintenance and repair planning, as well as cover depth determination for existing concrete structures. As stated before, only the data that are of relevance to this study will be presented for use in the process of comparison. Thus, only the carbonation data on 30 in-service bridges in the inland

environment of Johannesburg, South Africa age between 11 and 76 years, investigated by the author will be discussed in this study.

Measurements of carbonation depth using phenolphthalein solution sprayed on cores or wedges obtained from the concrete structures were performed. Yam also used carbonation data on concrete structures in the inland environment of South Africa obtained by Ballim and Lampacher (1996). The values for the measured depth of carbonation are also presented in these studies. These carbonation depth values, locations of the cores and compressive strength are available in the original study by Yam (2004), as well as in the published article by Alexander et al. (2007). Because of the wide scatter of the obtained carbonation depth results, the author grouped the data into exposure conditions and concrete grade to minimize the scatter and to gain better understanding of the carbonation rate values. Following a series of statistical analysis by the author on the depths of carbonation, the prediction models for inland environment presented in Table 6.12 were obtained.

Table 6.12: Carbonation prediction models for the inland environment taken from Yam (2004); Alexander et al. (2007)

Locality	Strength grade	Exposure condition	
		Exposed	Sheltered
		Prediction model	
Johannesburg	Grade 30	$d_c = 3.76t^{0.5}$	$d_c = 2.99t^{0.5}$
	Grade 35	$d_c = 3.20t^{0.5}$	$d_c = 3.95t^{0.5}$

Concrete strength grades of the assessed bridge elements were inferred by considering bridge practice in other localities within the country with known strength grades. Information from bridge drawings, measured core strength of bridge elements, similar elements with known strengths or from knowledge of strength based on common bridge design and construction practice was used in

estimating the “true” 28 day compressive strength for the structures assessed by the author. Since concrete strength changes with time and for meaningful comparisons of the rate of carbonation, the author normalized all strength values to 28 days, using standard procedures as given in Fulton (1977).

The prediction models presented in Table 6.12 for inland exposure condition are function of concrete strength grade. Thus only Models 3 and 4 developed in this study can be assessed. Since the inland exposure conditions presents the worst case for carbonation-induced corrosion of reinforcing steel, only the prediction for this exposure condition will be used in comparing the predictive ability, confidence and reliability of the developed models. Applying the above concrete grades and exposure conditions to the developed carbonation prediction models and using 7 days for the moist curing duration, models given in Equations 6.9 to 6.12 were obtained by fitting the respective rates of carbonation to the square root of time formula.

$D = 5.10\sqrt{t}$ (Model 3, exposed Grade 30) 6.9

$D = 4.25\sqrt{t}$ (Model 3, exposed Grade 35) 6.10

$D = 5.20\sqrt{t}$ (Model 4, exposed Grade 30) 6.11

$D = 4.33\sqrt{t}$ (Model 4, exposed Grade 35) 6.12

In order to compare the predictive ability, confidence and reliability of the developed models, the predicted depths of carbonation at various exposure times by the developed models was compared to predictions from Yam’s models. This comparison is presented in Figures 6.4 and 6.5 for Model 3 and Model 4 respectively.

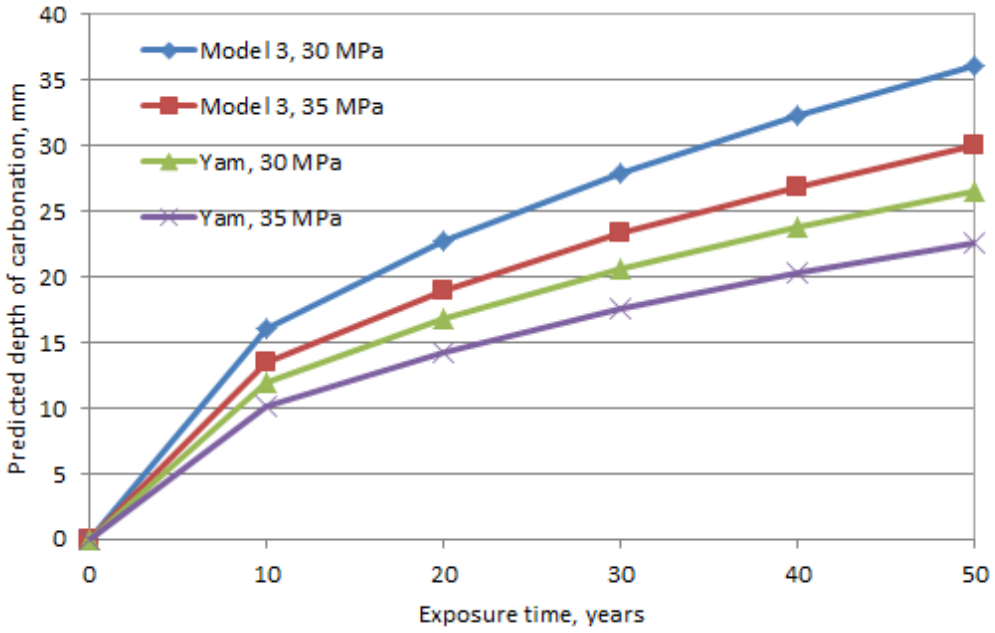


Figure 6.4: Comparison of predicted carbonation of Model 3 (Grade 30 and 35) and measured carbonation

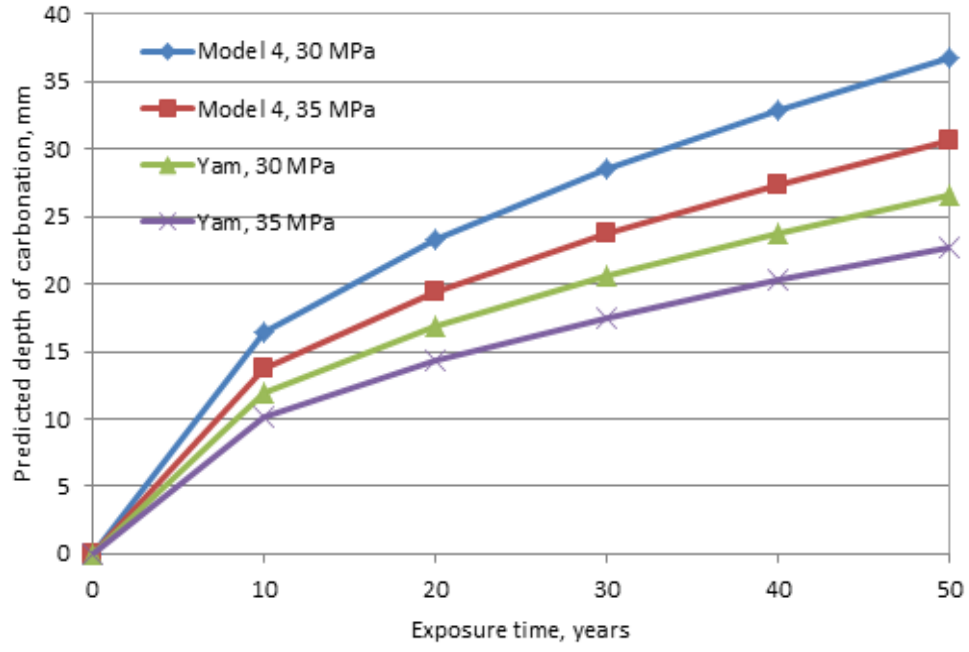


Figure 6.5: Comparison of predicted carbonation of Model 4 (Grade 30 and 35) and measured carbonation

Although Models 3 and 4 overestimated the carbonation in comparison to Yam's model, the differences between the carbonation predictions are not as high as predictions from Ballim and Lampacher or Lampacher models. The reason for the lower difference in carbonation prediction can be attributed to the statistical approach used by Yam in his derivation of the models. However, a discussion on the possible reasons for the differences in the carbonation predictions from Yam's study and the developed models will be provided in the section analyzing the differences in the predictions in measured and model predicted carbonation.

As stated before, all the developed models could not be assessed due to the limitations of the available information with the different studies. However, since the process of model formulation and development are similar, the confidence and reliability on carbonation predictions of the assessed models could be extended to the models that were not assessed.

6.3 Analyses of Difference between Predicted Carbonation from Developed Models and Measured Carbonation

A correction factor for the developed prediction models was contemplated in order to reduce or eliminate the observed differences between predicted and measured carbonation. However, the unquantifiable differences in material properties especially binder types between the two sets of carbonation data would not allow this option. Thus, the reasons for the closeness of the predicted carbonation to the measured carbonation or the consistent over-prediction of carbonation by the developed models were sought. This was approached from two perspectives, since the carbonation data used in the comparison were obtained on both laboratory samples and existing structures. While the laboratory carbonation studies were carried out in the mid 1990's with the casting of the concrete samples at about the same time, the carbonation studies on existing concrete structures were performed in the late 1990's with the concrete structures constructed between the 1960's and 1970's.

6.3.1 Laboratory cast concrete samples carbonation

Some of the likely reasons for the difference in carbonation depths predicted by the developed models and the measured values from laboratory concrete carbonation studies or the over predictions by the developed models are:

- **Varying climatic conditions over the short time of testing periods:** for instance, a particularly dry era with short, intermittent rain periods, rather than long and sustained rain periods – even with the same quantity of total rain affects or influences the rate of carbonation. These conditions affect the diffusion of CO_2 as well as the permeability of the concrete.
- **Increasing urbanization, manufacturing and vehicle usage in Johannesburg:** The increases in the above activities over the past 20 years, means that the CO_2 content must have increased. Thus, the probable reasons for the increased depth of carbonation noted in the present study.
- **Changes in cement characteristics**: The type of cement or binder used in making concrete influence it microstructure. The properties of cement have changed over the years mainly due to economic reasons. The present day "modern" cements are significantly finer with higher C_3S contents. This implies that its rate of hydration is high, with less later-age hydration, strength development or further pore refinement.

  Additionally, this cement will increase the heat of hydration and thus the drying shrinkage of the concrete with a possibility of micro crack and voids. This may create increased access for CO_2 to penetrate into the concrete. Similarly, admixture usage, results in generally lower binder content, for the same strengths – and therefore lower hydroxide contents in concrete.

6.3.2 Existing concrete structures carbonation

Reasons for the observed over prediction of carbonation by the developed models compared to the measured carbonation from existing concrete structures are similar to reasons given above for the laboratory carbonation studies. However,

some reasons are peculiar to the carbonation difference noted for existing concrete structures carbonation and the model predicted carbonation. The likely reasons for the observed difference in the carbonation predicted by the developed models and the measured carbonation from existing concrete structure are:

- **Cyclic wetting and drying effect on concrete:** This affects the rate of carbonation of concrete. When a concrete surface becomes saturated with water as a result of rain period, CO_2 diffusion into the concrete becomes negligible. The concrete has to dry out to the depth to which the carbonation front had reached just before the wetting period, in order for the concrete carbonation front to advance. In this manner, the rate of carbonation can be significantly reduced under continual cyclic wetting and drying conditions. Similarly, this condition also reduces the concrete pore structures and interconnectivity of the pores thus producing a less permeable concrete. This ultimately leads to reduction in the rate of carbonation. Thus, for concretes exposed to cyclic wetting and drying condition, the rate of carbonation is bound to be lower due to the reducing effect of this condition, particularly in the long-term for existing structures. This conditions may also lead to over prediction of carbonation the data obtained in the short- to medium-term were the effect is minimal is used in the development of prediction models.
- **Carbonation data used in the derivation of the models:** The developed models were derived from concrete carbonation data obtained in the medium-term, thus the reasons for the over predictions observed. Note that at early-age concrete covercrete is generally more porous because of the limited effect of curing. Similarly, the effect of decrease in the rate of carbonation with time of exposure is not fully captured at early-age. Note also that the formation and deposition of $CaCO_3$ through the process of carbonation densifies the pore structures of concrete and limits the passage of CO_2. These processes reduce the pore structure in concrete with depth and time, thus decreasing the rate of carbonation with increasing exposure time. All of the above mentioned processes are not captured by the early-age or medium-term carbonation measurements.

This is an added reason for over-prediction by the developed models. In the same light, since the models were derived from data obtained in the medium-term, using such a model to predict long-term carbonation introduces error by reducing the accuracy of the prediction.

From the foregoing, it is evident that the carbonation prediction by the developed models can be relied upon to be generally conservative in their prediction of long-term carbonation. This is based on the results of the comparison performed for some of the models and the likely reasons for the observed differences in the prediction of carbonation. Based on the above reasoning, Models 1, 4, 11, 12, and 14 which use mixture design, and 28 days compressive strength, oxygen permeability index, water sorptivity and accelerated carbonation rate values respectively as input parameters appear to provide the most reliable predictions.

This chapter has analysed the predictive ability of the developed models by comparing carbonation predictions from the models with historically measured carbonation from either laboratory or existing concrete structures in the inland environment. However, due to the limitations in applicability of the data obtained on old structures, not all the developed models could be assessed. Thus, with the limitation in the obtained data and the observed difference in the prediction of carbonation between the developed models and historically measured carbonation, selection of the most suitable models was based purely on statistical analysis. Nevertheless, the comparative analysis gives confidence and reliability to the carbonation prediction from the developed models since the predictions were sufficiently close to the measured carbonation values as well as being conservative. This makes the models suitable instruments for use in design-stage approximation of the likely rate of carbonation

The next chapter will draw together some of the important observation and conclusions noted in the research. The chapter will then conclude with the possible area for future research.

Chapter References

Alexander, M., Mackechnie, J. & Yam, W. (2007). *Carbonation of concrete bridge structures in three South African localities.* Cement and Concrete Composites, 29(10), 750-759.

Ananmalay, N. (1996). *Characterising the strength and durability performane of South African silica fume concretes*. MSc Dissertation, University of the Witwatersrand, Johannesbourg.

Ballim, Y. (1993). *Curing and the durability of concrete.* PhD Thesis, University of the Witwatersrand, Johannesburg.

Ballim, Y. & Lampacher, B. J. (1996). *Long-term carbonation of concrete structures in the Johannesburg environment.* JOURNAL-SOUTH AFRICAN INSTITUTION OF CIVIL ENGINEERS, 38, 5-9.

Fulton, F.S. (1977). *Concrete technology: a South African handbook.* 5th (Revised Metric) ed. Johannesburg: The Portland Cement Institute.

Lampacher, B. J. (2000). *Durability of concrete structures.* PhD, University of the Witwatersrand, Johannesburg.

Yam, W.K. (2004). *Carbonation of concrete bridge structures in three South African localities.* MSc (Eng.) Thesis. University of Cape Town, Cape Town; 2004.

CHAPTER 7

GENERAL CONCLUSIONS

7.1 Introduction

The main aim for this thesis was to develop carbonation prediction models for reinforced concrete structures in the inland environment of South Africa - Material, processing and environmental factors known to affect carbonation in concrete were given due consideration in the formulation of the models. The correlation of the rate of carbonation in concrete and the concrete mixture design and early-age characterisation parameters gave rise to a series of carbonation prediction models. The developed models reflect the concrete making materials and processing as well as the climatic conditions of exposure.

Through the carbonation study and model development, several conclusions can be drawn. This Chapter attempts to draw together the important observations and conclusions noted in the preceding chapters which touches on the potential durability performances of concrete, environmental exposure conditions and those relating to the predictions of durability and service life in concrete. Finally, a section is presented on the possible areas for future research in the field of concrete durability and deterioration and where possible, suggestions are made as to the form that such research may take.

7.2 Observations and Conclusions

a. Characterisation tests on concretes for comparative assessments based on fluid flow properties should be performed as early age as possible (preferably at 28 days) before exposure to the inland environment as the reliability of the tests results diminishes with exposure due to interactions between the material and atmospheric agents.

b. Accelerated carbonation tests for measuring potential durability of concrete need to be used with caution, although the test can be used to complement other characterisation tests since it is not a natural process. This is based on the fact that the acceleration process tends to change the microstructure of the concrete and its effect does not relate linearly to the increase or decrease in CO_2 concentration.
c. For concrete prepared at the same workability and compressive strength there is no significant difference between the rate of carbonation between plain and blended cement concrete because the increased tendency to carbonate by blended concrete because of the low carbonatable material is offset by it increased permeability.
d. Increasing the duration of moist curing and reducing the amount of addition of supplementary cementing materials has a significant effect on decreasing the rate of carbonation in concrete.
e. The micro-climate condition, especially the relative humidity, dictates the rate of carbonation of concrete in the inland environment. Thus, concrete samples in the outdoor sheltered sites presented the highest rate of carbonation. Although samples in this exposure site carbonate faster, the risk of reinforcement corrosion is likely to be low because the samples are protected from direct moisture effect.
f. Concrete samples in the outdoor exposed sites presented lower rate of carbonation compared to the sheltered sites but higher than for the indoor sites. Although samples in this exposure site presented moderate carbonation, the risk of reinforcement corrosion is likely to be high compared to the other two sites. This is as a result of the higher relative humidity and the cyclic wetting during rain period.
g. Good correlations were obtained between the concrete mixture design, early-age concrete characterisation parameters and the results of the carbonation rate of the concrete. This relationship gives high correlation coefficients.
h. Based on the good correlation coefficients between the concrete mixture design and early-age characterisation parameters and the rate of

carbonation, prediction models were derived. Comparisons of carbonation rates from the developed models with historical carbonation data are reasonably close, thus giving confidence and reliability to the developed models. These considerations satisfy an important objective of this research which was to develop reliable prediction models for the rate of carbonation in concrete exposed to an inland environment.

i. The developed prediction models are sensitive to the initial curing period of the concrete as well as the micro-climate of the exposure condition surrounding the concrete. Contrary to the other reported results, it was found that binder type, on its own is not statistically significant as a variable for the prediction of carbonation in concrete. This is based on the fact that the early-age characterisation parameters used vary with binder types.

Based on the statistical analysis and engineering judgments, the recommended models for use are presented in Table 7.1.

Table 7.1: Recommended models for use

Model	Prediction Equation
Model 1: Mixture Design	$K_{nat.} = 5.63 + 10.01\,(w/b) - 0.02(C) + \alpha_1 + \beta$
Model 2: Compressive Strength	$K_{nat.} = 14.26 - 0.18(f_c) + \alpha_2 + \beta$
Model 3: Oxygen Permeability Index	$K_{nat.} = 41.24 - 0.07(f_c) - 2.53(OPI) - 0.57(CH) + \beta$
Model 4: Water Sorptivity	$K_{nat.} = 13.75 - 0.06(f_c) + 0.34(WS) - 0.63(CH) + \beta$
Model 5: Accelerated Carbonation Rate	$K_{nat.} = 1.44 + 1.15(K_{acc.}) + \alpha_3 + \beta$

Where,

K_{nat} = natural carbonation rate, in mm/√years;

w/b = water/binder ratio;

C = cement content, in kg/m^3;

f_c = 28 day compressive strength of concrete, in MPa;

OPI = 28 day oxygen permeability of concrete;

WS = 28 day water sorptivity of the concrete;

CH = 28 day calcium hydroxide content of the concrete;

K_{acc} = 28 day accelerated carbonation rate of the concrete.

$\alpha_{1,2,3}$ = curing duration given to concrete and obtained from Table 7.2.

β = exposure condition of the concrete and obtained from Table 7.3.

Table 7.2: Model coefficients for curing duration

Curing duration	α_1	α_2	α_3
28 days	0	0	0
7 days	+1.61	-1.56	+0.74
3 days	+2.90	-1.79	+1.31

Table 7.3: Model coefficients for exposure condition

Exposure condition	β
Indoor	0
Outdoor sheltered	+1.07
Outdoor exposed	+-2.07

The presented models in Table 7.1 are for the prediction of carbonation rate in reinforced concrete structures located in the inland environment. These models can be applied:

- At the planning stage.
- At the design stage.
- At the construction stage.
- For service life prediction of proposed concrete structures.
- For maintenance and repair schedules of existing concrete structures.
- For residual service life prediction of existing concrete structures.

The model to be used will however depend on the type and quality of information available. A more detailed discussion of the use of each model is presented below.

Model 1 (Mixture design model): This model can be used at the planning stage of concrete structures when only the cement content and w/b ratio is known. An estimate of the likely curing duration would have to be made but this may be a designed specification. Should the concrete be specified to be cured for 3, 7 or 28 days, the appropriate value for use can be chosen from Table 7.2. Model 1 also requires a sense of the environment in which the concrete will be exposed. Where a concrete is to be exposed outdoor, the worst exposure scenario for corrosion of reinforcement should be obtained. The relevant exposure condition factor to use can be obtained from Table 7.3. If Model 1 is used the reliability of the prediction of the natural carbonation rate of concrete is 86% at the 5% confidence level.

Model 2 (Compressive strength model): This should be used when the mixture design detail of the concrete is not known but there is a measure of the 28 day compressive strength. However this model does require a curing duration of the concrete and knowledge of the exposure condition. These values can be obtained from Tables 7.2 and 7.3 respectively. Model 2 predicts the natural rate of carbonation in concrete with 75% reliability at the 5% confidence level.

Models 3 (Oxygen permeability index model) and Model 4 (Water sorptivity model): These models are to be used when the compressive strength of the

concrete is known and there is also a measure of the concrete fluid transport properties (Permeability and Sorptivity values) as well as the chemical composition of the concrete. Knowledge of the concrete curing duration and exposure condition is also necessary for prediction and the appropriate factor for these parameters can be obtained from Tables 7.2 and 7.3. Model 3 has a carbonation rate prediction reliability of 82% at the 5% confidence level while Model 4 has a carbonation rate prediction reliability of 85% at the 5% confidence level.

Model 5 (Accelerated carbonation model): Model 5 should be used when the accelerated carbonation of the concrete at 28 days is known. The accelerated carbonation condition should however be at 10±2% CO_2 concentration, 60±5% relative humidity and 22±1 ^{o}C temperature. Knowledge of the curing duration and exposure condition of the concrete are required and can be obtained from Tables 7.2 and 7.3 respectively. Model 5 has a reliability of 87% at the 5% confidence level in the prediction of the natural carbonation rate of the concrete.

Where all the above model input information is known, it is best to get a sense of the most reliable and the most conservative carbonation rate value, and should be used.

The carbonation prediction models presented above can more reliably be applied to estimate and or predict the rate of carbonation for the concrete structures which were constructed using “modern” cements and located in the inland environment. Thus, the carbonation prediction models developed in this research project can best be viewed as an aid to design for proposed concrete structures in terms of cover depth estimation, early-age concrete characterisation properties estimation and service life prediction. It can also be used for maintenance planning for existing concrete structures and residual service life prediction.

7.3 Recommendation for Future Research

a. Future research should be focused at quantifying the durability performance of concrete treated to other forms of curing conditions and exposure environments which are different from those used in this investigation. In particular, the effects of curing compounds used in the construction industry in Southern Africa, should be quantified with a view to facilitating specification of concrete durability performance as well as for the durability index tests.
b. The durability performance of concrete structures constructed using the durability index tests and exposed to the inland environment should be monitored in the long-term, since the depth of carbonation increases at a decreasing rate. Validation of the developed models should then be carried out with such carbonation data. This will improve the reliability and confidence of predictions.
c. Medium-term carbonation data from this study should be combined with long-term carbonation data obtained from concrete structures in the inland environment and a similar procedure of model development used in this research project followed for the development of more robust models that will cater for the cyclic effect of wetting and drying on the rate of carbonation in concrete.
d. The severity of the exposure condition needs to be determined more scientifically particularly with regard to the outdoor sheltered zone. More fundamental information is required about the interaction of carbon dioxide with the constituents of concrete. The effect of carbon dioxide dissolution in the concrete pore structure and diffusivity of the material is of particular interest when considering carbon dioxide ingress into concrete.
e. The relation between concrete mixture design and early-age parameters of a particular concrete and its resistance to deterioration in various aggressive environments must be studied further. The present study has considered the rate of carbonation as one part of a deterioration process.

Future studies should consider the corrosion processes in concrete, thus the propagation stage of reinforcement corrosion in concrete structures.

APPENDICES

Appendix A: Concrete compressive strength test results

Table A1: Individual concrete mass and compressive strength results

Binder type	Concrete mixture label	Age (days)	Mass (grams)	Compressive strength (MPa)
100% CEM I	PC-40	3	2529.6	47.4
			2531.6	45.8
			2530.2	46.5
		7	2535.5	64.6
			2564.4	63.0
			2542.1	62.8
		28	2525.5	77.0
			2566.4	74.6
			2542.8	76.2
	PC-50	3	2537.3	30.3
			2466.1	32.1
			2498.9	31.1
		7	2547.9	41.8
			2456.3	42.3
			2478.8	42.0
		28	2490.3	63.0
			2462.4	65.5
			2473.8	65.0
	PC-60	3	2443.0	23.4
			2388.9	22.2
			2399.2	23.6
		7	2452.6	31.1
			2471.1	32.0
			2438.9	31.5
		28	2409.7	51.2
			2486.6	48.2
			2513.6	48.3
	PC-75	3	2400.7	24.0
			2364.5	24.2
			2382.9	24.8
		7	2349.1	26.1
			2385.9	26.3
			2388.2	26.5
		28	2389.5	36.2
			2386.8	35.8
			2379.9	36.0

Table A1: Individual concrete mass and compressive strength results (Continued)

Binder type	Concrete mixture label	Age (days)	Mass (grams)	Compressive strength (MPa)
70/30 CEM I-FA	FA-40	3	2506.3	35.8
			2448.2	36.1
			2492.8	36.9
		7	2576.8	42.2
			2436.2	45.4
			2448.9	43.0
		28	2444.5	58.5
			2474.2	63.5
			2452.8	61.2
	FA-50	3	2480.1	21.8
			2439.0	22.1
			2446.2	22.3
		7	2437.6	30.7
			2481.3	31.6
			2470.2	31.0
		28	2461.0	48.0
			2441.2	48.3
			2449.4	48.9
	FA-60	3	2439.5	18.6
			2480.4	18.4
			2468.9	19.0
		7	2488.0	24.4
			2472.3	24.5
			2479.4	24.9
		28	2454.2	32.5
			2482.8	30.5
			2461.3	29.5
	FA-75	3	2436.4	14.0
			2406.2	13.2
			2424.9	13.6
		7	2448.9	16.5
			2432.4	15.7
			2456.7	16.0
		28	2460.5	23.1
			2455.8	22.5
			2459.2	23.0

Table A1: Individual concrete mass and compressive strength results (Continued)

Binder type	Concrete mixture label	Age (days)	Mass (grams)	Compressive strength (MPa)
50/50 CEM I-GGBS	SL-40	3	2464.4	24.3
			2513.0	24.9
			2492.3	25.1
		7	2434.8	34.0
			2416.8	33.9
			2422.6	34.2
		28	2488.0	63.9
			2497.9	61.5
			2492.1	63.0
	SL-50	3	2473.6	19.0
			2465.6	19.2
			2469.9	18.2
		7	2489.2	27.9
			2479.4	27.0
			2468.8	27.4
		28	2478.1	52.9
			2495.8	51.5
			2489.2	52.0
	SL-60	3	2442.7	13.5
			2456.3	14.1
			2449.8	13.8
		7	2448.8	17.6
			2466.4	18.8
			2459.2	18.3
		28	2465.2	36.8
			2490.7	39.1
			2478.9	37.5
	SL-75	3	2390.8	9.1
			2400.0	7.5
			2419.2	9.6
		7	2442.8	13.2
			2399.2	12.7
			2402.6	12.0
		28	2494.2	27.4
			2466.4	28.1
			2472.8	28.8

Table A1: Individual concrete mass and compressive strength results (Continued)

Binder type	Concrete mixture label	Age (days)	Mass (grams)	Compressive strength (MPa)
90/10 CEMI -CSF	SF-40	3	2500.5	49.0
			2480.8	53.2
			2499.2	51.0
		7	2511.0	69.6
			2517.1	72.5
			2508.2	70.5
		28	2481.2	89.5
			2512.2	92.0
			2492.8	92.7
	SF-50	3	2448.2	38.3
			2466.9	39.1
			2437.8	35.6
		7	2442.4	52.9
			2453.4	50.9
			2459.1	52.0
		28	2464.3	77.1
			2504.4	76.8
			2489.7	76.9
	SF-60	3	2437.1	28.0
			2419.2	25.9
			2428.2	26.9
		7	2441.7	37.5
			2426.9	36.8
			2434.8	37.0
		28	2460.3	58.6
			2435.9	60.8
			2449.2	59.0
	SF-75	3	2391.0	8.6
			2425.7	9.5
			2435.9	9.3
		7	2408.8	23.7
			2362.2	23.1
			2392.8	23.8
		28	2422.4	41.8
			2489.1	40.9
			2468.2	41.5

Table A1: Individual concrete mass and compressive strength results (Continued)

Binder type	Concrete mixture label	Age (days)	Mass (grams)	Compressive strength (MPa)
100% CEM V	CC-40	3	2411.0	8.3
			2391.2	7.3
			2409.8	7.9
		7	2466.9	23.1
			2425.3	22.4
			2435.6	22.8
		28	2432.2	40.2
			2419.4	41.6
			2429.8	40.8
	CC-50	3	2482.6	19.3
			2501.3	19.0
			2493.8	19.4
		7	2565.8	30.3
			2470.1	28.8
			2499.8	29.0
		28	2398.0	47.3
			2525.7	48.6
			2429.8	47.9
	CC-60	3	2480.9	16.5
			2421.4	17.6
			2411.8	16.8
		7	2445.6	23.2
			2499.3	23.4
			2489.7	23.8
		28	2468.9	37.9
			2478.2	36.6
			2474.8	37.0
	CC-75	3	2427.4	9.2
			2409.8	9.4
			2418.4	9.6
		7	2536.4	13.6
			2432.9	13.8
			2489.6	14.0
		28	2407.4	23.4
			2446.4	25.9
			2428.9	24.0

Appendix B: Concrete medium-term durability index test results

Table B1: Oxygen permeability results for site exposed concrete

Concrete mixture label	Exposure condition	Moist curing (days)	Exposure duration					
			6 months		12 months		18 months	
			OPI	*K* ($x10^{-10}$ m/s)	*OPI*	*K* ($x10^{10}$ m/s)	*OPI*	*K* ($x10^{10}$ m/s)
PC-50	Indoor	3	*	*	9.0	1.1E-09	8.6	2.5E-09
		7	8.6	2.5E-09	8.5	3.5E-09	8.7	2.2E-09
		28	8.7	1.9E-09	9.0	9.8E-09	8.4	3.9E-09
	Outdoor sheltered	3	8.7	2.9E-09	8.2	5.9E-09	8.3	5.2E-09
		7	8.4	4.0E-09	9.0	1.0E-09	8.6	2.6E-09
		28	8.7	2.0E-09	*	*	8.4	4.2E-09
	Outdoor exposed	3	8.8	1.7E-09	*	*	8.3	5.4E-09
		7	9.0	1.0E-09	*	*	8.5	3.0E-09
		28	8.9	1.3E-09	*	*	8.4	4.1E-09
FA-50	Indoor	3	8.7	2.2E-09	*	*	8.3	4.5E-09
		7	*	*	*	*	8.7	2.0E-09
		28	9.1	7.5E-10	*	*	8.8	1.5E-09
	Outdoor sheltered	3	*	*	8.9	1.3E-09	8.6	2.4E-09
		7	9.0	1.1E-09	8.7	2.2E-09	8.5	3.5E-09
		28	8.5	3.5E-09	*	*	8.8	1.4E-09
	Outdoor exposed	3	9.0	9.8E-09	9.1	7.5E-10	8.4	3.9E-09
		7	8.2	5.9E-09	*	*	8.8	1.5E-09
		28	9.0	1.0E-09	9.0	1.1E-09	8.4	4.5E-09
SL-50	Indoor	3	8.1	8.1E-09	8.5	3.5E-09	8.0	1.1E-08
		7	8.6	2.8E-09	*	*	*	*
		28	8.7	2.0E-09	*	*	8.2	5.9E-09
	Outdoor sheltered	3	8.5	2.9E-09	*	*	8.5	3.1E-09
		7	8.6	2.5E-09	*	*	8.6	2.4E-09
		28	8.3	4.6E-09	*	*	*	*
	Outdoor exposed	3	8.4	3.8E-09	8.5	3.1E-09	*	*
		7	8.1	8.4E-09	8.6	2.4E-09	8.6	2.3E-09
		28	8.7	2.0E-09	*	*	8.3	5.3E-09
SF-50	Indoor	3	*	*	*	*	8.6	2.5E-09
		7	*	*	8.6	2.3E-09	8.4	4.3E-09
		28	*	*	8.3	5.3E-09	8.8	1.7E-09
	Outdoor sheltered	3	*	*	*	*	8.6	2.6E-09
		7	8.5	3.1E-09	*	*	8.3	4.7E-09
		28	8.6	2.4E-09	*	*	*	*
	Outdoor exposed	3	*	*	*	*	8.4	4.2E-09
		7	*	*	*	*	8.7	1.8E-09
		28	8.6	2.3E-09	*	*	8.4	3.9E-09
			8.3	5.3E-09				

*Results discarded

Table B1: Oxygen permeability results for site exposed concrete (Continued)

Concrete mixture label	Exposure condition	Moist curing (days)	Exposure duration					
			6 months		12 months		18 months	
			OPI	*K* ($x10^{-10}$ m/s)	*OPI*	*K* ($x10^{10}$ m/s)	*OPI*	*K* ($x10^{10}$ m/s)
CC-50	Indoor	3	8.7	2.0E-09	*	*	8.9	1.4E-09
		7	8.2	6.3E-09	*	*	8.4	3.9E-09
		28	9.0	1.1E-09	8.5	3.1E-09	8.9	1.1E-09
	Outdoor sheltered	3	*	*	8.6	2.4E-09	8.6	2.4E-09
		7	*	*	*	*	8.6	2.4E-09
		28	8.4	3.7E-09	*	*	8.5	3.1E-09
	Outdoor exposed	3	8.5	3.4E-09	8.6	2.3E-09	8.4	3.6E-09
		7	8.2	6.2E-09	8.3	5.3E-09	8.4	3.6E-09
		28	9.0	9.2E-10	*	*	8.4	3.6E-09

*Results discarded

Table B2: Water sorptivity results for site exposed concrete

Concrete mixture label	Exposure condition	Moist curing (days)	Exposure duration					
			6 months		12 months		18 months	
			Sorptivity ($mm/hr^{0.5}$)	Porosity (%)	Sorptivity ($mm/hr^{0.5}$)	Porosity (%)	Sorptivity ($mm/hr^{0.5}$)	Porosity (%)
PC-50	Indoor	3	10.2	9.6	12.5	*	12.7	8.6
		7	8.6	9.9	10.9	*	12.1	8.6
		28	9.2	9.6	10.2	*	10.9	9.5
	Outdoor sheltered	3	9.5	10.2	11.3	*	13.0	8.5
		7	9.4	11.4	10.0	*	12.3	8.5
		28	10.5	9.6	10.8	*	9.8	8.6
	Outdoor exposed	3	9.8	9.4	7.3	*	9.5	7.6
		7	10.4	9.1	6.7	*	8.6	7.6
		28	10.7	9.2	9.3	*	9.5	8.4
FA-50	Indoor	3	10.8	10.6	11.9	*	12.0	9.8
		7	9.6	10.7	11.2	*	11.8	10.7
		28	9.7	10.7	9.6	*	9.7	10.4
	Outdoor sheltered	3	12.4	10.3	11.4	*	10.8	10.3
		7	10.8	10.4	10.6	*	9.7	11.1
		28	10.9	10.7	9.1	*	8.2	10.7
	Outdoor exposed	3	10.0	9.9	4.3	*	4.7	9.1
		7	9.3	10.6	5.1	*	4.7	8.5
		28	10.2	10.4	5.4	*	5.7	8.6
SL-50	Indoor	3	11.3	12.4	15.7	*	9.5	10.5
		7	8.7	11.6	12.1	*	8.4	10.4
		28	9.9	14.9	7.9	*	7.7	9.5
	Outdoor sheltered	3	11.7	10.2	11.7	*	8.4	10.7
		7	9.4	10.5	9.5	*	8.5	11.6
		28	9.1	*	15.5	*	8.3	10.9
	Outdoor exposed	3	9.8	11.9	6.0	*	6.7	8.6
		7	10.1	10.9	6.6	*	6.9	8.3
		28	8.6	10.6	8.4	*	7.2	7.9
SF-50	Indoor	3	6.4	*	*	*	9.0	*
		7	5.9	10.5	*	*	7.9	*
		28	5.9	11.3	*	*	7.1	*
	Outdoor sheltered	3	6.5	9.1	*	*	17.8	*
		7	7.3	9.2	*	*	16.6	*
		28	7.0	9.0	*	*	13.6	*
	Outdoor exposed	3	6.2	9.7	*	*	5.7	*
		7	6.8	9.9	*	*	6.2	*
		28	8.0	9.5	*	*	5.8	*

*Results discarded

Table B2: Water sorptivity results for site exposed concrete (Continued)

Concrete mixture label	Exposure condition	Moist curing (days)	Exposure duration					
			6 months		12 months		18 months	
			Sorptivity ($mm/hr^{0.5}$)	Porosity (%)	Sorptivity ($mm/hr^{0.5}$)	Porosity (%)	Sorptivity ($mm/hr^{0.5}$)	Porosity (%)
CC-50	Indoor	3	7.7	11.9	11.8	*	7.8	10.7
		7	4.6	11.6	9.6	*	7.4	9.6
		28	7.4	10.1	8.7	*	6.7	8.8
	Outdoor sheltered	3	10.1	11.0	9.0	*	8.7	10.1
		7	8.8	10.3	6.9	*	7.7	9.0
		28	8.3	*	6.4	*	7.0	8.0
	Outdoor exposed	3	8.1	*	4.5	*	6.0	8.1
		7	4.8	9.5	4.3	*	7.7	6.3
		28	4.6	*	4.7	*	7.7	5.6

*Results discarded

Appendix C: Micro-climate variation results of the exposure sites

Table C1: Annual micro-climate variations within the exposure sites

Month	Exposure site	CO_2 Concentration, %			Relative Humidity, %			Temperature, ^{O}C		
		Minimum	Maximum	Mean	Minimum	Maximum	Mean	Minimum	Maximum	Mean
January	Indoor	0.001	0.034	0.015	23.8	47.3	35.3	24.2	31.9	28.2
	Outdoor sheltered	0.002	0.194	0.024	10.2	92.3	57.4	11.9	33.0	21.3
	Outdoor exposed	0.002	0.194	0.021	10.2	92.3	57.9	11.9	32.8	20.9
February	Indoor	0.001	0.365	0.045	11.8	54.6	33.1	27.1	33.6	30.6
	Outdoor sheltered	0.002	0.053	0.035	10.5	90.7	54.1	14.7	30.1	22.7
	Outdoor exposed	0.001	0.336	0.032	7.3	88.9	51.2	15.4	37.8	24.2
March	Indoor	0.001	0.365	0.044	11.8	44.5	32.8	20.2	33.6	28.3
	Outdoor sheltered	0.013	0.056	0.037	17.6	85.3	58.9	13.0	28.6	20.4
	Outdoor exposed	0.001	0.312	0.021	11.6	82.2	55.2	14.2	33.7	22.1

Table C1: Annual micro-climate variations within the exposure sites (Continued)

Month	Exposure site	CO_2 Concentration, %			Relative Humidity, %			Temperature, ^{O}C		
		Minimum	Maximum	Mean	Minimum	Maximum	Mean	Minimum	Maximum	Mean
April	Indoor	0.014	0.058	0.037	17.6	50.8	32.3	20.2	29.3	24.8
	Outdoor sheltered	0.011	0.050	0.034	21.5	91.5	53.1	7.4	26.1	17.5
	Outdoor exposed	0.001	0.483	0.034	16.5	94.1	50.4	9.0	29.8	19.1
May	Indoor	0.013	0.056	0.041	13.0	57.3	26.9	17.7	26.0	23.0
	Outdoor sheltered	0.014	0.051	0.034	20.0	91.3	44.2	6.4	21.9	15.9
	Outdoor exposed	0.001	0.112	0.009	14.0	88.3	40.8	6.1	26.8	17.5
June	Indoor	0.007	0.061	0.045	7.02	41.2	22.7	17.3	25.3	22.4
	Outdoor sheltered	0.009	0.050	0.031	10.6	88.1	42.9	3.2	21.4	13.3
	Outdoor exposed	0.001	0.148	0.006	8.3	83.9	39.2	2.8	26.7	15.2

Table C1: Annual micro-climate variations within the exposure sites (Continued)

Month	Exposure site	CO_2 Concentration, %			Relative Humidity, %			Temperature, ^{O}C		
		Minimum	Maximum	Mean	Minimum	Maximum	Mean	Minimum	Maximum	Mean
July	Indoor	0.007	0.043	0.026	11.2	55.2	28.6	12.0	20.3	18.0
	Outdoor sheltered	0.011	0.035	0.014	7.3	77.7	33.9	3.9	22.9	15.6
	Outdoor exposed	0.030	0.09	0.023	6.8	96.5	48.5	0.1	26.3	11.7
August	Indoor	0.012	0.064	0.045	7.2	52.2	25.7	15.7	25.3	20.0
	Outdoor sheltered	0.004	0.051	0.032	11.6	99.4	42.2	3.3	22.6	13.4
	Outdoor exposed	0.001	0.383	0.016	6.52	91.1	36.8	2.2	32.3	16.0
September	Indoor	0.001	0.040	0.021	13.0	56.1	38.1	15.7	23.5	20.4
	Outdoor sheltered	0.001	0.140	0.006	10.9	75.1	34.7	9.0	27.3	20.6
	Outdoor exposed	0.004	0.029	0.042	9.1	98.1	54.0	4.0	31.3	15.9

Table C1: Annual micro-climate variations within the exposure sites (Continued)

Month	Exposure site	CO_2 Concentration, %			Relative Humidity, %			Temperature, ^{O}C		
		Minimum	Maximum	Mean	Minimum	Maximum	Mean	Minimum	Maximum	Mean
October	Indoor	0.001	0.037	0.006	17.6	62.3	41.9	21.0	26.1	23.3
	Outdoor sheltered	0.001	0.052	0.020	9.7	97.0	54.3	10.7	30.4	19.9
	Outdoor exposed	0.001	0.996	0.125	5.7	95.7	53.3	7.2	39.8	19.5
November	Indoor	0.001	0.068	0.013	25.4	49.2	37.7	25.9	33.7	29.4
	Outdoor sheltered	0.001	0.382	0.026	11.7	90.4	59.2	13.8	36.6	22.8
	Outdoor exposed	0.005	0.571	0.031	20.5	88.3	51.6	15.4	33.4	23.3
December	Indoor	0.001	0.269	0.014	23.9	51.2	36.0	24.3	35.5	30.6
	Outdoor sheltered	0.002	0.194	0.024	10.2	92.3	58.3	11.9	33.0	21.7
	Outdoor exposed	0.001	0.445	0.029	16.7	87.6	57.4	15.6	37.6	23.4

Appendix D: Concrete carbonation test results

Table D1: Natural indoor carbonation depth results for all concrete

Binder combination	Concrete mixture label	Moist curing (days)	Natural carbonation depths, d (mm)			
			Duration on indoor exposure site, t (years)			
			0.5	1	1.5	2
100% CEM I	PC-40	3	1.6	2.7	3.5	4.5
		7	1.1	1.7	2.3	2.1
		28	0.4	0.8	1.2	1.6
	PC-50	3	2.5	3.6	4.9	5.6
		7	1.9	2.6	3.4	4.2
		28	1.0	1.5	2.3	2.5
	PC-60	3	4.6	5.7	7.8	9.7
		7	3.1	4.3	5.7	6.5
		28	2.1	2.9	4.1	5.8
	PC-75	3	5.3	7.6	8.8	11.6
		7	3.7	5.1	6.8	8.7
		28	2.7	3.8	5.3	7.4
70/30 CEM I-FA	FA-40	3	3.5	4.8	5.8	12.5
		7	2.5	3.6	4.5	11.1
		28	1.2	2.0	2.7	8.7
	FA-50	3	4.4	5.7	8.2	14.5
		7	3.9	4.9	7.3	12.3
		28	2.4	3.6	5.1	10.3
	FA-60	3	5.4	8.4	9.7	16.4
		7	4.7	6.2	8.5	14.2
		28	2.9	4.4	6.5	12.0
	FA-75	3	8.9	12.3	15.7	21.5
		7	6.9	9.5	12.6	21.5
		28	4.1	6.2	9.0	16.9
50/50 CEM I-GGBS	SL-40	3	5.6	8.1	9.1	10.3
		7	4.4	6.1	7.3	8.1
		28	2.3	3.4	4.3	5.4
	SL-50	3	6.9	10.4	11.4	12.7
		7	5.3	7.6	9.3	10.4
		28	3.5	4.7	5.8	8.5
	SL-60	3	7.7	11.0	13.0	15.2
		7	7.2	10.6	12.2	13.2
		28	4.3	6.4	7.3	9.5
	SL-75	3	11.8	16.2	19.3	21.9
		7	10.3	13.8	15.1	18.4
		28	7.3	10.7	12.3	13.7

Table D1: Natural indoor carbonation depth results for all concrete (Continued)

Binder combination	Concrete mixture label	Moist curing (days)	Natural carbonation depths, d (mm)			
			Duration on indoor exposure site, t (years)			
			0.5	1	1.5	2
90/10 CEM I-CSF	SF-40	3	1.1	2.5	3.4	4.9
		7	0.2	1.4	2.5	3.4
		28	0.1	0.7	1.5	2.3
	SF-50	3	1.4	2.7	5.1	6.4
		7	1.4	2.7	4.1	5.1
		28	0.4	1.3	2.4	3.2
	SF-60	3	2.3	3.8	6.5	8.6
		7	1.8	3.4	5.3	7.1
		28	0.9	1.8	3.4	4.7
	SF-75	3	3.4	4.6	9.2	10.3
		7	3.2	4.6	7.6	9.5
		28	1.4	3.1	4.9	6.1
100% CEM V	CC-40	3	5.3	6.9	9.5	11.8
		7	3.7	5.3	6.7	8.0
		28	3.1	4.2	5.7	6.8
	CC-50	3	6.5	9.2	11.2	13.9
		7	5.6	8.1	9.9	11.5
		28	3.5	4.7	6.5	8.1
	CC-60	3	7.8	10.9	14.1	17.5
		7	6.9	9.8	11.7	13.7
		28	4.4	6.8	7.8	10.1
	CC-75	3	9.1	13.7	15.9	19.8
		7	8.4	12.6	14.7	18.0
		28	6.1	8.6	10.9	13.4

Table D2: Natural outdoor sheltered carbonation depth results for all concrete

Binder combination	Concrete mixture label	Moist curing (days)	Natural carbonation depths, d (mm)			
			Duration on outdoor sheltered exposure site, t (years)			
			0.5	1	1.5	2
100% CEM I	PC-40	3	2.3	3.2	4.5	5.6
		7	1.3	2.2	2.8	3.1
		28	0.6	1.2	1.5	1.9
	PC-50	3	3.9	5.7	6.5	7.3
		7	2.5	3.7	4.5	4.9
		28	1.3	2.2	2.8	3.5
	PC-60	3	5.1	7.1	8.7	10
		7	3.3	4.8	6.2	8.3
		28	2.1	3.2	4.3	6.6
	PC-75	3	6.5	8.9	11.0	13
		7	4.5	6.6	7.7	10.5
		28	3.5	5.1	6.2	8.3
70/30 CEM I-FA	FA-40	3	4.3	6.4	7.1	9.5
		7	2.5	3.9	4.9	7.8
		28	1.5	2.5	2.9	4.5
	FA-50	3	6.4	9.3	10.6	12.4
		7	5.3	7.9	8.9	11.2
		28	3.5	5.3	6.0	7.5
	FA-60	3	8.7	12.8	13.7	14.5
		7	6.4	8.3	10.6	13.4
		28	4.5	6.7	8.3	12
	FA-75	3	13.2	18.7	21.4	22.1
		7	9.8	13.7	17.3	21.3
		28	10.3	14.7	17.3	18.7
50/50 CEM I-GGBS	SL-40	3	5.5	7.5	9.3	10.1
		7	4.4	6.3	7.2	8.5
		28	2.6	3.7	4.2	5.3
	SL-50	3	7.4	10.9	12.7	13.4
		7	6.4	10.2	11.0	11.9
		28	4.5	6.6	7.5	8.1
	SL-60	3	9.6	12.4	14.9	18.1
		7	9.0	13.1	15.0	16.2
		28	5.0	7.1	8.3	10.4
	SL-75	3	14.7	19.7	23.4	25.3
		7	13.1	18.5	22.5	23.8
		28	6.8	9.9	11.4	12.9

Table D2: Natural outdoor sheltered carbonation depth results for all concrete (Continued)

Binder combination	Concrete mixture label	Moist curing (days)	Natural carbonation depths, d (mm)			
			Duration on outdoor sheltered exposure site, t (years)			
			0.5	1	1.5	2
90/10 CEM I-CSF	SF-40	3	0.8	1.6	2.8	3.9
		7	0.2	0.8	1.9	2.6
		28	0	0.7	1.4	2.6
	SF-50	3	1.9	2.8	4.7	6.1
		7	1.3	2.1	3.5	4.3
		28	0.7	1.4	2.7	3.3
	SF-60	3	2.8	5.3	7.8	10.7
		7	2.5	3.8	6.1	7.7
		28	1.7	2.5	4.4	6.2
	SF-75	3	4.7	6.9	10.1	13.2
		7	3.8	5.6	8.3	10.1
		28	3.2	4.4	6.9	8.7
100% CEM V	CC-40	3	5.3	7.9	9.8	12.5
		7	4.8	6.8	8.1	11.1
		28	4.2	5.6	7.1	8.7
	CC-50	3	7.4	10.5	12.3	14.5
		7	6.3	9.1	10.3	12.3
		28	5.5	7.7	8.9	10.3
	CC-60	3	8.5	12.4	14.6	16.4
		7	7.5	10.9	12.4	14.2
		28	5.8	8.9	9.7	12.0
	CC-75	3	11.2	16.3	19.3	21.5
		7	10.9	15.2	18.6	21.5
		28	8.6	13.5	15.8	16.9

Table D3: Natural outdoor exposed carbonation depth results for all concrete

Binder combination	Concrete mixture label	Moist curing (days)	Natural carbonation depths, d (mm)			
			Duration on outdoor exposed exposure site, t (years)			
			0.5	1	1.5	2
100% CEM I	PC-40	3	1.1	1.5	1.7	2.3
		7	0.5	0.8	1.0	1.3
		28	0.2	0.4	0.6	0.8
	PC-50	3	1.3	1.7	2.1	2.8
		7	1.1	1.5	1.8	2.1
		28	0.8	1.2	1.4	1.7
	PC-60	3	2.5	3.5	3.8	4.5
		7	1.8	2.5	3.0	3.5
		28	1.6	2.1	2.7	3.1
	PC-75	3	3.3	4.9	5.5	6.5
		7	2.9	3.9	4.5	5.7
		28	2.4	3.1	3.8	4.8
70/30 CEM I-FA	FA-40	3	2.3	3.3	4.2	4.5
		7	1.4	2.3	2.9	3.4
		28	0.8	1.5	2.0	2.3
	FA-50	3	3.4	4.8	6.3	6.8
		7	2.5	3.8	4.9	5.6
		28	2.2	3.3	4.1	4.7
	FA-60	3	4.9	7.3	8.1	9.5
		7	3.7	5.4	6.7	8.3
		28	3.4	4.8	6.2	7.5
	FA-75	3	7.1	9.8	11.7	13.4
		7	6.5	9.1	11.4	12.7
		28	5.5	7.7	10.0	12.8
50/50 CEM I-GGBS	SL-40	3	2.5	4.1	4.7	5.3
		7	2.1	3.0	3.8	5.2
		28	1.1	1.5	2.3	2.9
	SL-50	3	4.3	6.4	7.6	8.7
		7	3.2	4.4	6.0	7.5
		28	2.1	3.3	4.2	4.7
	SL-60	3	5.6	7.9	9.8	11.4
		7	4.0	6.1	7.5	9.1
		28	2.8	4.2	5.3	6.1
	SL-75	3	7.7	11.3	12.7	13.5
		7	6.5	10.0	11.2	12.9
		28	5.3	7.9	9.3	10.2

Table D3: Natural outdoor exposed carbonation depth results for all concrete (Continued)

Binder combination	Concrete mixture label	Moist curing (days)	Natural carbonation depths, d (mm)			
			Duration on outdoor exposed exposure site, t (years)			
			0.5	1	1.5	2
90/10 CEM I-CSF	SF-40	3	0	0.5	0.9	2.1
		7	0	0.2	0.6	1.6
		28	0	0.2	0.4	1.4
	SF-50	3	1.1	1.6	2.3	3.8
		7	1.0	1.3	2.1	2.4
		28	0.5	0.8	1.6	2.5
	SF-60	3	1.7	2.4	3.2	5.6
		7	1.6	1.9	2.9	3.7
		28	1.1	1.5	2.1	3.3
	SF-75	3	2.5	3.2	4.8	7.4
		7	2.1	3.2	4.1	6.1
		28	2.4	3.1	4.2	5.8
100% CEM V	CC-40	3	3.2	4.9	6.1	7.6
		7	2.9	4.2	5.3	6.1
		28	2.4	3.5	4.4	5.1
	CC-50	3	4.9	7.2	8.9	9.5
		7	3.8	5.5	7.2	8.3
		28	3.1	4.4	5.5	6.5
	CC-60	3	5.9	8.7	10.3	12.3
		7	4.4	6.5	8.3	9.4
		28	3.8	5.4	7.0	7.5
	CC-75	3	9.1	11.7	15.2	18.5
		7	7.1	9.5	12.4	13.3
		28	5.5	7.9	9.3	11.7

Table D4: Accelerated carbonation depth results for all concrete

Binder combination	Concrete mixture label	Moist curing (days)	Accelerated carbonation depths, d (mm)			
			Duration on accelerated exposure site, t (days)			
			7	14	21	28
100% CEM I	PC-40	3	1.7	2.4	3.6	4.1
		7	0.7	1.4	1.5	2.4
		28	0	0	0	0
	PC-50	3	4.3	7.1	8.3	9.8
		7	3.4	5.2	5.8	7.9
		28	2.7	3.7	5.3	6.1
	PC-60	3	6.1	9.8	12.4	13.3
		7	7.1	8.9	10.7	13.7
		28	5.3	7.5	10.2	10.9
	PC-75	3	11.2	15.4	18.0	21.7
		7	10.2	11.9	16.1	19.3
		28	8.9	10.8	14.3	17.2
70/30 CEM I-FA	FA-40	3	5.4	7.6	8.3	10.8
		7	4.4	5.8	6.7	8.9
		28	2.9	4.8	5.5	6.9
	FA-50	3	8.3	12.8	16.6	17.2
		7	6.9	10.4	11.9	14.7
		28	6.2	9.8	10.3	13.1
	FA-60	3	14.3	21.5	24.5	28.7
		7	12.9	15.3	20.4	23.9
		28	10.9	15.1	18.7	21.5
	FA-75	3	24.7	33.0	41.5	49.1
		7	19.6	32.5	38.5	41.3
		28	17.4	24.5	29.1	35.6
50/50 CEM I-GGBS	SL-40	3	7.8	10.8	12.3	15.1
		7	6.4	7.6	10.6	12.5
		28	4.6	7.1	7.5	9.3
	SL-50	3	10.7	14.9	19.5	21.8
		7	10.3	13.3	18.5	19.3
		28	8.7	10.5	13.4	16.7
	SL-60	3	15.9	24.1	27.8	32.0
		7	12.9	19.6	23.5	26.1
		28	10.9	13.8	17.8	21.4
	SL-75	3	21.3	-	-	-
		7	21.3	30.5	34.1	43.5
		28	15.3	17.5	23.8	28.5

- Carbonation depth exceeds 50 mm

Table D4: Accelerated carbonation depth results for all concrete (Continued)

Binder combination	Concrete mixture label	Moist curing (days)	Accelerated carbonation depths, d (mm)			
			Duration on accelerated exposure site, t (days)			
			7	14	21	28
90/10 CEM I-CSF	SF-40	3	3.2	4.3	4.9	5.5
		7	1.4	1.9	2.4	3.5
		28	0	0	0	0
	SF-50	3	4.9	7.6	8.3	9.7
		7	3.7	6.4	7.2	7.8
		28	3.9	5.8	6.3	7.3
	SF-60	3	8.6	11.2	13.1	16.3
		7	8.1	10.2	12.4	15.1
		28	6.5	9.1	11.3	13.5
	SF-75	3	15.1	22.3	27.3	29.8
		7	14.3	18.6	25.4	27.5
		28	12.7	18.7	22.9	26.2
100% CEM V	CC-40	3	10.1	16.4	18.6	21.3
		7	8.9	11.3	15.5	16.7
		28	7.2	8.5	10.7	14.8
	CC-50	3	13.8	22.1	25.5	29.5
		7	12.1	19.5	22.7	24.5
		28	10.1	15.5	17.3	20.7
	CC-60	3	26.1	31.4	40.3	49.7
		7	17.5	25.0	32.4	34.8
		28	14.3	20.5	25.3	29.3
	CC-75	3	30.1	-	-	-
		7	28.7	-	-	-
		28	24.1	33.8	43.5	47.9

- Carbonation depth exceeds 50 mm

Appendix E: Correlation analysis and scatter plots output

Table E1 gives the results of the bivariate analysis between the response variable and each predictor variables as well as the relationship among the predictor variables. While Figure E1 presents all the scatter plots between the variables. Tables E2 present the association between the categorical variables while Tables E3 gives the association between the continuous and categorical variables.

Table E1: Bivariate correlation

Correlations

		Knat	w_b	W	B	C	SCM	fc	OPI	WS	CH	CaO	Kacc
Knat	Pearson Correlation	1	.591**	.576**	-.584**	-.735**	.421**	-.777**	-.738**	.747**	-.744**	-.374**	.857**
	Sig. (2-tailed)		.000	.000	.000	.000	.000	.000	.000	.000	.000	.000	.000
	N	180	180	180	180	180	180	180	180	180	180	180	180
w_b	Pearson Correlation	.591**	1	.983**	-.994**	-.410**	-.189*	-.600**	-.823**	.759**	-.511**	-.302**	.734**
	Sig. (2-tailed)	.000		.000	.000	.000	.011	.000	.000	.000	.000	.000	.000
	N	180	180	180	180	180	180	180	180	180	180	180	180
W	Pearson Correlation	.576**	.983**	1	-.992**	-.409**	-.189*	-.606**	-.800**	.735**	-.513**	-.306**	.713**
	Sig. (2-tailed)	.000	.000		.000	.000	.011	.000	.000	.000	.000	.000	.000
	N	180	180	180	180	180	180	180	180	180	180	180	180
B	Pearson Correlation	-.584**	-.994**	-.992**	1	.412**	.190*	.608**	.817**	-.751**	.515**	.305**	-.725**
	Sig. (2-tailed)	.000	.000	.000		.000	.010	.000	.000	.000	.000	.000	.000
	N	180	180	180	180	180	180	180	180	180	180	180	180
C	Pearson Correlation	-.735**	-.410**	-.409**	.412**	1	-.816**	.647**	.585**	-.517**	.834**	.674**	-.790**
	Sig. (2-tailed)	.000	.000	.000	.000		.000	.000	.000	.000	.000	.000	.000
	N	180	180	180	180	180	180	180	180	180	180	180	180
SCM	Pearson Correlation	.421**	-.189*	-.189*	.190*	-.816**	1	-.312**	-.112	.080	-.571**	-.532**	.391**
	Sig. (2-tailed)	.000	.011	.011	.010	.000		.000	.134	.285	.000	.000	.000
	N	180	180	180	180	180	180	180	180	180	180	180	180
fc	Pearson Correlation	-.777**	-.600**	-.606**	.608**	.647**	-.312**	1	.742**	-.718**	.723**	.262**	-.761**
	Sig. (2-tailed)	.000	.000	.000	.000	.000	.000		.000	.000	.000	.000	.000
	N	180	180	180	180	180	180	180	180	180	180	180	180
OPI	Pearson Correlation	-.738**	-.823**	-.800**	.817**	.585**	-.112	.742**	1	-.855**	.660**	.270**	-.871**
	Sig. (2-tailed)	.000	.000	.000	.000	.000	.134	.000		.000	.000	.000	.000
	N	180	180	180	180	180	180	180	180	180	180	180	180
WS	Pearson Correlation	.747**	.759**	.735**	-.751**	-.517**	.080	-.718**	-.855**	1	-.572**	-.115	.858**
	Sig. (2-tailed)	.000	.000	.000	.000	.000	.285	.000	.000		.000	.125	.000
	N	180	180	180	180	180	180	180	180	180	180	180	180
CH	Pearson Correlation	-.744**	-.511**	-.513**	.515**	.834**	-.571**	.723**	.660**	-.572**	1	.690**	-.828**
	Sig. (2-tailed)	.000	.000	.000	.000	.000	.000	.000	.000	.000		.000	.000
	N	180	180	180	180	180	180	180	180	180	180	180	180
CaO	Pearson Correlation	-.374**	-.302**	-.306**	.305**	.674**	-.532**	.262**	.270**	-.115	.690**	1	-.475**
	Sig. (2-tailed)	.000	.000	.000	.000	.000	.000	.000	.000	.125	.000		.000
	N	180	180	180	180	180	180	180	180	180	180	180	180
Kacc	Pearson Correlation	.857**	.734**	.713**	-.725**	-.790**	.391**	-.761**	-.871**	.858**	-.828**	-.475**	1
	Sig. (2-tailed)	.000	.000	.000	.000	.000	.000	.000	.000	.000	.000	.000	
	N	180	180	180	180	180	180	180	180	180	180	180	180

**. Correlation is significant at the 0.01 level (2-tailed).

*. Correlation is significant at the 0.05 level (2-tailed).

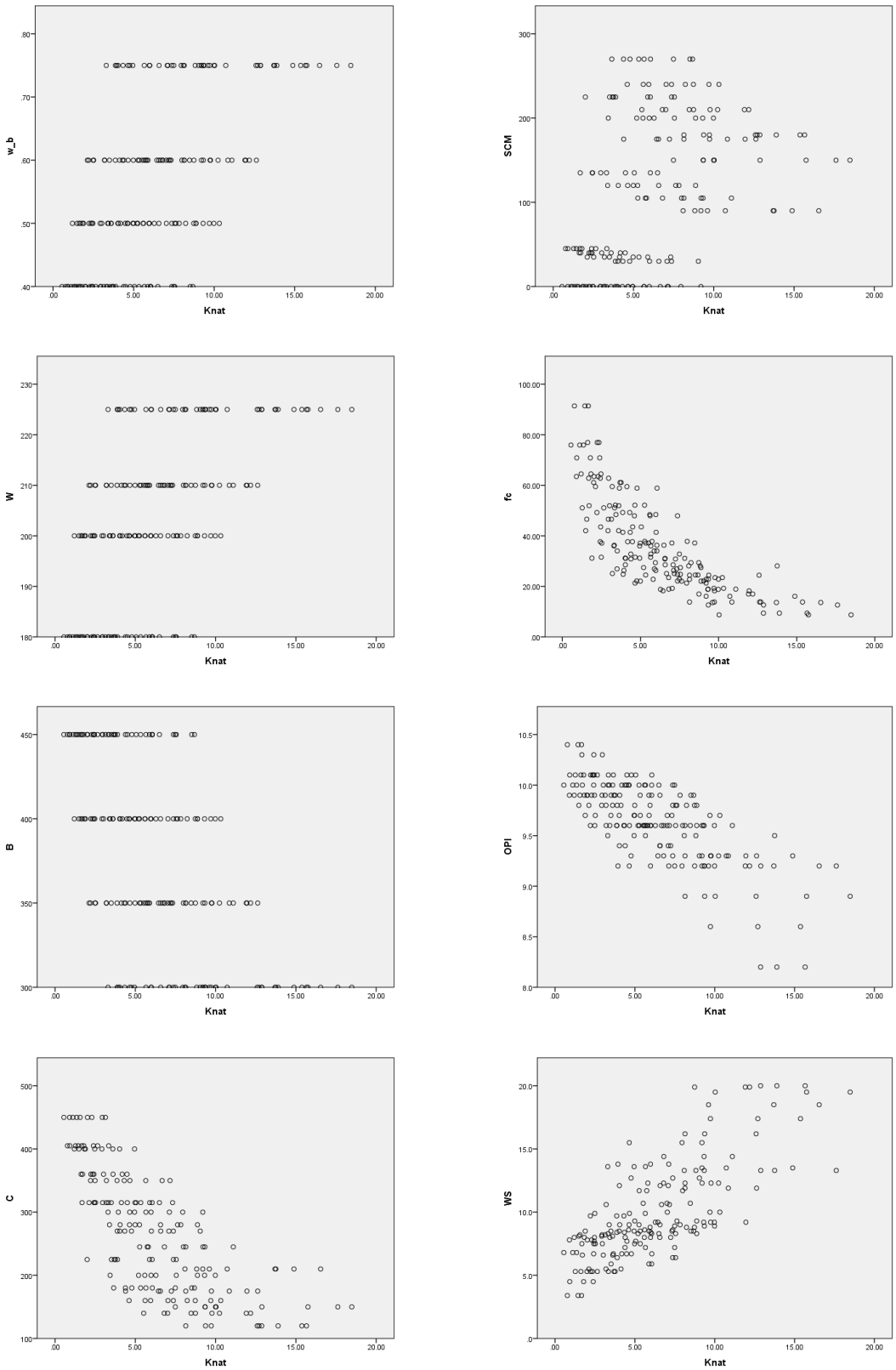


Figure E1: Scatter plots of the variables

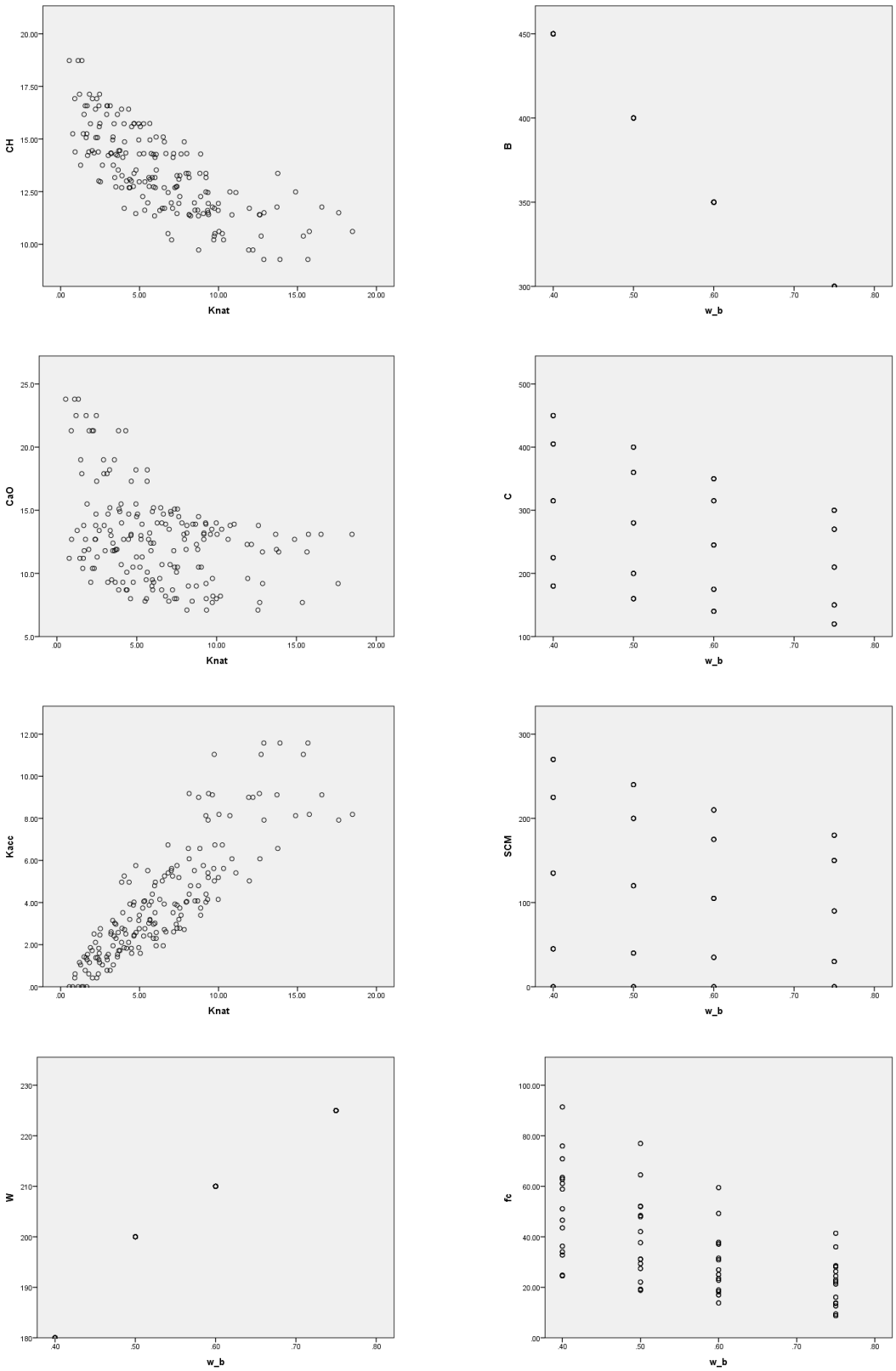


Figure E1: Scatter plots of the variables (continued)

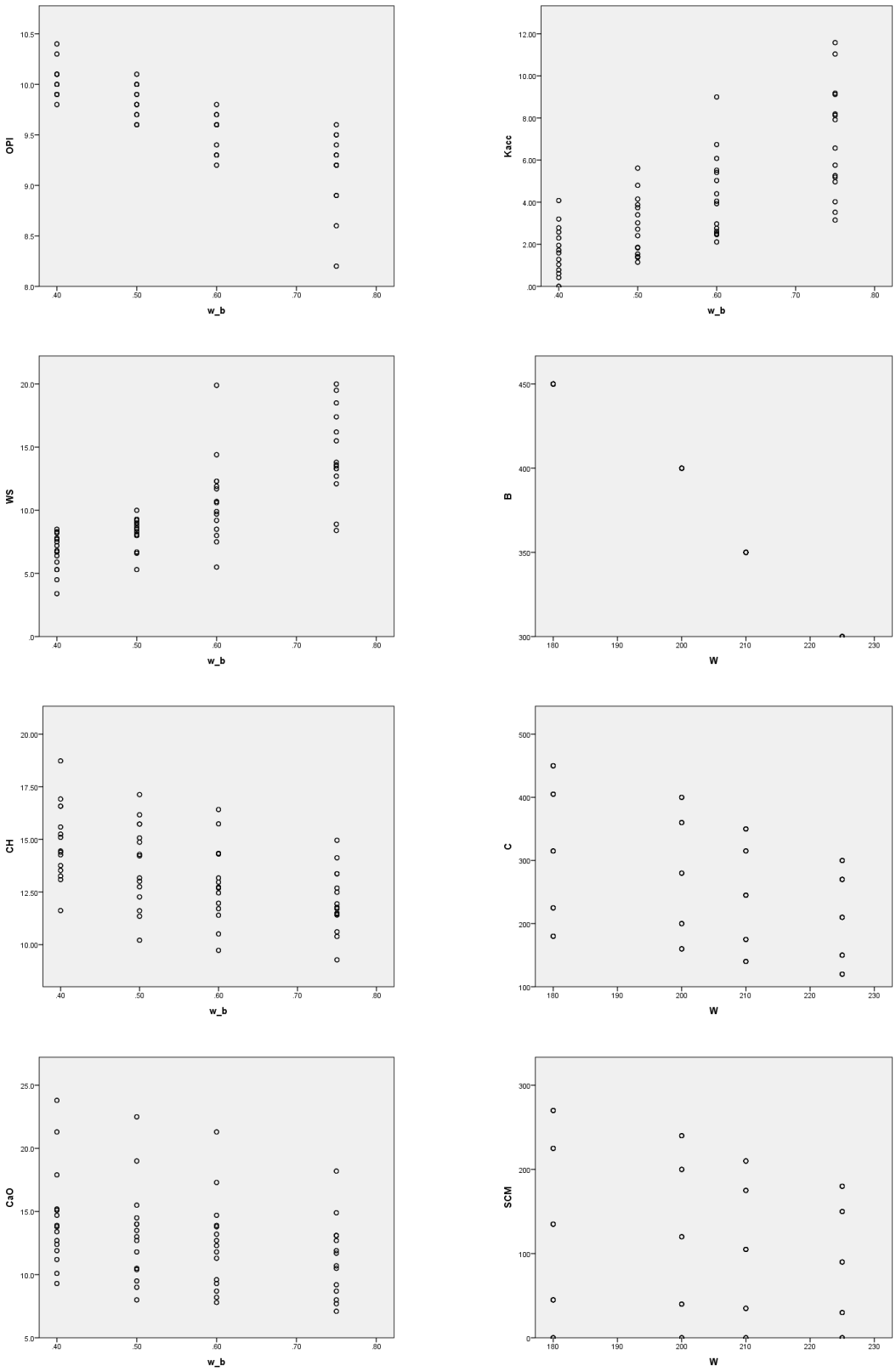


Figure E1: Scatter plots of the variables (continued)

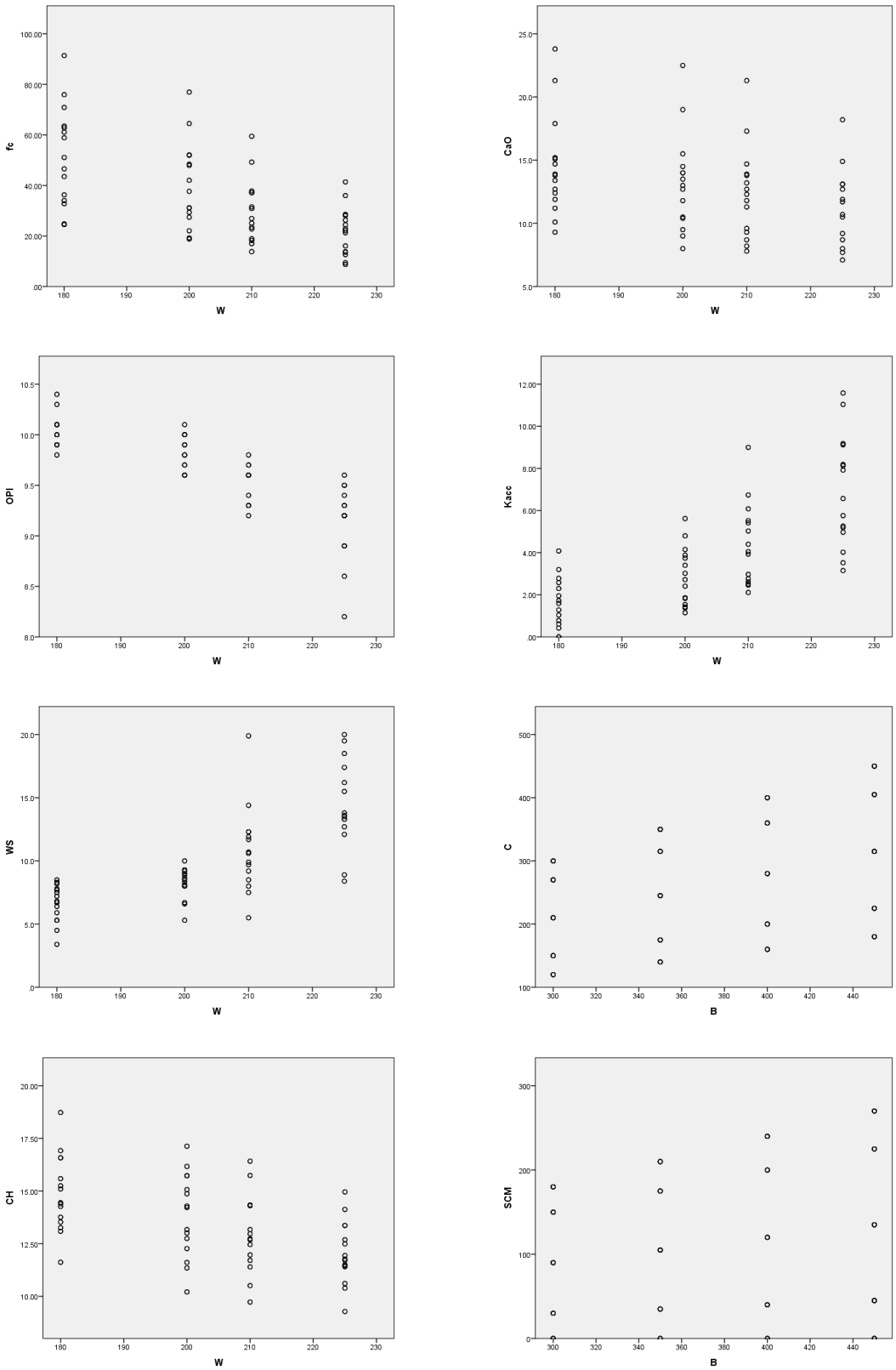


Figure E1: Scatter plots of the variables (continued)

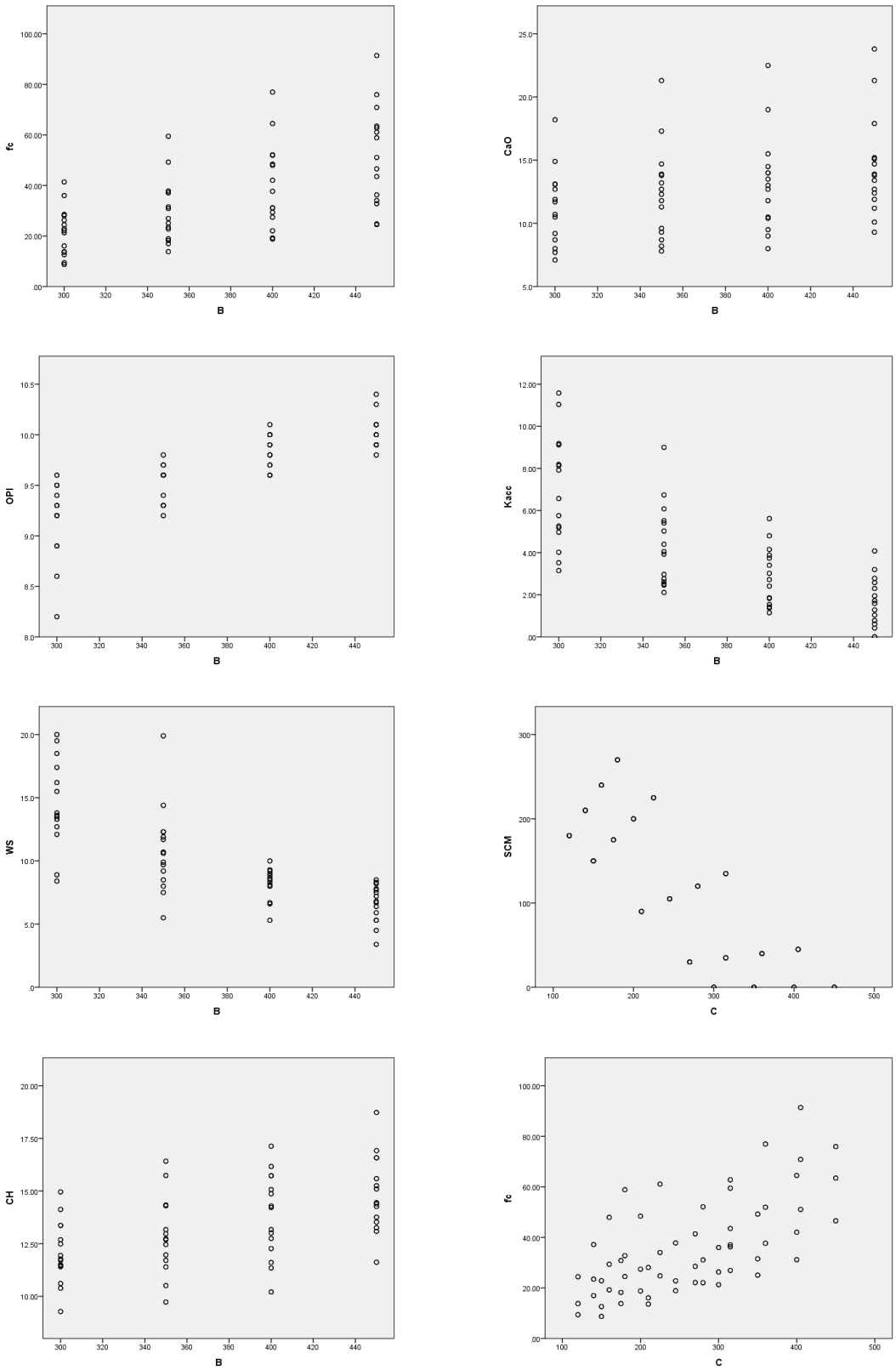


Figure E1: Scatter plots of the variables (continued)

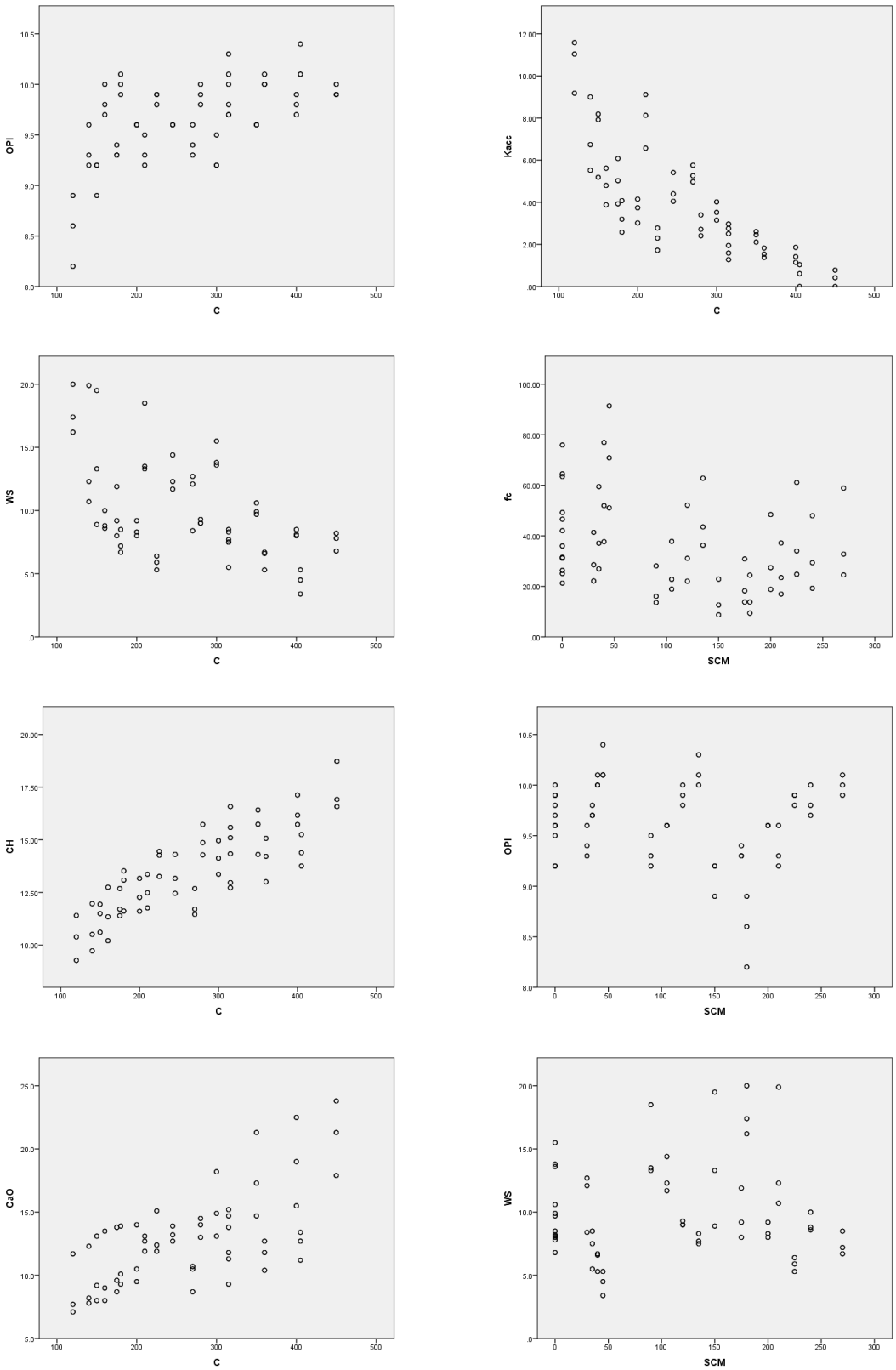


Figure E1: Scatter plots of the variables (continued)

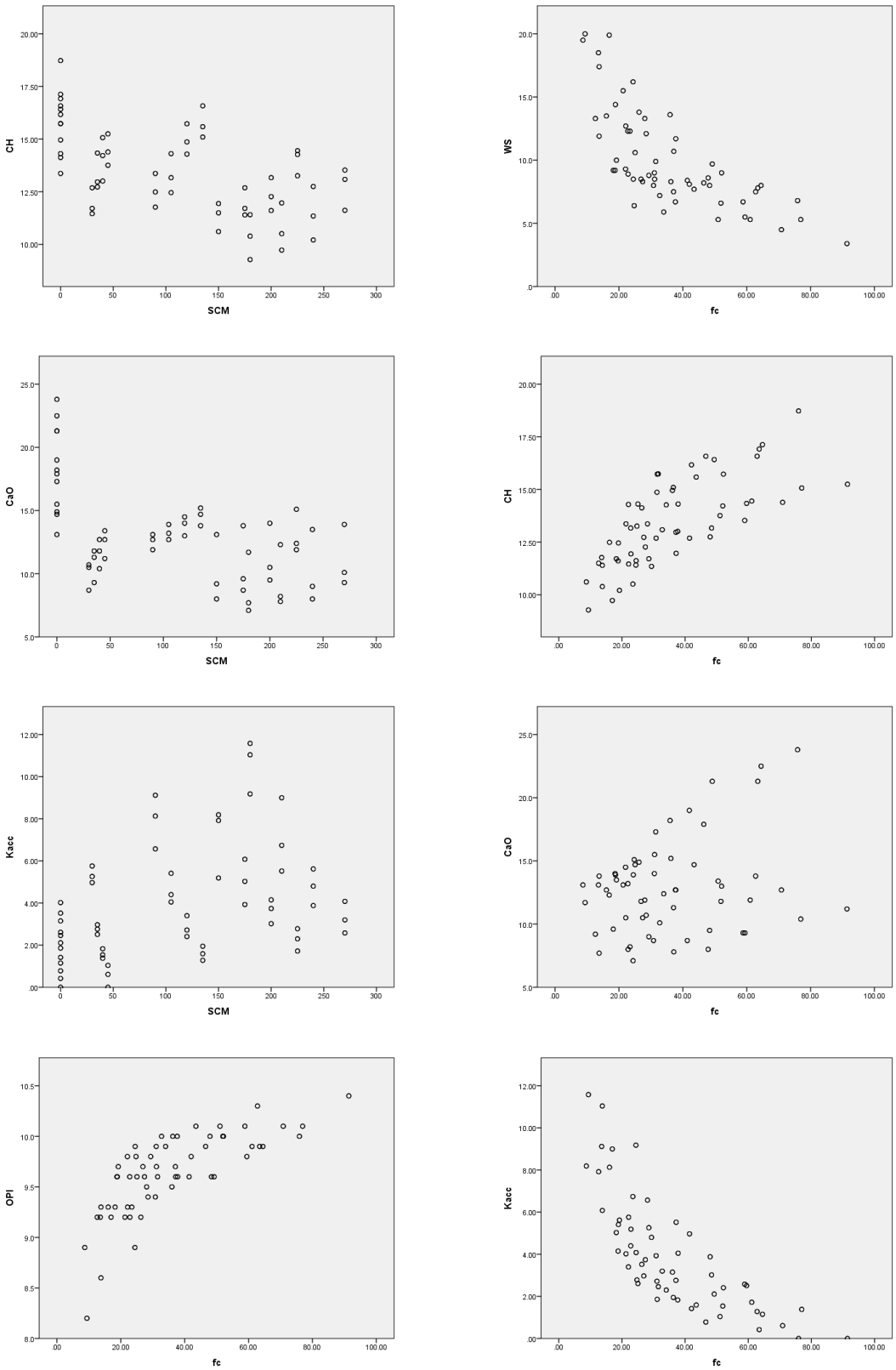


Figure E1: Scatter plots of the variables (continued)

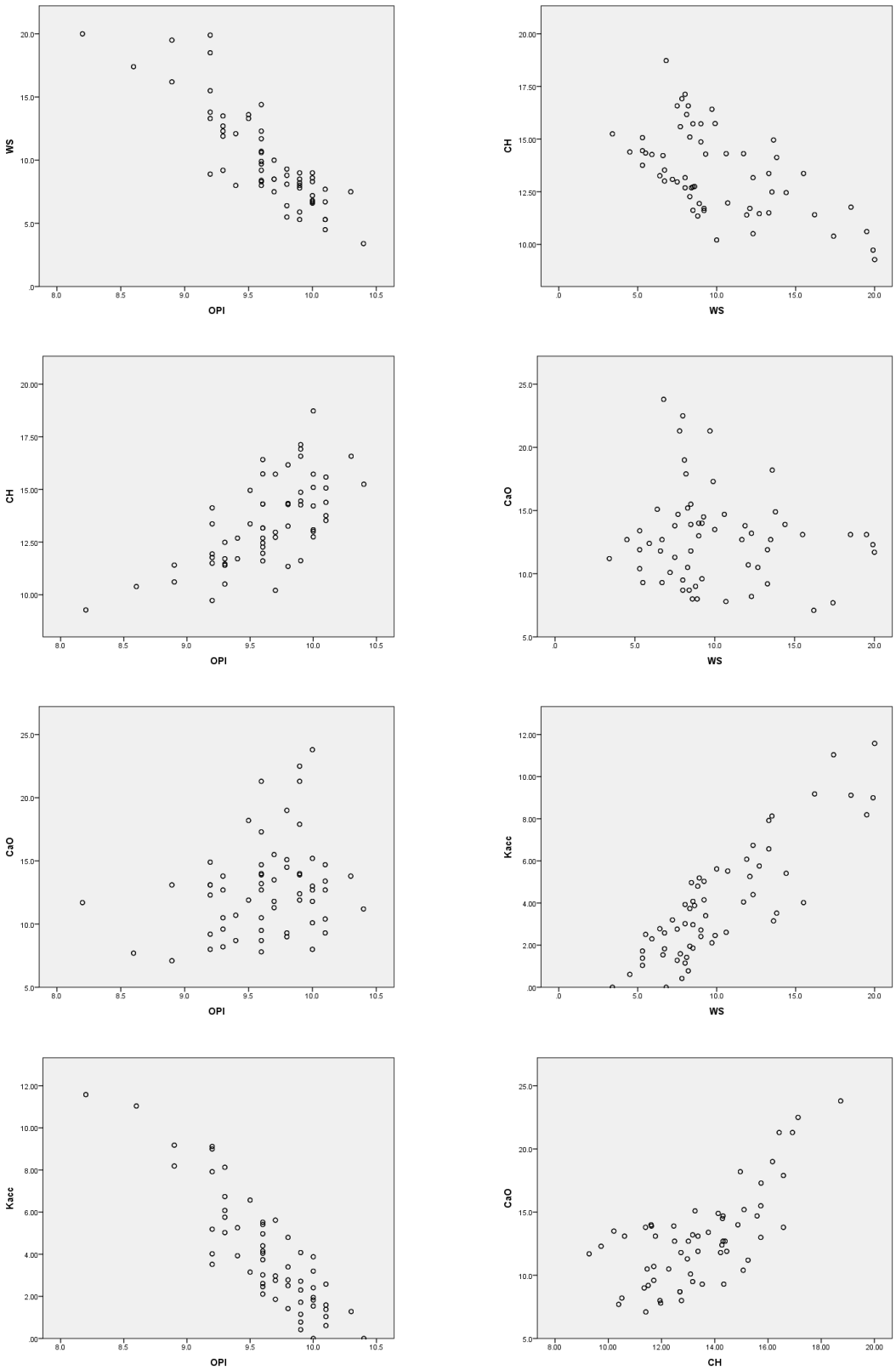


Figure E1: Scatter plots of the variables (continued)

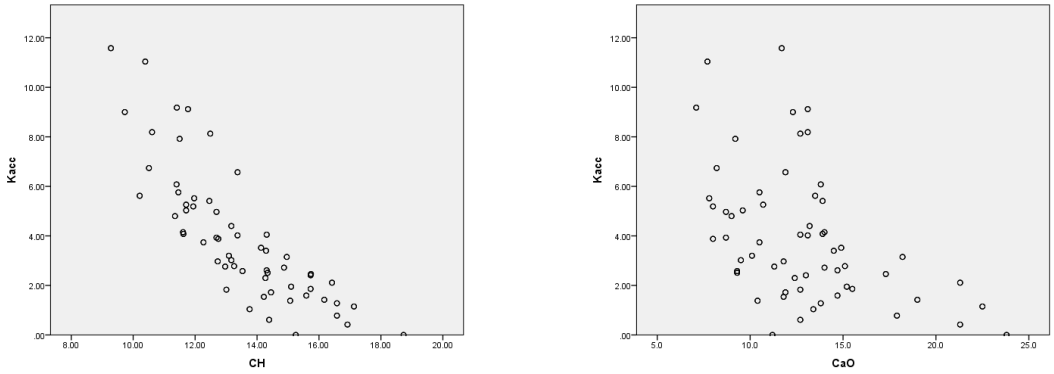


Figure E1: Scatter plots of the variables (continued)

Table E2: Association between the categorical variables

BT vs CP

Symmetric Measures

		Value	Approx. Sig.
Nominal by Nominal	Phi	.000	1.000
	Cramer's V	.000	1.000
N of Valid Cases		180	

a. Not assuming the null hypothesis.

b. Using the asymptotic standard error assuming the null hypothesis.

BT vs EC

Symmetric Measures

		Value	Approx. Sig.
Nominal by Nominal	Phi	.000	1.000
	Cramer's V	.000	1.000
N of Valid Cases		180	

a. Not assuming the null hypothesis.

b. Using the asymptotic standard error assuming the null hypothesis.

CP vs EC

Symmetric Measures

		Value	Approx. Sig.
Nominal by Nominal	Phi	.000	1.000
	Cramer's V	.000	1.000
N of Valid Cases		180	

a. Not assuming the null hypothesis.

b. Using the asymptotic standard error assuming the null hypothesis.

Table E3: Association between the continuous and categorical variables

ANOVA

Knat

	Sum of Squares	df	Mean Square	F	Sig.
Between Groups	854.034	4	213.508	22.765	.000
Within Groups	1641.279	175	9.379		
Total	2495.312	179			

ANOVA

w_b

	Sum of Squares	df	Mean Square	F	Sig.
Between Groups	.000	4	.000	.000	1.000
Within Groups	3.009	175	.017		
Total	3.009	179			

ANOVA

W

	Sum of Squares	df	Mean Square	F	Sig.
Between Groups	.000	4	.000	.000	1.000
Within Groups	48093.750	175	274.821		
Total	48093.750	179			

ANOVA

B

	Sum of Squares	df	Mean Square	F	Sig.
Between Groups	.000	4	.000	.000	1.000
Within Groups	562500.000	175	3214.286		
Total	562500.000	179			

ANOVA

C

	Sum of Squares	df	Mean Square	F	Sig.
Between Groups	1316250.000	4	329062.500	188.884	.000
Within Groups	304875.000	175	1742.143		
Total	1621125.000	179			

ANOVA

SCM

	Sum of Squares	df	Mean Square	F	Sig.
Between Groups	1316250.000	4	329062.500	720.951	.000
Within Groups	79875.000	175	456.429		
Total	1396125.000	179			

ANOVA

Fc

	Sum of Squares	df	Mean Square	F	Sig.
Between Groups	14126.782	4	3531.696	12.993	.000
Within Groups	47569.229	175	271.824		
Total	61696.012	179			

ANOVA

OPI

	Sum of Squares	df	Mean Square	F	Sig.
Between Groups	4.360	4	1.090	7.661	.000
Within Groups	24.900	175	.142		
Total	29.260	179			

ANOVA

WS

	Sum of Squares	df	Mean Square	F	Sig.
Between Groups	515.268	4	128.817	10.306	.000
Within Groups	2187.437	175	12.500		
Total	2702.705	179			

ANOVA

CH

	Sum of Squares	df	Mean Square	F	Sig.
Between Groups	427.060	4	106.765	61.456	.000
Within Groups	304.021	175	1.737		
Total	731.081	179			

ANOVA

CaO

	Sum of Squares	df	Mean Square	F	Sig.
Between Groups	1582.587	4	395.647	81.622	.000
Within Groups	848.283	175	4.847		
Total	2430.869	179			

ANOVA

Kacc

	Sum of Squares	df	Mean Square	F	Sig.
Between Groups	449.752	4	112.438	23.383	.000
Within Groups	841.489	175	4.809		
Total	1291.241	179			

ANOVA

Knat

	Sum of Squares	df	Mean Square	F	Sig.
Between Groups	252.962	2	126.481	9.984	.000
Within Groups	2242.351	177	12.669		
Total	2495.312	179			

ANOVA

w_b

	Sum of Squares	df	Mean Square	F	Sig.
Between Groups	.000	2	.000	.000	1.000
Within Groups	3.009	177	.017		
Total	3.009	179			

ANOVA

W

	Sum of Squares	df	Mean Square	F	Sig.
Between Groups	.000	2	.000	.000	1.000
Within Groups	48093.750	177	271.716		
Total	48093.750	179			

ANOVA

B

	Sum of Squares	df	Mean Square	F	Sig.
Between Groups	.000	2	.000	.000	1.000
Within Groups	562500.000	177	3177.966		
Total	562500.000	179			

ANOVA

C

	Sum of Squares	df	Mean Square	F	Sig.
Between Groups	.000	2	.000	.000	1.000
Within Groups	1621125.000	177	9158.898		
Total	1621125.000	179			

ANOVA

SCM

	Sum of Squares	df	Mean Square	F	Sig.
Between Groups	.000	2	.000	.000	1.000
Within Groups	1396125.000	177	7887.712		
Total	1396125.000	179			

ANOVA

fc

	Sum of Squares	df	Mean Square	F	Sig.
Between Groups	20981.194	2	10490.597	45.606	.000
Within Groups	40714.817	177	230.027		
Total	61696.012	179			

ANOVA

OPI

	Sum of Squares	df	Mean Square	F	Sig.
Between Groups	1.417	2	.709	4.504	.012
Within Groups	27.843	177	.157		
Total	29.260	179			

ANOVA

WS

	Sum of Squares	df	Mean Square	F	Sig.
Between Groups	252.727	2	126.363	9.129	.000
Within Groups	2449.978	177	13.842		
Total	2702.705	179			

ANOVA

CH

	Sum of Squares	df	Mean Square	F	Sig.
Between Groups	88.095	2	44.048	12.125	.000
Within Groups	642.986	177	3.633		
Total	731.081	179			

ANOVA

CaO

	Sum of Squares	df	Mean Square	F	Sig.
Between Groups	63.268	2	31.634	2.365	.097
Within Groups	2367.601	177	13.376		
Total	2430.869	179			

ANOVA

Kacc

	Sum of Squares	df	Mean Square	F	Sig.
Between Groups	57.397	2	28.698	4.117	.018
Within Groups	1233.844	177	6.971		
Total	1291.241	179			

ANOVA

Knat

	Sum of Squares	df	Mean Square	F	Sig.
Between Groups	304.900	2	152.450	12.319	.000
Within Groups	2190.412	177	12.375		
Total	2495.312	179			

ANOVA

w_b

	Sum of Squares	df	Mean Square	F	Sig.
Between Groups	.000	2	.000	.000	1.000
Within Groups	3.009	177	.017		
Total	3.009	179			

ANOVA

W

	Sum of Squares	df	Mean Square	F	Sig.
Between Groups	.000	2	.000	.000	1.000
Within Groups	48093.750	177	271.716		
Total	48093.750	179			

ANOVA

B

	Sum of Squares	df	Mean Square	F	Sig.
Between Groups	.000	2	.000	.000	1.000
Within Groups	562500.000	177	3177.966		
Total	562500.000	179			

ANOVA

C

	Sum of Squares	df	Mean Square	F	Sig.
Between Groups	.000	2	.000	.000	1.000
Within Groups	1621125.000	177	9158.898		
Total	1621125.000	179			

ANOVA

SCM

	Sum of Squares	df	Mean Square	F	Sig.
Between Groups	.000	2	.000	.000	1.000
Within Groups	1396125.000	177	7887.712		
Total	1396125.000	179			

ANOVA

fc

	Sum of Squares	df	Mean Square	F	Sig.
Between Groups	.000	2	.000	.000	1.000
Within Groups	61696.012	177	348.565		
Total	61696.012	179			

ANOVA

OPI

	Sum of Squares	df	Mean Square	F	Sig.
Between Groups	.000	2	.000	.000	1.000
Within Groups	29.260	177	.165		
Total	29.260	179			

ANOVA

WS

	Sum of Squares	df	Mean Square	F	Sig.
Between Groups	.000	2	.000	.000	1.000
Within Groups	2702.705	177	15.270		
Total	2702.705	179			

ANOVA

CH

	Sum of Squares	df	Mean Square	F	Sig.
Between Groups	.000	2	.000	.000	1.000
Within Groups	731.081	177	4.130		
Total	731.081	179			

ANOVA

CaO

	Sum of Squares	df	Mean Square	F	Sig.
Between Groups	.000	2	.000	.000	1.000
Within Groups	2430.869	177	13.734		
Total	2430.869	179			

ANOVA

Kacc

	Sum of Squares	df	Mean Square	F	Sig.
Between Groups	.000	2	.000	.000	1.000
Within Groups	1291.241	177	7.295		
Total	1291.241	179			

Appendix F: Regression analysis output

The results of the multiple linear regression analysis between the response variables and the individual sets of the predictor variables are presented.

This Appendix contains the following output results for each of the fourteen models:

- ANOVA table;
- Model Summary table;
- Coefficients table;
- Histogram;
- P-P plot;
- Scatter plots;
- Partial regression plots.

Model 1 – *w/b, C, CP, EC*

Model Summary[b]

Model	R	R Square	Adjusted R Square	Std. Error of the Estimate	Durbin-Watson
1	.930[a]	.864	.860	1.39902	1.412

a. Predictors: (Constant), OutdoorExposed, SevenDays, C, w_b, Threedays, OutdoorSheltered

b. Dependent Variable: Knat

ANOVA[a]

Model		Sum of Squares	df	Mean Square	F	Sig.
1	Regression	2156.707	6	359.451	183.650	.000[b]
	Residual	338.605	173	1.957		
	Total	2495.312	179			

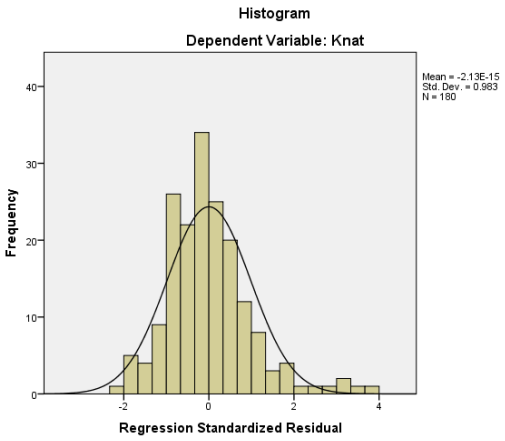
a. Dependent Variable: Knat

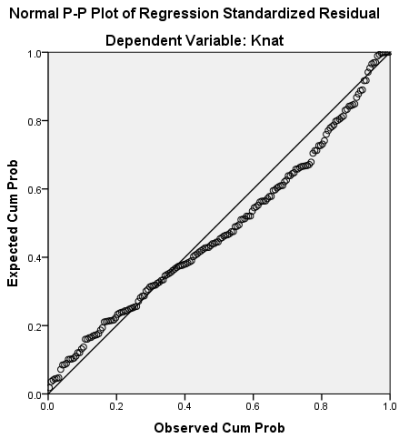
b. Predictors: (Constant), OutdoorExposed, SevenDays, C, w_b, Threedays, OutdoorSheltered

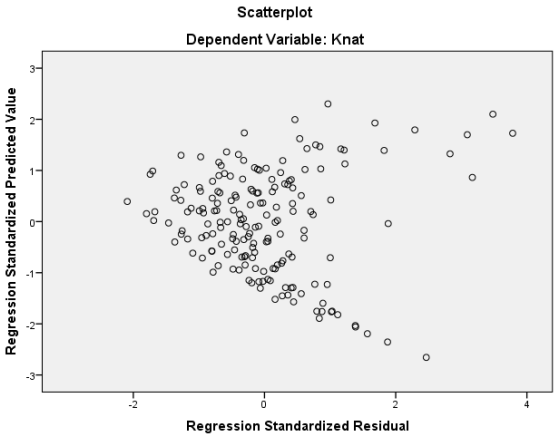
Coefficients[a]

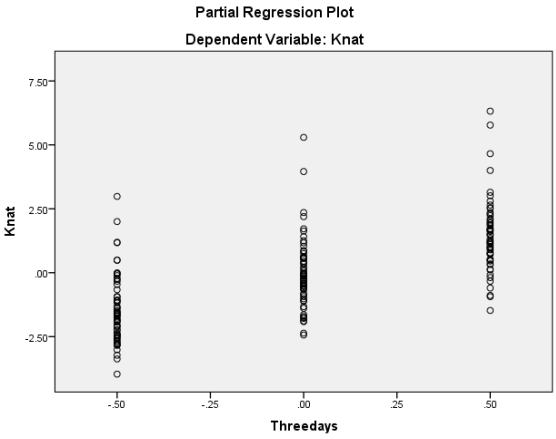
Model		Unstandardized Coefficients		Standardized Coefficients	t	Sig.	95.0% Confidence Interval for B		Correlations			Collinearity Statistics	
		B	Std. Error	Beta			Lower Bound	Upper Bound	Zero-order	Partial	Part	Tolerance	VIF
1	(Constant)	5.625	.729		7.721	.000	4.187	7.063					
	w_b	10.010	.884	.348	11.321	.000	8.265	11.755	.591	.652	.317	.832	1.202
	C	-.023	.001	-.592	-19.294	.000	-.026	-.021	-.735	-.826	-.540	.832	1.202
	Threedays	2.898	.255	.367	11.346	.000	2.394	3.402	.265	.653	.318	.750	1.333
	SevenDays	1.606	.255	.203	6.286	.000	1.102	2.110	.020	.431	.176	.750	1.333
	OutdoorSheltered	1.066	.255	.135	4.174	.000	.562	1.570	.266	.302	.117	.750	1.333
	OutdoorExposed	-2.069	.255	-.262	-8.100	.000	-2.573	-1.565	-.329	-.524	-.227	.750	1.333

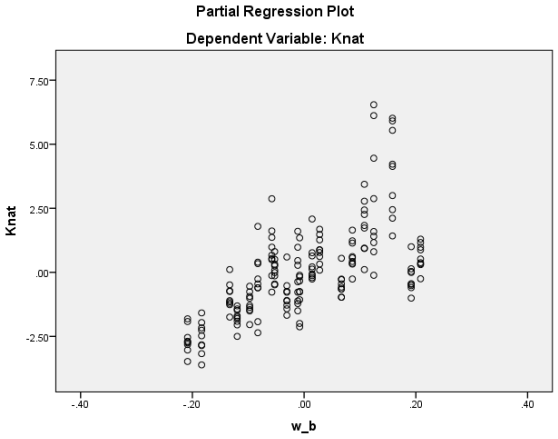
a. Dependent Variable: Knat

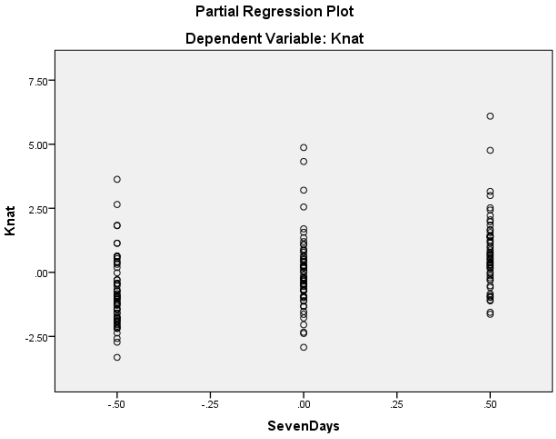


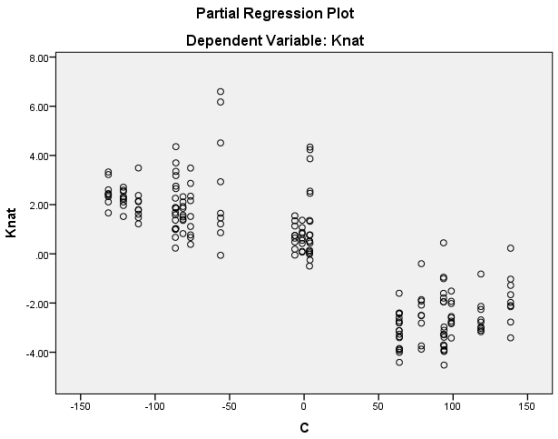


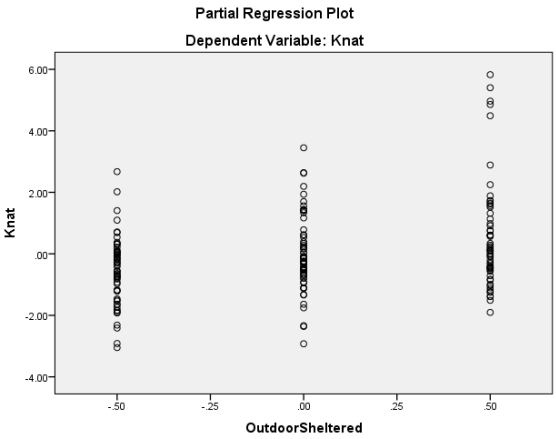

Scatterplot
Dependent Variable: Knat
Regression Standardized Predicted Value
Regression Standardized Residual

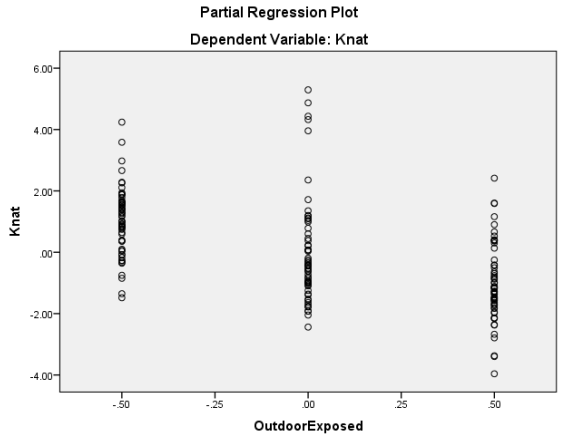

Partial Regression Plot
Dependent Variable: Knat
Knat
Threedays


Partial Regression Plot
Dependent Variable: Knat
Knat
w_b


Partial Regression Plot
Dependent Variable: Knat
Knat
SevenDays


Partial Regression Plot
Dependent Variable: Knat
Knat
C


Partial Regression Plot
Dependent Variable: Knat
Knat
OutdoorSheltered


Partial Regression Plot
Dependent Variable: Knat
Knat
6.00
4.00
2.00
.00
-2.00
-4.00
-.50
-.25
.00
.25
.50
OutdoorExposed

Model 2 – *w/b, BT, CP, EC*

Model Summary[b]

Model	R	R Square	Adjusted R Square	Std. Error of the Estimate	Durbin-Watson
1	.956[a]	.915	.910	1.11987	1.522

a. Predictors: (Constant), OutdoorExposed, SevenDays, CEMV, w_b, CEMICSF, CEMIGGBS, Threedays, OutdoorSheltered, CEMIFA

b. Dependent Variable: Knat

ANOVA[a]

Model		Sum of Squares	df	Mean Square	F	Sig.
1	Regression	2282.115	9	253.568	202.191	.000[b]
	Residual	213.197	170	1.254		
	Total	2495.312	179			

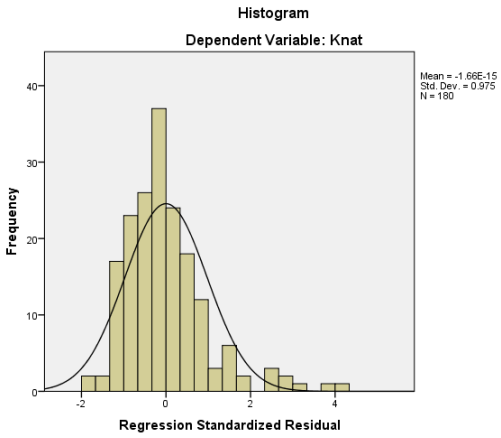
a. Dependent Variable: Knat

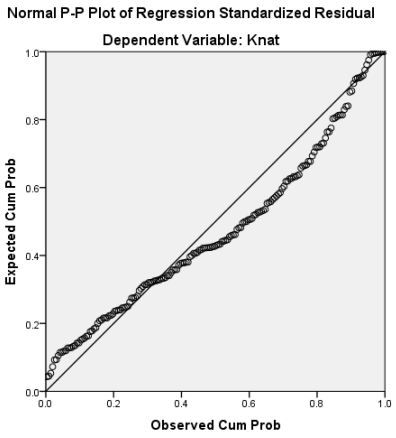
b. Predictors: (Constant), OutdoorExposed, SevenDays, CEMV, w_b, CEMICSF, CEMIGGBS, Threedays, OutdoorSheltered, CEMIFA

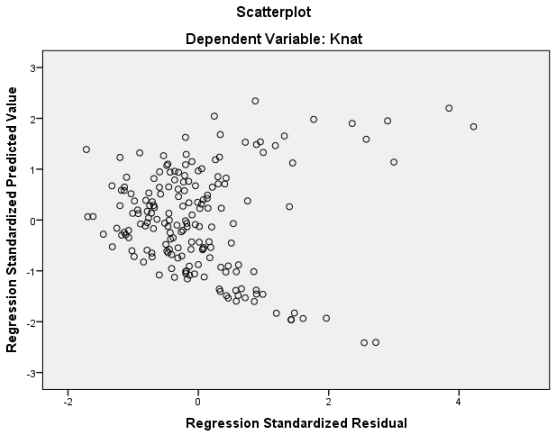
Coefficients[a]

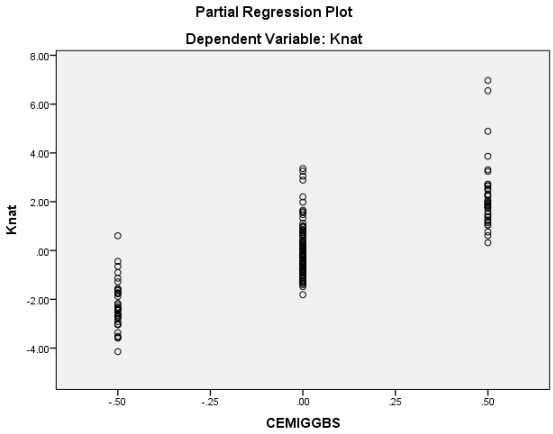
Model		Unstandardized Coefficients		Standardized Coefficients	t	Sig.	95.0% Confidence Interval for B		Correlations			Collinearity Statistics	
		B	Std. Error	Beta			Lower Bound	Upper Bound	Zero-order	Partial	Part	Tolerance	VIF
1	(Constant)	-7.033	.441		-15.944	.000	-7.903	-6.162					
	w_b	17.005	.646	.591	26.342	.000	15.731	18.279	.591	.896	.591	1.000	1.000
	CEMIFA	3.603	.264	.387	13.648	.000	3.081	4.124	.132	.723	.306	.625	1.600
	CEMIGGBS	4.488	.264	.482	17.001	.000	3.966	5.009	.251	.794	.381	.625	1.600
	CEMICSF	.020	.264	.002	.076	.940	-.501	.541	-.349	.006	.002	.625	1.600
	CEMV	4.996	.264	.537	18.928	.000	4.475	5.517	.319	.824	.424	.625	1.600
	Threedays	2.898	.204	.367	14.175	.000	2.495	3.302	.265	.736	.318	.750	1.333
	SevenDays	1.606	.204	.203	7.853	.000	1.202	2.009	.020	.516	.176	.750	1.333
	OutdoorSheltered	1.066	.204	.135	5.215	.000	.663	1.470	.266	.371	.117	.750	1.333
	OutdoorExposed	-2.069	.204	-.262	-10.119	.000	-2.472	-1.665	-.329	-.613	-.227	.750	1.333

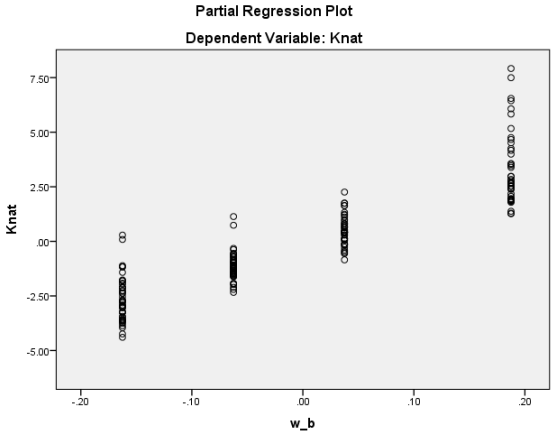
a. Dependent Variable: Knat

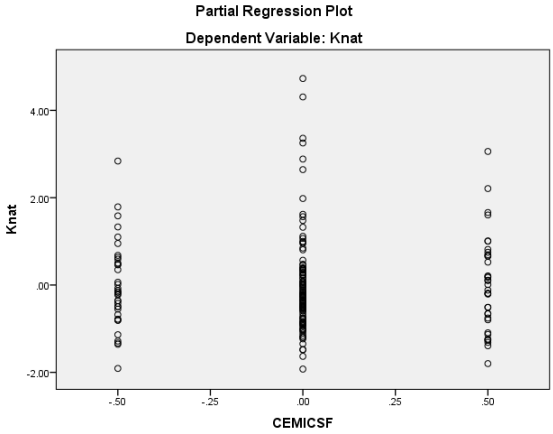


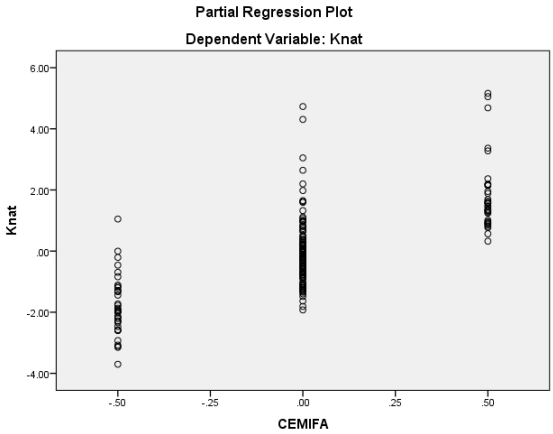


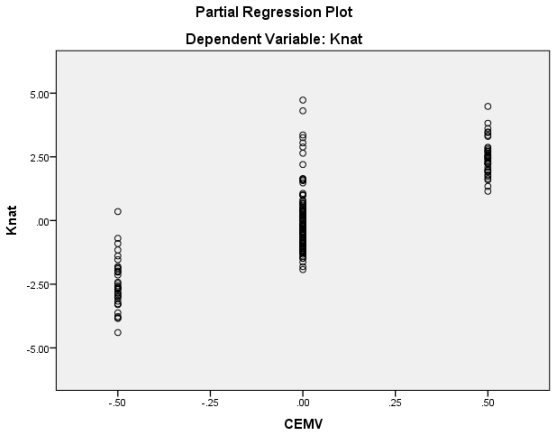

Scatterplot
Dependent Variable: Knat
Regression Standardized Predicted Value
Regression Standardized Residual

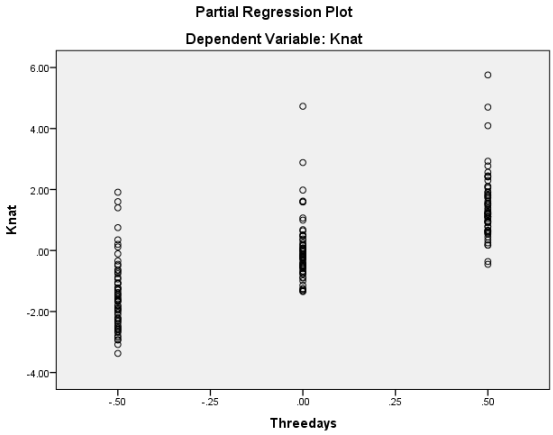

Partial Regression Plot
Dependent Variable: Knat
Knat
CEMIGGBS

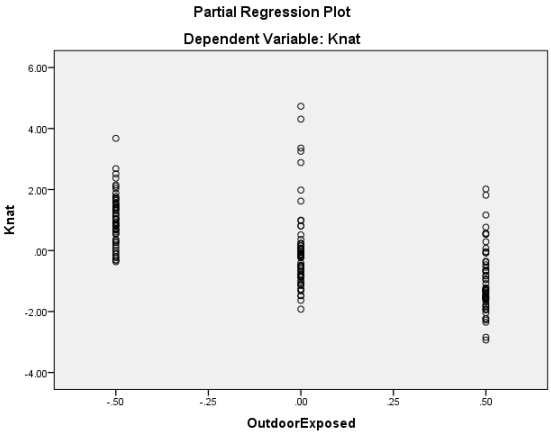

Partial Regression Plot
Dependent Variable: Knat
Knat
w_b

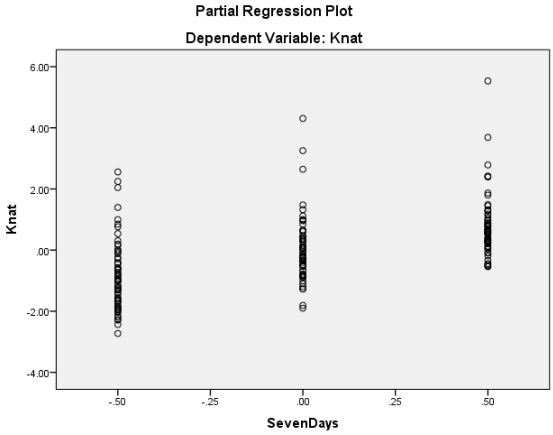

Partial Regression Plot
Dependent Variable: Knat
Knat
CEMICSF

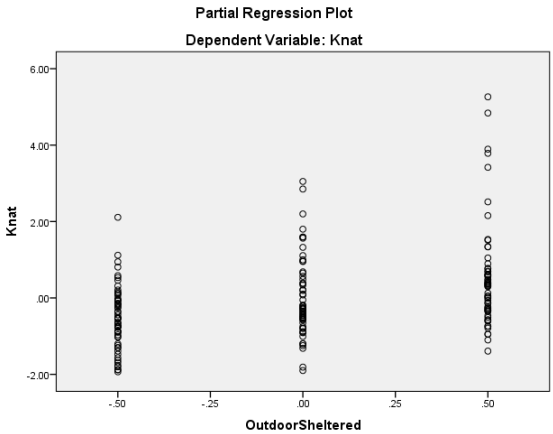

Partial Regression Plot
Dependent Variable: Knat
Knat
CEMIFA


Partial Regression Plot
Dependent Variable: Knat
Knat
CEMV


Partial Regression Plot
Dependent Variable: Knat
Knat
Threedays


Partial Regression Plot
Dependent Variable: Knat
Knat
OutdoorExposed


Partial Regression Plot
Dependent Variable: Knat
Knat
SevenDays


Partial Regression Plot
Dependent Variable: Knat
Knat
OutdoorSheltered

Model 3 – f_c, *EC*

Model Summary[b]

Model	R	R Square	Adjusted R Square	Std. Error of the Estimate	Durbin-Watson
1	.852[a]	.726	.722	1.97007	1.274

a. Predictors: (Constant), OutdoorExposed, fc, OutdoorSheltered

b. Dependent Variable: Knat

ANOVA[a]

Model		Sum of Squares	df	Mean Square	F	Sig.
1	Regression	1812.226	3	604.075	155.642	.000[b]
	Residual	683.087	176	3.881		
	Total	2495.312	179			

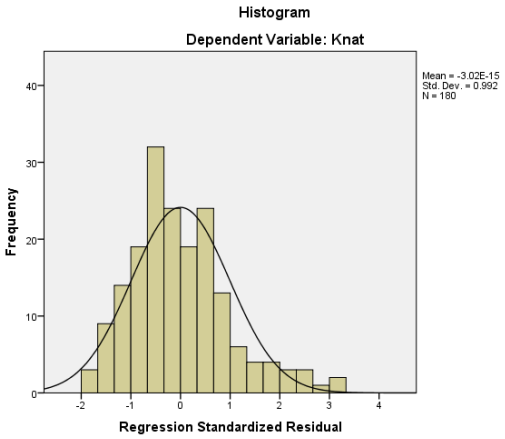
a. Dependent Variable: Knat

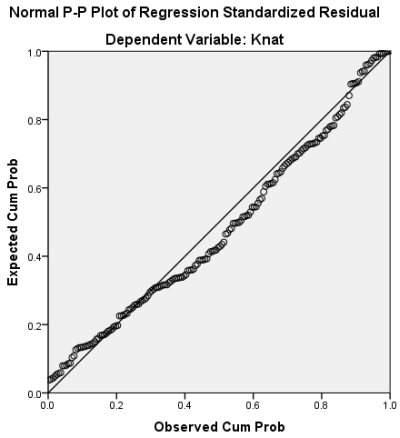
b. Predictors: (Constant), OutdoorExposed, fc, OutdoorSheltered

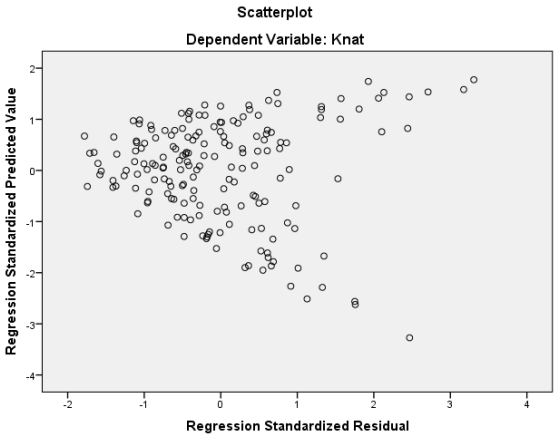
Coefficients[a]

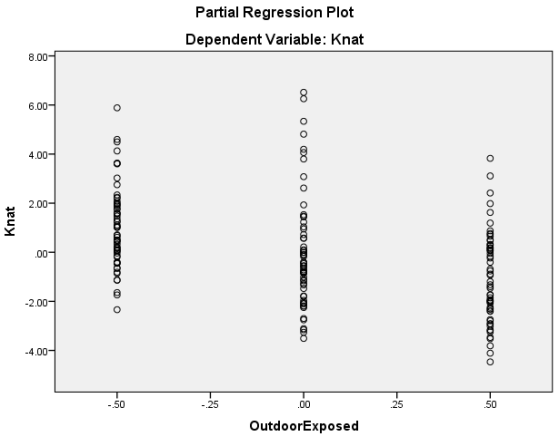
Model		Unstandardized Coefficients		Standardized Coefficients	t	Sig.	95.0% Confidence Interval for B		Correlations			Collinearity Statistics	
		B	Std. Error	Beta			Lower Bound	Upper Bound	Zero-order	Partial	Part	Tolerance	VIF
1	(Constant)	12.265	.382		32.130	.000	11.511	13.018					
	fc	-.156	.008	-.777	-19.707	.000	-.172	-.141	-.777	-.830	-.777	1.000	1.000
	OutdoorSheltered	1.066	.360	.135	2.964	.003	.356	1.776	.266	.218	.117	.750	1.333
	OutdoorExposed	-2.069	.360	-.262	-5.752	.000	-2.779	-1.359	-.329	-.398	-.227	.750	1.333

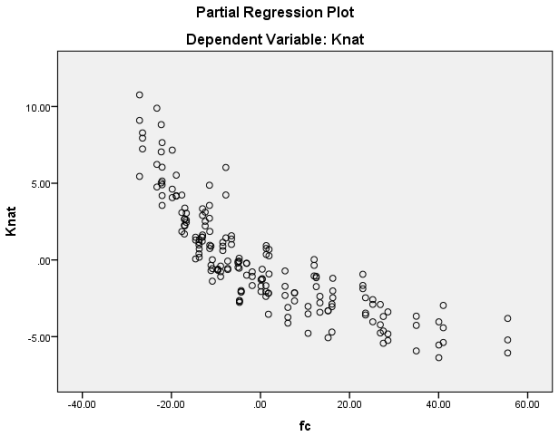
a. Dependent Variable: Knat

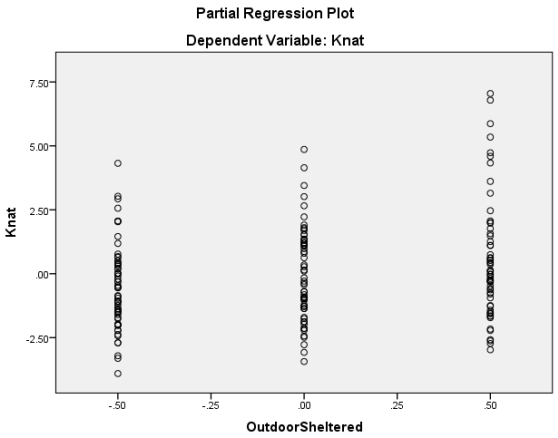





Scatterplot
Dependent Variable: Knat
Regression Standardized Predicted Value
Regression Standardized Residual


Partial Regression Plot
Dependent Variable: Knat
Knat
OutdoorExposed


Partial Regression Plot
Dependent Variable: Knat
Knat
fc


Partial Regression Plot
Dependent Variable: Knat
Knat
OutdoorSheltered

Model 4 – f_c, *CP, EC*

Model Summary[b]

Model	R	R Square	Adjusted R Square	Std. Error of the Estimate	Durbin-Watson
1	.870[a]	.757	.750	1.86687	1.364

a. Predictors: (Constant), OutdoorExposed, SevenDays, fc, OutdoorSheltered, Threedays

b. Dependent Variable: Knat

ANOVA[a]

Model		Sum of Squares	df	Mean Square	F	Sig.
1	Regression	1888.886	5	377.777	108.394	.000[b]
	Residual	606.426	174	3.485		
	Total	2495.312	179			

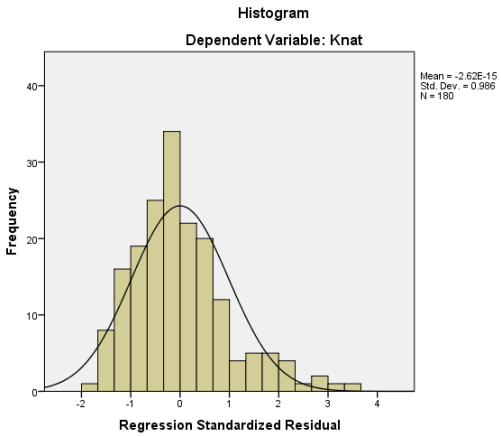
a. Dependent Variable: Knat

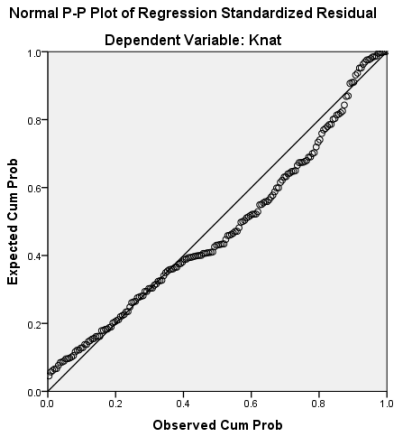
b. Predictors: (Constant), OutdoorExposed, SevenDays, fc, OutdoorSheltered, Threedays

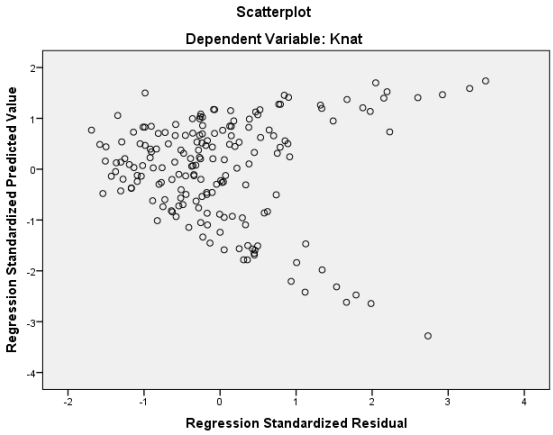
Coefficients[a]

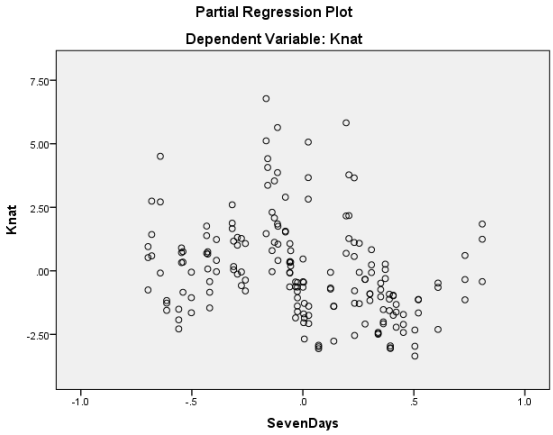
Model		Unstandardized Coefficients		Standardized Coefficients	t	Sig.	95.0% Confidence Interval for B		Correlations			Collinearity Statistics	
		B	Std. Error	Beta			Lower Bound	Upper Bound	Zero-order	Partial	Part	Tolerance	VIF
1	(Constant)	14.260	.560		25.451	.000	13.154	15.366					
	fc	-.181	.009	-.899	-19.542	.000	-.199	-.163	-.777	-.829	-.730	.660	1.515
	Threedays	-1.788	.417	-.226	-4.290	.000	-2.610	-.965	.265	-.309	-.160	.502	1.993
	SevenDays	-1.561	.377	-.198	-4.137	.000	-2.306	-.816	.020	-.299	-.155	.612	1.635
	OutdoorSheltered	1.066	.341	.135	3.128	.002	.393	1.739	.266	.231	.117	.750	1.333
	OutdoorExposed	-2.069	.341	-.262	-6.070	.000	-2.742	-1.396	-.329	-.418	-.227	.750	1.333

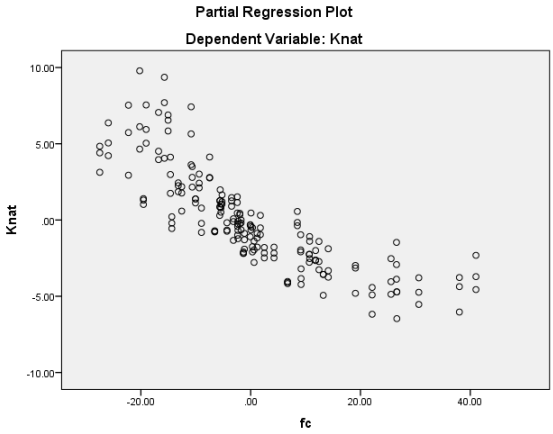
a. Dependent Variable: Knat

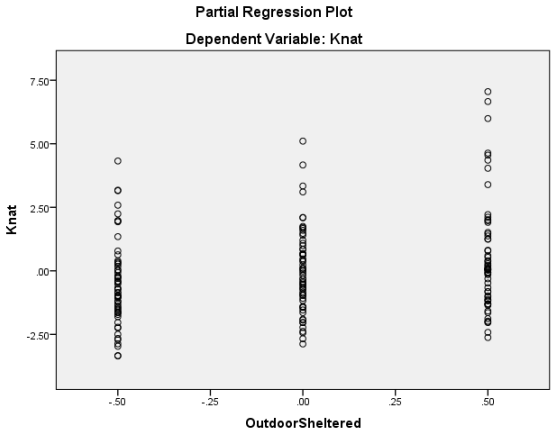


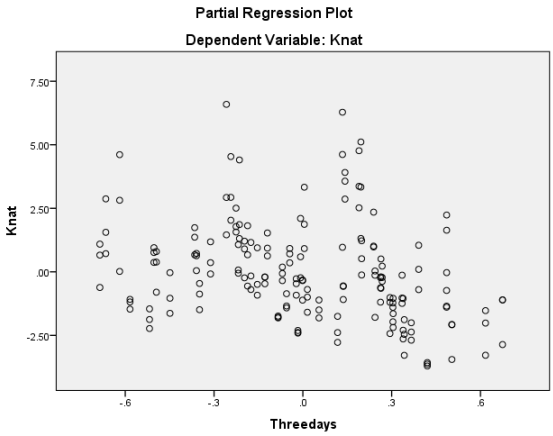


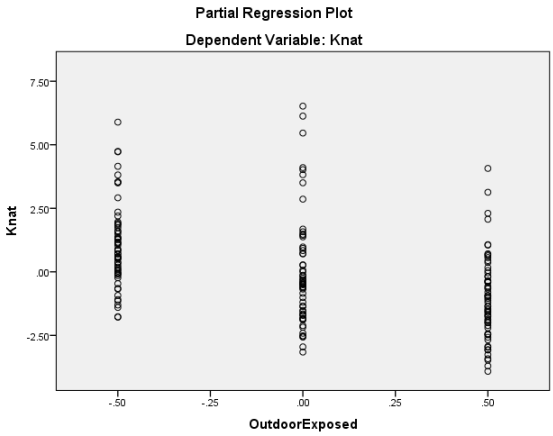

Scatterplot
Dependent Variable: Knat
Regression Standardized Predicted Value
Regression Standardized Residual


Partial Regression Plot
Dependent Variable: Knat
Knat
SevenDays


Partial Regression Plot
Dependent Variable: Knat
Knat
fc


Partial Regression Plot
Dependent Variable: Knat
Knat
OutdoorSheltered


Partial Regression Plot
Dependent Variable: Knat
Knat
Threedays


Partial Regression Plot
Dependent Variable: Knat
Knat
OutdoorExposed

Model 5 - *OPI, EC*

Model Summary[b]

Model	R	R Square	Adjusted R Square	Std. Error of the Estimate	Durbin-Watson
1	.817[a]	.667	.661	2.17295	1.089

a. Predictors: (Constant), OutdoorExposed, OPI, OutdoorSheltered

b. Dependent Variable: Knat

ANOVA[a]

Model		Sum of Squares	df	Mean Square	F	Sig.
1	Regression	1664.291	3	554.764	117.492	.000[b]
	Residual	831.021	176	4.722		
	Total	2495.312	179			

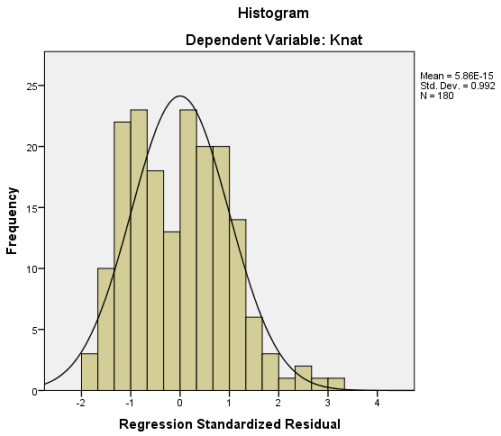
a. Dependent Variable: Knat

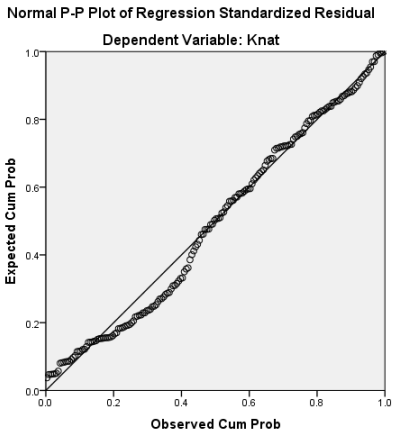
b. Predictors: (Constant), OutdoorExposed, OPI, OutdoorSheltered

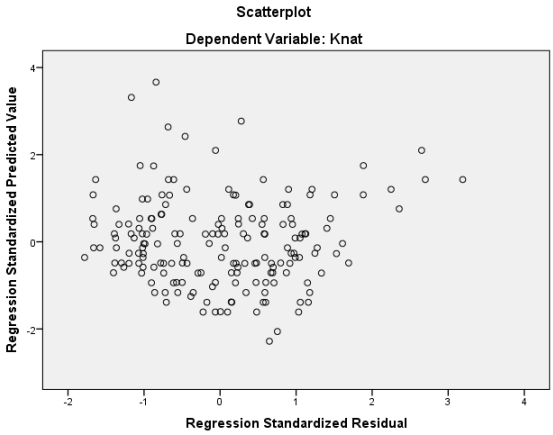
Coefficients[a]

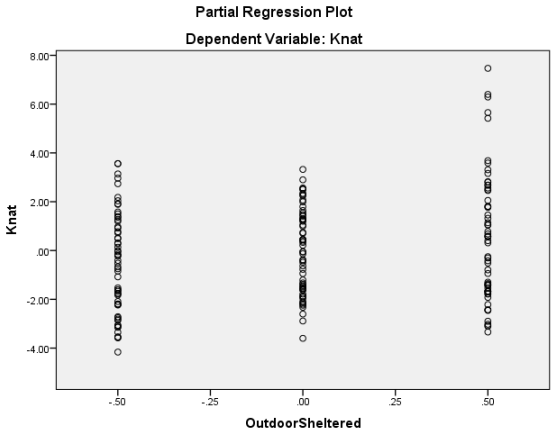
Model		Unstandardized Coefficients		Standardized Coefficients	t	Sig.	95.0% Confidence Interval for B		Correlations			Collinearity Statistics	
		B	Std. Error	Beta			Lower Bound	Upper Bound	Zero-order	Partial	Part	Tolerance	VIF
1	(Constant)	72.317	3.880		18.639	.000	64.660	79.974					
	OPI	-6.816	.402	-.738	-16.968	.000	-7.609	-6.023	-.738	-.788	-.738	1.000	1.000
	OutdoorSheltered	1.066	.397	.135	2.687	.008	.283	1.849	.266	.199	.117	.750	1.333
	OutdoorExposed	-2.069	.397	-.262	-5.215	.000	-2.852	-1.286	-.329	-.366	-.227	.750	1.333

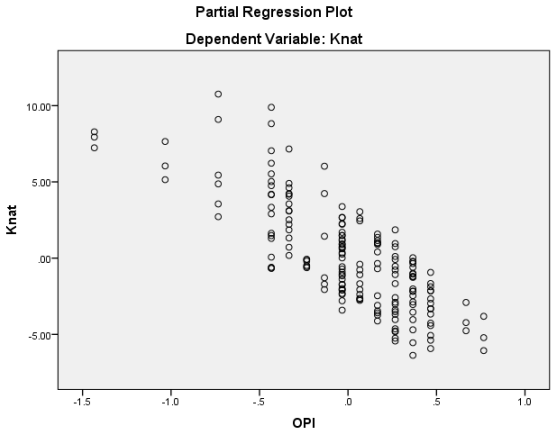
a. Dependent Variable: Knat

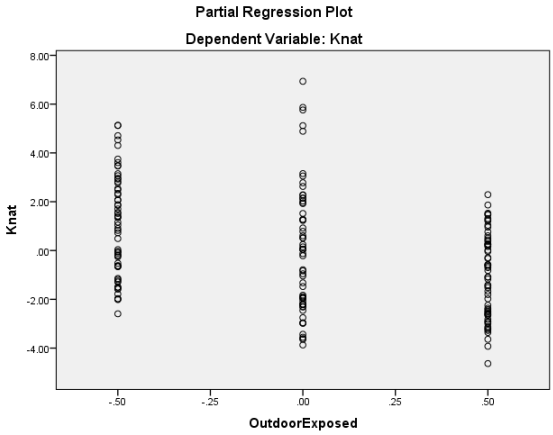












Model 6 - *WS, EC*

Model Summary[b]

Model	R	R Square	Adjusted R Square	Std. Error of the Estimate	Durbin-Watson
1	.825[a]	.680	.674	2.13049	1.049

a. Predictors: (Constant), OutdoorExposed, WS, OutdoorSheltered

b. Dependent Variable: Knat

ANOVA[a]

Model		Sum of Squares	df	Mean Square	F	Sig.
1	Regression	1696.452	3	565.484	124.584	.000[b]
	Residual	798.860	176	4.539		
	Total	2495.312	179			

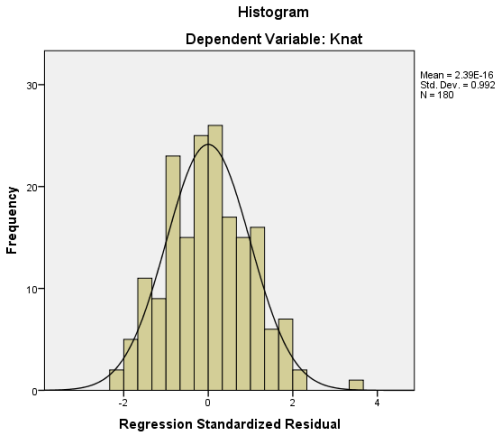
a. Dependent Variable: Knat

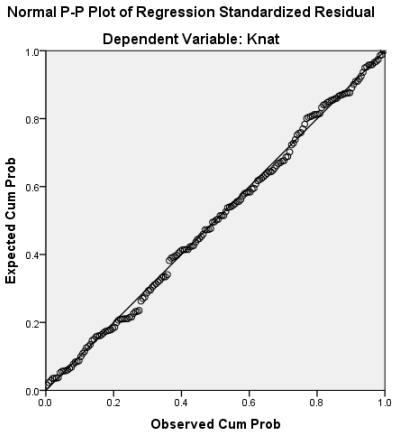
b. Predictors: (Constant), OutdoorExposed, WS, OutdoorSheltered

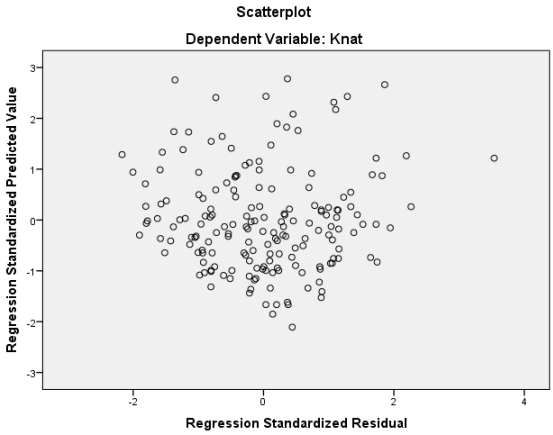
Coefficients[a]

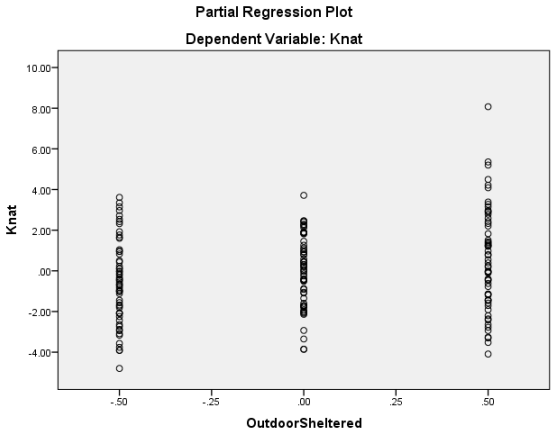
Model		Unstandardized Coefficients		Standardized Coefficients	t	Sig.	95.0% Confidence Interval for B		Correlations			Collinearity Statistics	
		B	Std. Error	Beta			Lower Bound	Upper Bound	Zero-order	Partial	Part	Tolerance	VIF
1	(Constant)	-.541	.495		-1.093	.276	-1.517	.435					
	WS	.718	.041	.747	17.509	.000	.637	.798	.747	.797	.747	1.000	1.000
	OutdoorSheltered	1.066	.389	.135	2.741	.007	.299	1.834	.266	.202	.117	.750	1.333
	OutdoorExposed	-2.069	.389	-.262	-5.319	.000	-2.836	-1.301	-.329	-.372	-.227	.750	1.333

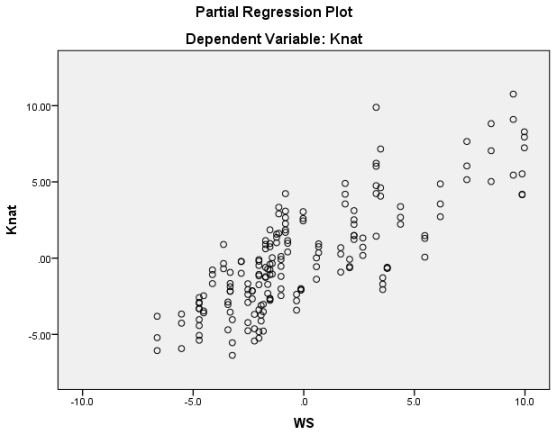
a. Dependent Variable: Knat

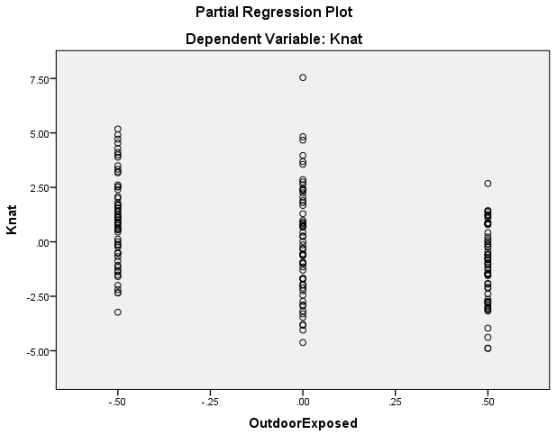












Model 7 - *fc, OPI, EC*

Model Summary[b]

Model	R	R Square	Adjusted R Square	Std. Error of the Estimate	Durbin-Watson
1	.886[a]	.784	.779	1.75416	1.280

a. Predictors: (Constant), OutdoorExposed, OPI, OutdoorSheltered, fc

b. Dependent Variable: Knat

ANOVA[a]

Model		Sum of Squares	df	Mean Square	F	Sig.
1	Regression	1956.826	4	489.207	158.985	.000[b]
	Residual	538.486	175	3.077		
	Total	2495.312	179			

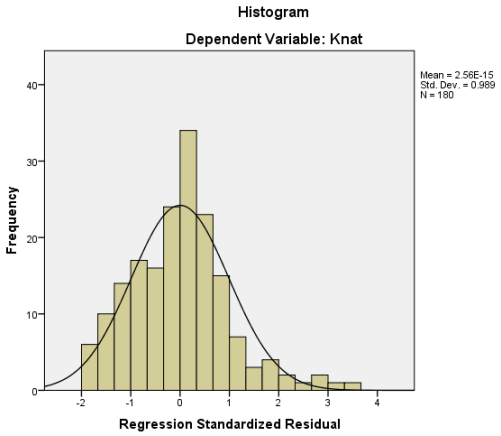
a. Dependent Variable: Knat

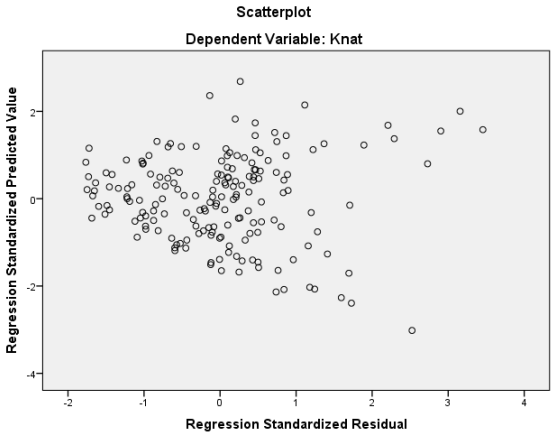
b. Predictors: (Constant), OutdoorExposed, OPI, OutdoorSheltered, fc

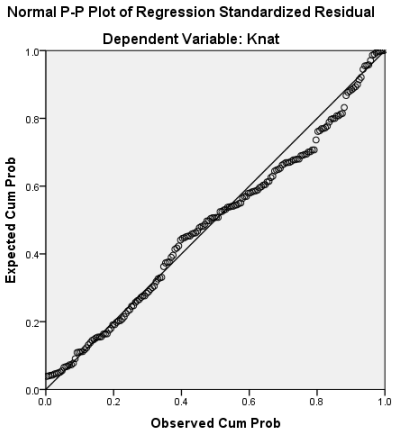
Coefficients[a]

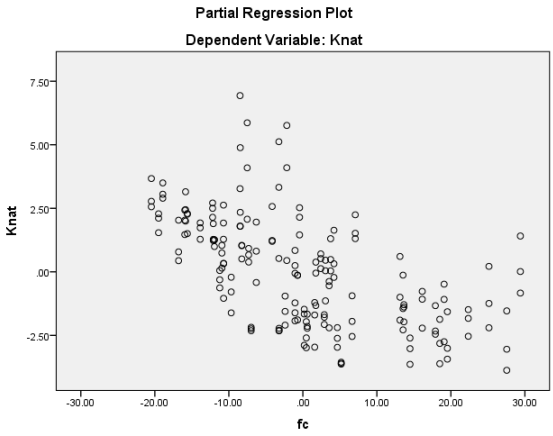
Model		Unstandardized Coefficients		Standardized Coefficients	t	Sig.	95.0% Confidence Interval for B		Correlations			Collinearity Statistics	
		B	Std. Error	Beta			Lower Bound	Upper Bound	Zero-order	Partial	Part	Tolerance	VIF
1	(Constant)	42.287	4.393		9.627	.000	33.618	50.957					
	fc	-.103	.011	-.511	-9.750	.000	-.124	-.082	-.777	-.593	-.342	.449	2.225
	OPI	-3.316	.484	-.359	-6.855	.000	-4.271	-2.361	-.738	-.460	-.241	.449	2.225
	OutdoorSheltered	1.066	.320	.135	3.329	.001	.434	1.698	.266	.244	.117	.750	1.333
	OutdoorExposed	-2.069	.320	-.262	-6.460	.000	-2.701	-1.437	-.329	-.439	-.227	.750	1.333

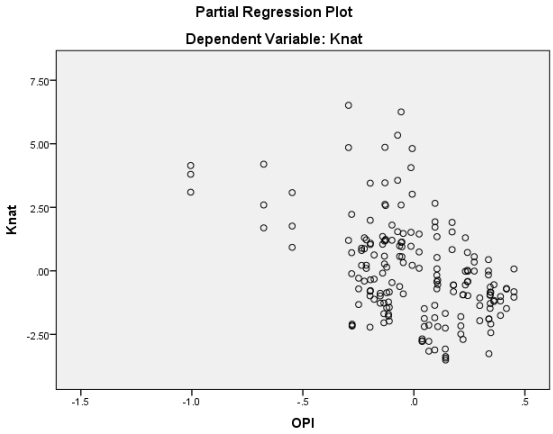
a. Dependent Variable: Knat

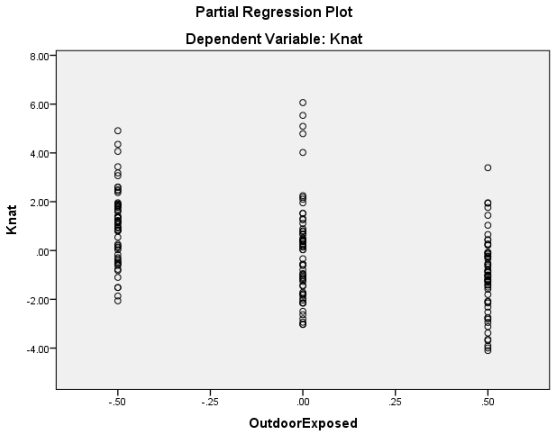


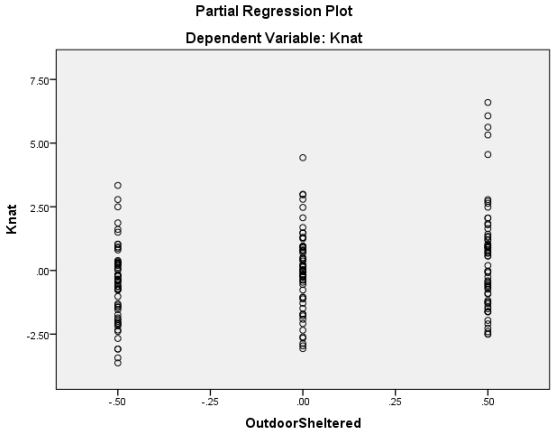












Model 8 - *fc, WS, EC*

Model Summary[b]

Model	R	R Square	Adjusted R Square	Std. Error of the Estimate	Durbin-Watson
1	.894[a]	.800	.795	1.68931	1.061

a. Predictors: (Constant), OutdoorExposed, WS, OutdoorSheltered, fc

b. Dependent Variable: Knat

ANOVA[a]

Model		Sum of Squares	df	Mean Square	F	Sig.
1	Regression	1995.903	4	498.976	174.848	.000[b]
	Residual	499.409	175	2.854		
	Total	2495.312	179			

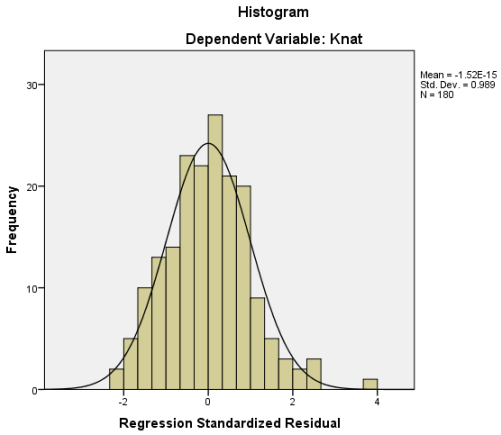
a. Dependent Variable: Knat

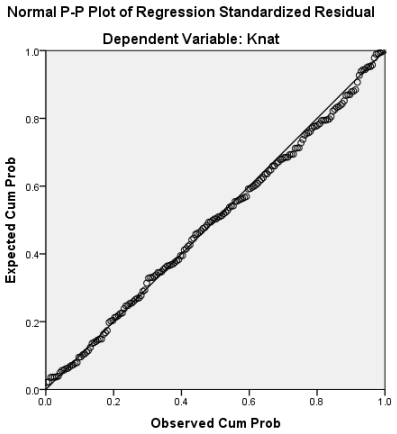
b. Predictors: (Constant), OutdoorExposed, WS, OutdoorSheltered, fc

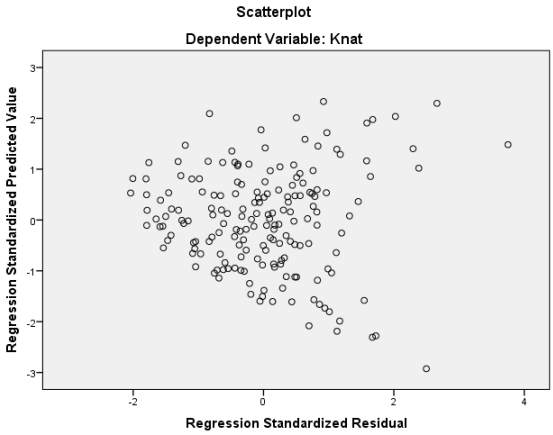
Coefficients[a]

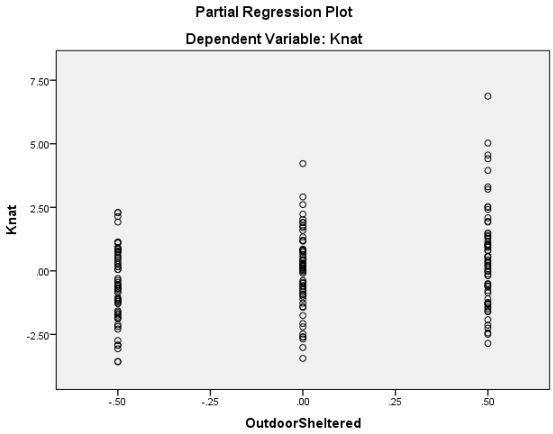
Model		Unstandardized Coefficients		Standardized Coefficients	t	Sig.	95.0% Confidence Interval for B		Correlations			Collinearity Statistics	
		B	Std. Error	Beta			Lower Bound	Upper Bound	Zero-order	Partial	Part	Tolerance	VIF
1	(Constant)	6.491	.791		8.211	.000	4.931	8.052					
	fc	-.100	.010	-.498	-10.244	.000	-.119	-.081	-.777	-.612	-.346	.485	2.063
	WS	.374	.047	.390	8.023	.000	.282	.467	.747	.519	.271	.485	2.063
	OutdoorSheltered	1.066	.308	.135	3.457	.001	.457	1.675	.266	.253	.117	.750	1.333
	OutdoorExposed	-2.069	.308	-.262	-6.708	.000	-2.678	-1.460	-.329	-.452	-.227	.750	1.333

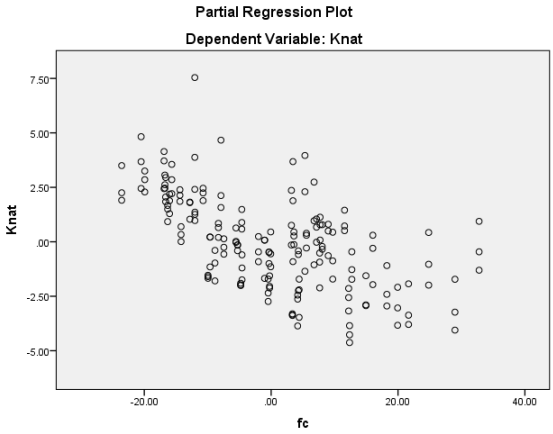
a. Dependent Variable: Knat

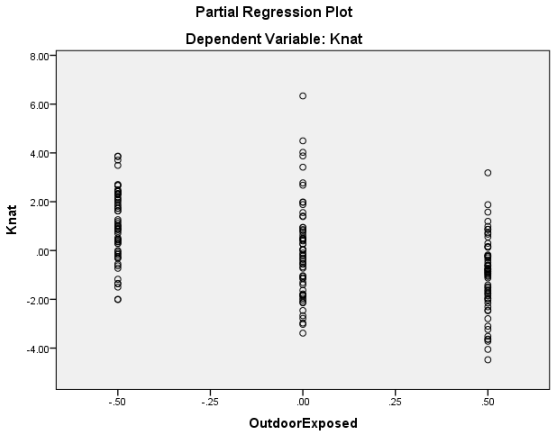


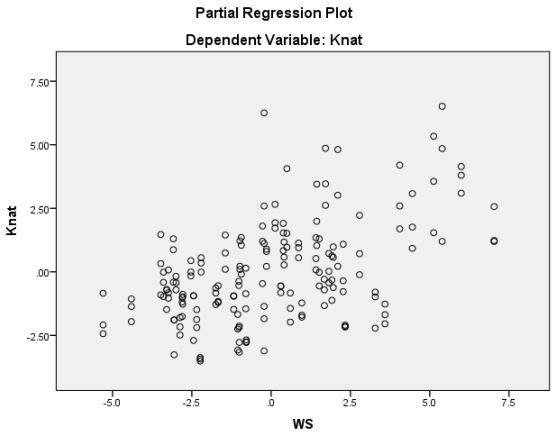



Scatterplot
Dependent Variable: Knat
Regression Standardized Predicted Value
Regression Standardized Residual


Partial Regression Plot
Dependent Variable: Knat
Knat
OutdoorSheltered


Partial Regression Plot
Dependent Variable: Knat
Knat
fc


Partial Regression Plot
Dependent Variable: Knat
Knat
OutdoorExposed


Partial Regression Plot
Dependent Variable: Knat
Knat
WS

Model 9 – *OPI, CH, EC*

Model Summary[b]

Model	R	R Square	Adjusted R Square	Std. Error of the Estimate	Durbin-Watson
1	.885[a]	.784	.779	1.75669	1.402

a. Predictors: (Constant), OutdoorExposed, CH, OutdoorSheltered, OPI

b. Dependent Variable: Knat

ANOVA[a]

Model		Sum of Squares	df	Mean Square	F	Sig.
1	Regression	1955.269	4	488.817	158.400	.000[b]
	Residual	540.043	175	3.086		
	Total	2495.312	179			

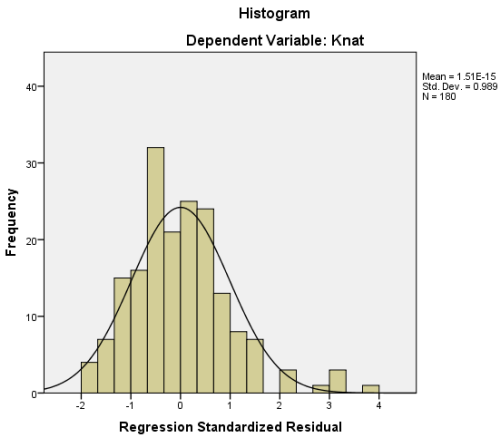
a. Dependent Variable: Knat

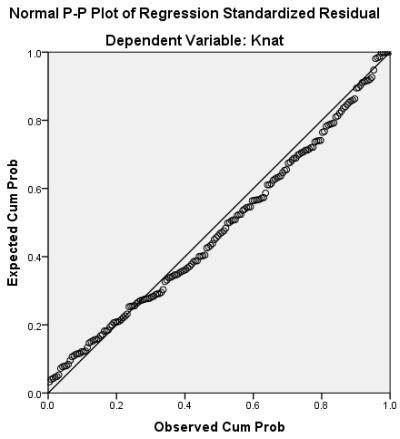
b. Predictors: (Constant), OutdoorExposed, CH, OutdoorSheltered, OPI

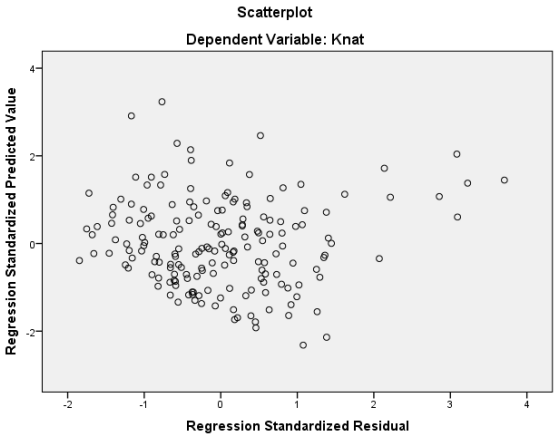
Coefficients[a]

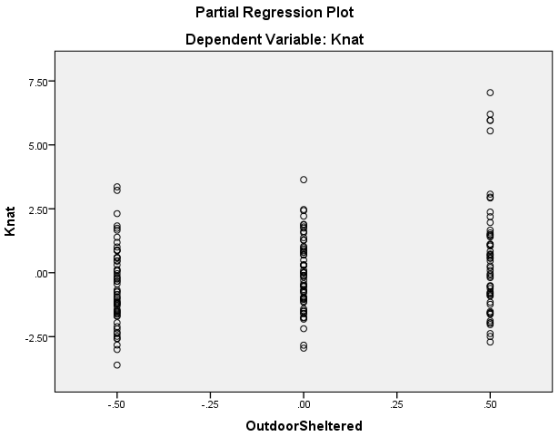
Model		Unstandardized Coefficients		Standardized Coefficients	t	Sig.	95.0% Confidence Interval for B		Correlations			Collinearity Statistics	
		B	Std. Error	Beta			Lower Bound	Upper Bound	Zero-order	Partial	Part	Tolerance	VIF
1	(Constant)	56.890	3.516		16.180	.000	49.951	63.830					
	OPI	-4.043	.432	-.438	-9.348	.000	-4.896	-3.189	-.738	-.577	-.329	.564	1.773
	CH	-.840	.087	-.455	-9.710	.000	-1.011	-.669	-.744	-.592	-.341	.564	1.773
	OutdoorSheltered	1.066	.321	.135	3.324	.001	.433	1.699	.266	.244	.117	.750	1.333
	OutdoorExposed	-2.069	.321	-.262	-6.450	.000	-2.702	-1.436	-.329	-.438	-.227	.750	1.333

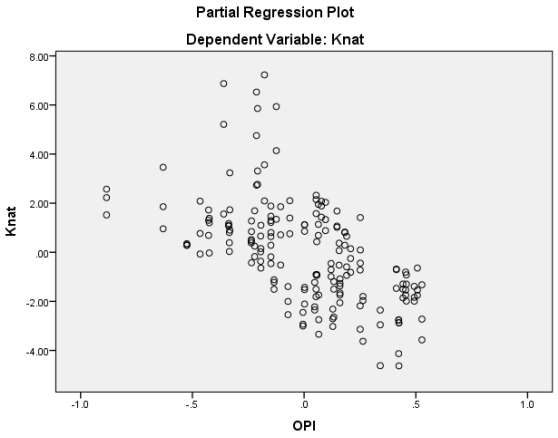
a. Dependent Variable: Knat

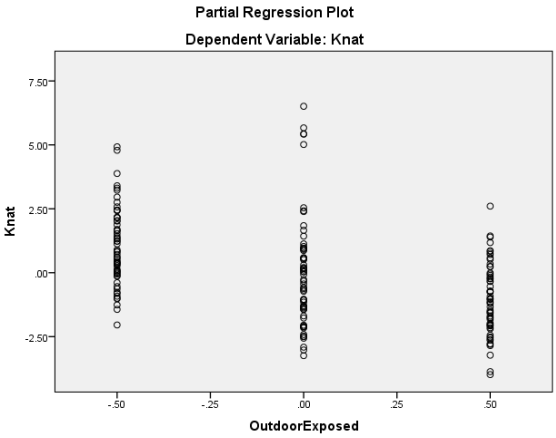


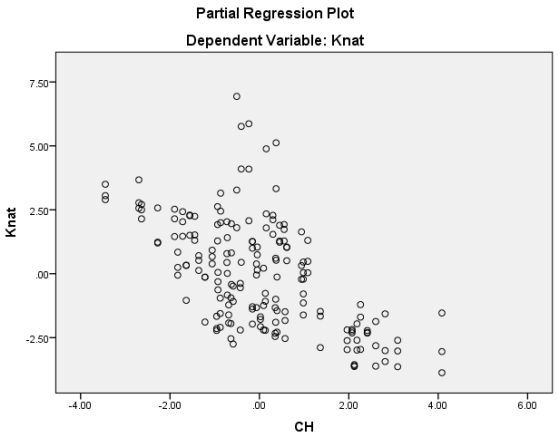



Scatterplot
Dependent Variable: Knat
Regression Standardized Predicted Value
Regression Standardized Residual


Partial Regression Plot
Dependent Variable: Knat
Knat
OutdoorSheltered


Partial Regression Plot
Dependent Variable: Knat
Knat
OPI


Partial Regression Plot
Dependent Variable: Knat
Knat
OutdoorExposed


Partial Regression Plot
Dependent Variable: Knat
Knat
CH

Model 10 – *WS, CH, EC*

Model Summary[b]

Model	R	R Square	Adjusted R Square	Std. Error of the Estimate	Durbin-Watson
1	.911[a]	.829	.825	1.56145	1.491

a. Predictors: (Constant), OutdoorExposed, CH, OutdoorSheltered, WS

b. Dependent Variable: Knat

ANOVA[a]

Model		Sum of Squares	df	Mean Square	F	Sig.
1	Regression	2068.641	4	517.160	212.114	.000[b]
	Residual	426.671	175	2.438		
	Total	2495.312	179			

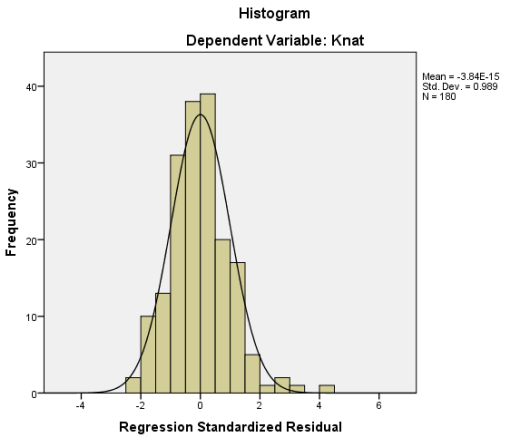
a. Dependent Variable: Knat

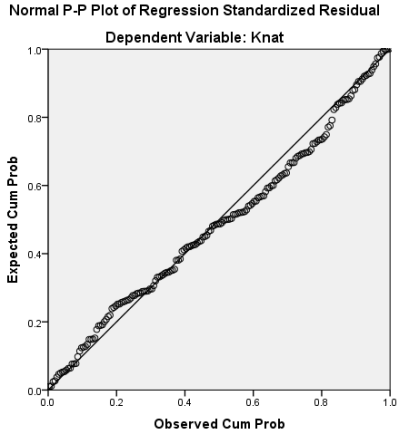
b. Predictors: (Constant), OutdoorExposed, CH, OutdoorSheltered, WS

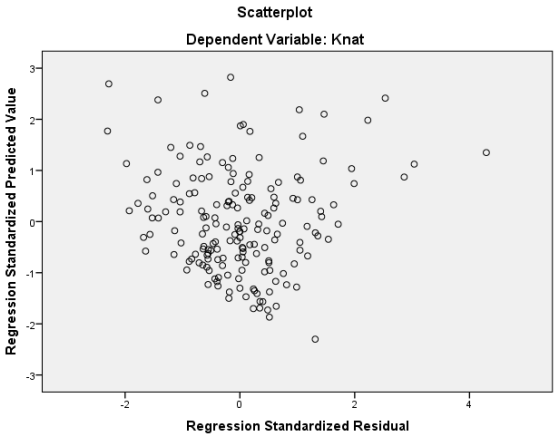
Coefficients[a]

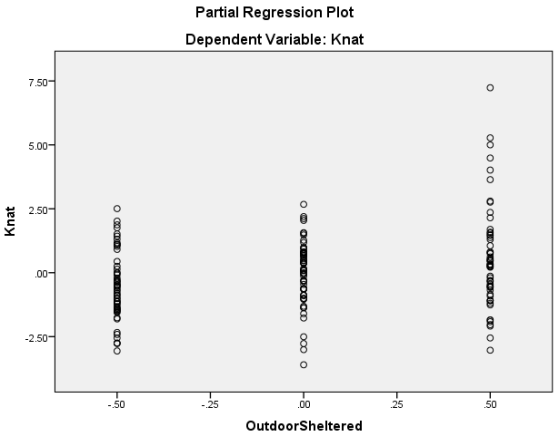
Model		Unstandardized Coefficients		Standardized Coefficients	t	Sig.	95.0% Confidence Interval for B		Correlations			Collinearity Statistics	
		B	Std. Error	Beta			Lower Bound	Upper Bound	Zero-order	Partial	Part	Tolerance	VIF
1	(Constant)	13.740	1.211		11.343	.000	11.349	16.131					
	WS	.459	.037	.478	12.534	.000	.387	.531	.747	.688	.392	.673	1.486
	CH	-.870	.070	-.471	-12.355	.000	-1.009	-.731	-.744	-.683	-.386	.673	1.486
	OutdoorSheltered	1.066	.285	.135	3.740	.000	.504	1.629	.266	.272	.117	.750	1.333
	OutdoorExposed	-2.069	.285	-.262	-7.257	.000	-2.631	-1.506	-.329	-.481	-.227	.750	1.333

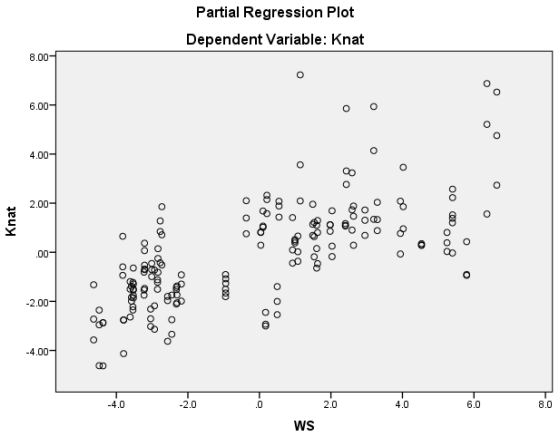
a. Dependent Variable: Knat

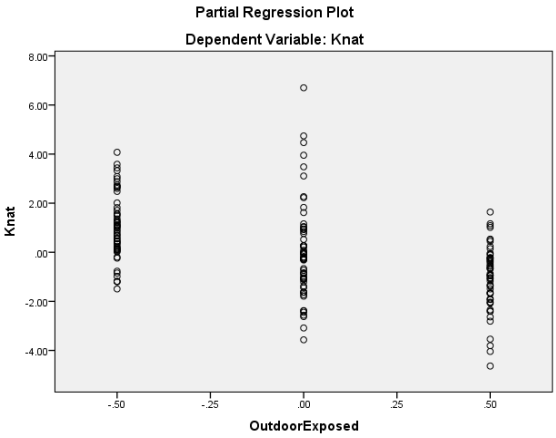


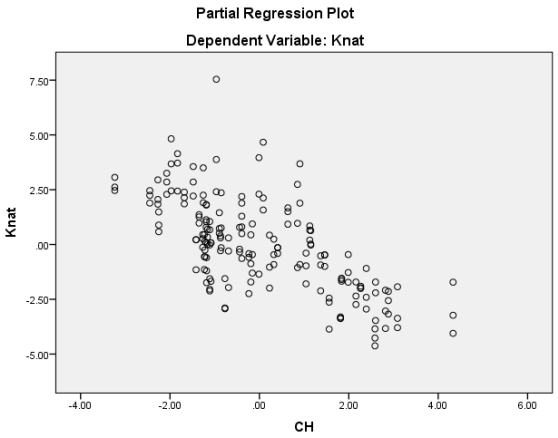



Scatterplot
Dependent Variable: Knat
Regression Standardized Predicted Value
Regression Standardized Residual


Partial Regression Plot
Dependent Variable: Knat
Knat
OutdoorSheltered


Partial Regression Plot
Dependent Variable: Knat
Knat
WS


Partial Regression Plot
Dependent Variable: Knat
Knat
OutdoorExposed


Partial Regression Plot
Dependent Variable: Knat
Knat
CH

Model 11 – f_c, *OPI, CH, EC*

Model Summary[b]

Model	R	R Square	Adjusted R Square	Std. Error of the Estimate	Durbin-Watson
1	.909[a]	.827	.822	1.57635	1.507

a. Predictors: (Constant), OutdoorExposed, CH, OutdoorSheltered, OPI, fc

b. Dependent Variable: Knat

ANOVA[a]

Model		Sum of Squares	df	Mean Square	F	Sig.
1	Regression	2062.942	5	412.588	166.039	.000[b]
	Residual	432.370	174	2.485		
	Total	2495.312	179			

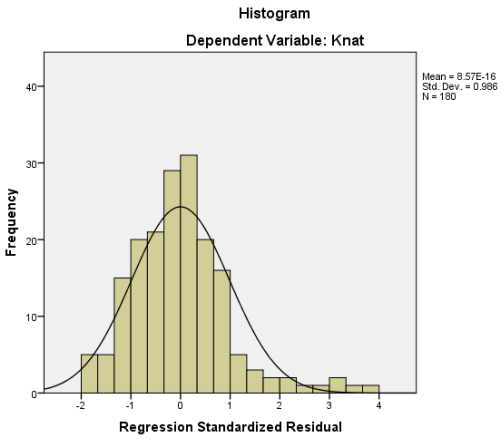
a. Dependent Variable: Knat

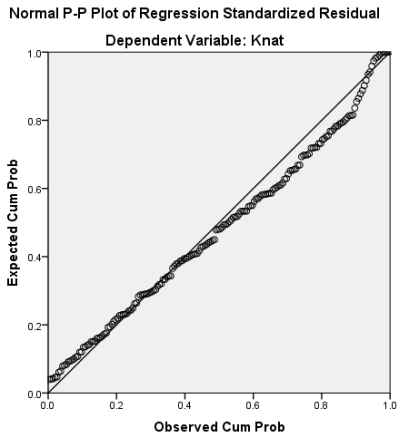
b. Predictors: (Constant), OutdoorExposed, CH, OutdoorSheltered, OPI, fc

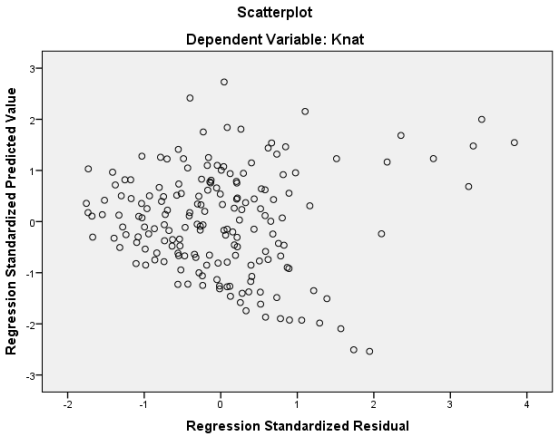
Coefficients[a]

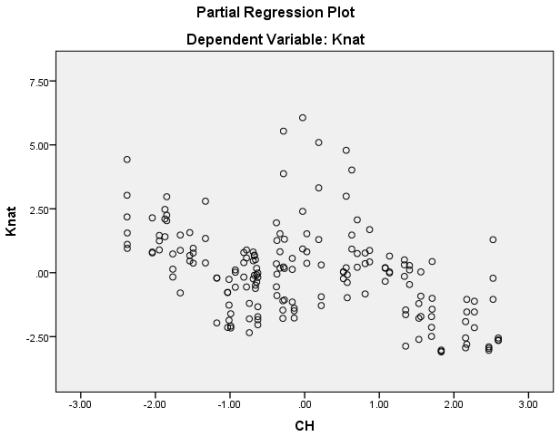
Model		Unstandardized Coefficients		Standardized Coefficients	t	Sig.	95.0% Confidence Interval for B		Correlations			Collinearity Statistics	
		B	Std. Error	Beta			Lower Bound	Upper Bound	Zero-order	Partial	Part	Tolerance	VIF
1	(Constant)	41.239	3.951		10.438	.000	33.441	49.036					
	fc	-.070	.011	-.350	-6.583	.000	-.091	-.049	-.777	-.447	-.208	.353	2.835
	OPI	-2.529	.451	-.274	-5.607	.000	-3.420	-1.639	-.738	-.391	-.177	.417	2.396
	CH	-.573	.088	-.310	-6.535	.000	-.746	-.400	-.744	-.444	-.206	.443	2.259
	OutdoorSheltered	1.066	.288	.135	3.705	.000	.498	1.634	.266	.270	.117	.750	1.333
	OutdoorExposed	-2.069	.288	-.262	-7.188	.000	-2.637	-1.501	-.329	-.479	-.227	.750	1.333

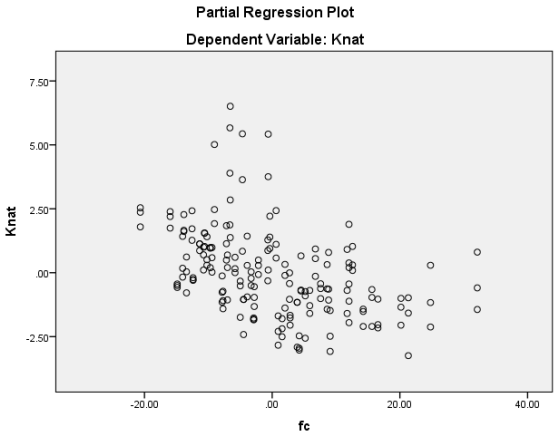
a. Dependent Variable: Knat

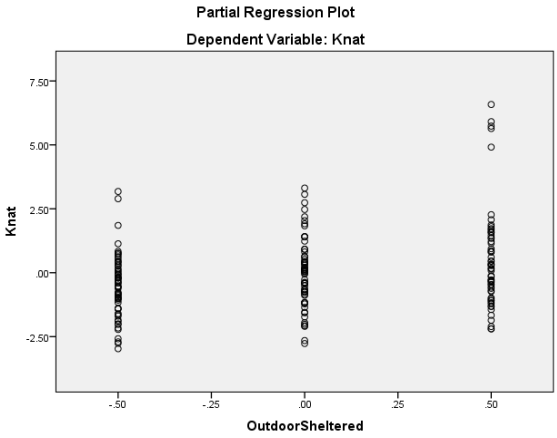


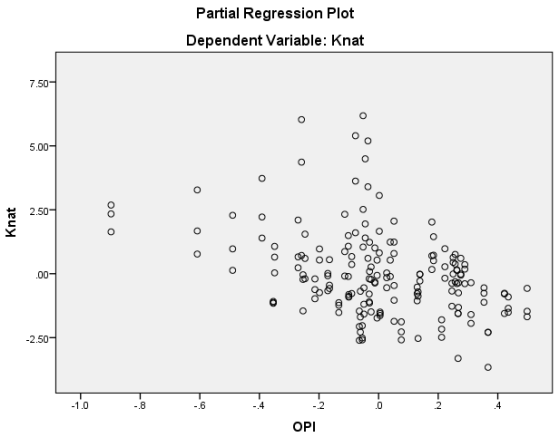


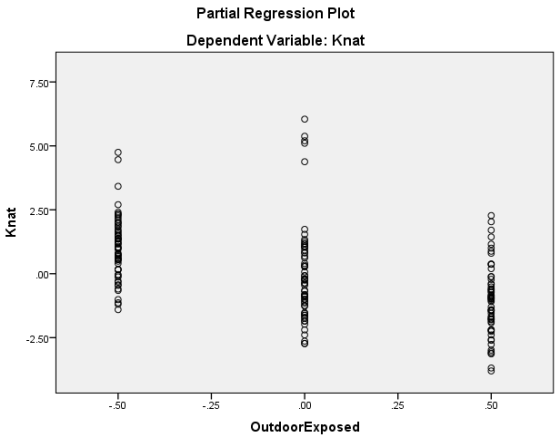

Scatterplot
Dependent Variable: Knat
Regression Standardized Predicted Value
Regression Standardized Residual


Partial Regression Plot
Dependent Variable: Knat
Knat
CH


Partial Regression Plot
Dependent Variable: Knat
Knat
fc


Partial Regression Plot
Dependent Variable: Knat
Knat
OutdoorSheltered


Partial Regression Plot
Dependent Variable: Knat
Knat
OPI


Partial Regression Plot
Dependent Variable: Knat
Knat
OutdoorExposed

Model 12 – *fc, WS, CH, EC*

Model Summary[b]

Model	R	R Square	Adjusted R Square	Std. Error of the Estimate	Durbin-Watson
1	.925[a]	.855	.851	1.44216	1.452

a. Predictors: (Constant), OutdoorExposed, CH, OutdoorSheltered, WS, fc

b. Dependent Variable: Knat

ANOVA[a]

Model		Sum of Squares	df	Mean Square	F	Sig.
1	Regression	2133.420	5	426.684	205.153	.000[b]
	Residual	361.892	174	2.080		
	Total	2495.312	179			

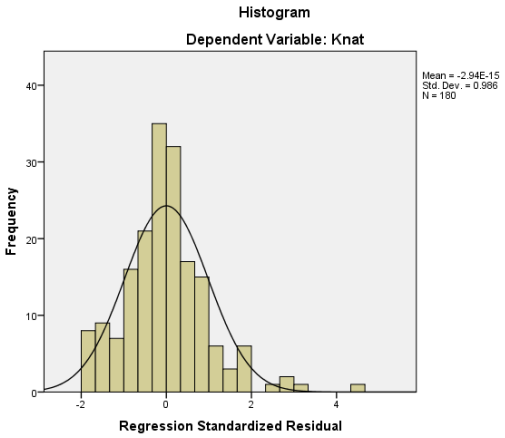
a. Dependent Variable: Knat

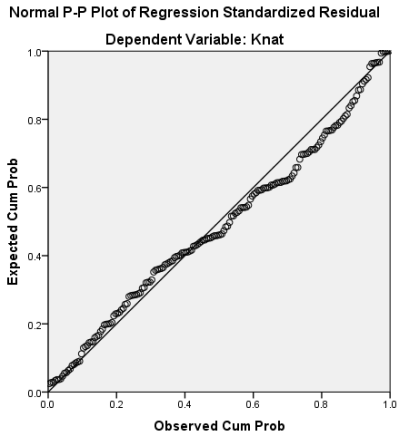
b. Predictors: (Constant), OutdoorExposed, CH, OutdoorSheltered, WS, fc

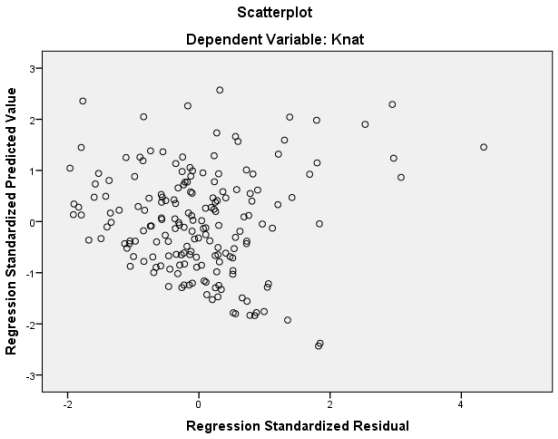
Coefficients[a]

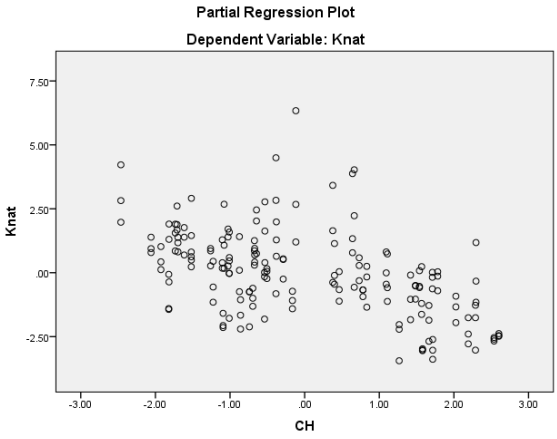
Model		Unstandardized Coefficients		Standardized Coefficients	t	Sig.	95.0% Confidence Interval for B		Correlations			Collinearity Statistics	
		B	Std. Error	Beta			Lower Bound	Upper Bound	Zero-order	Partial	Part	Tolerance	VIF
1	(Constant)	13.747	1.119		12.287	.000	11.539	15.955					
	fc	-.056	.010	-.277	-5.581	.000	-.075	-.036	-.777	-.390	-.161	.339	2.948
	WS	.339	.040	.353	8.453	.000	.260	.418	.747	.540	.244	.479	2.088
	CH	-.632	.078	-.342	-8.131	.000	-.785	-.479	-.744	-.525	-.235	.471	2.124
	OutdoorSheltered	1.066	.263	.135	4.049	.000	.546	1.586	.266	.293	.117	.750	1.333
	OutdoorExposed	-2.069	.263	-.262	-7.857	.000	-2.589	-1.549	-.329	-.512	-.227	.750	1.333

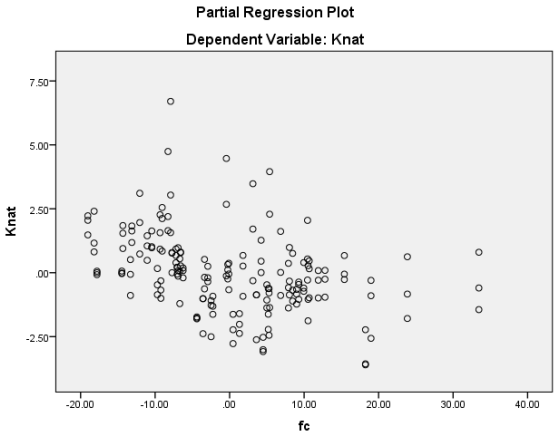
a. Dependent Variable: Knat

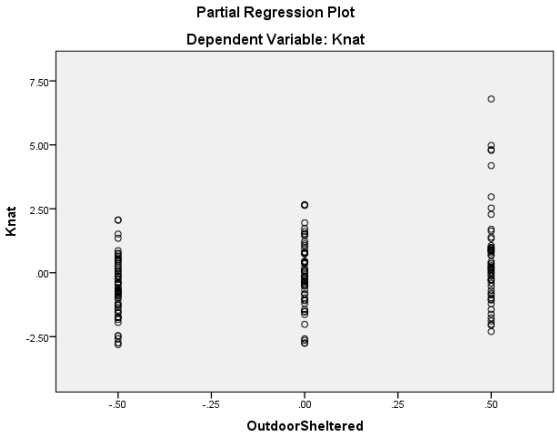


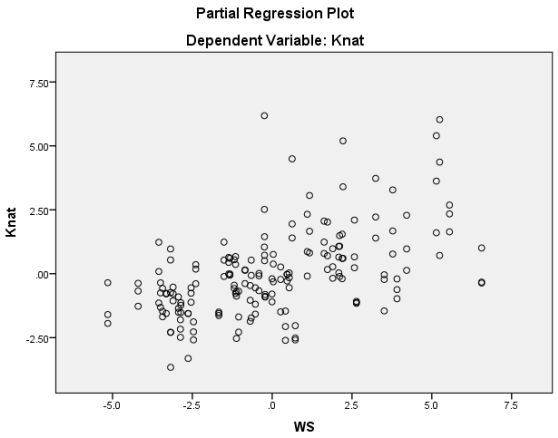


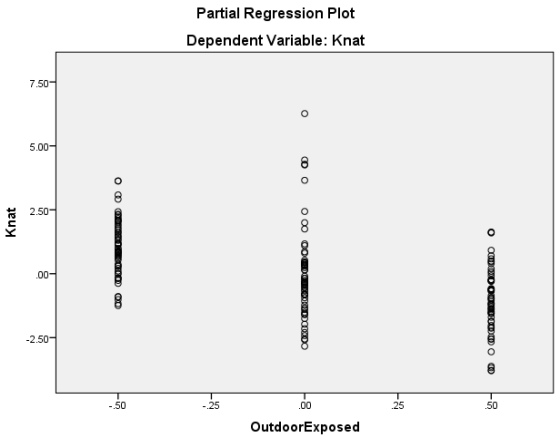

Scatterplot
Dependent Variable: Knat
Regression Standardized Predicted Value
Regression Standardized Residual


Partial Regression Plot
Dependent Variable: Knat
Knat
CH


Partial Regression Plot
Dependent Variable: Knat
Knat
fc


Partial Regression Plot
Dependent Variable: Knat
Knat
OutdoorSheltered


Partial Regression Plot
Dependent Variable: Knat
Knat
WS


Partial Regression Plot
Dependent Variable: Knat
Knat
OutdoorExposed

Model 13 – K_{acc}, *EC*

Model Summary[b]

Model	R	R Square	Adjusted R Square	Std. Error of the Estimate	Durbin-Watson
1	.926[a]	.857	.854	1.42583	1.160

a. Predictors: (Constant), OutdoorExposed, Kacc, OutdoorSheltered

b. Dependent Variable: Knat

ANOVA[a]

Model		Sum of Squares	df	Mean Square	F	Sig.
1	Regression	2137.505	3	712.502	350.469	.000[b]
	Residual	357.807	176	2.033		
	Total	2495.312	179			

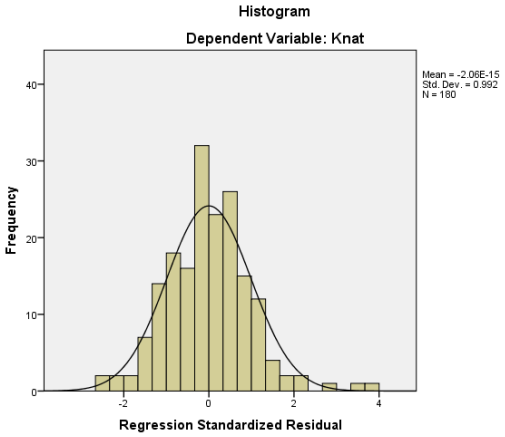
a. Dependent Variable: Knat

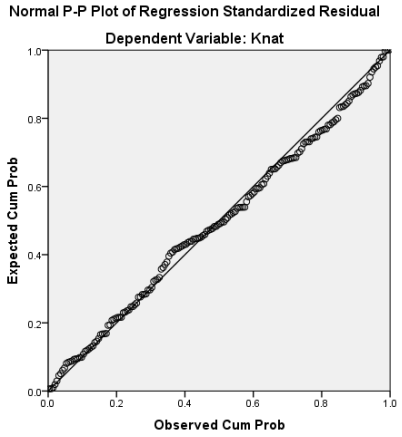
b. Predictors: (Constant), OutdoorExposed, Kacc, OutdoorSheltered

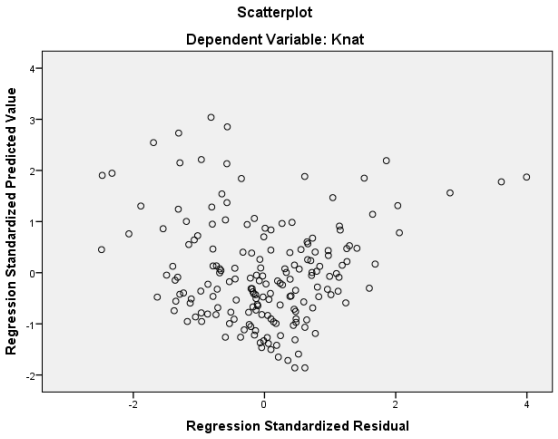
Coefficients[a]

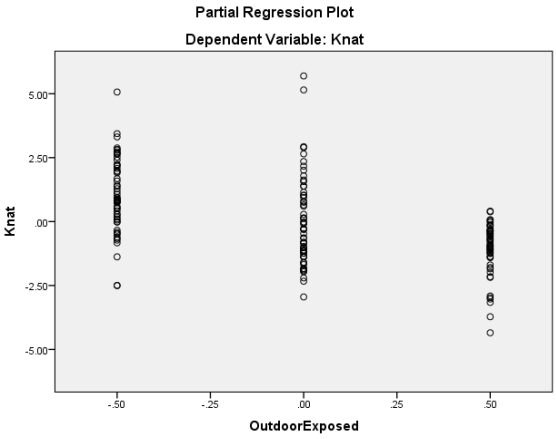
Model		Unstandardized Coefficients		Standardized Coefficients	t	Sig.	95.0% Confidence Interval for B		Correlations			Collinearity Statistics	
		B	Std. Error	Beta			Lower Bound	Upper Bound	Zero-order	Partial	Part	Tolerance	VIF
1	(Constant)	1.961	.242		8.118	.000	1.484	2.437					
	Kacc	1.191	.040	.857	30.024	.000	1.113	1.270	.857	.915	.857	1.000	1.000
	OutdoorSheltered	1.066	.260	.135	4.096	.000	.552	1.580	.266	.295	.117	.750	1.333
	OutdoorExposed	-2.069	.260	-.262	-7.947	.000	-2.583	-1.555	-.329	-.514	-.227	.750	1.333

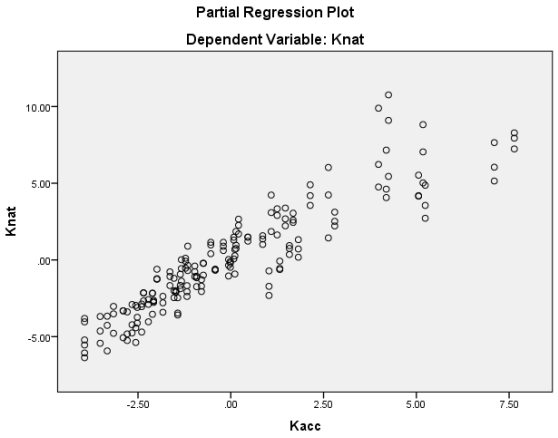
a. Dependent Variable: Knat

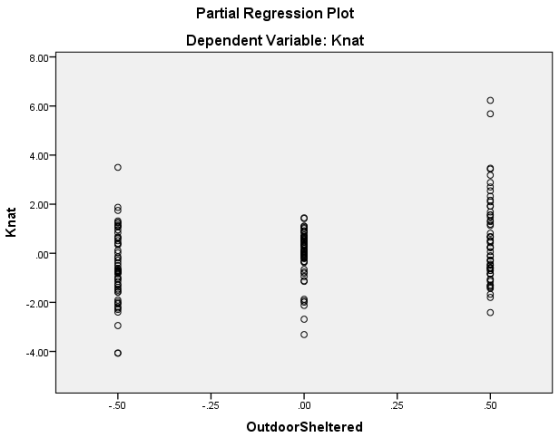





Scatterplot
Dependent Variable: Knat
Regression Standardized Predicted Value
Regression Standardized Residual


Partial Regression Plot
Dependent Variable: Knat
Knat
OutdoorExposed


Partial Regression Plot
Dependent Variable: Knat
Knat
Kacc


Partial Regression Plot
Dependent Variable: Knat
Knat
OutdoorSheltered

Model 14 – K_{acc}, *CP, EC*

Model Summary[b]

Model	R	R Square	Adjusted R Square	Std. Error of the Estimate	Durbin-Watson
1	.936[a]	.876	.873	1.33102	1.343

a. Predictors: (Constant), OutdoorExposed, SevenDays, Kacc, OutdoorSheltered, Threedays

b. Dependent Variable: Knat

ANOVA[a]

Model		Sum of Squares	df	Mean Square	F	Sig.
1	Regression	2187.053	5	437.411	246.901	.000[b]
	Residual	308.259	174	1.772		
	Total	2495.312	179			

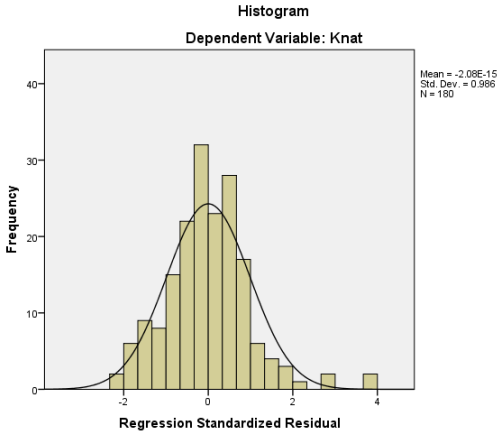
a. Dependent Variable: Knat

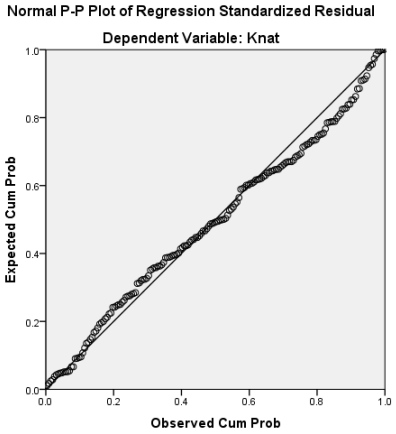
b. Predictors: (Constant), OutdoorExposed, SevenDays, Kacc, OutdoorSheltered, Threedays

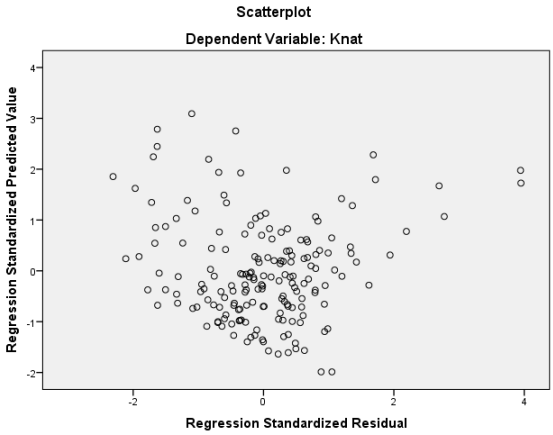
Coefficients[a]

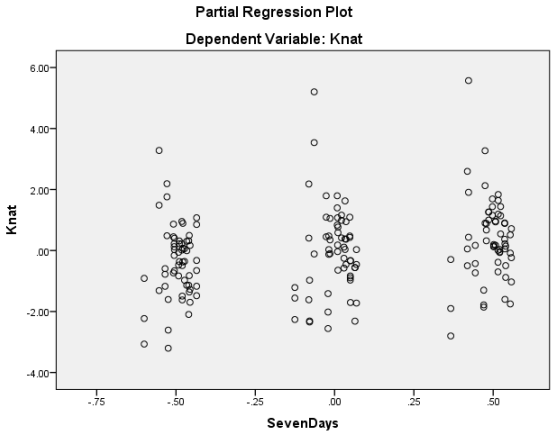
Model		Unstandardized Coefficients		Standardized Coefficients	t	Sig.	95.0% Confidence Interval for B		Correlations			Collinearity Statistics	
		B	Std. Error	Beta			Lower Bound	Upper Bound	Zero-order	Partial	Part	Tolerance	VIF
1	(Constant)	1.442	.253		5.693	.000	.942	1.942					
	Kacc	1.149	.038	.827	30.325	.000	1.074	1.224	.857	.917	.808	.956	1.047
	Threedays	1.311	.249	.166	5.273	.000	.820	1.801	.265	.371	.140	.717	1.395
	SevenDays	.744	.245	.094	3.040	.003	.261	1.227	.020	.225	.081	.740	1.352
	OutdoorSheltered	1.066	.243	.135	4.387	.000	.587	1.546	.266	.316	.117	.750	1.333
	OutdoorExposed	-2.069	.243	-.262	-8.513	.000	-2.548	-1.589	-.329	-.542	-.227	.750	1.333

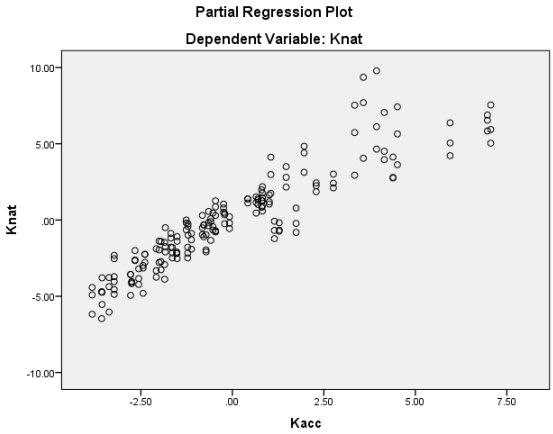
a. Dependent Variable: Knat

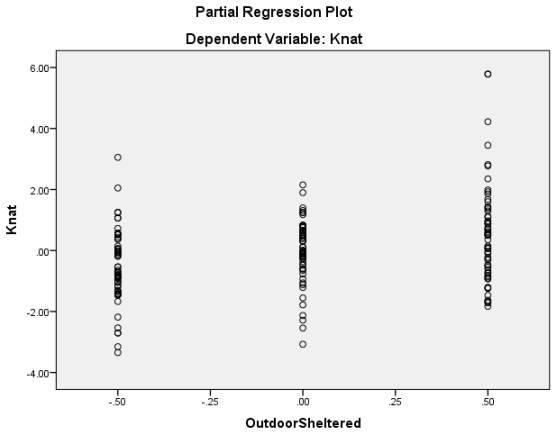


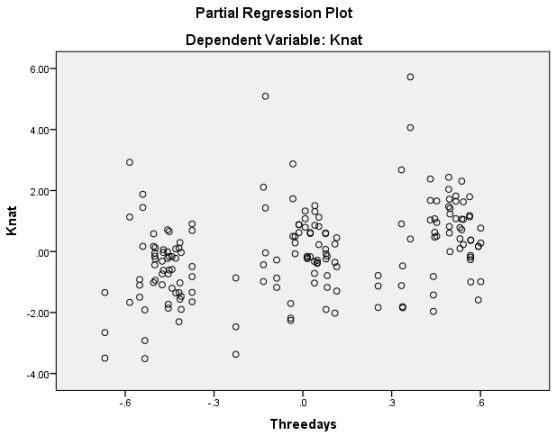


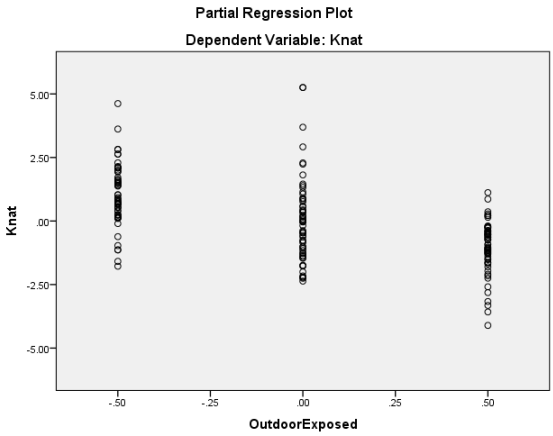

Scatterplot
Dependent Variable: Knat
Regression Standardized Predicted Value
Regression Standardized Residual


Partial Regression Plot
Dependent Variable: Knat
Knat
SevenDays


Partial Regression Plot
Dependent Variable: Knat
Knat
Kacc


Partial Regression Plot
Dependent Variable: Knat
Knat
OutdoorSheltered


Partial Regression Plot
Dependent Variable: Knat
Knat
Threedays


Partial Regression Plot
Dependent Variable: Knat
Knat
OutdoorExposed

Appendix G: Natural carbonation rate determination for the indoor exposure

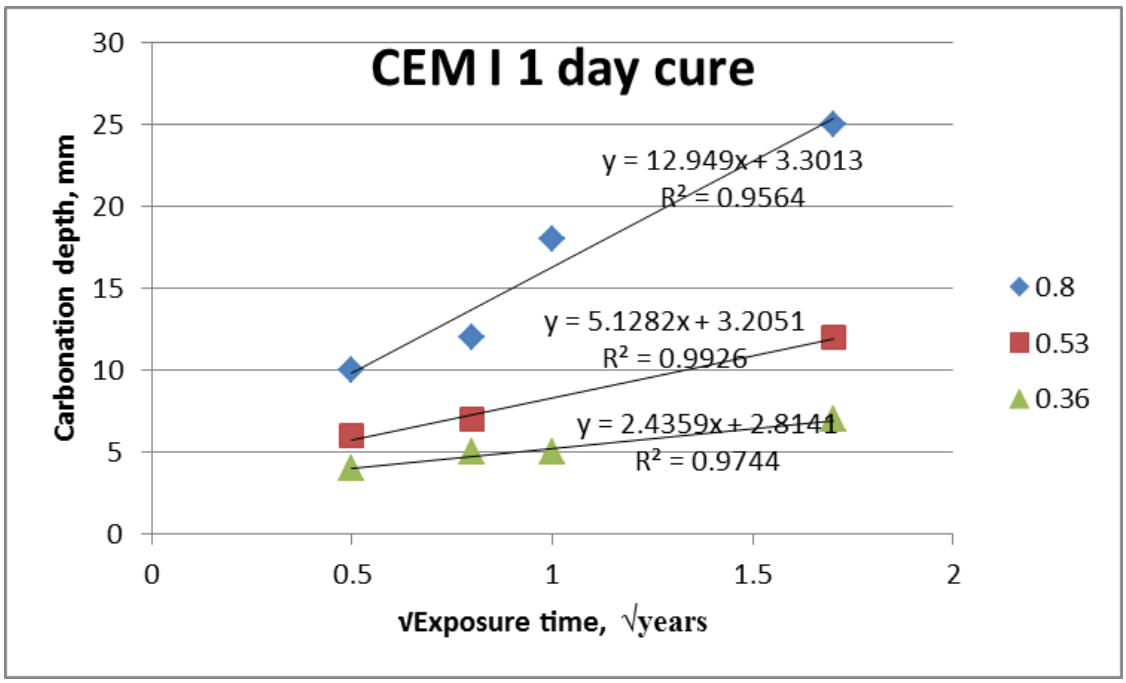


Figure G1: Carbonation depth vs. square root of exposure period

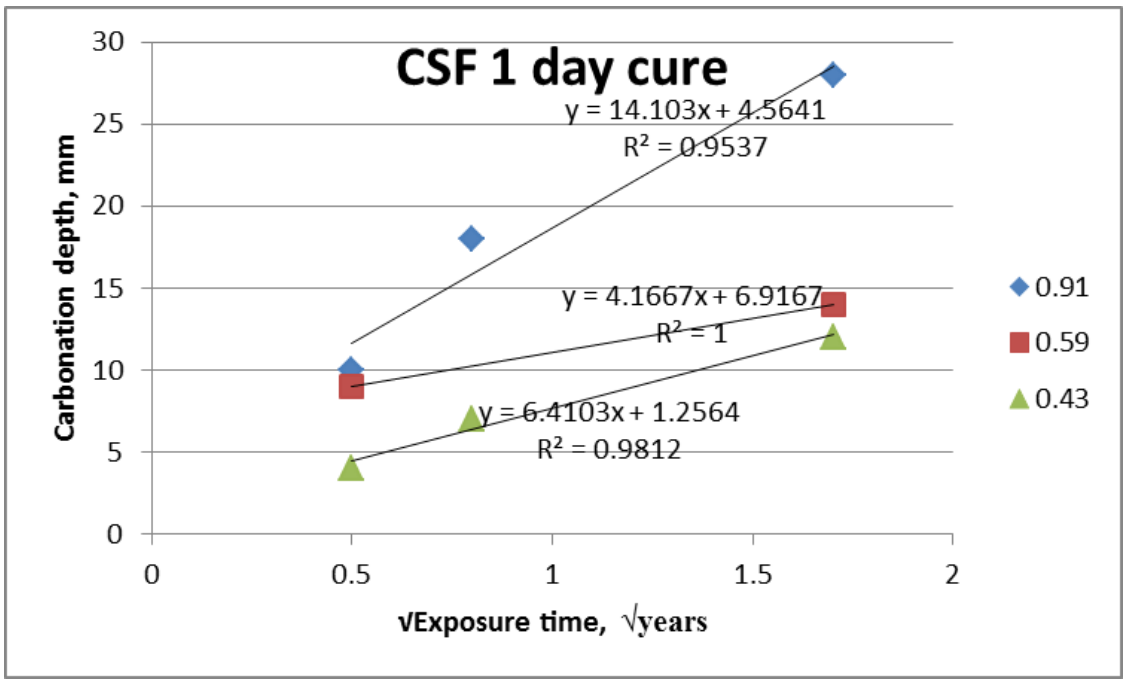


Figure G2: Carbonation depth vs. square root of exposure period

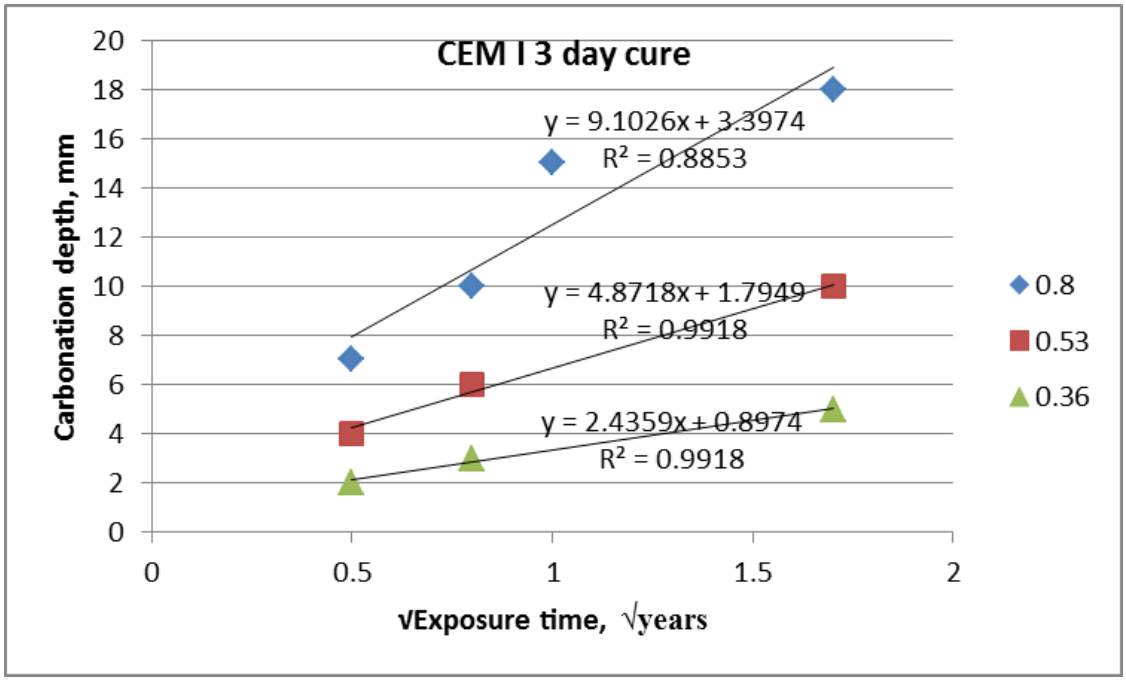


Figure G3: Carbonation depth vs. square root of exposure period

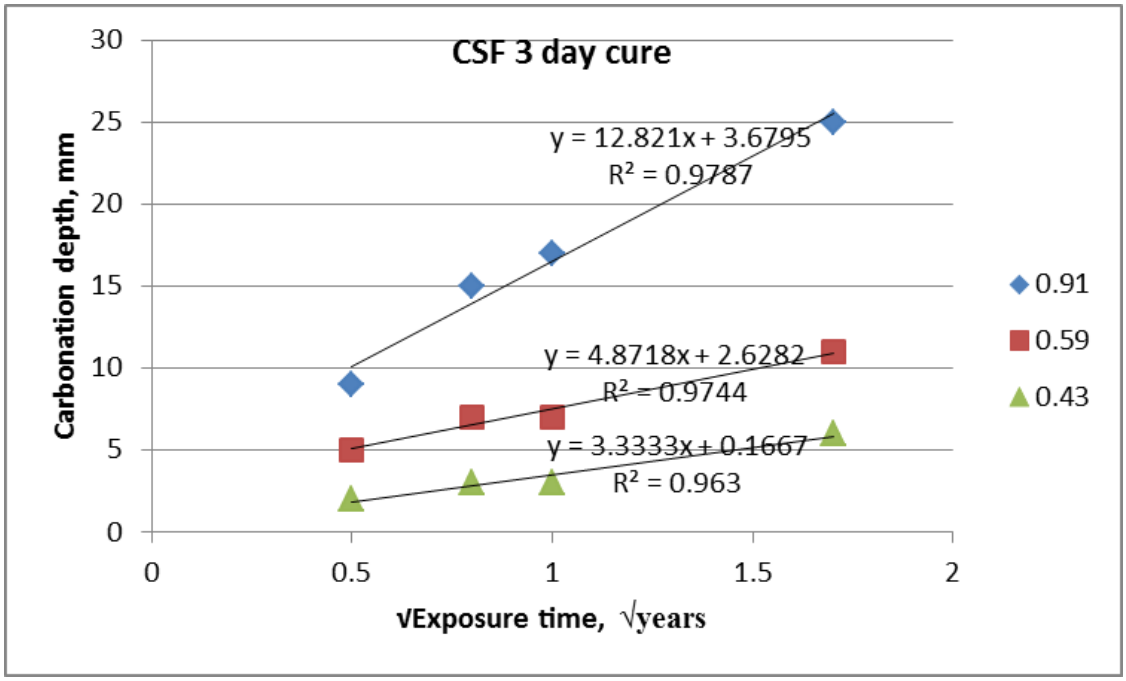


Figure G4: Carbonation depth vs. square root of exposure period

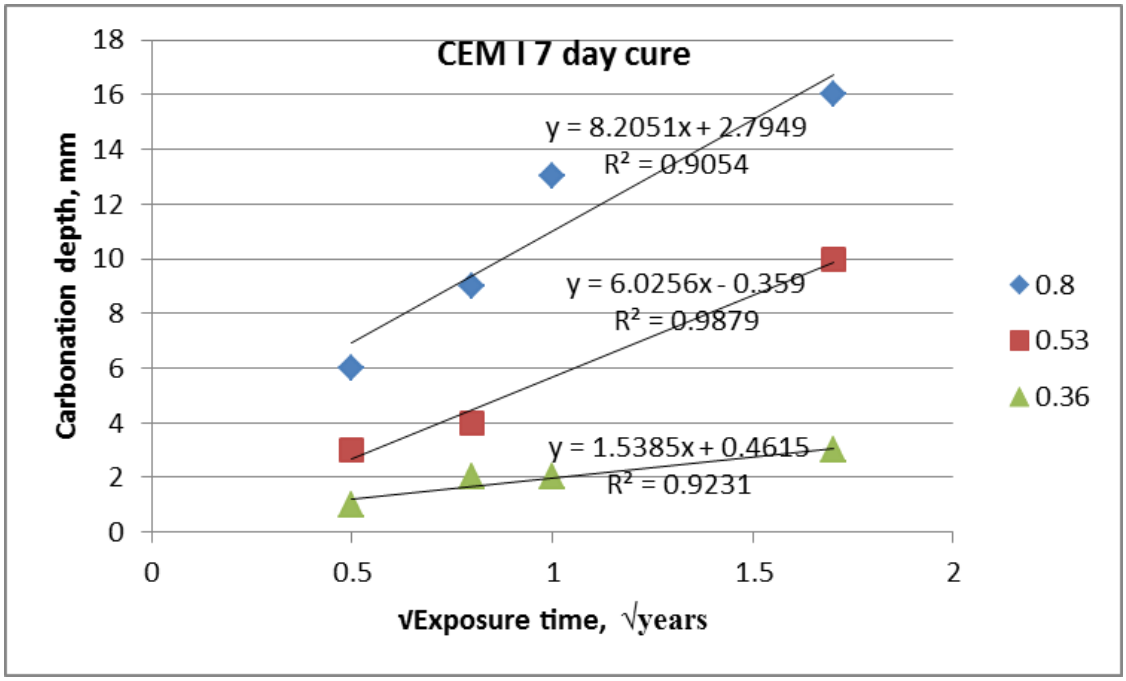


Figure G5: Carbonation depth vs. square root of exposure period

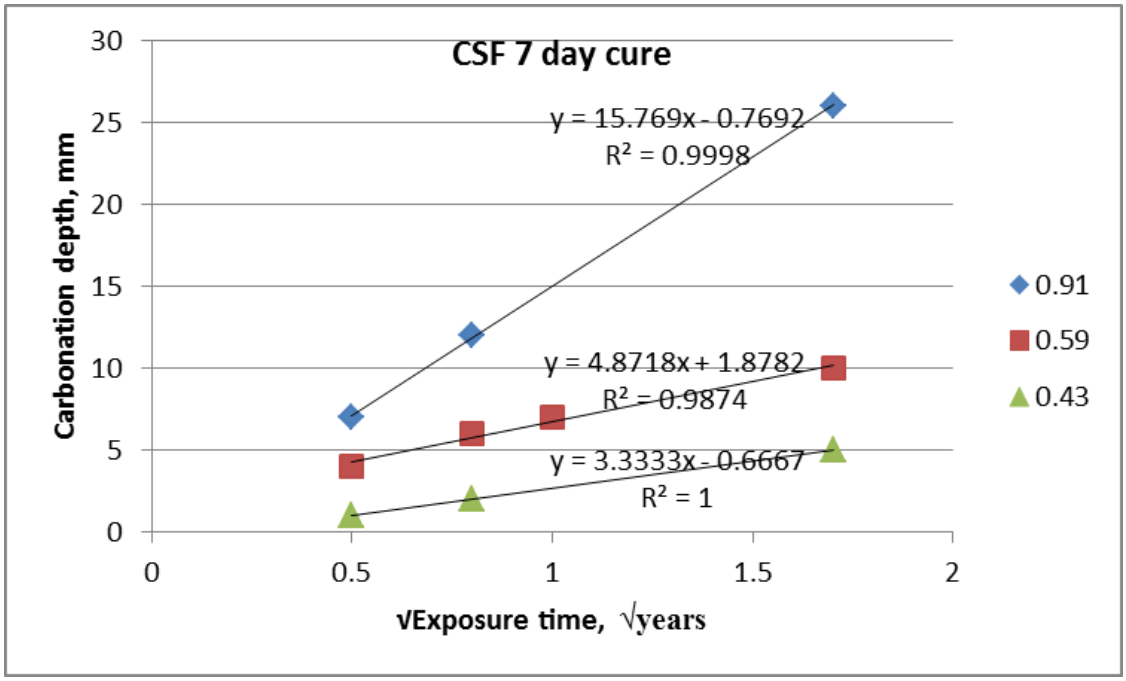


Figure G6: Carbonation depth vs. square root of exposure period

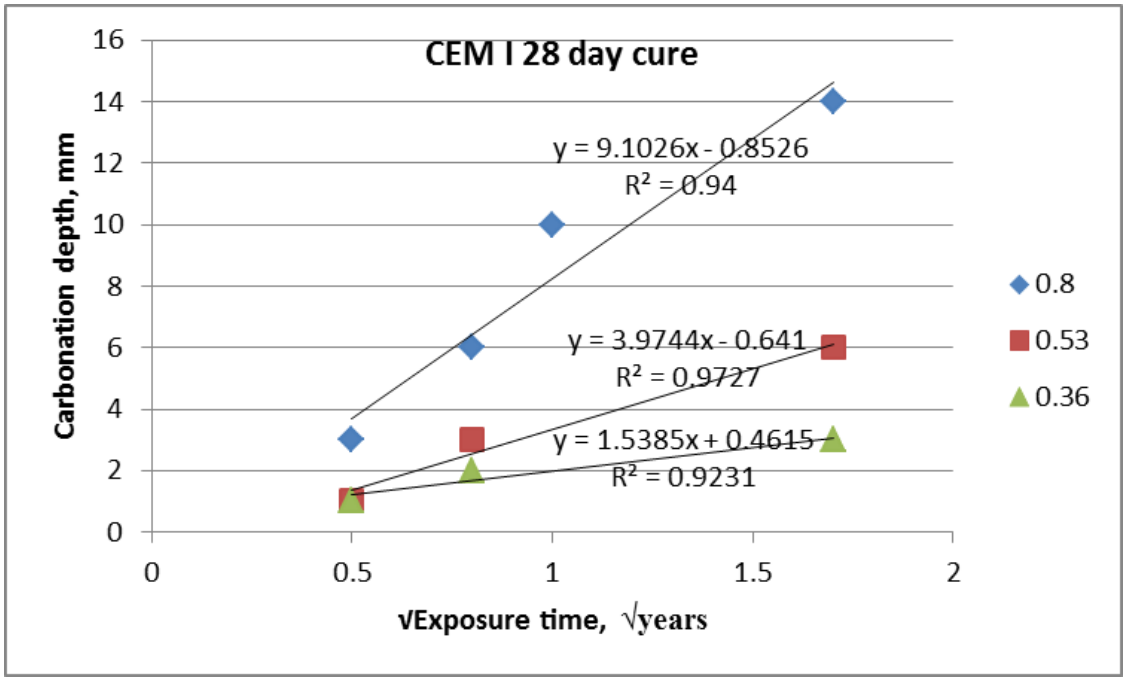


Figure G7: Carbonation depth vs. square root of exposure period

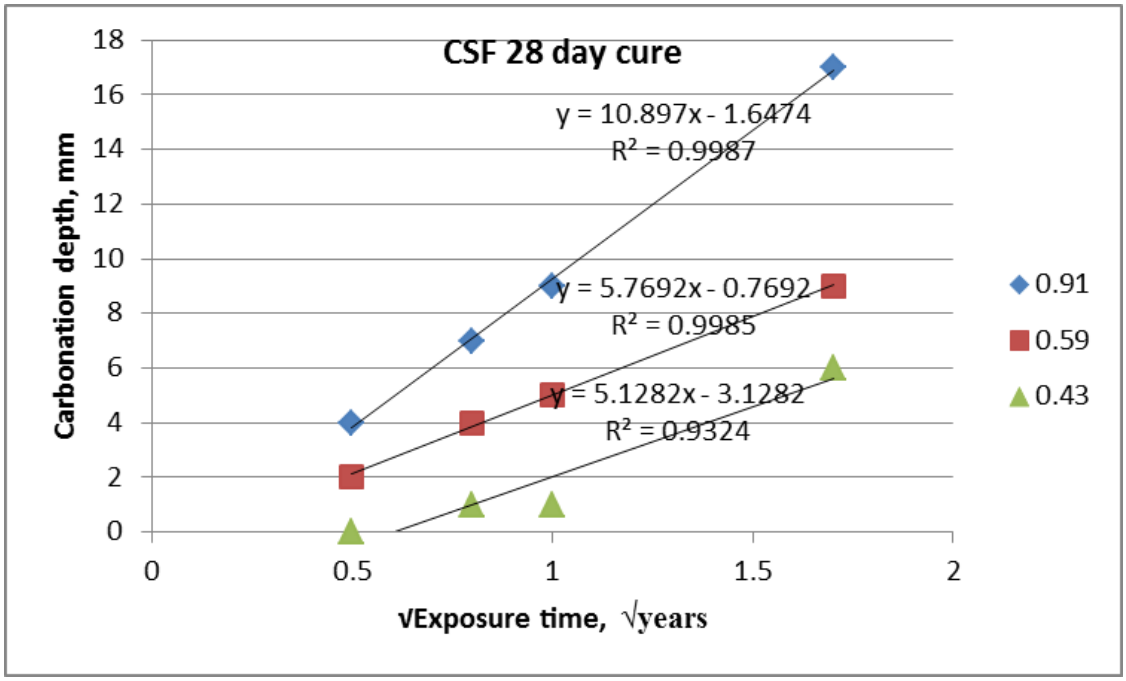


Figure G8: Carbonation depth vs. square root of exposure period